UNIVERSITAT ROVIRA I VIRGILI

COMPUTATIONAL MECHANISTIC STUDIES IN GOLD(I) CATALYSIS AND DESIGN OF NEW CHIRAL LIGANDS

Immaculada Escofet Miquel

UNIVERSITAT ROVIRA i VIRGILI

Computational Mechanistic Studies in Gold(I) Catalysis and Design of New Chiral Ligands

Imma Escofet Miquel
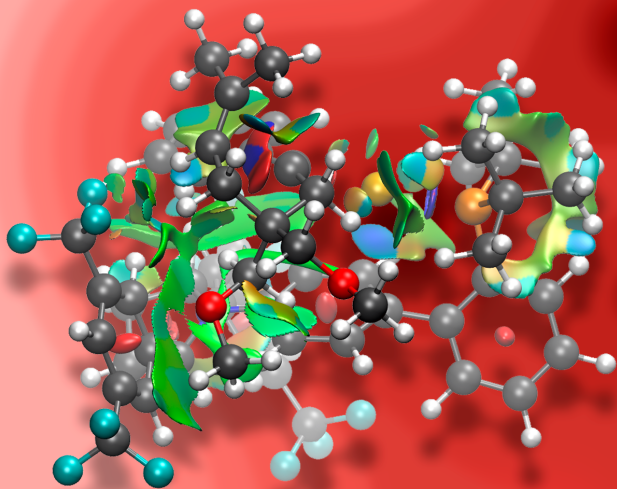
DOCTORAL THESIS
2020

UNIVERSITAT ROVIRA I VIRGILI
COMPUTATIONAL MECHANISTIC STUDIES IN GOLD(I) CATALYSIS AND DESIGN OF NEW CHIRAL LIGANDS
Immaculada Escofet Miquel

UNIVERSITAT ROVIRA I VIRGILI
COMPUTATIONAL MECHANISTIC STUDIES IN GOLD(I) CATALYSIS AND DESIGN OF NEW CHIRAL LIGANDS
Immaculada Escofet Miquel

Imma Escofet Miquel

Computational Mechanistic Studies in Gold(I) Catalysis and Design of New Chiral Ligands

DOCTORAL THESIS

Supervised by Professor Antonio M. Echavarren

Institut Català d´Investigació Química (ICIQ)

Tarragona 2020

UNIVERSITAT ROVIRA I VIRGILI
COMPUTATIONAL MECHANISTIC STUDIES IN GOLD(I) CATALYSIS AND DESIGN OF NEW CHIRAL LIGANDS
Immaculada Escofet Miquel

I STATE that the present study, entitled "**Computational Mechanistic Studies in Gold(I) Catalysis and Design of New Chiral Ligands**", presented by Imma Escofet Miquel for the award of the degree of Doctor, has been carried out under my supervision at the Institut Català d´Investigació Química (ICIQ).

Tarragona, June 12th, 2020

Doctoral Thesis Supervisor

Prof. Antonio M. Echavarren

UNIVERSITAT ROVIRA I VIRGILI
COMPUTATIONAL MECHANISTIC STUDIES IN GOLD(I) CATALYSIS AND DESIGN OF NEW CHIRAL LIGANDS
Immaculada Escofet Miquel

A la meva família i a l'Ernest

UNIVERSITAT ROVIRA I VIRGILI
COMPUTATIONAL MECHANISTIC STUDIES IN GOLD(I) CATALYSIS AND DESIGN OF NEW CHIRAL LIGANDS
Immaculada Escofet Miquel

*"Em van ensenyar que el camí del
progrés no és ni ràpid ni fàcil"*

Marie Curie

UNIVERSITAT ROVIRA I VIRGILI
COMPUTATIONAL MECHANISTIC STUDIES IN GOLD(I) CATALYSIS AND DESIGN OF NEW CHIRAL LIGANDS
Immaculada Escofet Miquel

Aquesta tesi doctoral s'ha dut a terme a l'Institut Català d'Investigació Química i ha estat supervisada pel Professor A. M. Echavarren, a qui agraeixo l'oportunitat de formar-me en el seu grup i l'absoluta confiança dipositada en mi des del primer dia. Moltes gràcies Antonio per transmetre'm la teva passió per la química i la feina ben feta, per tota l'orientació i ajuda i, també, per estar sempre disposat a ensenyar.

Agraeixo a la Sònia Gavaldà, la meva companya i amiga i la més eficient coordinadora de grup. Per donar-me sempre suport, ajudar-me en tot moment i per tenir un gran cor.

Voldria agrair a tots els membres de l'ASR de l'ICIQ, per la seva professionalitat. Gràcies a les unitats: HTE, Chromtae, CRTU, HRMS, NMR, X-Ray, tallers mecànic i del vidre. A la Dr. Gisela Colet per tots els consells i solucions ràpides als problemes. I a tots els altres departaments de l'ICIQ per facilitar-nos tant la feina, especialment IT, CSOL i SHEQ.

Són molts els membres que han passat pel grup Echavarren durant aquests anys, a tots ells i elles els agraeixo haver pogut aprendre'n tant i alhora gaudir de la seva companyia i col·laboració. Gràcies als que em vau obrir la porta del lab, avui dia ja doctors: Morgane Gaydou, Yahui Wang, Anthony Pitaval, Madeleine Livendhal, Núria Huguet, Katya Smirnova, Masha Kirillova, Pilar Calleja (per ser com ets) i Bart Herlé. Agraeixo molt l'ajuda incondicional de l'Anna Homs i de la Carla Obradors amb qui vaig treballar colze a colze i en vaig aprendre tantes coses i amb qui, he anat sembrant una bonica amistat. També, voldria agrair als doctors: Paul McGonigal, Philipp Holstein, Javier Carreras, Ana Pereira, Tania Jiménez, Juan Sarria, Ophélie Quinonero, Jean S. Suppo, Estíbaliz Coya, Jin-Ming Yang, Andrey Konovalov, Miguel Peña, Michael Muratore (for the interesting discussions), Óscar Pablo, Fedor Miloserdov (thanks for you help), Xiao-Li Pei (for your positive energy), Araceli Fernández (gracias por tantos buenos momentos y por tu apoyo). Als últims doctors del grup: Zhouting Rong, Xiang Yin, Eric Tan, Ruth Dorel, Elena de Orbe (por haberme guiado por el mundo computacional, por sus consejos y nuestras conversaciones sobre química y la vida). Especial agraïment també a la Sofia Ferrer per haver estat sempre una gran companya dins i fora del laboratori. A totes aquelles persones amb qui he tingut el plaer de poder col·laborar: Dr. Beatrice Ranieri (gracias Bea por tu amistad, lealtad y tu gran ayuda), Dr. Laura López (pels nostres inicis a l'HTE, també al Dr. Xisco Caldentey). Les ara ja doctores: Anna Homs (amb qui vaig començar a investigar la química de l'or), Carla Obradors (per la seva feina impecable) i Cristina García (por su constancia y energía), Dr. Hanna Bruss & Dr. Masha Kirillova & Dr. Dagmar Scharnagel for your excellent results and very interesting discussions. A la Dr. Maria Besora, per ajudar-me tant quan m'he intentat entendre amb un ordinador, gràcies per la teva dedicació i paciència! Especial menció també, pels meus últims companys de projecte: Giuseppe Zucarrello (for your very well done work), Joan G. Mayans, Alba H. Pérez i l'Helena Armengol (per tenir sempre els braços oberts per fer-te una abraçada). Als nous membres del grup: Otilia Stoica, Mauro Mato, Ulysse Caniparolli, Àlex Martí, Gala Ogalla i especialment a la Margherita Zanini (pels teus muffins i ànims quan no hi veia la llum, gràcies Marghe!). A mis "super-users": Ana Arroyo, Eduardo García e Inma Martín por ayudarme tanto estos últimos meses ¡y siempre de tan buen humor! I també als doctors: Allegra Franchino, Rémi Blieck, Leonardo Nannini, Marc Montesinos i Franco Della Felice.Thank you all!

I would like to thank to my previous research group in The University of Aberdeen where I learnt how to work in a laboratory and spent a very special year some time ago, thanks to Dr. Laurent Trembleau, Dr. Michael Simpson, and Dr. Sarah Nicoll.

No puc oblidar-me de la bona gent que he conegut a Tarragona i amb qui els dinars dels divendres seran sempre recordats: Basti, Toni, Pep (gràcies per fer-me riure tant i per ser un bon amic), Edu, Carla, Anna, Beatrice, Paco, Noelia i Lucía (gracias a los tres por tanta energía). També, vull agraïr als meus companys de cotxe, amb qui tots els km per l'AP-7 han sigut molt més entretinguts: Guillem, Anna i Dídac. I a les "gretels" que fan que l'hora de dinar cada dia sigui més divertida: Noemí, Laura i Sònia.

Agraeixo als amics de la UB, amb qui vaig començar l'aventura de la química ja fa uns anys i de tant en tant encara trobem temps per seguir compartint moments memorables junts: Elena, Carles, Raul, Iris, Joan i Laura.

A les meves granadenques preferides, per fer-me sempre costat i ajudar-me sense demanar mai res a canvi: Mireia, Carme, Maria, Mònica, Anna i a tots els integrants de l'anomenada "Colla Pessigolla". Amb vosaltres he gaudit de moments molt especials: viatges inoblidables, balls de bastons, esquiades, rutes muntanyenques i també hem fet vàries obres de teatre junts; Litus, a tu també, gràcies! També, agraeixo als amics de Vilafranca, on sempre m'he sentit com a casa: Helena, Faust i Emma (gràcies per tant d'amor i somriures junts). Lluís, Núria i Joan per les nostres escapades i per ser-hi sempre.

I am very grateful to share my passion for wine with "my winos": Dominique, Maria and Esme. Thank ladies for such a wonderful time together and for all your support.

Voldria agrair també a la meva segona família d'Avinyonet, per acollir-me tan bé i donar-me suport sempre: Teresa (la iaia), Gemma i Mota (els meus "xuelus ongoing"), Salvador, Josefina, Cristina, Núria i Isaac.

Agraeixo a aquelles persones que sempre han cregut en mi i m'han donat força. Per sobre de tot, als meu pares, Carles i Mercè, per estimar-me tant i fer-ho sempre el millor que han pogut i més! A la meva germana Montse (amb qui sempre he fet pinya i és per a mi un exemple a seguir), al meu cunyat Enric i als meus nebots, Àlex i Xavi (amb qui he compartit molt d'amor i rialles). Als meus avis, àvies, tiets i tietes, per ser com són i lluitar cada dia per seguir essent una família unida. Als meus cosins i cosines, que des que vam néixer, han estat un puntal a la meva vida: Jordi, Ernest, Josep i Andrea (i els petitons Pau i Toni, gràcies per tants bons moments junts i pels que vindran a Alemanya o Catalunya), Francesc (gràcies xic per no fallar-me mai), Gemma (gràcies Nona per ser-hi sempre), Ferran i Agnès (la més fidel confident i amiga, gràcies per tant Mimo!), Mercè, Sergi, Carlos i Maria (ànims amb la tesi!), Jordi i Irina, i a tu David, que sempre et portaré al cor.

Finalment, voldria agrair al meu company de vida, l'Ernest (per mi, l'Erni) per creure sempre en mi i donar-me tanta energia positiva quan més ho he necessitat. Per les teves abraçades en els moments més durs i per tot el que junts hem anat construint aquests anys. Gràcies per estimar-me tant, aquesta tesi, també és teva.

UNIVERSITAT ROVIRA I VIRGILI
COMPUTATIONAL MECHANISTIC STUDIES IN GOLD(I) CATALYSIS AND DESIGN OF NEW CHIRAL LIGANDS
Immaculada Escofet Miquel

At the moment of writing this thesis, the results presented herein have been published in:

A Case Study on the Formation of *trans*-Fused Bicyclo[5.1.0]octanes: On the Structure of Cyclopropyl Gold(I) Carbene-Type Intermediates.
Escofet, I.; Armengol-Relats, H.; Bruss, H.; Besora, M.; Echavarren, A. M.
Manuscript in preparation.

Acetylene as a Dicarbene Equivalent via Gold(I) Catalysis: Total Synthesis of Waitziacuminone in One Step
Scharnagel, D.; Escofet, I.; Armengol-Relats, H.; de Orbe, M. E.; Korber, J. N.; Echavarren, A. M.
Angew. Chem. Int. Ed. **2020**, *59*, 4888–4891.

Enantioselective Folding of Enynes by Gold(I) Catalysts with a Remote C_2-Chiral Element
Zuccarello, G.; Mayans, J. G.; Escofet, I.; Scharnagel, D.; Kirillova, M. S.; Peŕez-Jimeno, A. H.; Calleja, P.; Boothe, J. R.; Echavarren, A. M.
J. Am. Chem.Soc. **2019**, 141, 30, 11858–11863.

Enantioselective Synthesis of Cyclobutenes by Intermolecular [2+2] Cycloaddition with Non-C_2 Symmetric Digold Catalysts
García-Morales, C.; Ranieri, B.; Escofet, I.; López-Suárez, L.; Obradors, C.; Konovalov, A.; Echavarren. A. M.
J. Am. Chem. Soc. **2017**, *139*, 13628–13631. – Highlighted in *Synfacts*, **2018**, *14*, 66.

Anatomy of Gold Catalysts: Facts and Myths
Ranieri, B.; Escofet, I.; Echavarren, A. M.
Org. Biomol. Chem. **2015**, 13, 7103 - 7118.

Modular chiral gold(I) phosphite complexes
Delpont, N.; Escofet, I.; Pérez-Galán, P.; Spiegl, D.; Raducan, M.; Bour, C.; Sinisi, R.; Echavarren, A. M.
Catal. Sci. Technol. **2013**, 3, 3007-3012.

On the Silver Effect and the Formation of Chloride-Bridged Digold Complexes
Homs, A; Escofet, I; Echavarren. A. M.
Org. Lett. **2013**, *15*, 5782–5785.

In addition, other results which are not that related to the topic of this thesis have been published in:

Functional-Group-Tolerant, Silver-Catalyzed N-N Bond Formation by Nitrene Transfer to Amines
Maestre, L.; Dorel, R.; Pablo, O.; Escofet, I.; Sameera, W. M. C.; Alvarez, E.; Maseras, F.; Diaz-Requejo, M. M.; Echavarren, A. M.; Perez, P. J.
J. Am.Chem.Soc. **2017**, 139, 2216-2223.

Development of ^{18}F-fluorinatable dendrons and their application to cancer cell targeting
Trembleau, L.; Simpson, M.; Cheyne, R. W.; Escofet, I.; Appleyard, V.; Murray, K.; Sharp, S.; Thompson, A.; Smith, T. A. D.
New J. Chem., **2011**, 35, 2496-2502.

UNIVERSITAT ROVIRA I VIRGILI
COMPUTATIONAL MECHANISTIC STUDIES IN GOLD(I) CATALYSIS AND DESIGN OF NEW CHIRAL LIGANDS
Immaculada Escofet Miquel

UNIVERSITAT ROVIRA I VIRGILI
COMPUTATIONAL MECHANISTIC STUDIES IN GOLD(I) CATALYSIS AND DESIGN OF NEW CHIRAL LIGANDS
Immaculada Escofet Miquel

Table of Contents

Chapter II: Computational Study of the Gold(I)-Catalyzed Activation of Acetylene

Chapter III: Enantioselective Gold(I) Catalysis

General Conclusions

UNIVERSITAT ROVIRA I VIRGILI
COMPUTATIONAL MECHANISTIC STUDIES IN GOLD(I) CATALYSIS AND DESIGN OF NEW CHIRAL LIGANDS
Immaculada Escofet Miquel

UNIVERSITAT ROVIRA I VIRGILI
COMPUTATIONAL MECHANISTIC STUDIES IN GOLD(I) CATALYSIS AND DESIGN OF NEW CHIRAL LIGANDS
Immaculada Escofet Miquel

Prologue

This Doctoral Thesis manuscript has been divided into four main parts, a general introduction on gold(I) catalysis and three research chapters, which are preceded by the abstract and general objectives of the Thesis and followed by the general conclusions. Each research chapter comprises five sections including a specific introduction on the research topic, the objectives, the results and discussion, the conclusions and the experimental section. The references and numbering are organized by chapters.

The **General Introduction** provides an overview of the basic principles of homogeneous gold(I) catalysis focusing on the activation of alkynes, the cycloisomerizations of enynes, the intermolecular reactions of alkynes with alkenes, the enantioselective gold(I) catalysis and a computational perspective on gold(I) catalysis.

The **Chapter I** collects the computational investigations on the nature of cyclopropyl gold(I) carbenes in cycloisomerization reactions together with mechanistic study on the formation of *trans*-fused cyclopropanes by gold(I)-catalyzed cascades reactions. Experimental part of this chapter was carried out by Dr. Hanna Bruss and Helena Armengol i Relats, for coherence some of their results have been discussed briefly. The computational study on the nature of intermediates has been performed in collaboration with Dr. Maria Besora (URV).

The **Chapter II** contains a computational study of intermolecular gold(I)-catalyzed acetylene activation. Experimental part of this chapter was carried out by Dr. Dagmar Scharnagel, Helena Armengol i Relats, M. Elena de Orbe and J. Nepomuk Korber, for coherence some of their results have been discussed briefly. This work has been published in *Angew. Chem. Int. Ed*. **2020**, *59*, 4888–4891.

The **Chapter III** has been divided in three main parts. The synthesis of chiral phosphite monogold(I) complexes and its applications in gold(I)-catalyzed transformations. Initial studies on the phosphite ligand synthesis were performed by Patricia Pérez-Galán, Mihai Raducan, Dr. Christophe Bour and Dr. Riccardo Sinisi, these results are not discussed in this Thesis. This work has been done in collaboration with Nicolas Delpont and Dr. Dirk Spiegl and has been published in *Catal. Sci. Technol.* **2013**, 3, 3007−3012. Second part of this chapter is focus on the development of broad scope enantioselective synthesis of cyclobutenes by intermolecular [2+2] cycloaddition of alkynes with alkenes using Josiphos digold(I) catalysts. This work was performed in collaboration with Cristina García-Morales, Dr. Laura López-Suárez. Kinetic studies were performed by Cristina García-Morales. The computed enantioinduction model was performed by Dr. Andrey I. Konovalov. This work has been published in *J. Am. Chem. Soc.* **2017**, *139*, 13628–13631. Finally, a computational study on the mode of action of the new pyrrolidinyl-biphenyl phosphine gold(I) complexes will be presented. Experimetnal part of this project was carried out by Giuseppe Zuccarello, Joan G. Mayans, Dr. Dagmar Scharnagel, Dr. Mariia S. Kirillova, Alba H. Pérez-Jimeno, Pilar Calleja and Jordan R. Boothe, for coherence some of their results have been discussed briefly. This work has been published in *J. Am. Chem. Soc.* **2019**, *141*, 11858–11863.

UNIVERSITAT ROVIRA I VIRGILI
COMPUTATIONAL MECHANISTIC STUDIES IN GOLD(I) CATALYSIS AND DESIGN OF NEW CHIRAL LIGANDS
Immaculada Escofet Miquel

List of Abbreviations and Acronyms

In this manuscript, the abbreviations and acronyms most commonly used in organic and organometallic chemistry have been used following the recommendations of "Guidelines of Authors" of the Journal of Organic Chemistry.

Additional abbreviations and acronyms used in this manuscript are listed below:

APCI	atmospheric pressure chemical ionization
BAr$_4$$^{F-}$	tetrakis[3,5-bis(trifluoromethyl)phenylborate]
BF$_4$	tetrafluoroborate
BINAP	2,2'-bis(diphenylphosphino)-1,1'-binaphthyl
BINOL	1,1'-binaphthol
BIPHEP	(Biphenyl-2,2'-diyl)bis(diphenylphosphine)
dr	diastereomeric ratio
ee	enantiomeric excess
er	enantiomeric ratio
DAD	diode array detector
ESI	electrospray ionization
JohnPhos	(2-biphenyl)di-*tert*-butylphosphine
Int	intermediate
IPr	1,3-bis(2,4,6-trimethylphenyl)imidazole-2-ylidene
L	ligand
MALDI matrix assisted laser desorption ionization	
MeOBIPEP	bis(diphenylphosphino)-6,6'-dimethoxy-1,1'-biphenyl
MeCN	acetonirile
MS	mass spectrometry/molecular sieves
MW	microwave irradiation
NBO	natural bond orbital
NHC	N-heterocyclic carbene
NTf$_2$$^{-}$	bis(trifluoromethyl)imidiate
OTf^{-}	triflate
ORTEP	oak ridge thermal ellipsoid plot
PF$_6$$^{-}$	hexafluorophosphate
SbF$_6$$^{-}$	hexafluoroantimonate
SEGPHOS	4,4'-bi-1,3-benzodioxole-5,5'-diylbis(diphenylphosphane)
SFC	Supercritical Fluid Chromatography
*t*BuXPhos	2-(di-*tert*-butylphosphino)-2',4',6'-triisopropyl-1,1'-biphenyl
tmbn	trimethoxybenzonitrile
TS	transition state
XPhos	2-Dicyclohexylphosphino-2',4',6'-triisopropylbiphenyl

UNIVERSITAT ROVIRA I VIRGILI
COMPUTATIONAL MECHANISTIC STUDIES IN GOLD(I) CATALYSIS AND DESIGN OF NEW CHIRAL LIGANDS
Immaculada Escofet Miquel

Abstract

Research in homogeneous gold catalysis has provided unique tools for the ready construction of molecular complexity through the selective activation of alkynes. Over the last years, our research group focused on the development of novel synthetic methodologies enabled by gold(I) catalysis, the study of the intriguing mechanisms of these transformations, and the design and preparation of new gold(I) complexes with improved catalytic activities. In this context, the nature of intermediates in gold(I)-catalyzed cycloisomerization reactions has been particularly puzzling. In order to shed light on the mechanism of these transformations, we have performed detailed computational studies. Thus, we investigated the nature of cyclopropyl gold(I) carbenes and their different canonical possible forms. Benchmark of DFT methods together with QTAIM theory and NBO analysis confirmed the presence of different intermediates in cycloisomerizations of enynes. As particularly challenging case, we have also computed the selective formation of *trans*-fused cyclopropanes by gold(I)-catalyzed cyclization cascade of functionalized dienynes.

Recently, we discovered a gold(I)-catalyzed system for the incorporation of acetylene gas into complex frameworks. Formation of only one diastereomer of biscyclopropanes by reaction of *trans*-stilbene with acetylene has been rationalized by means of DFT calculations.

Despite the success of gold(I) in homogeneous catalysis for the selective activation of multiple C-C bonds, highly enantioselective reactions are still relatively scarce, particularly in the context of intermolecular transformations. This is mainly due to the preference of gold(I) to form linear two-coordinated complexes, in which the chiral ligand is located far away from the reacting center in the enantio-determining step. Therefore, we prepared a series of novel chiral phosphite gold(I) complexes and tested their activity in the enantioselective formal [4+2] cycloaddition of 1,6-arylenynes.

We developed the enantioselective intermolecular gold(I)-catalyzed [2+2] cycloaddition of terminal alkynes and alkenes using non C_2-chiral Josiphos digold(I) complexes as catalysts. Our mechanistic studies indicate that only one of the gold(I) centers is directly involved in the activation of the alkyne, although the second one is required to induce the enantioselectivity. We demonstrated that both ligand exchange and electrophilic addition can be turnover-limiting steps in this catalytic cycloaddition.

To address the limitations on enantioselective catalysis, our group has designed a new class of chiral gold(I) catalysts containing remote C_2-symmetric 2,5-disubstituted pyrrolidines that promote different enantioselective cyclizations in good to excellent enantioselectivities. We elucidated the mode of action of our novel catalysts by means of DFT calculations. As revealed by NCI plots, we proposed that the catalyst exerts the stereocontrol by non-covalent interactions between the aryl groups on the pyrrolidine moiety and the aryl groups of the substrate. In addition, 2nd generation of chiral ligands have been investigated in order to determine the role of each component in the enantioselectivity.

UNIVERSITAT ROVIRA I VIRGILI
COMPUTATIONAL MECHANISTIC STUDIES IN GOLD(I) CATALYSIS AND DESIGN OF NEW CHIRAL LIGANDS
Immaculada Escofet Miquel

General Objectives

The aims of this Doctoral Thesis were:

- To perform a computational study of gold(I) catalyzed cycloisomerizations by Density Functional Theory in order to lay the mechanistic bases for further developments.
- The detailed computational examination of the high selectivity of intermolecular gold(I)-catalyzed acetylene activation.
- Synthesis of new chiral gold(I) catalysts based on ligand design, development of a general enantioselective gold(I)-catalyzed transformations and systematic computational investigation of the mode of enantioinduction.

Each chapter of this manuscript provides a more detailed description of the corresponding objectives.

UNIVERSITAT ROVIRA I VIRGILI
COMPUTATIONAL MECHANISTIC STUDIES IN GOLD(I) CATALYSIS AND DESIGN OF NEW CHIRAL LIGANDS
Immaculada Escofet Miquel

General Introduction

UNIVERSITAT ROVIRA I VIRGILI
COMPUTATIONAL MECHANISTIC STUDIES IN GOLD(I) CATALYSIS AND DESIGN OF NEW CHIRAL LIGANDS
Immaculada Escofet Miquel

UNIVERSITAT ROVIRA I VIRGILI
COMPUTATIONAL MECHANISTIC STUDIES IN GOLD(I) CATALYSIS AND DESIGN OF NEW CHIRAL LIGANDS
Immaculada Escofet Miquel

General Introduction

Anatomy of gold catalysis

For many years, gold has only been considered an unreactive noble metal and its potential as catalyst was neglected. The outburst of activity in gold chemistry was centered on heterogenous catalysis during the 80's, when the group of Hutchings discovered that vinyl chloride could be obtained by the hydrochlorination of acetylene catalyzed by metallic gold and the group of Haruta disclosed that, under similar heterogeneous conditions in the presence of gold, carbon monoxide could be oxidized at room temperature.[1] It was not only until the late 90's when the group of Teles reported the first important application of Au(I) complexes in homogeneous catalysis, namely the formation of acetals by addition of methanol to alkynes, under mild conditions (Scheme 1).[2]
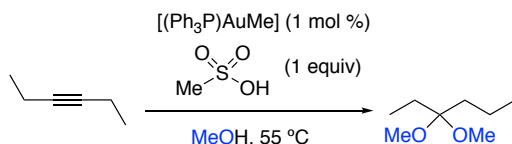
Scheme 1. First reaction of alkynes in homogeneous catalysis.

Likewise, together with the development of phenol synthesis by Hashmi using simple gold(III) salts,[3] our group and those of Fürstner and Toste discovered that cationic gold(I) complexes were the most powerful catalysts for the electrophilic activation of alkynes towards a variety of nucleophiles. Since then, homogeneous gold catalysis has seen an almost exponential growth leading to the development of a plethora of synthetic transformations for the build-up of molecular complexity (Figure 1).[4]

This is mainly due to the high ability of gold(I) to selectively activate π-bonds, which can be rationalized by the relativistic effects.[5] It is known that relativistic effects arise from the high speed of electrons spinning around a heavy nucleus. As a consequence, the mass of the electron increases, which leads to their energetic stabilization, and thus, a contraction of the *s* and *p* orbitals. This entails that the electrons occupying the *d* and *f* orbitals experience destabilization and expansion and are weakly attracted by the nucleus. This effect is much more significant for those elements having their 4*f* and 5*d* orbitals filled, reaching a maximum for gold (Au electronic configuration: [Xe] $4f^{14} \, 5d^{10} \, 6s^1$). Hence, the contraction

1 (a) Hutchings, G. J. *J. Catal.* **1985**, *96*, 292–295. (b) Haruta, M.; Kobayashi, T.; Sano, H.; Yamada, N. *Chem. Lett.* **1987**, *16*, 405–408. (c) Hutchings, G. J. *ACS Cent. Sci.* **2018**, 4, 1095–1101.
2 Teles, J. H.; Brode, S.; Chabanas, M. *Angew. Chem. Int. Ed.* **1998**, *37*, 1415–1418.
3 Hashmi, A. S. K.; Frost, T. M.; Bats, J. W. *J. Am. Chem. Soc.* **2000**, *122*, 11553–11554.
4 (a) Martín-Matute, B.; Cárdenas, D. J.; Echavarren A. M. *Angew. Chem. Int. Ed.* **2001**, *40*, 4754–4757. (b) Martín-Matute, B.; Nevado, C.; Cárdenas, D. J.; Echavarren A. M. *J. Am. Chem. Soc.* **2003**, *125*, 5757–5766. (c) Jiménez-Nuñez, E.; Echavarren, A. M. *Chem. Commun.* **2007**, 333–346. (d) Jiménez-Núñez, E.; Echavarren, A. M. *Chem. Rev.* **2008**, *108*, 3326–3350. (e) Fürstner, A. *Chem. Soc. Rev.* **2009**, *38*, 3208–3221. (f) Obradors, C.; Echavarren, A. M. *Acc. Chem. Res.* **2014**, *47*, 902–912. (g) Fensterbank, L.; Malacria, M. *Acc. Chem. Res.* **2014**, *47*, 953–965. (h) Dorel, R.; Echavarren, A. M. *Chem. Rev.* **2015**, *115*, 9028–9072. (i) Pflästerer, D.; Hashmi, A. S. K. *Chem. Soc. Rev.* **2016**, *45*, 1331–1367. (j) Echavarren, A. M.; Muratore; M.; López-Carrillo, V.; Escribano-Cuesta, A.; Huguet, N.; Obradors, C. *Org. React.* **2017**, *92*, 1–288.
5 Gorin, D.; Toste, F. D. Nature, **2007**, *446*, 395–403. See also references cited herein.

UNIVERSITAT ROVIRA I VIRGILI
COMPUTATIONAL MECHANISTIC STUDIES IN GOLD(I) CATALYSIS AND DESIGN OF NEW CHIRAL LIGANDS
Immaculada Escofet Miquel

General Introduction

of the gold 6*s* orbital causes the expansion of the 5*d* orbitals, which minimize the electron-electron repulsion. This phenomenon not only explains the aurophilic interactions and the highest electronegativity of gold (2.4) among the transition metals but also its soft Lewis acidic character.
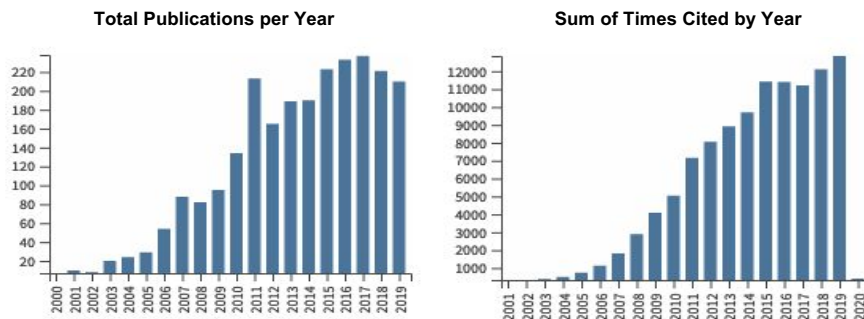
Figure 1. Publications and citations report per year for the topic "gold(I) catalysis" from Scopus.

Gold(I) complexes adopt a linear dicordination geometry, although higher coordination numbers are also possible (3 or 4).[6] This structural preference of gold(I) can also be justified by relativistic effects since the hybridization of *s/d* or *s/p* orbitals is very efficient due to the small differences in energy among *s*, *p* and *d* states. Gold(I) linear two-coordinated complexes do not undergo spontaneous oxidative addition[7] or promote β-hydride elimination. Nevertheless, recent discoveries have demonstrated that by rational ligand design, gold(I) can promote oxidative addition.[8] In addition, to date, only square planar gold(III) complexes have been claimed to promote β-hydride elimination.[9]

Gold(IIII) complexes present a square planar geometry, are harder Lewis acids than their gold(I) counterparts, and thus, catalytically active in many transformations. It has been observed that switching from gold(I) to gold(III) has an important effect, even leading to divergent reaction outcomes.[10] However, in the presence of oxidable substrates, they can be

---

6   (a) Gimeno, M. C.; Laguna, A. *Chem. Rev.* **1997**, *97*, 511–522. (b) Joost, M.; Amgoune, A.; Bourissou, D. *Angew. Chem. Int. Ed.* **2015**, *54*, 15022–15045.

7   Livendahl, M.; Goehry, C.; Maseras, F.; Echavarren, A. M. *Chem. Commun.* **2014**, *50*, 1533–1536.

8   (a) Joost, M.; Zeineddine, A.; Estévez, L.; Mallet-Ladeira, S.; Miqueu, K.; Amgoune, A.; Bourissou, D. *J. Am. Chem. Soc.* **2014**, *136*, 14654–14657. (b) Guenther, J.; Mallet-Ladeira, S.; Estevez, L.; Miqueu, K.; Amgoune, A.; Bourissou, D. *J. Am. Chem. Soc.* **2014**, *136*, 1778–1781. (c) Cambeiro, X. C.; Ahlsten, N.; Larrosa, I. *J. Am. Chem. Soc.* **2015**, 137, 15636−15639. (d) Wu, C. Y.; Horibe, T.; Jacobsen, C. B.; Toste, F. D. *Nature,* **2015**, *517*, 449–454. (e) Zeineddine, A.; Estévez, L.; Mallet-Ladeira, S.; Miqueu, K.; Amgoune, A.; Bourissou, D. *Nat. Commun.* **2017**, *8*, 565–572. (f) Cadge, J. A.; Sparkes, H. A.; Bower, J. F.; Rusell, C. A. *Angew. Chem. Int. Ed.* **2020**, *59*, 6617–6621.

9   (a) Mankad, N. P.; Toste, F. D. *Chem. Sci.* **2012**, *3*, 72–76. (b) Klatt, G.; Xu, R.; Pernpointner, M.; Molinari, L.; Quang Hung, T.; Rominger, F.; Hashmi, A. S. K.; Köppel, H. *Chem. Eur. J.* **2013**, *19*, 3954–3961. (c) Castiñeira Reis, M.; López, C. S.; Kraka, E.; Cremer, D.; Faza, O. N. *Inorg. Chem.* **2016**, *55*, 8636–8645. (d) Rekhroukh, F.; Estevez, L.; Mallet-Ladeira, S.; Miqueu, K.; Amgoune, A.; Bourissou, D. *J. Am. Chem. Soc.* **2016**, *138*, 11920−11929. (e) Kumar, R.; Krieger, J.-P.; Gómez-Bengoa, E.; Fox, T.; Linden, A.; Nevado, C. *Angew. Chem. Int. Ed.* **2017**, *56*, 12862–12865.

10   (a) Hashmi, A. S.; Weyrauch, J. P.; Rudolph, M.; Kurpejovi, E. *Angew. Chem. Int. Ed.* **2004**, *43*, 6545–6547 (b) Wong, M. K. *Adv. Synth. Catal.* **2013**, *355*, 2055–2070. (c) Yang, Y.; Hu, W.; Ye, X.; Wang, D.; Shi, X. *Adv. Synth. Catal.* **2016**, *358*, 2583–2588. (d) Ranieri, B.; Escofet, I.; Echavarren, A. M. *Org. Biomol. Chem*. **2015**, *13***,** 7103–7118, and references cited therein.

UNIVERSITAT ROVIRA I VIRGILI
COMPUTATIONAL MECHANISTIC STUDIES IN GOLD(I) CATALYSIS AND DESIGN OF NEW CHIRAL LIGANDS
Immaculada Escofet Miquel

General Introduction

easily reduced to Au(I) or Au(0). From a practical point of view, gold(I) complexes can be easily used as catalysts in many transformations in air, without an inert atmosphere, due to its redox stability.

In the early years of gold catalysis, gold(I) as well as gold(III) were mainly used as chloride salts. However, it was promptly realized that ligands play a fundamental role in modulating the reactivity and the selectivity of gold(I) catalysts in the activation of alkynes, allenes, and alkenes.[4f,11] As a consequence of the L-Au bond contraction, the nature of the complex can be highly modulated by the electronic and steric properties of the ligand. The development of this chemistry led to the design and synthesis of ligands to successfully achieve the desired reactivity.

Generally, complexes with donating ligands that are sterically hindered are the most useful catalysts. Gold(I) complexes with phosphite ligands are more electrophilic than those bearing better σ-donating phosphines or N-heterocyclic carbenes (Figure 2). Gold(I) complexes show intermediate electrophilicity when bearing phosphines. Commercially available bulky dialkyl biphenyl phosphines, initially developed for Pd-catalyzed cross-coupling reactions, are the most common phosphines in gold-catalyzed transformations.[12]
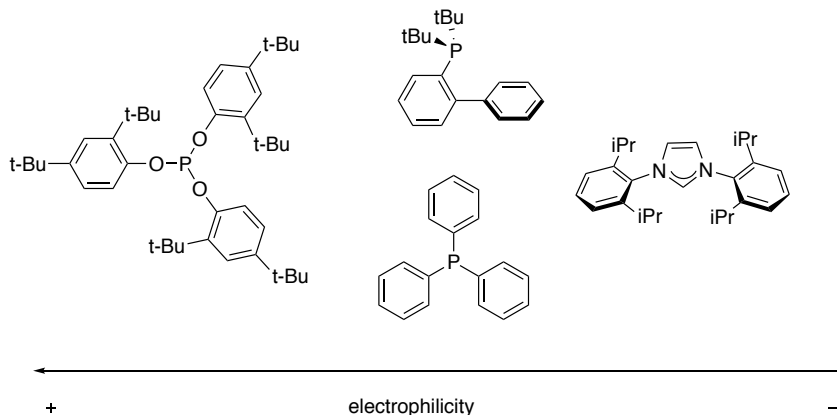
Figure 2. Typical ligands used for gold(I) complexes classified by electrophilicity.

Gold(I) complexes can be readily prepared either by reduction of NaAuCl$_4$ with 2,2'-thiodiethanol in the presence of the L (ligand) or following a more practical procedure by the direct reaction of L with commercially available Me$_2$SAuCl (Scheme 2).

11   (a) Hashmi, A. S. K.; *Chem. Rev.* **2007**, *107*, 3180–3211. (b) Gorin, D. J.; Sherry, B. D.; Toste, F. D. *Chem. Rev.* **2008**, 108, 3351–3378. (c) Hashmi, A. S. K.; *Acc. Chem. Res.* **2014**, *47*, 864–876.
12   (a) Kaye, S.; Fox, J. M.; Hicks, F. A.; Buchwald, S. L. *Adv. Synth. Catal.*, **2001**, *343*, 789–794. (b) Nevado, C.; Echavarren, A. M. *Synthesis* **2005**, *2*, 167–182. (c) Hashmi, A. S. K.; Haufe, P.; Schmid, C.; Rivas Nass, A.; Frey, W. *Chem. Eur. J.* **2006**, *12*, 5376–5382. (d) Kusama, H.; Miyashita, Y.; Takay, J.; Iwasawa, N. *Org. Lett.* **2006**, *8*, 289–292. (e) Shapiro, N. D.; Toste, F. D. *J. Am. Chem. Soc.* **2007**, *129*, 4160–4161. (f) Ye, L.; Cui, L.; Zhang, L. *J. Am. Chem. Soc.* **2010**, *132*, 3258–3259.

UNIVERSITAT ROVIRA I VIRGILI
COMPUTATIONAL MECHANISTIC STUDIES IN GOLD(I) CATALYSIS AND DESIGN OF NEW CHIRAL LIGANDS
Immaculada Escofet Miquel

General Introduction
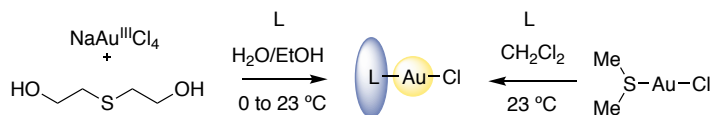
Scheme 2. Common synthesis of LAuCl complexes.

Although the majority of catalytic applications have been developed using neutral gold(I) complexes [LAuCl], their activation is usually needed to create a formal vacancy. This activation takes place by the abstraction of the chloride so that the substrate could coordinate to gold *via* an associative mechanism.[13] Active gold(I) complexes can be generated *in situ* by treatment with a chloride scavenger, usually silver(I) salts, in the presence of the substrate, to form insoluble AgCl (Scheme 3, (a)).[14] However, we observed that in the absence of a coordinating substrate, much less reactive chloride-bridged dinuclear gold(I) complexes are formed [LAuClAuL]X (Scheme 3, (c)). The formation of these species is responsible for the so-called "silver effects".[15] Due to this fact, the most convenient way to abstract chloride is either preparing a neutral complex [LAuX] where X$^-$ is a weakly coordinating anion such as NTf$_2^-$ or OTf$^-$ (Scheme 3, (d)) or cationic complexes [LAuL']X, where L' is a neutral weakly coordinating ligand such as MeCN or PhCN, and X$^-$ is a weakly coordinating counterion (SbF$_6^-$, BF$_4^-$, or PF$_6^-$) (Scheme 3, (b)). These cationic complexes can directly enter to the catalytic cycle preventing the formation of chloride-bridged species.[10d] It is worth mentioning that some of these easily handled and air stable cationic complexes are commercially available nowadays.

The effects of counterions in gold catalysis, both kinetics and selectivity, have also been discussed recently.[16] Despite the fact that [LAu$^+$] species are very often invoked in mechanistic proposals, the existence of these "naked gold" complexes as stable, isolable species in solution have not been proven yet.[17]

13 (a) Nieto-Oberhuber, C.; López, S.; Muñoz, M. P.; Cárdenas, D. J.; Buñuel, E.; Nevado, C.; Echavarren, A. M. *Angew. Chem. Int. Ed.* **2005**, *44*, 6146–6148. (b) H. Schmidbaur, A. Schier, *Organom.* **2010**, *29*, 2–23. (c) Amijs, C. H. M.; López-Carrillo, V.; Raducan, M.; Pérez-Galán, P.; Ferrer, C.; Echavarren, A. M. *J. Org. Chem*. **2008**, *73*, 7721–7730.

14 (a) Preisenberger, M.; Schier, A.; Schmidbaur, H.; *J. Chem. Soc. Dalton Trans*. **2009**, 1645–1650. (b) Partyka, D. V.; Robilotto, T. J.; Zeller, M.; Hunter, A. D.; Gray, T. G. *Organometallics* **2008**, *27*, 28–32.

15 (a) Zhu, Y.; Day, C. S.; Zhang, L.; Hauser, K. J.; Jones, A. C. *Chem Eur. J.* **2013**, *19*, 12264–12271. (b) Homs, A.; Escofet, I.; Echavarren, A. M. *Org. Lett.* **2013**, *15*, 5782–5785. (c) Lu, Z.; Han, J.; Hammond, G. B.; Xu, B. *Org. Lett.* **2015**, *17*, 4534–4537. (d) Zhdanko, A.; Maier, M. E. *ACS Catal.* **2015**, *5*, 5994−6004.

16 (a) Homs, A.; Obradors, C.; Lebœuf, D.; Echavarren, A. M. *Adv. Synth. Catal.* **2014**, *356*, 221–228. (b) Jia, M.; Bandini, M. *ACS Catal.* **2015**, *5*, 1638–1652.

17 (a) Weber, S. D.; Zahner, D.; Rominger, F.; Straub, B. F. *Chem. Commun.* **2012**, *48*, 11325–11327. (b) Veenboer, R. M. P.; Collado, A.; Dupuy, S.; Lebl, T.; Falivene, L.; Cavallo, L.; Cordes, D. B.; Slawin, A. M. Z.; Cazin, C. S. J.; Nolan, S. P. *Organometallics* **2017**, *36*, 2861–2869.

UNIVERSITAT ROVIRA I VIRGILI
COMPUTATIONAL MECHANISTIC STUDIES IN GOLD(I) CATALYSIS AND DESIGN OF NEW CHIRAL LIGANDS
Immaculada Escofet Miquel

General Introduction

A multipurpose precatalyst with an electron-donating 2,4,6-trimethylmethoxybenzonitrile as ligand, [Au(tmbn)₂](SF₆), can be also used for the *in situ* preparation of a wide variety of cationic complexes [LAu(tmbn)]SbF₆, bearing L phosphines or NHC.[18]
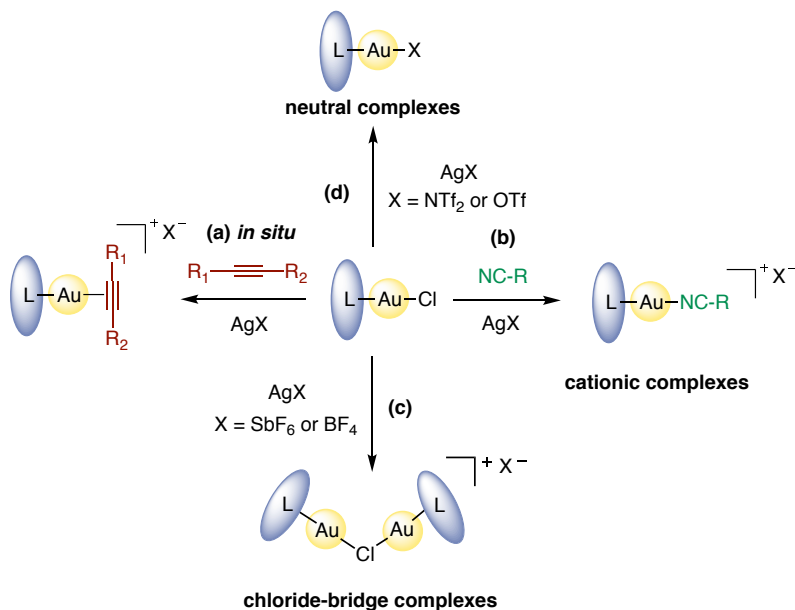
Scheme 3. Activation modes of LAuCl and possible side-products.

Gold(I) complexes selectively activate alkynes in the presence of other functional groups, including alkenes. However, there is no thermodynamic preference of gold(I) to coordinate alkynes. Hence, the alkynophilicity of gold(I)[4c] is directly related to the higher reactivity of the resulting (η^2-alkyne)gold(I) species **1** towards nucleophilic attack.[19a] In general, the attack of the nucleophiles takes place in outer-sphere *anti*-fashion manner giving rise to *trans*-alkenyl gold complexes **2** (Scheme 4).[19]
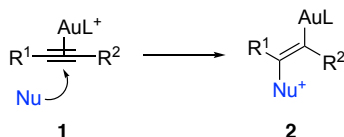
Scheme 4. Markovnikov nucleophilic attack to (η^2-alkyne)gold(I) complexes.

A wide range of nucleophiles has been used in both inter- and intramolecular gold(I) catalyzed transformations including arenes, heteroarenes, water, alcohols, amines, imines,

18   Raducan, M.; Rodríguez-Escrich, C.; Cambeiro, X. C.; Escudero-Adán, E. C.; Pericàs, M. A.; Echavarren, A. M. *Chem. Commun.* **2011**, *47*, 4893–4895.
19   (a) García-Mota, M.; Cabello, N.; Maseras, F.; Echavarren, A. M.; Pérez-Ramírez, J.; López, N. *ChemPhysChem.* **2008**, *9*, 1624–1629. (b) Hashmi, A. S. K.; Weyrauch, J. P.; Frey, W.; Bats, N. W. *Org. Lett.* **2004**, *6*, 4391–4394. (c) Kennedy-Smith, J. J.; Staben, S. T.; Toste, F. D. *J. Am. Chem. Soc.* **2004**, *126*, 4526–4527.

UNIVERSITAT ROVIRA I VIRGILI
COMPUTATIONAL MECHANISTIC STUDIES IN GOLD(I) CATALYSIS AND DESIGN OF NEW CHIRAL LIGANDS
Immaculada Escofet Miquel

General Introduction

thiols, sulfoxides, and *N*-oxides, affording *anti*-addition products **2**.[4,20] On the other hand, a direct *syn* insertion of alkynes and allenes into gold-silicon bonds has also been disclosed.[21]

Reactions catalyzed by gold(I) typically proceed by multistep pathways. Although labelling and kinetic experiments together with DFT studies have been crucial for the proposal of coherent mechanisms, relatively few relevant intermediates in gold catalysis have been isolated.[22] Since most of reactions proceed under mild conditions, gold(I) has been involved in many total syntheses of natural products and biologically relevant compounds.[20e]

Cycloisomerizations of 1,*n*-Enynes

Cycloisomerization of enynes has gained great attraction for the construction of diverse molecular frameworks from simple substrates. In particular, cycloisomerizations of 1,6-enynes are one of the most extensively studied.[4d,4f] Gold(I) forms (η^2-alkyne)gold(I) species **I** that react intermolecularly with the tethered alkene to give either cyclopropyl gold(I) carbenes intermediates **II** and **III** deriving by anti-5-*exo*-dig or 6-*endo*-dig cyclization, respectively (Scheme 5). Intermediates **II** and **III** can evolve by different skeletal rearrangements, in the absence of internal and external nucleophiles. Moreover, both intermediates **II** and **III** have been found to be highly delocalized cationic species by means of DFT calculations.[13,23]

Cyclopropyl gold carbene **II**, can undergo a single-cleavage skeletal rearrangement when the distal carbon of the alkene moiety migrates to the terminal carbon of the alkyne to form 1,3-dienes **4** (Scheme 5, purple). Alternatively, intermediate **II** can evolve through a double-cleavage rearrangement, resulting in the formal insertion of the terminal alkene carbon into the alkyne carbons giving rise to carbene **IV** that afford product **3**, after α-hydrogen

20   (a) Mizushima, E.; Sato, K.; Hayashi, T.; Tanaka, M. *Angew. Chem. Int. Ed.* **2002**, *41*, 4563–4565. (b) Ferrer, C.; Echavarren, A. M. *Angew. Chem. Int. Ed.* **2006**, *45*, 1105–1109. (c) Nakamura, I.; Sato, T.; Yamamoto, Y. *Angew. Chem. Int. Ed.* **2006**, *45*, 4473–4475. (d) Istrate, F. M.; Gagosz, F. *Org. Lett.* **2007**, *9*, 3181–3184. (e) Hashmi, A. S. K.; Rudolph, M. *Chem. Soc. Rev.* **2008**, *37*, 1766–1775. (f) Davies, P. W.; Albrecht, S. J. C. *Angew. Chem. Int. Ed.* **2009**, *48*, 8372–8375. (g) Krauter, C. M.; Hashmi A. S. K.; Pernpointner, M. *ChemCatChem* **2010**, *2*, 1226–1230. (h) Qian, J.; Liu, Y.; Cui, J.; Xu, Z. *J. Org. Chem.* **2012**, *77*, 4484–4490. (i) Shi, S.; Wang, T.; Yang, W.; Rudolph, M.; Hashmi, A. S. K. *Chem. Eur. J.* **2013**, *19*, 6576–6580. (j) Debrouwer, W.; Heugebaert, T. S. A.; Roman, B. I. A.; Stevens, C. V. *Adv. Synth. Catal.* **2015**, *357*, 2975–3006. (k) Molawi, K.; Delpont, N.; Echavarren, A. M. *Angew. Chem. Int. Ed.* **2010**, *49*, 3517–3519. (l) López-Suárez, L.; Riesgo, L.; Bravo, F.; Ransom, T. T.; Beutler, J.; Echavarren, A. M. *Chem. Med. Chem.* **2016**, *11*, 1003–1007.

21   Joost, M.; Gualco, P.; Mallet-Ladeira, S.; Amgoune, A.; Bourissou, D. *Angew. Chem. Int. Ed.* **2013**, *52*, 7160–7163.

22   (a) Pyykkö, P. *Angew. Chem. Int. Ed.* **2004**, *43*, 4412–4456. (b) Hashmi, A. S. K. *Angew. Chem. Int. Ed.* **2010**, *49*, 5232–5241. (c) Liu, L. P.; Hammond, G. B. *Chem. Soc. Rev.* **2012**, *41*, 3129–3139. (d) Sameera, W. M. C.; Maseras, F. *WIREs Comput. Mol. Sci.* **2012**, *2*, 375–385. (e) Thiel, W. *Angew. Chem. Int. Ed.* **2014**, *53*, 8605–8613 (f) Jones, A. C. *Top. Curr. Chem.* **2015**, *357*, 133–166. (g) Ferrer, S.; Echavarren, A. M. *Organometallics* **2018**, *37*, 781–786.

23   (a) Nieto-Oberhuber, C.; Muñoz, M. P.; Buñuel, E.; Nevado, C.; Cárdenas, D. J.; Echavarren, A. M. *Angew. Chem. Int. Ed.* **2004**, *43*, 2402–2406. (b) Ferrer, C.; Raducan, M.; Nevado, C.; Claverie, C. K.; Echavarren, A. M. *Tetrahedron* **2007**, *63*, 6306–6316. (c) Soriano, E.; Marco-Contelles, J. *Acc. Chem. Res.* **2009**, *42*, 1026–1036. (d) Escribano-Cuesta, A.; Pérez-Galán, P.; Herrero-Gómez, E.; Sekine, M.; Braga, A. A. C.; Maseras, F.; Echavarren, A. M. *Org. Biomol. Chem.* **2012**, *10*, 6105–6111.

UNIVERSITAT ROVIRA I VIRGILI
COMPUTATIONAL MECHANISTIC STUDIES IN GOLD(I) CATALYSIS AND DESIGN OF NEW CHIRAL LIGANDS
Immaculada Escofet Miquel

General Introduction

elimination (Scheme 5, green). Even though both (Z and E) configurations are possible for product **3**, Z-**3** are more commonly obtained.[24]
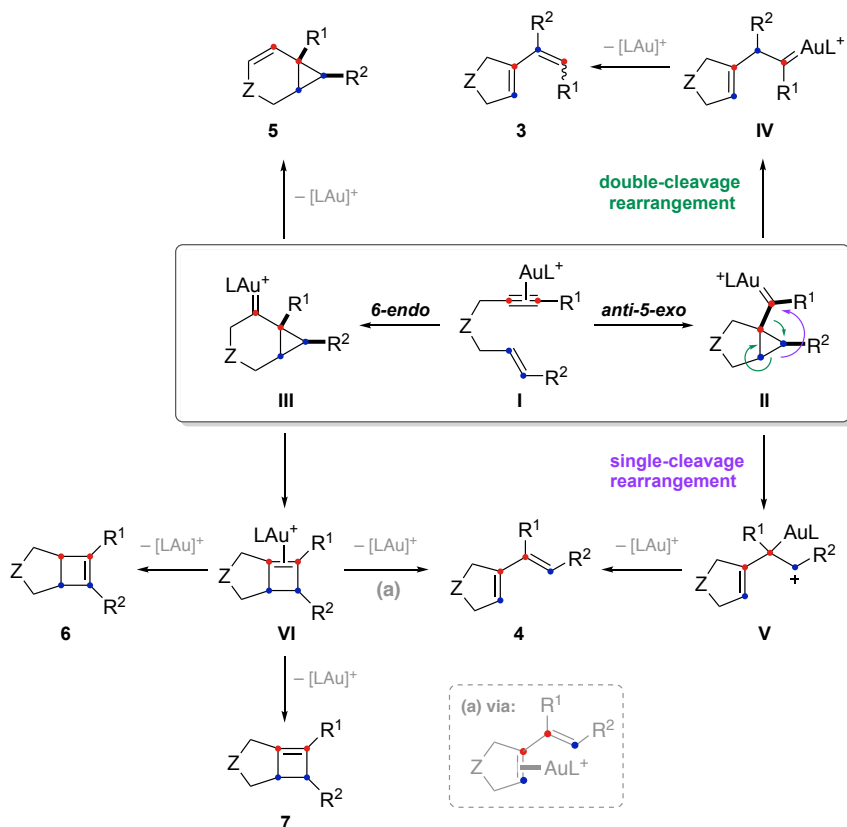
Scheme 5. General pathways for cycloisomerizations of 1,6-enynes catalyzed by Au(I).

On the other hand, intermediate **III,** resulting from 6-*endo*-dig cyclization of **I**, can give bicyclo[4.1.0]hept-2-ene derivatives **5** upon 1,2-H shift and protodeauration.[25] Additionally, ring expansion of the cyclopropane moiety of intermediate **III** renders (^{2}-cyclobutene)-gold(I) complexes **VI** that can either undergo ring opening to afford 1,3-dienes **4** (via (η^2-alkene)gold(I) complexes) or isomerization to form **6**.[13,23] Interestigly, cyclobutenes type **7** have only been isolated in few cases as a product of cycloisomerization of 1-6,enynes[13a,23d,26b,30] whereas the macrocyclization of higher 1,n-enynes (n≥7) give rise

24   (a) Ota, K.; Chatani, N. *Chem. Commun.* **2008**, 2906–2907. (b) Ota, K.; Lee, S. I.; Tang, J.-M.; Takachi, M.; Nakai, H.; Morimoto, T.; Sakurai, H.; Kataoka, K.; Chatani, N. *J. Am. Chem. Soc.* **2009**, *131*, 15203–15211.

25   (a) Nieto-Oberhuber, C.; Muñoz, M. P.; López, S.; Jiménez-Núñez, E.; Nevado, C.; Herrero-Gómez, E.; Raducan, M.; Echavarren, A. M. *Chem. Eur. J.* **2006**, *12*, 1677–1693. (b) Nieto-Oberhuber, C.; Pérez-Galán, P.; Herrero-Gómez, E.; Lauterbach, T.; Rodríguez, C.; López, S.; Bour, C.; Rosellón, A.; Cárdenas, D. J.; Echavarren, A. M. *J. Am. Chem. Soc.* **2008**, *130*, 269–279. (c) Lee, Y. T.; Kang, Y. K.; Chung, Y. K. *J. Org. Chem.* **2009**, *74*, 7922–7934.

UNIVERSITAT ROVIRA I VIRGILI
COMPUTATIONAL MECHANISTIC STUDIES IN GOLD(I) CATALYSIS AND DESIGN OF NEW CHIRAL LIGANDS
Immaculada Escofet Miquel

General Introduction

selectively to relatively less strained cyclobutenes via a formal [2+2] cycloaddition.[26] Thus, cyclobutene-fused product **9** was obtained by a diastereoselective gold(I) catalyzed [2+2] macrocyclization reaction of 1,10-enyne **8**. This methodology was applied for the total synthesis of both rumphellaone A and hushinone, natural products that contain tetrasubstituted cyclobutene moiety (Scheme 6).[27] Moreover, 1,5- and 1,7-enynes react intramolecularly in a similar manner as their 1,6-enyne counterparts.[28]
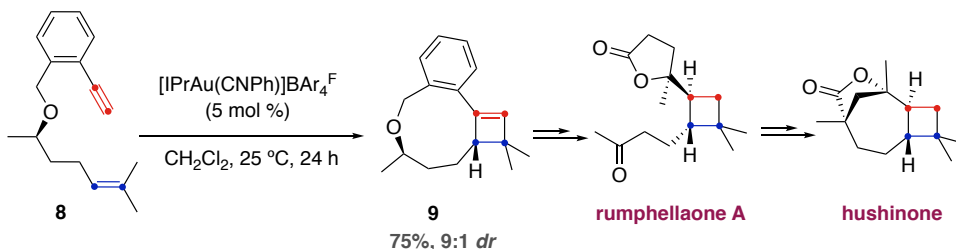
Scheme 6. Au(I)-catalyzed macrocyclization of enyne 8 for the synthesis of natural products.

Cycloisomerizations of 1,*n*-enynes also lead to the formation of alkoxy-, hydroxy- or aminocyclization products in the presence of external nucleophiles (e.g. alcohols, water, amines or ketones) that attack the cyclopropyl gold(I) carbene formed in a stereospecific and regioselective manner.[23a,25a,29]

A formal [4+2] cycloaddition reaction can also occur when the alkyne of the enyne is substituted with an aryl ring leading to tricyclic scaffolds **10** (Scheme 7).[25,30] The reaction commences with the formation of cyclopropyl gold(I) carbene **VIII-a** via a 5-*exo*-dig pathway that can open to form the aryl stabilized cation **VIII-b**. Then, Friedel-Crafts-type reaction takes places to give **IX** which upon re-aromatization and protodemetalation leads to the formation of **10**.

26   (a) Lee, S. I.; Kim, S. M.; Choi, M. R.; Kim, S. Y.; Chung, Y. K. *J. Org. Chem.* **2006**, *71*, 9366–9372. (b) Odabachian, Y.; Gagosz, F. *Adv. Synth. Catal.* **2009**, *351*, 379–386. (c) Ito, H.; Ohmiya, H.; Sawamura, M. *Org. Lett.* **2010**, *12*, 4380–4383. (d) Brooner, R. E. M.; Brown, T. J.; Widenhoefer, R. A. *Angew. Chem. Int. Ed.* **2013**, *52*, 6259–6261.

27   (a) Obradors, C.; Leboeuf, D.; Aydin, J.; Echavarren, A. M. *Org. Lett.* **2013**, *15*, 1576–1579. (b) Ranieri, B.; Obradors, C.; Mato, M.; Echavarren, A. M. *Org. Lett.* **2016**, *18*, 1614–1617.

28   (a) Sun, J.; Conley, M.; Zhang, L.; Kozmin, S. *J. Am. Chem. Soc.* **2006**, *128*, 9705–9710. (b) López-Carrillo, V.; Huguet, N.; Mosquera, Á.; Echavarren, A. M. *Chem. Eur. J.* **2011**, *17*, 10972–10978. (c) Cabello, N.; Rodríguez, C.; Echavarren, A. M. *Synlett* **2007**, 1753–1758.

29   (a) Zhang, L.; Kozmin, S. A. *J. Am. Chem. Soc.* **2005**, *127*, 6962–6963. (b) Fürstner, A.; Morency, L. *Angew. Chem. Int. Ed.* **2008**, *47*, 5030–5033. (c) Buzas, A. K.; Istrate, F. M.; Gagosz, F. *Angew. Chem. Int. Ed.* **2007**, *46*, 1141–1144. (d) Chao, C.-M.; Toullec, P. Y.; Michelet, V. *Tetrahedron Lett.* **2009**, *50*, 3719–3722.

30   Nieto-Oberhuber, C.; López, S.; Echavarren, A. M. *J. Am. Chem. Soc.* **2005**, *127*, 6178–6179.

UNIVERSITAT ROVIRA I VIRGILI
COMPUTATIONAL MECHANISTIC STUDIES IN GOLD(I) CATALYSIS AND DESIGN OF NEW CHIRAL LIGANDS
Immaculada Escofet Miquel

General Introduction
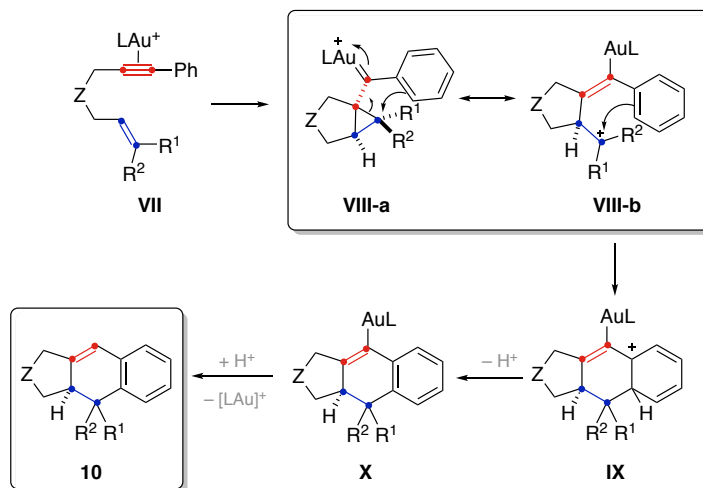
Scheme 7. Mechanistic proposal for the intramolecular [4+2] cycloaddition reaction of aryl-substituted 1,6-enynes type **VII**.

Intermolecular Gold(I) Catalyzed Reactions of Alkynes with Alkenes

Although a significant progress has been made in the intramolecular gold(I) catalyzed reactions of alkynes with alkenes to obtain complex polycyclic structures, the development of intermolecular transformations is still challenging.[31] In this scenario, both unsaturated substrates (alkynes and alkenes) are plausible ligands for gold(I) and present a similar association constants.[32] Furthermore, dimerization or polymerization of the alkenes promoted by gold catalyst can also take place as side reactions.[33]

Nonetheless, several gold(I) catalyzed intermolecular transformations have been recently developed, opening the door to the construction of complex molecular frameworks from simple starting materials.[31,34] In 2010, our research group reported the regioselective formation of cyclobutenes of type **11** from terminal alkynes with alkenes by using cationic gold(I) complexes with sterically hindered *t*BuXPhos ligand (Scheme 8).[34a]

---

31   (a) Muratore, M. E.; Homs, A.; Obradors, C.; Echavarren, A. M. *Chem. Asian. J.* **2014**, *9*, 3066–3082. (b) García-Morales, C.; Echavarren, A. M. *Synlett* **2018**, *29*, 2225–2237.

32   (a) Brown, T. J.; Dickens, M. G.; Widenhoefer, R. A. *J. Am. Chem. Soc.* **2009**, *131*, 6350–6351. (b) Brown, T. J.; Widenhoefer, R. A. *J. Organomet. Chem.* **2011**, *696*, 1216–1220. (c) Brooner, R. E. M.; Widenhoefer, R. A. *Angew. Chem. Int. Ed.* **2013**, *52*, 11714–11724.

33   (a) Urbano, J.; Hormigo, A. J.; de Frémont, P.; Nolan, P.S.; Díaz-Requejo, M. M.; Pérez, P. J. *Chem. Commun.* **2008**, 759–761. (b) Brown, T. J.; Dickens, M. G.; Widenhoefer, R. A. *Chem. Commun.* **2009**, 6451–6453.

34   (a) López-Carrillo, V.; Echavarren, A. M. *J. Am. Chem. Soc.* **2010**, *132*, 9292–9294. (b) de Orbe, M. E.; Amenós, L.; Kirillova, M. S.; Wang, Y.; López-Carrillo, V.; Maseras, F.; Echavarren, A. M. *J. Am. Chem. Soc.* **2017**, *139*, 10302–10311. (c) de Orbe, M. E.; Echavarren, A. M. Eur. *J. Org. Chem.* **2018**, *22*, 2740–2752.

UNIVERSITAT ROVIRA I VIRGILI
COMPUTATIONAL MECHANISTIC STUDIES IN GOLD(I) CATALYSIS AND DESIGN OF NEW CHIRAL LIGANDS
Immaculada Escofet Miquel

General Introduction
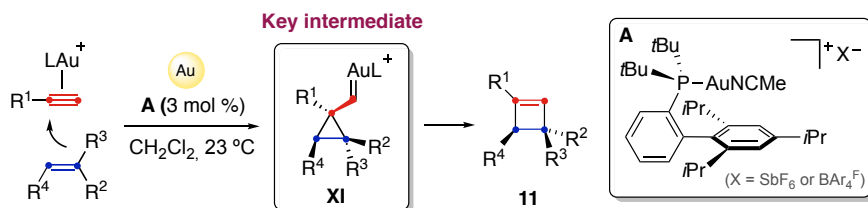
Scheme 8. Intermolecular [2+2] cycloaddition of terminal alkynes with alkenes.

These reactions proceed through the same key cyclopropyl gold carbene intermediate **XI** as in the aforementioned cycloisomerizations of 1,*n*-enynes (n>7), that upon ring opening delivers the cyclobutene. Likewise, the formation of the unreactive σ,π-(alkyne)digold(I) species was found as a secondary process in this transformation. Anion effects proved to be crucial and new cationic gold(I) catalysts were designed by using a bulky and less acidic BAr$_4$$^{F-}$ as counterion, instead of SbF$_6$$^-$, leading to 10-30% increase in the isolated yields using this new complex.[16a] A 1:1 mixture of diastereomeric cyclobutenes **12** was obtained when the reaction took place between phenylacetylene and the deuterated alkene which indicates that free rotation can occur at the C3-C4 bond of the intermediate **XII** followed by ring expansion (Scheme 9).
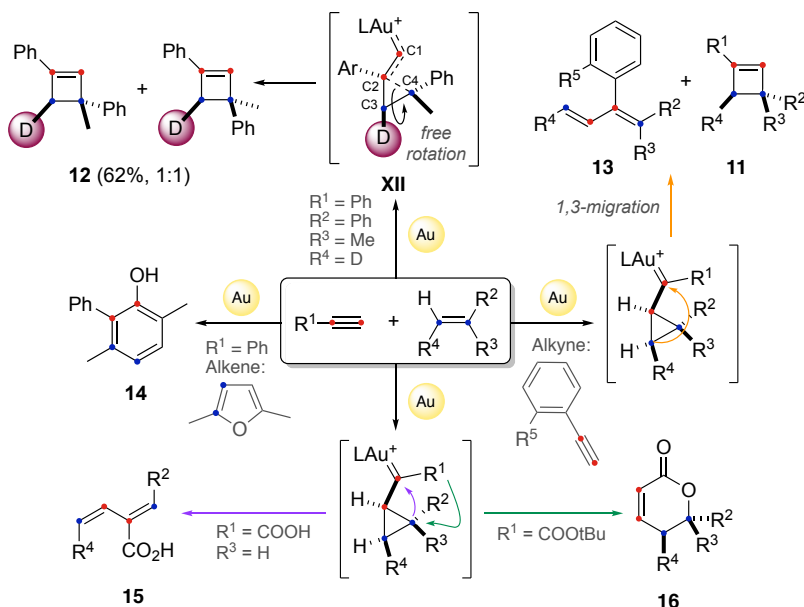
Scheme 9. Intermolecular [2+2] gold(I) catalyzed reactions of different types of alkenes and alkynes and deuterated alkene experiment.

Interestingly, under the same reaction conditions, 1,3-dienes **13** can be obtained together with cyclobutenes **11**, when using *ortho*-substituted aryl alkynes (Scheme 9, orange).[34b]

UNIVERSITAT ROVIRA I VIRGILI
COMPUTATIONAL MECHANISTIC STUDIES IN GOLD(I) CATALYSIS AND DESIGN OF NEW CHIRAL LIGANDS
Immaculada Escofet Miquel

General Introduction

Moreover, alkyl-, vinyl- and (hetero)arylalkynes react with different furans under gold(I) catalysis to give rise to a variety of phenols **14** in very good yields.[35] Propiolic acid and some of its derivatives can also take part in a gold(I) catalyzed intermolecular reaction with 1,1-di- or trisubstituted alkenes leading to α,β-unsaturated δ-lactones **16** by a formal [4+2] annulation. Indeed, upon the formation of the corresponding cyclopropyl gold carbene, the more substituted carbon of the alkene is attacked intermolecularly by the propiolate moiety (Scheme 9, green). The enantioselective version of this transformation has also been reported, being the first asymmetric example of an intermolecular cycloadditon catalyzed by gold(I) (see **Chapter III**). Nonetheless, when using 1,2-disubstituted alkenes, 1,3-dienes **15** were obtained by stereospecific cross metathesis-type reaction that arises from a stepwise rearrangement (Scheme 9, purple).[36]
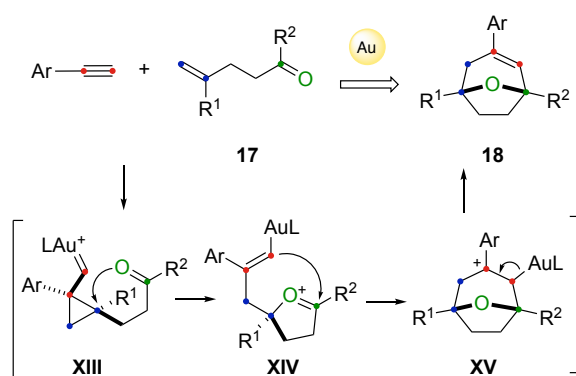
Scheme 10. [2+2+2] intermolecular cycloaddition of arylalkynes with oxoalkenes.

Our group also discovered a particular important gold(I)-catalyzed [2+2+2] cycloaddition of terminal arylalkynes with ketoalkenes **17** that affords 8-oxabicyclo[3.2.1]oct-3-enes **18**, a structural motif present in biologically active natural products (Scheme 10).[37] This process occurs both regio- and stereoselectively and forms cyclopropyl gold carbene **XIII**, bearing a carbonyl group at the alkenyl side chain that attacks the most substituted position of the alkene, building an oxonium cation **XIV**. This intermediate undergoes a Prins reaction leading to benzylic cation **XV**, which gives rise to oxabicyles **18** upon metal elimination and ligand exchange.

35   (a) Hashmi, A. S. K.; Blanco, M. C.; Kurpejović, E.; Frey, W.; Bat, J. W. *Adv. Synth. Catal.* **2006**, *348*, 709–713. (b) Huguet, N.; Leboeuf, D.; Echavarrenx, A. M. *Chem. Eur. J.* **2013**, *19*, 6581–6585.

36   Yeom, H.-S.; Koo, J.; Park, H.-S.; Wang, Y.; Liang, Y.; Yu, Z.-X.; Shin, S. *J. Am. Chem. Soc.* **2012**, *134*, 208–211.

37   (a) Obradors, C; Echavarren, A. M. *Chem. Eur. J.* **2013**, *19*, 3547–3551. (b) Li, B.; Zhao, Y.-J.; Lai, Y.-C.; Loh, T.-P. *Angew. Chem. Int. Ed.* **2012**, 51, 8041–8045. (c) Bai. Y.; Tao, W.; Ren, J.; Wang, Z. *Angew. Chem. Int. Ed.* **2012**, 51, 4112–4116.

UNIVERSITAT ROVIRA I VIRGILI
COMPUTATIONAL MECHANISTIC STUDIES IN GOLD(I) CATALYSIS AND DESIGN OF NEW CHIRAL LIGANDS
Immaculada Escofet Miquel

General Introduction

Enantioselective Gold(I) Catalysis

Despite the success of gold(I) in homogeneous catalysis, the development of efficient asymmetric transformations has been relatively slow-paced. One of the pioneering examples in this field referred to the use of a chiral ferrocenylphophine-gold(I) catalyst in the enantioselective aldol reaction between aldehydes **19** and isocyanoacetates **20**, where gold acts as a Lewis acid upon the activation of carbonyl group (Scheme 11).[38]
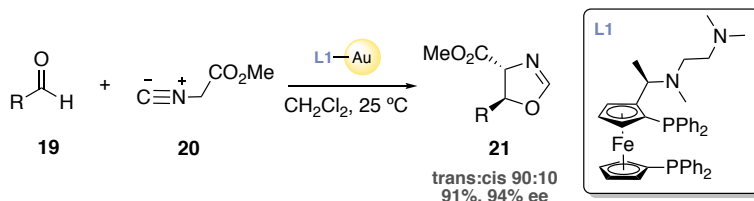
Scheme 11. Pioneer example of enantioselective gold(I)-catalyzed synthesis of oxazolines **21**.

However, highly enantioselective reactions of broad scope are still relatively scarce and the major achievements were only reported recently.[39] This slow development is rationalized by the aforementioned propensity of gold(I) to form linear two-coordinated complexes in which the chiral ligand (L*) is very distant from the reaction center. The problem due to the distance between the substrate and the ligand is further exacerbated by the outer-sphere attack of the nucleophiles (Figure 3).[40]
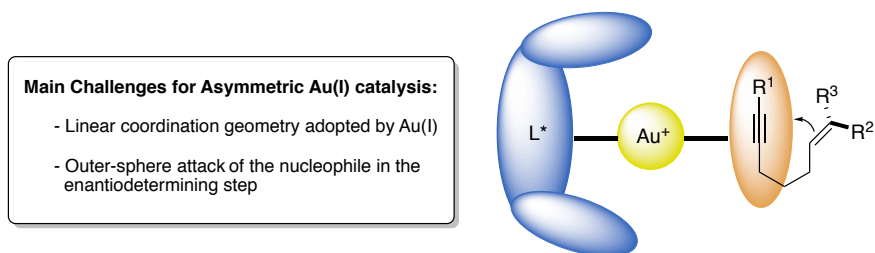
Figure 3. General coordination mode and main challenges for asymmetric Au(I) catalysis.

In 2005, our group developed the first example of a gold(I) catalyzed enantioselective alkoxycyclization of 1,6-enynes **22** using a chiral bis(gold) complex bearing Tol-BINAP ligand (Scheme 12, Figure 4).[41] Although high enantioselectivites (94% *ee*) were achieved

38   Ito, Y.; Sawamura, M.; Hayashi, T. *J. Am. Chem. Soc.* **1986**, *108*, 6405–6406.
39   (a) Fairlamb, I. J. S. *Angew. Chem. Int. Ed.* **2004**, 43, 1048–1052. (b) Bongers, N.; Krause, N. *Angew. Chem. Int. Ed.* **2008**, *47*, 2178–2181. (c) Widenhoefer, R. A. *Chem. Eur. J.* **2008**, *14*, 5382–5391. (d) Sengupta, S.; Shi, X. *ChemCatChem.* **2010**, *2*, 609–619. (e) Lee, A.-L. *Annu. Rep. Prog. Chem.,* Sect. B, **2010**, *106*, 428–446. (f) Shapiro, N. D.; Toste, F. D. *Synlett* **2010**, 2010, 675–691. (g) Pradal, A.; Toullec, P. Y.; Michelet, V. *Synthesis* **2011**, 1501–1514. (h) Wang, Y. M.; Lackner, A. D.; Toste, F. D. *Acc. Chem. Res.* **2014**, *47*, 889–901. (i) Li, Y.; Li, W.; Zhang, J. *Chem. Eur. J.* **2017**, *23*, 467–512.
40   Zi, W.; Toste, F. D. *Chem. Soc. Rev.* **2016**, *45*, 4567–4589.
41   Muñoz, M. P.; Adrio, J.; Carretero, J. C.; Echavarren, A. M. *Organometallics,* **2005**, *24*, 1293–1300.

UNIVERSITAT ROVIRA I VIRGILI
COMPUTATIONAL MECHANISTIC STUDIES IN GOLD(I) CATALYSIS AND DESIGN OF NEW CHIRAL LIGANDS
Immaculada Escofet Miquel

General Introduction

for a sulfone derivative, surprisingly, racemic product was obtained when a malonate was used. This result highlights how crucial can be the nature of the tether in the cyclization of enynes.
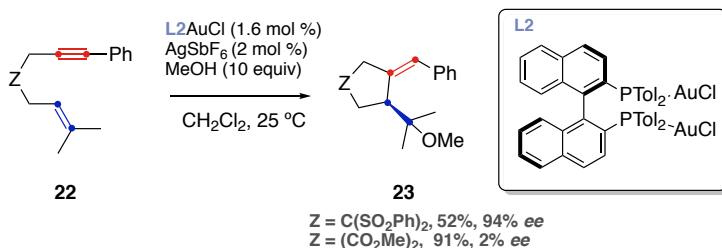
Scheme 12. Enantioselective methoxycyclization reaction of enynes **22**.

Based on these promising results, several examples of enantioselective gold(I) reactions have been recently disclosed, mainly in the field of intramolecular hydrofunctionalization of allenes with carbo- and heteronucleophiles.[42] Digold complexes of bidentate phosphines, such as BINAP, SEGPHOS, BIPHEP, are the most often employed catalysts for these transformations (Figure 4).
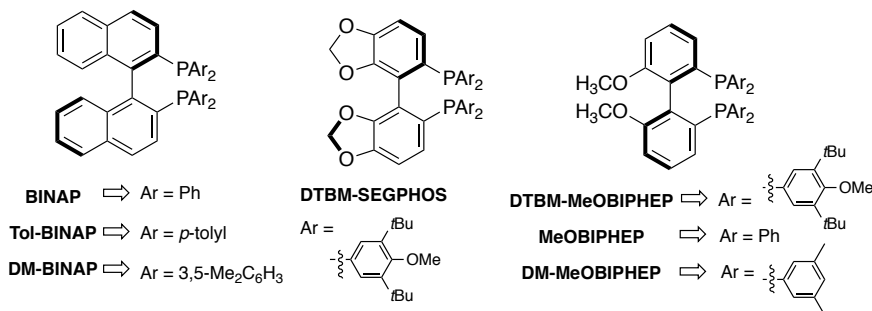
Figure 4. Typical ligands used in asymmetric gold(I) catalysis.

The use of DTBM-SEGPHOS ligand (Figure 4) in gold(I) catalysis was disclosed by the group of Toste in the intermolecular cyclopropanation of sterically hindered pivalate propargylic ester **25** and styrenes of type **24** (Scheme 13).[43] The proposed transition state showed an outer-sphere attack of the vinyl group by a 90º angle with respect to gold(I) carbene that facilitates the enantiodiscrimination giving rise to cycloproane **26** in 94% *ee*.

42   (a) Zhang, Z.; Liu, C.; Kinder, R. E.; Han, X.; Qian, H.; Widenhoefer, R. A. *J. Am. Chem. Soc.* **2006**, *128*, 9066–9073. (b) Tarselli, M. A.; Chianese, A. R.; Lee, S. L.; Gagné, M. R. *Angew. Chem. Int. Ed.* **2007**, *46*, 6670–6673. (c) Luzung, M. R.; Mauleón, P.; Toste, F. D. *J. Am. Chem. Soc.* **2007**, *129*, 12402–12403. (d) Zhang, Z.; Widenhoefer, R. A. *Angew. Chem. Int. Ed.* **2007**, *46*, 283–285. (e) Zhang, Z.; Bender, C. F.; Widenhoefer, R. A. *Org. Lett.* **2007**, *9*, 2887–2889. (f) LaLonde, R. L.; Sherry, B. D.; Kang, E. J.; Toste, F. D. *J. Am. Chem. Soc.* **2007**, *129*, 2452–2453.

43   Johansson, M. J.; Gorin, D. J.; Staben, S. T.; Toste, F. D. *J. Am. Chem. Soc.* **2005**, *127*, 18002–18003.

UNIVERSITAT ROVIRA I VIRGILI
COMPUTATIONAL MECHANISTIC STUDIES IN GOLD(I) CATALYSIS AND DESIGN OF NEW CHIRAL LIGANDS
Immaculada Escofet Miquel

General Introduction
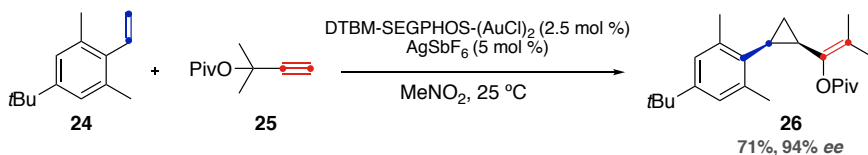
Scheme 13. Enantioselective intermolecular cyclopropanation of alkene **24** using pivalate ester **25**.

Later, the synthesis of tricyclic compounds type of **28** was reported from arylenynes **27** in excellent yields and 92-93% *ee* when using bimetallic gold(I) complexes based on MeOBIPHEP (Scheme 14).[44] These results confirmed the possibility of further develop efficient enantioselective gold(I)-catalyzed transformations of substituted enynes.
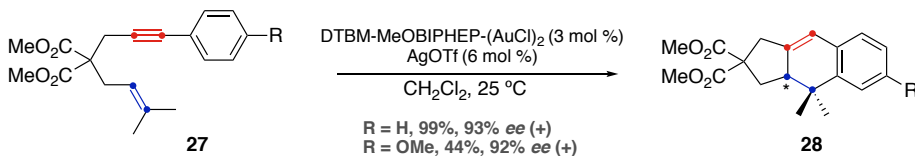
Scheme 14. Asymmetric gold(I)-catalyzed cyclization of arylenynes **27**.

Monogold complexes based on monodentate phosphoramidites and phosphites chiral ligands have also demonstrated to be potential catalyst for the enantioselective gold(I)-catalyzed reactions (Figure 5).[45]
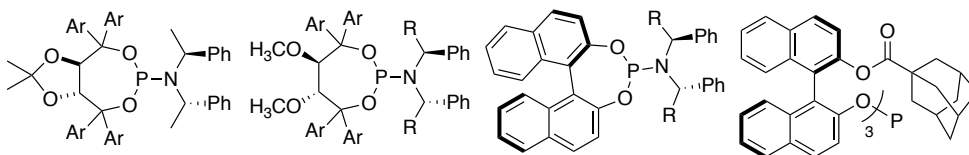
Figure 5. Commonly used phosphoroamidites and phosphite ligands in asymmetric Au(I) catalysis.

Moreover, important anion effects have been observed in the enantioselecivity of several gold(I)-catalyzed transformations.[46] As an example, the hydroalkoxylation of **29** to **30** proceed in very good yields and high enantiomeric ratios when the cyclization was performed with chiral phosphate counterion **31**. Thus, the chiral information could be successfully transfered from the counterion *via* tight ion pairs. Nonetheless, it was later

44   Chao, C.-M.; Vitale, M. R.; Toullec, P. Y.; Genêt, J.-P.; Michelet, V. *Chem. Eur. J.* **2009**, *15*, 1319–1323.
45   (a) Alonso, I.; Trillo, B.; López, F.; Montserrat, S.; Ujaque, G.; Castedo, L.; Lledós, A.; Mascareñas, J. L. *J. Am. Chem. Soc.* **2009**, *131*, 13020–13030. (b) González, A. Z.; Toste, F. D. *Org. Lett.* **2009**, *12*, 200–203. (c) Teller, H.; Flügge, S.; Goddard, R.; Fürstner, A. *Chem. Int. Ed.* **2010**, 49, 1949–1953. (d) González, A. Z.; Benitez, D.; Tkatchouk, E.; Goddard, W. A.; Toste, F. D. *J. Am. Chem. Soc.* **2011**, *133*, 5500–5507.
46   (a) Hamilton, G. L.; Kang, E. J.; Mba, M.; Toste, F. D. *Science,* **2007**, *317*, 496–499. (b) Aikawa, K.; Kojima, M.; Mikami, K. *Angew. Chem. Int. Ed.* **2009**, *48*, 6073–6077. (c) Aikawa, K.; Kojima, M.; Mikami, K. *Adv. Synth. Catal.* **2010**, *352*, 3131–3135. (d) Tu, X.; Gong, L. *Angew. Chem. Int. Ed.* **2012**, *51*, 11346–11349. (e) Butler, K. L.; Tragni, M.; Widenhoefer, R. A. *Angew. Chem. Int. Ed.* **2012**, *51*, 5175–5178. (f) Zhang, Z.; Smal, V.; Retailleau, P.; Voituriez, A.; Frison, G.; Marinetti, A.; Guinchard, X.; *J. Am. Chem. Soc.* **2020**, *142*, 3797–3805.

UNIVERSITAT ROVIRA I VIRGILI
COMPUTATIONAL MECHANISTIC STUDIES IN GOLD(I) CATALYSIS AND DESIGN OF NEW CHIRAL LIGANDS
Immaculada Escofet Miquel

General Introduction

demonstrated that this strategy based on the synergistic use of chiral counterions to mediate the enantiodescrimination failed for substrates with terminal alkynes due to the formation of inactive alkynylgold(I) complexes **33** as a result of terminal alkyne deprotonation of **32** mediated by gold(I) complex bearing **31** ligands (Scheme 15).[47] Recently, it has been demonstrated that tethering a metal complex to its phosphate chiral counterion via phosphine ligand leads to good enansioselectivities in some gold(I)-catalyzed reactions.[46f]
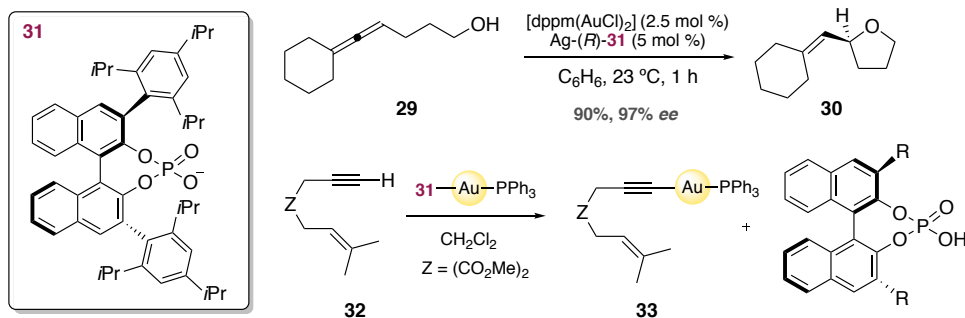
Scheme 15. Binaphtol-based chiral counterion-mediated enantioselective gold(I)-catalyzed synthesis of **30** and formation of inactive alkynylgold(I) complex **33**.

Finally, very recent progress relies on the design of new ligands such as sulfonamides,[48] helically chiral phosphine ligands,[49] and the use of axially chiral monodentate phosphine ligands with a remote cooperative functionality (Figure 6).[50] Sulfonamides PC-Phos was used as ligand in the efficient synthesis of chiral tetrahydrocarbolines as a result of *N*-allenamides cyclization, whereas Xiang-Phos gold(I) complexes were found to be effective catalysts for the enantioselective cyclopropanation of indenes and trisubstituted alkenes. The intermolecular (3+2) cycloaddition of 2-(1-alkynyl)-2-alken-1-ones with 3-stylindoles was achieved in high enantiomeric ratios when using gold(I) catalyst attached with the Ming-Phos ligand. On the other hand, phosphathiahelicenes has been prepared in modular manner and applied for 1,6-enynes cyclizations.

Most of the recent advances just mentioned were reported simultaneously to some results developed in this Doctoral Thesis.

---

47   Raducan, M.; Moreno, M.; Bour, C.; Echavarren, A. M. *Chem. Commun.* **2012**, *48*, 52–54.
48   (a) Wang, Y.; Zhang, P.; Di, X.; Dai, Q.; Zhang, Z.-M.; Zhang, J. *Angew. Chem., Int. Ed.* **2017**, *56*, 15905–15909. (b) Wang, Y.; Zhang, Z.-M.; Liu, F.; He, Y.; Zhang, J. *Org. Lett.* **2018**, *20*, 6403–6406. (c) Zhang, P.-C.; Wang, Y.; Zhang, Z.-M.; Zhang, J. *Org. Lett.* **2018**, *20*, 7049–7052.
49   (a) Yavari, K.; Aillard, P.; Zhang, Y.; Nuter, F.; Retailleau, P.; Voituriez, A.; Marinetti, A. *Angew. Chem., Int. Ed.* **2014**, *53*, 861–865. (b) Aillard, P.; Dova, D.; Magne, V.; Retailleau, P.; Cauteruccio, S.; Licandro, E.; Voituriez, A.; Marinetti, A. *Chem. Commun*. **2016**, *52*, 10984–10987.
50   (a) Wang, Z.; Nicolini, C.; Hervieu, C.; Wong, Y.-F.; Zanoni, G.; Zhang, L. *J. Am. Chem. Soc.* **2017**, *139*, 16064–16067. (b) Cheng, X.; Wang, Z.; Quintanilla, C. D.; Zhang, L. *J. Am. Chem. Soc.* **2019**, *141*, 3787–3791.

UNIVERSITAT ROVIRA I VIRGILI
COMPUTATIONAL MECHANISTIC STUDIES IN GOLD(I) CATALYSIS AND DESIGN OF NEW CHIRAL LIGANDS
Immaculada Escofet Miquel

General Introduction
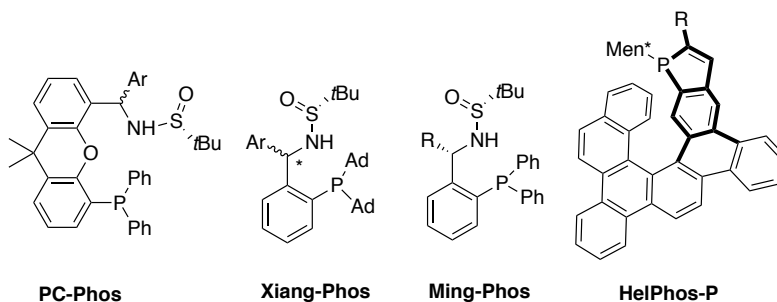
Figure 6. Chiral ligands designed bearing sulfonamides and phosphathiahelicenes that have recently been used in asymmetric gold(I)-catalyzed transformations.

Computational Perspective on Gold(I) Catalysis

Together with the development of new synthetic methodologies based on gold(I) catalysis, there is still a need of understanding the often highly intriguing reaction mechanisms involved in these processes. During the last decades, computational chemistry became a very useful tool that allowed to model, explain and predict properties of gold(I)-catalyzed reactions.[22,23,51] The combination of experimental and computational chemistry opens the door to the development of new reactions in a rational manner together with the rapid screening of molecular systems. Additionally, thanks to the considerable evolution of theoretical chemistry, a wide variety of systems can be covered by this branch of chemistry.[52] Quantum Mechanics (QM) allows to describe little systems with very high accuracy whereas for large systems such as proteins, Molecular Mechanics (MM) or multi-scale model based on a combination of QM/MM, are the most convenient models.

The size of systems studied in this Thesis (up to 150 atoms) is small enough to apply accurate Quantum Mechanics (QM), specifically those based on Density Functional Theory (DFT).

Quantum Mechanics (QM): This model, in contrast to MM, make no reference whatsoever to chemical bonding, treating molecules as collection of nuclei and electrons. The energy and molecular properties are obtained by laws of quantum mechanics, namely the Schrödinger equation:

$$\mathbf{H\Psi} = E\mathbf{\Psi}$$

Where $\mathbf{\Psi}$ is a many-electron wavefunction and $\mathbf{H}$ is the Hamiltonian. The solution of this equation leads to electronic structure and energy. However, since the exact solution for

---

51   (a) Pyykkö, P. *Chem. Soc. Rev.* **2008**, 37, 1967–1997. (b) Shapiro, N. D.; Toste, F. D. *Proc. Nat. Acad. Sci.* **2008**, *105,* 2779–2782. (c) Tsipis, A. C. *Coord. Chem. Rev.* **2014**, *272*, 1–29.

52   (a) Ziegler, T.; Autschbach, J. *Chem. Rev.* **2005**, *105*, 2695–2722. (b) Houk, K. N.; Cheong, P. H.-Y. *Nature* **2008**, *455*, 309.

UNIVERSITAT ROVIRA I VIRGILI
COMPUTATIONAL MECHANISTIC STUDIES IN GOLD(I) CATALYSIS AND DESIGN OF NEW CHIRAL LIGANDS
Immaculada Escofet Miquel

General Introduction

the Schrödinger equation is not possible for many-electrons systems, different QM Methods have been taken to solve it, differing on the approximations:

- **Semiempiricals:** these methods solve an approximate form of the Schrödinger equation taking parameters from experiments. It can be useful for large systems (1000 or more atoms) but to have accurate energies, very good parameters that define the system are required.

- *Ab initio*: these methods aim to solve the Schrödinger equation leading to the computation of the wavefunction for a given nuclear coordinates. Hartree-Fock (HF) is the least expensive *ab initio* method, although it does not provide accurate results. However, these wavefunction-based methods can be improved and converged toward the exact solution of Schrödinger equation. Among the *ab initio* methods, CCSD(T) (coupled-cluster model with single and double excitations corrected by perturbative triples) has become very popular, despite its use is restricted to benchmark studies on very small systems due to high computational cost.[53] Many efforts has been put into the development of low cost methods that by implemented approximations in *ab initio* methods without loss of accuracy. Very recently, the group of Neese developed the Domain-based Local Pair Natural Orbital Method (DLPNO).[54] This correlation method takes advantage of the locality of the electron correlation by means of Pair Natural Orbitals (PNOs). The application of PNOs in correlated calculations drastically reduced the computational cost of the methods with very small errors. The addition of perturbative treatment of the triple excitation led to the DLPNO-CCSD(T) model that allows obtaining high accurate energies in the faster and easier way. This method has recently been used as calibration for benchmark studies of the performance of density functionals.[55] This model will be used in this Thesis in **Chapter I**.

- **Density Functional Theory (DFT):** following laws of quantum mechanics, this electronic structure method solves the Schrödinger equation using mathematical approximations to calculate the electron density. These methods, which provide a time-economic way to handle many electron systems, were developed by Walter Kohn.[56] DFT methods are similar to *ab initio* methods at a much less computational cost since it is not necessary to calculate the many electron wavefunction. According to Honenberg-Kohn theorems,[57] the energy of a system can be expressed as a functional of the electron density function $\rho(r)$, which only depends on three spatial coordinates. Thus, a functional can be used to calculate the energy of a system from the electron density function without computing the

53   Pitonak, M.; Holka, F.; Neogrady, P.; Urban, M. *THEOCHEM*. **2006**, *768*, 79–89.
54   (a) Riplinger, C.; Sandhoefer, B.; Hansen, A; Neese, F. *J. Chem. Phys*. **2013**, *139*, 134101. (b) Sparta, M.; Neese, F. *Chem. Soc. Rev*. **2014**, *43*, 5032–5041.
55   Iron, M. A.; Janes, T. *J. Phys. Chem*. **2019**, *123*, 3761–3781.
56   Koch, W.; Holthausen, M. C. *A Chemist's Guide to Density Functional Theory*; Wiley–VCH: Weinheim, **2001**.
57   Honenberg, P; Koch, W. *Phys. Rev*. **1964**, *136*, B864–B871.

UNIVERSITAT ROVIRA I VIRGILI
COMPUTATIONAL MECHANISTIC STUDIES IN GOLD(I) CATALYSIS AND DESIGN OF NEW CHIRAL LIGANDS
Immaculada Escofet Miquel

General Introduction

wavefunction. The electron density is defined as the probability of finding one electron in an infinitesimal volume. Contrary to Hartree-Fock theory, DFT methods include electron correlation. The exchange-correlation energy as function of the electron density function must be approximated into two parts, the exchange and the correlation. The accuracy of DFT computational results depends on the quality of the exchange-correlation functional. DFT is the theoretical method used to obtain the major part of the results in this Thesis (**Chapters I**, **II** and **III**).

Several type of functionals have been developed that can be divided in two families:

- Pure Functionals: The first generation of functionals is the Local Density approximation (LDA), which assumes that the functional only depends on the density at the specific coordinate. The exchange part is obtained from highly accurate Thomas-Fermi-Dirac method,[58] whereas the correlation part derives from highly accurate simulations of the uniform electron gas, such as VWN.[59] However, they are not appropriated for transition-metal catalyzed reaction mechanists studies in which electronic density changes rapidly. The next generation of functionals that allows to more properly describe the electronic density are based on the Generalized Gradient Approximation (GGA). GGA takes into account the gradient of density at the same coordinate, both in exchange and in the correlation functionals. Some examples on GGA methods that we have used in this Thesis are:

  o **PBE**[60] was developed by Perdew based on quantum mechanical principles. It calculates the correlation with analytical equations.
  o **TPSS**,[61] whose name comes from the authors initials (Tao, Perdew, Staroverov and Scuseria). This exchange functional was developed to calculate the exchange-correlation energy without taking into account empirical parameters.
  o **B97D**,[62] developed by Grimme in 2006, based on Becke's methods.
  o **PB86**[63] is composed of the Becke 1988 exchange functional and the Perdew 88 correlation functional. This functional has been used for the efficient mechanistic calculation of

58   (a) Fermi, E. Rend. *Accad. Lincei.* **1927**, *6*, 602–607. (b) Dirac, P. A. M. *Proc. Camb. Phil. Soc.* **1930**, *26*, 376–385.
59   Vosko, S. H.; Wilk, L.; Nusair, M. *Can. J. Phys.* **1980**, *58*, 1200–1211.
60   Perdew, J. P.; Burke, K.; Ernzerhof, M. *Phys. Rev. Lett.* **1996**, *77*, 3865–3868.
61   Tao, J.; Perdew, J. P. *Phys. Rev. Lett.* **2003**, *91*, 146401.
62   Grimme, S. *J. Comput. Chem.* **2006**, *27,* 1787–1799.
63   (a) Becke, A. D. *Phys. Rev. A.* **1988**, *38*, 3098–3100. (b) Perdew, J. P. *Phys. Rev. B.* **1986**, *33,* 8822–8824.

UNIVERSITAT ROVIRA I VIRGILI
COMPUTATIONAL MECHANISTIC STUDIES IN GOLD(I) CATALYSIS AND DESIGN OF NEW CHIRAL LIGANDS
Immaculada Escofet Miquel

General Introduction

enantioselective gold(I)-catalyzed reactions. (see **Chapter I and III**).

The accuracy of GGA functionals can be improved by using meta-GGA approaches (not only the first derivate of the density is taken into account but also the second derivate, Laplacian).

- Hybrid Functionals: The combination of GGA methods with certain percentage of Hartree-Fock (which include a component of the exact exchange with the rest of exchange-correlation energies from other sources) lead to the development of hybrid functionals. They can provide improved results respect to pure functionals. Some hybrid functionals that we have used in this Thesis are:

  - **B3LYP**,[64] the most popular functional, it was obtained from a combination of exchange functional B88 and LYP correlational functionals developed by Paar and co-workers. This functional has been widely used for the study of reactions catalyzed by gold(I) (see **Chapter I**).[13, 23, 25]

  - **B3PW91**[59] specifies BPW91 functional with the non-local correlation provided by Perdew 86/Wang 91.

  - **PBE0**[65] hybrid functional of the pure PBE developed by Adamo. It uses 25% exact exchange and 75% DTF exchange. It is also known as PBE1PBE or PBE hybrid.

  - **BMK**,[66] developed by Boese and Martin in 2004, is a τ-dependent hybrid functional.

  - **Minnesota functionals**,[67] developed by the group of Truhlar. M06 functionals are based on the combination of meta-hybrid-GGA that use the first and second derivate of the density together with some contribution of HF exchange. Among the whole family of Minnesota functionals, **M06** is the most popular. M06 has been widely used for the mechanistic studies of gold(I)-catalyzed transformations (see **Chapter II**).[13,23,25]

In the study of reaction mechanisms, calculation of free energies is fundamental to obtain the thermodynamics for the minimum structures and also, kinetics for transition states.

64   (a) Becke, A. D. *J. Chem. Phys*. **1993**, *98*, 5648–5652. (b) Lee, C.; Tang, W.; Parr, R. G. *Phys. Rev. B*. **1988**, *37*, 785–789.
65   Adamo, C. *J. Chem. Phys*. **1999**, *110*, 6158–6170.
66   Boese, A. D.; Martin, J. M. *J. Chem. Phys*. **2004**, *121*, 3405–3416.
67   Zao, Y.; Truhlar, D. G. *Theor. Chem. Account*. **2008**, *120*, 215–241.

UNIVERSITAT ROVIRA I VIRGILI
COMPUTATIONAL MECHANISTIC STUDIES IN GOLD(I) CATALYSIS AND DESIGN OF NEW CHIRAL LIGANDS
Immaculada Escofet Miquel

General Introduction

Hence, Density Functional Theory is the most economical and accurate option to compute reaction pathways since it considers the electrons of the system. Thus, this theory will be used along this Doctoral Thesis (**Chapter I**, **II** and **III**) together with *ab initio* DLPNO-CCSD(T) model as calibration for benchmark studies in **Chapter I**.

It is known that DFT methods do not describe accurately dispersion interactions, especially for medium-range and long-range interactions like van der Waals force. Thus, this limitation can become detrimental when dispersion interactions have an important effect in the chemical system under study. To face this problem, Grimme and co-workers developed an approach based on the inclusion of dispersion interactions into DFT.[57,68] This approach has been used in this Thesis and is named **DFT-D3**.

Moreover, the reaction medium (solvent) can strongly affect chemical reactivity, so that the inclusion of solvent is generally crucial in the optimization process. Computationally, the stabilization of intermediates and transition states can change dramatically the mechanistic pathways. Luckily, tools have been developed to include solvation effects into DFT calculation in two distinct methodologies:

- **Explicit Models:** they do include explicitly a certain number of molecules of the solvent to mimic the real concentration of solute into the solvent. Although this method allows to describe the solute-solvent interactions, it is unaffordable for our study. The addition of an explicit number of molecules to have similar conditions than real concentration of solute into solvent is not efficient since the number of atoms in the system would increases dramatically and thus, the computational cost.

- **Implicit Models:** they do consider a solvent as a continuous medium at the solute to be inside a cavity with a fixed dielectric constant. Despite being easily affordable, it might not be accurate enough to describe solute-solvent interactions (when solvent plays a role on the mechanism). There are several continuum solvation models that allow to compute energies in solution. This is done by an iterative process, in which the dielectric medium produces an electrostatic interaction with the solute and *vice versa*, until the mutual polarization reaches the self-consistency (Self-Consistent Reaction Field, SCRF).[69] In this Thesis, we will use:
    - **Polarizable Continuum Model (PCM):**[70] this method models the solvent as a polarizable continuum and is based on the Poisson-Boltzmann equation, which is solved by the Integral-Equation-Formalism (IEP). For that reason, PCM can be also named as IEP-PCM.

68   Grimme, S.; Antony, J.; Ehrlich, S.; Krieg, H. *J. Chem. Phys.* **2010**, *132*, 154104.
69   Tomasi, J.; Mennucci, B.; Cammi, R. *Chem. Rev.* **2005**, *105*, 2999–3094.
70   Cossi, M.; Barone, V.; Cammi, R.; Tomasi, J. *Chem. Phys. Lett.* **1996**, *255*, 327–335.

UNIVERSITAT ROVIRA I VIRGILI
COMPUTATIONAL MECHANISTIC STUDIES IN GOLD(I) CATALYSIS AND DESIGN OF NEW CHIRAL LIGANDS
Immaculada Escofet Miquel

General Introduction

- **Solvation Model based on Density (SMD):**[71] this model is based on Born equation, which is an approximation of Poisson's equation for cavity shapes. Despite both models being very similar, SMD uses a set of specifically parametrized radii to create a cavity.

71   Marenich, A. V.; Cramer, C. J.; Truhlar, D. G. *J. Phys.Chem. B.* **2009**, *113*, 6378–6396.

Chapter I: Computational Study of Gold(I)-Catalyzed Cycloisomerization Reactions

UNIVERSITAT ROVIRA I VIRGILI
COMPUTATIONAL MECHANISTIC STUDIES IN GOLD(I) CATALYSIS AND DESIGN OF NEW CHIRAL LIGANDS
Immaculada Escofet Miquel

UNIVERSITAT ROVIRA I VIRGILI
COMPUTATIONAL MECHANISTIC STUDIES IN GOLD(I) CATALYSIS AND DESIGN OF NEW CHIRAL LIGANDS
Immaculada Escofet Miquel

Chapter I

Introduction

Structure of Alkene and Alkyne Gold(I) Complexes

As highlighted in the **General Introduction**, gold(I) is a π-electrophilic Lewis acid[1] that can form stable π-complexes with alkynes,[2] alkenes,[3] allenes[4] and 1,3-dienes,[5] whose structures have been characterized by NMR and X-ray crystallography (Scheme 1).[2,6]

Scheme 1. Analysis of the structure of alkene and alkyne gold(I) complexes.
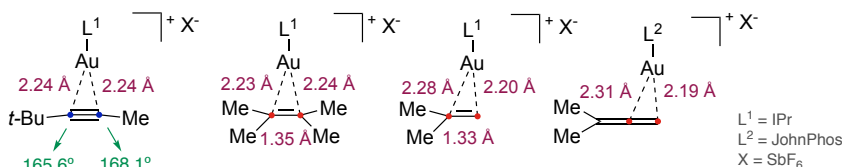
Symmetrical η^2-coordination of gold(I) to the alkyne[2] was observed even for unsymmetrical alkynes (equal distance, between gold and both alkyne carbons, 2.24 Å), in which the triple bond length was found to be identical to that of a free alkyne, even though a significant deviation from linearity of the alkyne moiety was detected (Scheme 1, green). Similarly, for symmetric alkenes,[3] the coordination was found to be symmetrical. However, different ligand-metal-substrate angles as well as bond lengths suggested that steric factors control the orientation of the unsaturation. Hence, terminal alkenes[3] bind unsymmetrically with gold(I) resulting in shorter bonds with the less substituted carbon atom. Likewise, gold(I) coordinates preferentially to the less substituted double bond in allenes.[4]

The nature of gold-unsaturation bond can be rationalized by the Dewar-Chatt-Ducanson model as a donor-acceptor interaction between the substrate and the metal.[7] Thus, it can be described as a combination of σ-donation of the substrate to the metal (Figure 1, right) and a back-bonding π-interaction (donation of the metal to the π^* orbitals of alkyne) (Figure 1, left). Computational studies have been used to better understand the contribution of these

1   Yamamoto, Y. *J. Org. Chem.* **2007**, *72*, 7817–7831.
2   (a) Flügge, S.; Anoop, A.; Goddard, R.; Thiel, W.; Fürstner, A. *Chem. Eur. J.* **2009**, *15*, 8558–856. (b) Zuccaccia, D.; Belpassi, L.; Rocchigiani, L.; Tarantelli, F.; Macchioni, A. *Inorg. Chem.* **2010**, *49*, 3080–3082. (c) Hooper, T. N.; Green, M.; Russell, C. A. *Chem. Commun.* **2010**, *46,* 2313–2315. (d) Brown, T. J.; Widenhoefer, R. A. *J. Organomet. Chem.* **2011**, *696*, 1216–1220.
3   (a) Brown, T. J.; Dickens, M. G.; Widenhoefer, R. A. *J. Am. Chem. Soc.* **2009**, *131*, 6350–6351. (b) Broomer, R. E. M.; Widenhoefer, R. A. *Organometallics* **2012**, *31*, 768–771. (c) Brooner, R. E. M.; Brown, T. J.; Widenhoefer, R. A. *Chem. Eur. J.* **2013**, *19*, 8276–8284.
4   (a) Brown, T. J.; Sugie, A.; Dickens, M. G.; Widenhoefer, R. A. *Organometallics* **2010**, *29*, 4207–4209. (b) Brown, T. J.; Sugie, A.; Leed, M. G. D.; Widenhoefer, R. A. *Chem. Eur. J.* **2012**, *18*, 6959–6971. (c) Johnson, A.; Laguna, A.; Gimeno, M. C. *J. Am. Chem. Soc.* **2014**, *136*, 12812–12815.
5   (a) Sanguramath, R. A.; Hooper, T. N.; Butts, C. P.; Green, M.; McGrady, J. E.; Russell, C. A. *Angew. Chem. Int. Ed.* **2011**, *50*, 7592–7595. (b) Brooner, R. E. M.; Widenhoefer, R. A. *Organometallics* **2011**, *30*, 3182-3193. (c) Krossing, I. *Angew. Chem. Int. Ed.* **2011**, *50*, 11576–11578.
6   (a) Shapiro, N. D.; Toste, F. D. *Proc. Natl. Acad. Sci. U.S.A.* **2007**, *104*, 43569–13573. (b) Brooner, R. E. M.; Widenhoefer, R. A. *Angew. Chem. Int. Ed.* **2013**, *52*, 11714–11724.
7   (a) Dewar, M. J. S. *Bull. Soc. Chim. Fr.* **1951**, *18*, C71–C79. (b) Chatt, J.; Duncanson, L. A. *J. Chem. Soc.* **1953**, 2939–2947.

UNIVERSITAT ROVIRA I VIRGILI
COMPUTATIONAL MECHANISTIC STUDIES IN GOLD(I) CATALYSIS AND DESIGN OF NEW CHIRAL LIGANDS
Immaculada Escofet Miquel

Chapter I

interactions.[6a,8] In the case of gold(I), $5d$ orbitals are too low in energy for a significant back bonding to π^* orbitals but not to empty non-bonding orbitals, leading to unsubstantial back-donation. For this reason, alkynes can be described as strong two-electron σ-donors but rather weak π-acceptors towards gold(I). Moreover, this modest back-donation can differ depending on the ligand, substrate rigidity towards deformation, as well as the distance between the metal and the substrate.
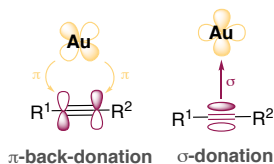
Figure 1. Dewar-Chatt-Duncanson model for gold.

Nature of Cyclopropyl Gold(I) Carbenes

Although gold(I) carbenes have been proposed as crucial intermediates of many gold(I)-catalyzed transformations, there is some controversy regarding the nature and the electronic structure of these species (carbenic or cationic character of C–Au bond).[9,10,11] This debate is further exacerbated due to the high reactivity of carbenes, which makes their isolation very challenging. However, both gold(I) carbenes and gold(I)-stabilized carbocations are exactly the same species represented in a different way by their resonance forms (Scheme 2).
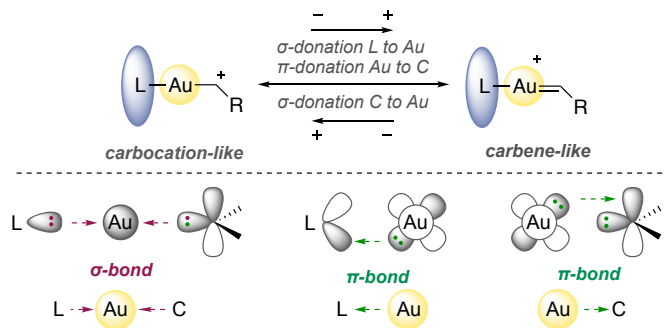
Scheme 2. Bonding model and nature of gold(I) carbenes.

The bonding model of gold (I) carbenes proposes a 3 center–4 electron σ-hyperbond in which both the ligand and the carbene moiety can donate their paired electrons to gold

8   (a) Hertwig, R. A.; Koch, W.; Schröder, D.; Schwarz, H.; Hrusak, J.; Schwerdtfeger, P. *J. Phys. Chem.* **1996**, *100*, 12253–12260. (b) Nechaev, M. S.; Rayón, V. M.; Frenking, G. *J. Phys. Chem. A.* **2004**, *108*, 3134–3142.

9   Harris, R. J.; Widenhoefer, R. A. *Chem. Soc. Rev.* **2016**, *45*, 4533–4551 and references cited therein.

10   (a) Fürstner, A.; Morency, L. *Angew. Chem. Int. Ed.* **2008**, *47*, 5030–5033. (b) Hashmi, A. S. K. *Angew. Chem. Int. Ed.* **2008**, *47*, 6754–6756. (c) Seidel, G.; Mynnot, R.; Fürstner, A. *Angew. Chem. Int. Ed.* **2009**, *48*, 2510–2513. (d) Benitez, D.; Shapiro, N. D.; Tkatchouk, E.; Wang, Y.; Goddard, W. A.; Toste, F. D. *Nat. Chem.* **2009**, *1*, 482–486. (e) Echavarren, A. M. *Nat. Chem.* **2009**, 431–433.

UNIVERSITAT ROVIRA I VIRGILI
COMPUTATIONAL MECHANISTIC STUDIES IN GOLD(I) CATALYSIS AND DESIGN OF NEW CHIRAL LIGANDS
Immaculada Escofet Miquel

Chapter I

(Scheme 2, purple), along with orthogonal weak π-backbonding in which gold back-donates electron density from two filled 5*d* orbitals to the ligand and carbene (Scheme 2, green). Therefore, both ligands and substituents will have a notable influence on the reactivity and bonding of these resulting gold carbenes. For example, good σ-donating ancillary ligands such as NHC will increase the carbene-like character of the intermediate by π–backdonation from gold to carbon.[11]

Gold(I) carbenes could be considered Fischer carbenes due to their high electrophilic character resulting from the weak metal-to-carbon π-backdonation. Although gold(I) intermediates are too highly reactive to be readily isolated, some progress has been done in the observation of these key species.[12] However, many of these species have only been isolated with stabilizing functional groups attached to the carbenic carbon. Thus, there was a lack of well-defined gold(I) carbene intermediates. Very recently, our group has generated and spectroscopically characterized mesityl gold(I) carbenes **2** for the first time in solution.[13] Chloride abstraction of chloro(mesityl)methylgold(I) carbenoids **1** with GaCl₃ gave rise to reactive gold(I) carbenes **2** that were fully characterized by NMR at -90ºC.
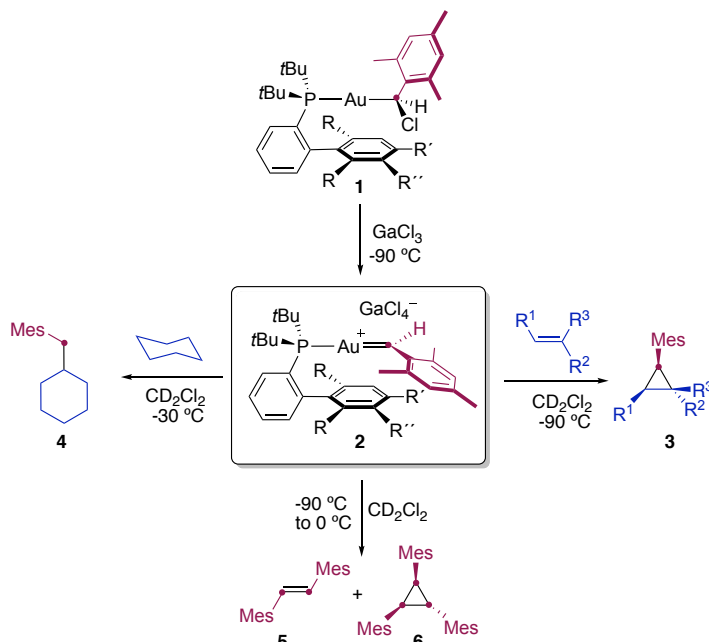
Scheme 3. Formation and reactivity of mesityl gold(I) carbenes **2**.

11   Wang, Y.; Muratore, M. E.; Echavarren, A. M. *Chem. Eur. J.* **2015**, *21*, 7332–7339.
12   (a) Seidel, G.; Fürstner, A. *Angew. Chem. Int. Ed.* **2014**, *53*, 4807–4811. (b) Hussong, M. W.; Rominger, F.; Krämer, P.; Straub, B. F. *Angew. Chem. Int. Ed.* **2014**, *53*, 9372–9375. (c) Harris, R. J.; Widenhoefer, R. A. *Angew. Chem. Int. Ed.* **2014**, *53*, 9369–9371. (d) Joost, M.; Estévez, L.; Mallet-Ladeira, S.; Miqueu, K.; Amgoune, A.; Bourissou, D. *Angew. Chem. Int. Ed.* **2014**, *53*, 14512–14516. (e) Wang, J.; Cao, X.; Lv, S.; Zhang, C.; Xu, S.; Shi, M.; Zhang, J. *Nature Comm.* **2017**, *8*, 14625–14635. (f) Zeineddine, A.; Rekhroukh, F.; Carrizo, E. D. S.; Mallet-Ladeira, S.; Miqueu, K.; Amgoune, A.; Bourissou, D. *Chem. Int. Ed.* **2018**, *57*, 1306–1310.
13   García-Morales, C.; Pei, X.-L.; Sarria Toro, J. M.; Echavarren, A. M. *Angew. Chem. Int. Ed.* **2019**, *58*, 3957–3961.

UNIVERSITAT ROVIRA I VIRGILI
COMPUTATIONAL MECHANISTIC STUDIES IN GOLD(I) CATALYSIS AND DESIGN OF NEW CHIRAL LIGANDS
Immaculada Escofet Miquel

Chapter I

Interestingly, these species undergo further transformations at low temperature such as cyclopropanation of alkenes affording **3**, as well as preparation intermolecular C-H insertion leading to product **4**, and formation of alkenes **5** and cyclopropanes **6** (Scheme 3).

The Janus-like character of cyclopropyl gold(I) carbenes has been intensively discussed, stressing their carbocation nature.[14] Three possible potential structures, have been observed: **I, II**, and **III**. Intermediates **I** were found to be highly distorted species so that, by stretching the C2-C4 bond, gold(I)-stabilized homoallylic carbocations **III** can be generated. Similarly, semi-opened cyclopropanes of type **II** can also be considered (Table 1).[15] DFT calculations have proved that the substitution pattern of the enyne and the ligand used dictate the carbenic or cationic nature of the gold(I) intermediate[14]. Therefore, intermediate **II**, which has the longest distance between C2-C3 (1.742 Å), was found to be the most relevant structure when R = H and Me, whereas for R = cyclopropyl or *p*-MeOC6H4 the structure of the intermediate resembles that of open carbocation intermediate **III**.
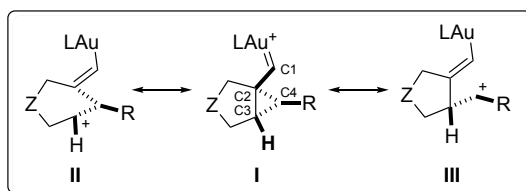
R	d(C$_1$-C$_2$)	d(C$_2$-C$_3$)	d(C$_2$-C$_4$)
H	1.378	1.742	1.569
Me	1.372	1.720	1.622
Cyclopropyl	1.356	1.586	1.987
p-MeOC$_6$H$_4$	1.344	1.578	2.328

Table 1. Canonical structures of cyclopropyl gold(I) carbenes, **I – II – III,** and their calculated bond distances by DFT at the B3LYP/6-31G(d) (C, H, P) and LANL2DZ (Au) level in CH$_2$Cl$_2$ (PCM). L = PH$_3$. Distances expressed in Å.

Likewise, for those cases in which **III** is the most relevant description of the structure, the stereospecificity of the reaction could be affected by the rotation around the C3–C4 bond. This was indeed the case for 1,6-enynes **7** and **8**, which have strongly electron-donating cyclopropyl substituent (R) in the alkene moiety, and react non-stereospecifically. Hence, both (*E*)-**7** and (*Z*)-**8** isomers unexpectedly give rise to the same *cis*-product **9** upon the treatment with gold(I) catalyst (Scheme 4). Although the key cyclopropyl gold(I) carbene species have never been isolated or characterized spectroscopically, their presence in these

14   (a) Nieto-Oberhuber, C.; López, S.; Muñoz, M. P.; Cárdenas, D. J.; Buñuel, E.; Nevado, C.; Echavarren, A. M. *Angew. Chem. Int. Ed.* **2005**, *44*, 6146–6148. (b) Fürstner, A.; Davies, P. W.; *Angew. Chem. Int. Ed.* **2007**, *46*, 3410–3449. (c) Cabello, N.; Jiménez-Núñez, E.; Buñuel, E.; Cárdenas, D. J.; Echavarren, A. M. *Eur. J. Org. Chem.* **2007**, 4217–4223. (d) Pérez-Galán, P.; Martin, N. J. A.; Campaña, A. G.; Cárdenas, D. J.; Echavarren, A. M. *Chem. Asian. J.* **2011**, *6*, 482–486.
15   Jiménez-Núñez, E.; Claverie, C. K.; Bour, C.; Cárdenas, D. J.; Echavarren, A. M. *Angew. Chem. Int. Ed.* **2008**, *47*, 7892–7895.

UNIVERSITAT ROVIRA I VIRGILI
COMPUTATIONAL MECHANISTIC STUDIES IN GOLD(I) CATALYSIS AND DESIGN OF NEW CHIRAL LIGANDS
Immaculada Escofet Miquel

Chapter I

transformations could be confirmed by trapping them inter- and intramolecularly with different types of nucleophiles.[16]
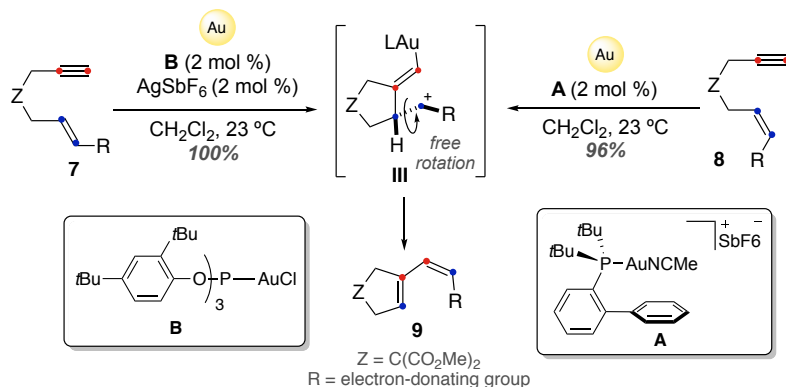
Scheme 4. Gold(I) catalyzed *cis*-selective single-cleavage rearrangements of enynes **7** and **8**.

Trapping of Intermediates and Cyclopropanation of Enynes

An example of how ligands can contribute on the cationic or carbenic character of gold(I) carbenes is the nucleophilic addition of indoles **11** to 1,6-enynes **10** (Scheme 5).[17] In this reaction, the ratio between products **12** and **13** depends on the ligand used.
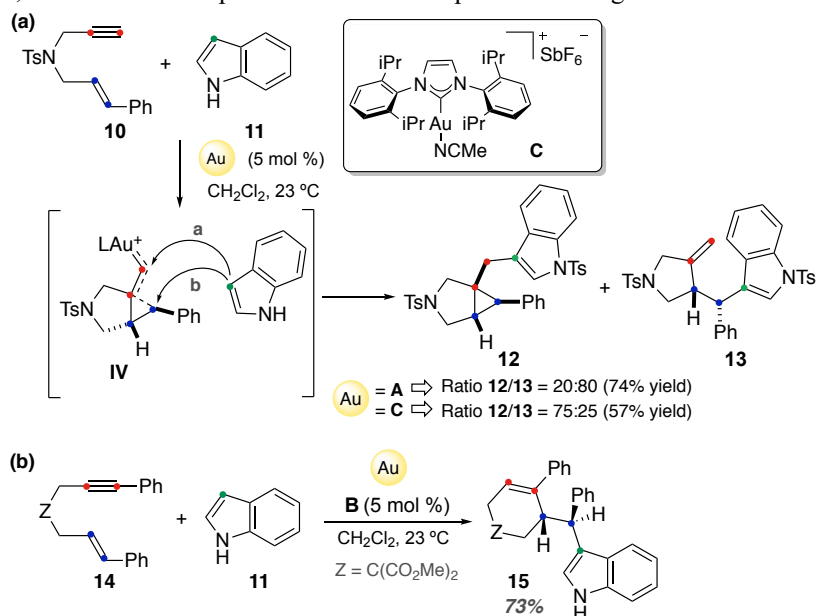
Scheme 5. Gold(I)-catalyzed intermolecular trapping of the carbenes by indole **11**.

16   (a) Pérez-Galán, P.; Herrero-Gómez, E.; Hog, D. T.; Martin, N. J. A.; Maseras, F.; Echavarren, A. M. *Chem. Sci.* **2011**, *2*, 141–149. (b) Calleja, P.; Pablo, O.; Ranieri, B.; Gaydou, M.; Pitaval, A.; Moreno, M.; Raducan, M.; Echavarren, A. M. *Chem. Eur. J.* **2016**, *22*, 13613–13618.

17   Amijs, C. H. M.; Lopez-Carrillo, V.; Raducan, M.; Pérez-Galán, P.; Ferrer, C.; Echavarren, A. M. *J. Org. Chem.* **2008**, *73*, 7721–7730.

UNIVERSITAT ROVIRA I VIRGILI
COMPUTATIONAL MECHANISTIC STUDIES IN GOLD(I) CATALYSIS AND DESIGN OF NEW CHIRAL LIGANDS
Immaculada Escofet Miquel

Chapter I

As mentioned before, the use of NHC ligands (catalyst **C**) enhances the carbene-like nature of intermediate **IV**, thus indole **11** would attack to the carbenic carbon (Scheme 5a, path **a**) to afford mainly product **12** (like **I**, Table 1). However, the trapping of **IV** by indole **11** would take place to the carbocationic center (Scheme 5a, path **b**) when using catalyst **A**, bearing JohnPhos-type ligand, which favors the formation of open carbocation type **III** delivering **13** as major product (Table 1). The 6-*endo-dig* pathway was predominant for the addition of indole **11** to enyne **14** giving rise to **15** stereospecifically in the presence of catalyst **B** (Scheme 5b) *via* intermediate type **III** (Table 1).

On the other hand, the intermediacy of cyclopropyl gold(I) carbenes in cycloisomerizations of 1,*n*-enynes has been demonstrated by their trapping with alkenes.[16,18] Hence, tetracyclic compound **17** was obtained stereoselectively by the reaction of dienyne **16** with catalyst **D** (Scheme 6a). According to DFT calculations, this reaction proceeds through intermediate **V** (type of **I**, Table 1), which upon cyclopropanation of the second double bond gives rise to **17**. A similar model was proposed for the intermolecular cyclopropanation 1,6-enyne **18** by norbornene **19** to effort product **20** (Scheme 6b). In this case, the cyclopropanation reaction was concerted since the alkene was symmetrical, whereas styrenes (more polarized alkenes) reacted in a stepwise fashion.[18f] However, even in this case, since the two new C–C bonds were formed from the same face of the alkene, the overall process was stereospecific.
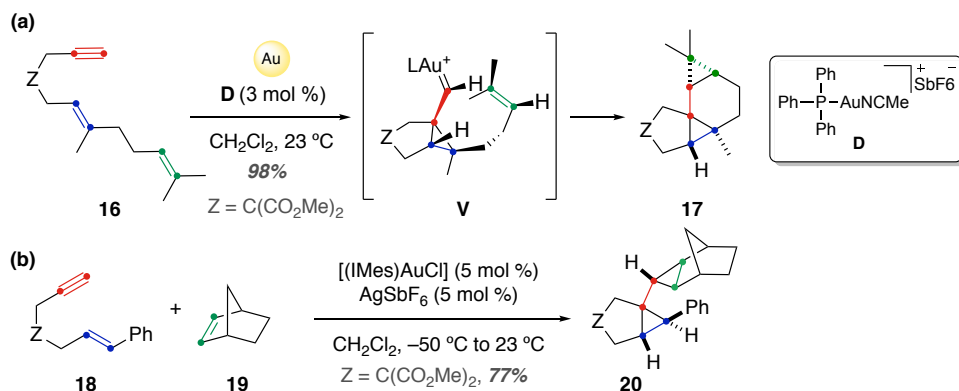
Scheme 6. Examples on the gold(I)-catalyzed intra- and intermolecular cyclopropanation of enynes **16** and **18**, respectively, catalyzed by gold(I).

In addition, dienynes that contain an OR group at the propargylic position such as **21**, led to tricyclic compound **22** *via* tandem cyclization/1,5-OR migration/intramolecular

18   (a) Nieto-Oberhuber, C.; Muñoz, M. P.; Buñuel, E.; Nevado, C.; Cárdenas, D. J.; Echavarren, A. M. *Angew. Chem. Int. Ed.* **2004**, *43*, 2402–2406. (b) Nieto-Oberhuber, C.; López, S.; Muñoz, M. P.; Jiménez-Núñez, E.; Buñuel, E.; Cárdenas, D. J.; Echavarren, A. M. *Chem. Eur. J.* **2006**, *12*, 1694–1702. (c) Kim, S. M.; Park, J. H.; Choi, S. Y.; Chung, Y. K. *Angew. Chem. Int. Ed.* **2007**, *46*, 6172–6175. (d) López, S.; Herrero-Gómez, E.; Pérez-Galán, P.; Nieto-Oberhuber, C.; Echavarren, A. M. *Angew. Chem. Int. Ed.* **2006**, *45*, 6029–6032. (e) Prieto, A.; Fructos, M. R.; Díaz-Requejo, M. M.; Pérez, P.; Pérez-Galán, P.; Delpont, N.; Echavarren, A. M. *Tetrahedron* **2009**, *65*, 1790–1793. (f) Batiste, L.; Fedorov, A.; Chen, P. *Chem. Commun.* **2010**, *46*, 3899–3901. (g) Leboeuf, D.; Gaydou, M.; Wang, Y.; Echavarren, A. M. *Org. Chem. Front.* **2014**, *1*, 759–764.

UNIVERSITAT ROVIRA I VIRGILI
COMPUTATIONAL MECHANISTIC STUDIES IN GOLD(I) CATALYSIS AND DESIGN OF NEW CHIRAL LIGANDS
Immaculada Escofet Miquel

Chapter I

cyclopropanation process catalyzed by gold(I) (Scheme 7).[16b,18g,19a] Thus, the reaction proceeded through intermediate **VI** (cyclopropyl gold carbene type of **I**, Table 1), which evolved by intramolecular attack of the ether moiety attached to the propargylic position at the electrophilic site of the cyclopropane. Then, α,β-unsaturated gold carbene intermediate **VIII** would be formed upon the cleavage of the oxonium bridge **VII** and it would undergo an intramolecular cyclopropanation with the alkene at the side chain to form **22**. According to deuterium labelling experiments, in the presence of an external nucleophile such as CD3OD, intermediate **VI** was trapped intermolecularly prior to the aforementioned cyclopropanation with the pending alkene, giving rise to the epimer **23** in a moderate yield. Interestingly, tetracyclic compounds type **22** bearing the scaffold present in the sesquiterpenes globulol and epiglobulol.[19] Hence, this method has been applied for the shortest total syntheses of (–)-epiglobulol, 4α-7α-aromadendranediol and (–)-4β,7α-aromadendranediol by a stereodivergent gold(I)-catalyzed reaction which establishes four stereogenic centers from a single one in (*E,E*)-farnesol.[19b] Although gold(I)-catalyzed polycyclizations of enynes often involve intramolecular cyclopropanation reactions to afford complex ring systems with *cis*-fused cyclopropanes type **22**, the corresponding *trans*-fused cyclopropanes were only occasionally obtained as minor products.[19,21]
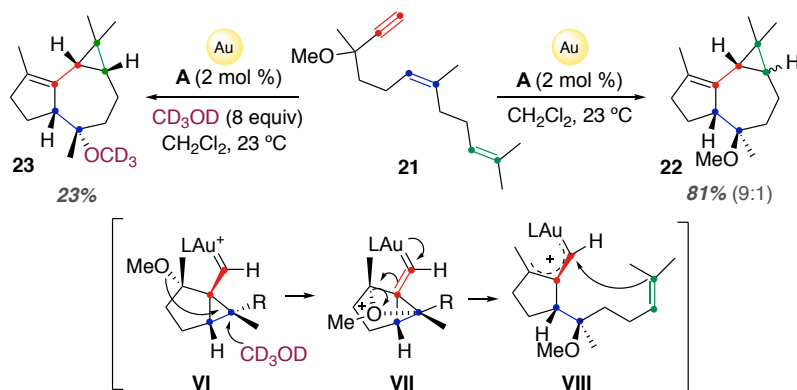
Scheme 7. Gold(I)-catalyzed tandem cyclization, 1,5-propargylic ether migration followed by intramolecular cyclopropanation of dienyne **21**.

Our group also discovered a noteworthy cyclization of 1,*n*-enynes bearing a carbonyl group at the alkenyl side chain to give oxatricyclic compounds by formal [2+2+2] alkyne/alkene/carbonyl cycloaddition cascade.[20] This cascade cycloaddition was applied to build the core of several oxygen-bridged sesquiterpenoids such as (+)-orientalol F[21] (**29**)

19   (a) Jiménez-Núñez, E.; Raducan, M.; Lauterbach, T.; Molawi, K.; Solorio, C. R.; Echavarren, A. M. *Angew. Chem. Int. Ed.* **2009**, *48*, 6152–6155. (b) Carreras, J.; Livendahl, M.; McGonigal, P. R.; Echavarren, A. M. *Angew. Chem. Int. Ed.* **2014**, *53*, 4896–4899.

20   (a) Jiménez-Núñez, E.; Claverie, C. K.; Nieto-Oberhuber, C.; Echavarren, A. M. *Angew. Chem. Int. Ed.* **2006**, *45*, 5452–5455. (b) Calleja, P.; Muratore, M. E.; Jiménez, T.; Echavarren, A. M. *Synthesis* **2016**, *48*, 3183–3198. (c) Related results with oximes: Muratore, M. E.; Konovalov, A. I.; Armengol-Relats, H.; Echavarren, A. M. *Chem. Eur. J.* **2018**, *24*, 15613–15621.

21   Jiménez-Núñez, E.; Molawi, K.; Echavarren, A. M. *Chem. Commun.* **2009**, 7327–7329.

UNIVERSITAT ROVIRA I VIRGILI
COMPUTATIONAL MECHANISTIC STUDIES IN GOLD(I) CATALYSIS AND DESIGN OF NEW CHIRAL LIGANDS
Immaculada Escofet Miquel

Chapter I

and (–)-englerin A (**30**)[22a] (Scheme 8). Interestingly, another total synthesis of **30** was also disclosed by using this gold(I)-catalyzed cascade as the key step.[22b] Later, due to remarkable and unique antitumor activity of the (–)-englerin A towards certain types of renal cancer, several analogues have been prepared in our group leading to the discovery of new potent compounds with broader biological profile.[22c,22d]

Oxo-1,6-enynes **24** react in the presence of AuCl by a formal [2+2+2] cycloaddition that allows the formation of two C–C and one C–O bonds to obtain predominantly oxatricyclic compounds **25**, together with minor amounts of diene **26** (Scheme 8).
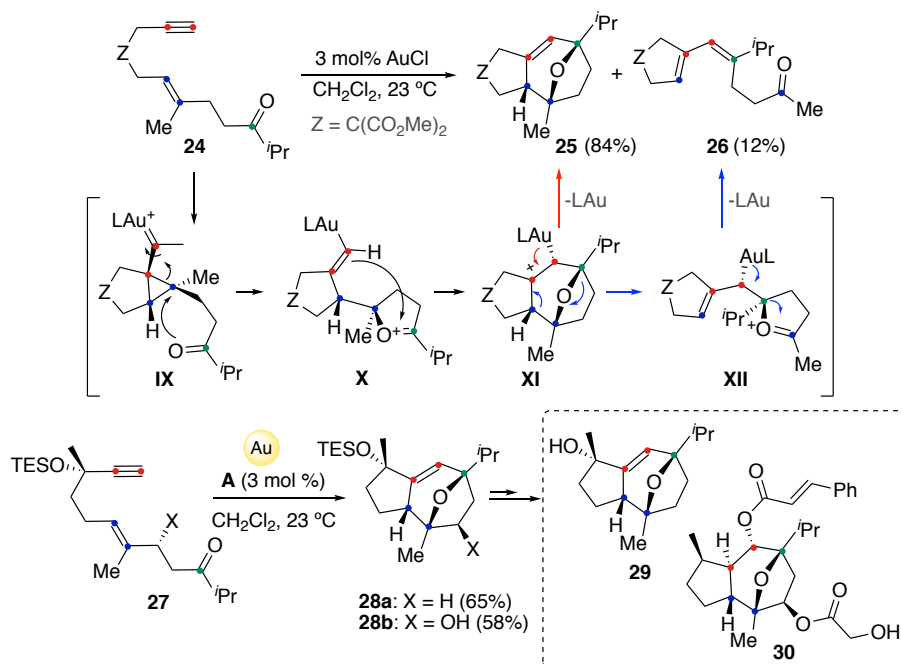
Scheme 8. Intramolecular [2+2+2] alkyne/alkene/carbonyl cycloaddition of oxo-1,6-enynes.

These reactions take place *via* intramolecular nucleophilic attack of the ketone to cycloproplyl gold(I) carbene **IX** (type of **I**, Table 1) delivering oxonium cations **X** stereospecifically. Then, intermediate **X** undergoes a Prins-type cyclization forming tertiary carbocation **XI**. Demetallation from **XI** would deliver product **25** (Scheme 8, red), whereas diene **26** would be obtained by an alternative elimination with fragmentation of the seven-membered ring scaffold through intermediate **XII** and final demetallation (Scheme 8, blue).

22   (a) Molawi, K.; Delpont, N.; Echavarren, A. M. *Angew. Chem. Int. Ed.* **2010**, *49*, 3517–3519. (b) Zhou, Q.; Chen, X.; Ma, D. *Angew. Chem. Int. Ed.* **2010**, *49*, 3513–3515. (c) López-Suárez, L.; Riesgo, L.; Bravo, F.; Ransom, T. T.; Beutler, J. A.; Echavarren, A. M. *Chem. Med. Chem.* **2016**, *11*, 1003–1007. (d) Patents: Beutler, J. A.; Echavarren, A. M.; López, L.; Bravo, F.; Riesgo, L.; Ranson, T. T. (NCI-ICIQ). Ref. WO/2016/168281; Echavarren, A. M.; Molawi, K.; Delpont, N. (ICIQ). Ref.WO/2011/120886.

UNIVERSITAT ROVIRA I VIRGILI
COMPUTATIONAL MECHANISTIC STUDIES IN GOLD(I) CATALYSIS AND DESIGN OF NEW CHIRAL LIGANDS
Immaculada Escofet Miquel

Chapter I

Moreover, trapping of the cyclopropyl gold(I) carbene by carbonyl groups was also carried out when using an external ketone or aldehyde in the presence of a 1,6-enyne.[23]

Trans-Fused Cyclopropanes by Gold(I)-Catalyzed Cyclization of Dienynes

In our studies towards the total synthesis of jatrophalactone (**35**),[24] a naturally occurring diterpenoid isolated in 2012 from the roots of *Jatropha curcas*, we serendipitously found a system in which the selective construction of pentacyclic skeleton by gold(I)-catalyzed cyclization of dienynes leads unexpectedly to *trans*-fused cyclopropanes **34** (Scheme 9).
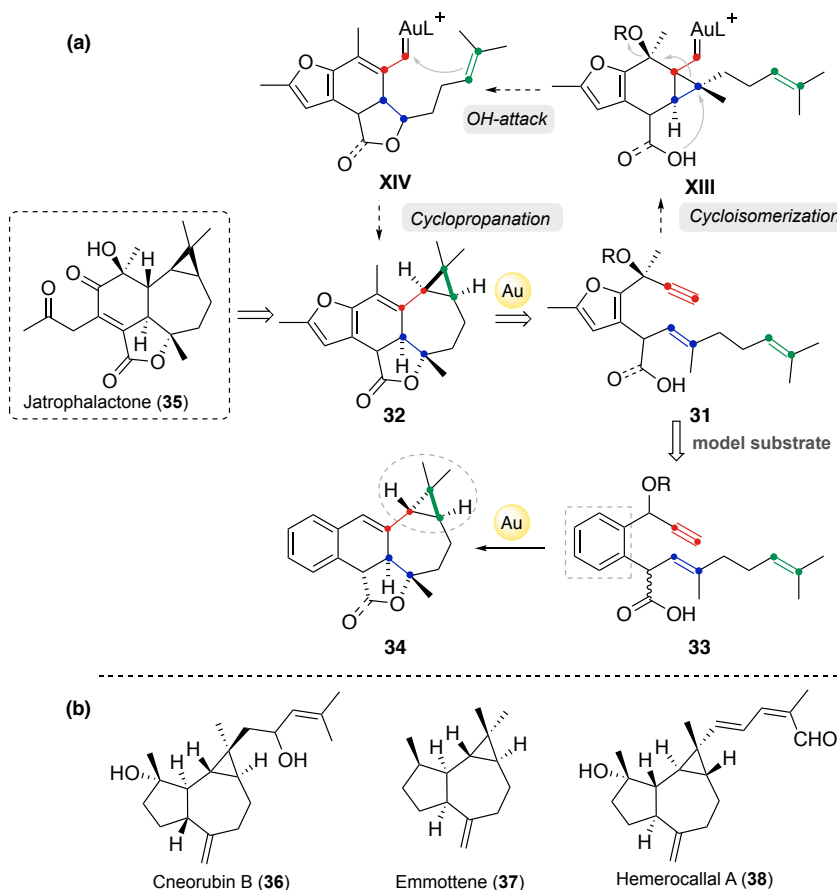
Scheme 9. (a) Proposed retrosynthesis of jatrophalactone **35** and model substrate **31** for the gold(I)-catalyzed cycloisomerization key step. (b) Natural products bearing a *trans*-fused cyclopropane.

23   (a) Escribano-Cuesta, A.; López-Carrillo, V.; Janssen, D.; Echavarren, A. M. *Chem. Eur. J.* **2009**, *15*, 5646–5650. (b) Huguet, N.; Echavarren, A. M. *Synlett* **2012**, *23*, 49–53. (c) Huple, D. B.; Liu, R. S. *Chem. Commun.* **2012**, *48*, 10975–10977.
24   (a) Liu, J.-Q.; Yang, Y.-F.; Wang, C.-F.; Li, Y.; Qiu, M.-H. *Tetrahedron.* **2012**, *68*, 972–976. (b) The experimental part of this project has been performed by: Dr. Hanna Bruss and Helena Armengol i Relats.

UNIVERSITAT ROVIRA I VIRGILI
COMPUTATIONAL MECHANISTIC STUDIES IN GOLD(I) CATALYSIS AND DESIGN OF NEW CHIRAL LIGANDS
Immaculada Escofet Miquel

Chapter I

Jatrophalactone showed cytotoxic activity against five cancer cell lines: HL-60 (human promyelocytic leukemia), SMMC-7721 (human hepatocarcinoma), A-549 (adenocarcinomic human alveolar basal epithelial cells), MCF-7 (breast cancer) and SW480 (colon carcinoma) cell lines.[24a] To date, no total synthesis of this natural product has been reported. Thus, we envisioned that after the coordination of gold to the alkyne, dienyne **31** would undergo a 6-*endo-dig* cycloisomerization delivering cyclopropyl gold carbene **XIII**, which, after intramolecular nucleophilic attack of the OH moiety to the carbene, would lead to the formation of intermediate **XIV**. Product **32** would later be obtained upon cyclopropanation of the terminal alkene. Functionalization and oxidative ring opening of furan **32** would give rise to natural product, jatrophalactone **35 (**Scheme 9a).

In order to explore the feasibility of this transformation, simpler model substrate **33** has been designed having a phenyl ring instead of a less stable furan moiety. To our surprise, however, product **34** obtained in this reaction bears a *trans*-fused cyclopropane, which a rather unexpected stereochemical feature. Although, the rare *trans*-bicyclo[5.1.0]-octane motif is present in some natural products[25] such as emmottene, cneorubin B and hemerocallal A (Scheme 9b), the formation of this ring system is challenging because it is naturally traced back to (*E*)-cycloheptenes, which are unstable at room temperature.[26] Thus, we decided to study in detail the formation of these *trans*-cyclopropane compounds that had only been obtained before as minor byproducts in similar cyclization cascade reactions catalyzed by gold(I).[21]

Dienynes[27] **33a, 39**, and **40** reacted with catalyst **A** almost instantaneously. Surprisingly, (*E*)-configured enynes **39a** and **40a** containing a free hydroxy group afforded *trans*-fused cyclopropanes **41** as single diastereomers in 45-50% yield, along with naphthalene derivate **42** (14% yield). The relative configuration of **41** was confirmed by X-ray diffraction analysis (Scheme 10).

Likewise, carboxylic acid **33a** also yielded a *trans*-fused cyclopropane **34a** as a single diastereomer. Again, naphthalene byproduct **42** was isolated as a minor product by a formal loss of a CO_2 molecule. The analogous mixtures of (*Z*)-configured **39b** and **40b** reacted to give an inseparable mixture of isomers **43** and **44** in moderate yield, together with (*Z*)-**42** (Scheme 10). Remarkably, when the two isomers of **39b** were separated by semi-preparative chromatography and exposed to gold(I)-catalysis, the same mixture of **43** and **44** was obtained, although the reaction was much cleaner for one of them.[27] The relative

25   (a) Cronan Jr., J. M.; Daviau, T. R.; Pannell, L. K.; Cardellina II, J. H. *J. Org. Chem.* **1995**, *60*, 6864–6865. (b) Brochini, C. B.; Roque, N. F. *J. Braz. Chem. Soc.* **2000**, *11*, 361–364. (c) Yang, Z.; Chen, H.; Li, Y. *Helv. Chim. Acta.* **2003**, *86*, 3305–3309.

26   (a) Gassman, P.; Williams, F. J.; Seter, J. *J. Am. Chem. Soc.* **1968**, *90*, 6893–6895. (b) Kirmse W.; Hase, C. *Angew. Chem. Int. Ed.* **1968**, *7*, 891–892. (c) Cain, D.; Pawar, D.M.; Noe, E. A. *J. Mol. Struc. Theochem.* **2004**, *674*, 251–255. (d) Squillacote, M. E.; DeFellipis, J.; Shu, Q. *J. Am. Chem. Soc.* **2005**, *127*, 15983–15988.

27   Escofet, I.; Armengol-Relats, H.; Bruss, H.; Besora, M.; Echavarren, A. M. Manuscript in preparation.

UNIVERSITAT ROVIRA I VIRGILI
COMPUTATIONAL MECHANISTIC STUDIES IN GOLD(I) CATALYSIS AND DESIGN OF NEW CHIRAL LIGANDS
Immaculada Escofet Miquel

Chapter I

configuration of both pentacyclic products was assigned by NOE NMR experiments, which are clearly distinct from **41** (obtained from the *(E)*-configured precursor).
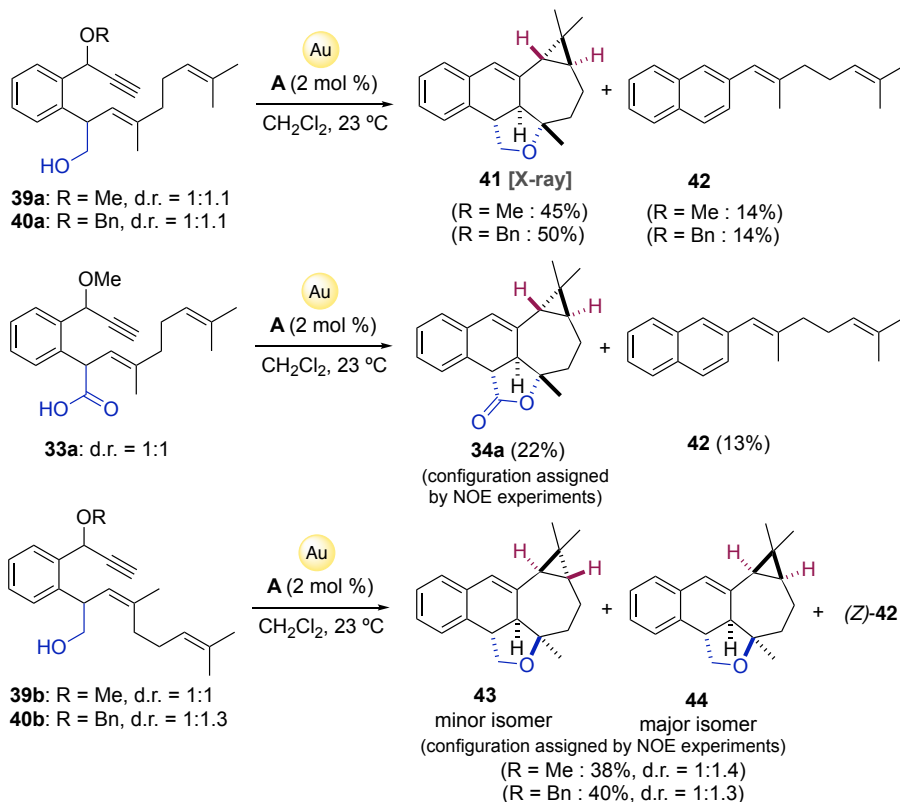
Scheme 10. Gold(I) catalyzed cyclization cascade reactions of **33a**, **39a-b** and **40a-b**.

Moreover, in order to better understand how the side chain can interfere in the stereoselectivity of these transformations, other dienynes were prepared[27] for control experiments (Scheme 11). Therefore, simpler substrates **45-46**, missing the benzylic hydroxymethyl group, were submitted to gold(I) catalysis giving products **47**, **47'** and **48** as single diastereomers in *ca* 50% yield. All of these products featured a *cis*-fused cyclopropane, which was confirmed by X-ray diffraction analysis. The reactions prove to be stereospecific with respect to the configuration of the alkene, as in many other gold(I)-catalyzed transformations. In the same way, products **50** and **52** were obtained as single diastereomers upon the reaction of the dienynes **49a** and **49b** with catalyst **A**. Deprotection of TBS group would give rise to crystalline primary alcohols **51** and **53**, whose relative configuration was confirmed by X-ray diffraction (Scheme 11).

Since all these simpler dienynes lacking an internal nucleophile afforded *cis*-cyclopropanes, we proposed that the formation of the fused tetrahydrofuran ring plays a crucial role in the final cyclopropanation step. To further demonstrate the need of the internal nucleophile, new dienyne derivatives **54** were prepared containing a longer chain moiety (Scheme 12).[27]

UNIVERSITAT ROVIRA I VIRGILI
COMPUTATIONAL MECHANISTIC STUDIES IN GOLD(I) CATALYSIS AND DESIGN OF NEW CHIRAL LIGANDS
Immaculada Escofet Miquel

Chapter I
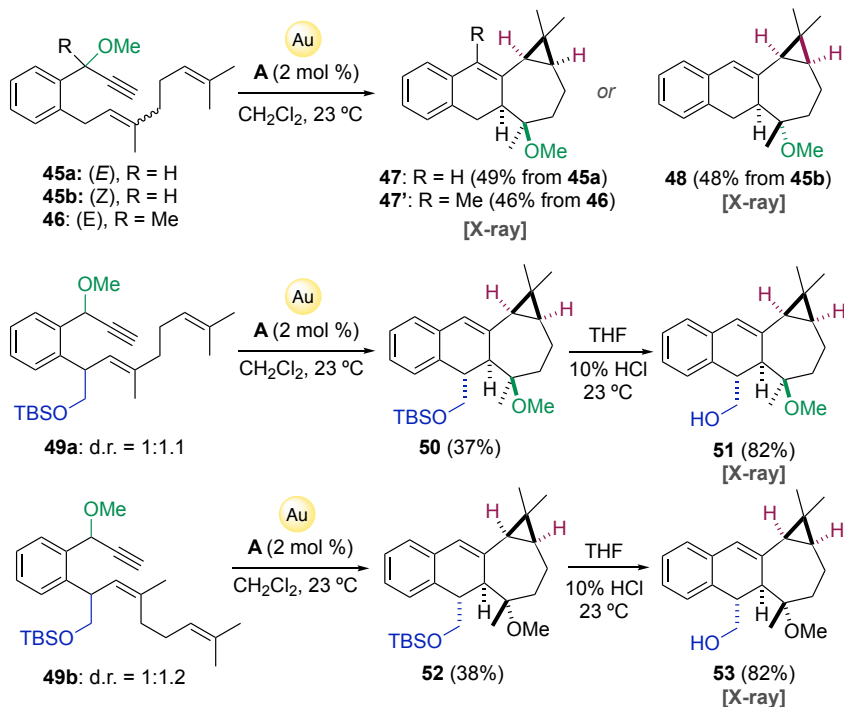
Scheme 11. Gold(I)-catalyzed cycloisomerizations of simpler dienynes **45**, **46**, and **49**.

First attempts to prepare tetracyclic compound **55** under the standard reaction conditions failed due to decomposition of starting material. Therefore, dienyne **54** underwent gold(I)-catalyzed cyclization cascade when lowering the temperature to -20 ºC leading to the formation of **55** in low yield (7%), together with naphthalene **56** as the main product (25%). However, when catalyst **C** with more donating IPr was used, the selectivity improved towards desired tetracyclic product **55**. The relative configuration of **55** was assigned by NOE experiments as a *cis*-fused cyclopropane. According to this last control experiment, we conclude that a longer and more flexible chain does not always translate into easier formation of *trans*-fused cyclopropanes.
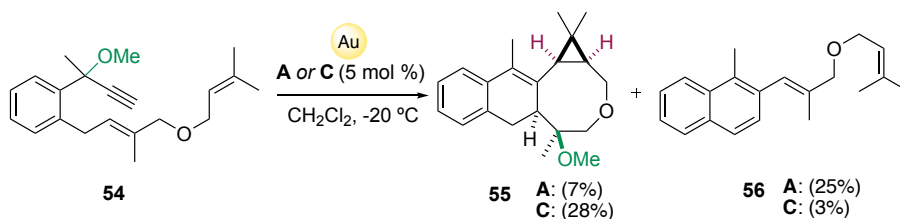
Scheme 12. Gold(I)-catalyzed cycloisomerizations of substrate **54**.

UNIVERSITAT ROVIRA I VIRGILI
COMPUTATIONAL MECHANISTIC STUDIES IN GOLD(I) CATALYSIS AND DESIGN OF NEW CHIRAL LIGANDS
Immaculada Escofet Miquel

Chapter I

Objectives

Cyclopropyl gold(I) carbenes intermediates **I** are highly distorted species that can also be represented as gold-stabilized homoallylic carbocations **III** and semi-opened systems like **II**.[14] DFT calculations have proved that both the substitution pattern of the enyne and the ligand used can dictate the carbenic or cationic nature of the gold(I) intermediate. Also, when the open carbocation **III** is the most relevant structure, the stereospecificity of the reaction could be affected by the C3–C4 bond rotation (Table 1). Although this crucial cyclopropyl gold carbene intermediate has never been isolated or fully characterized, its presence in gold(I) catalyzed transformations has been confirmed in several examples by its trapping inter- and intramolecularly with different types of nucleophiles.[16] However, we decided that further computational studies on cycloisomerizations reactions catalyzed by gold(I) are needed to more fully determine the nature of cyclopropyl gold(I) carbenes. Therefore, a detailed computational study has been performed exploring the nature of these species and their reactivity in cycloisomerizations of different enynes.
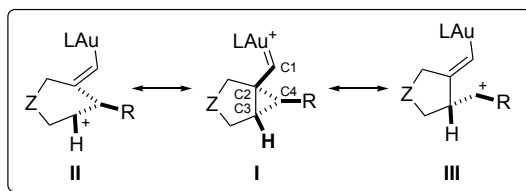
Table 1. Canonical structures of cyclopropyl gold(I) carbenes, **I–II–III**.

In this context, intrigued both by the selective formation of *trans*-fused cyclopropane **34** (Scheme 13) and the different selectivity of (*E*)-/(*Z*)-dienynes in the new gold(I)-catalyzed cyclization cascade reactions, we decided to study the mechanism of this transformation by means of DFT methods.
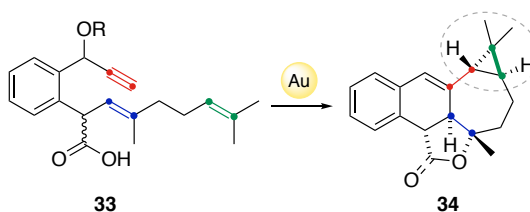
Scheme 13. Gold(I)-catalyzed cyclization of functionalized dienyne **33**.

UNIVERSITAT ROVIRA I VIRGILI
COMPUTATIONAL MECHANISTIC STUDIES IN GOLD(I) CATALYSIS AND DESIGN OF NEW CHIRAL LIGANDS
Immaculada Escofet Miquel

Chapter I

Results and Discussion

Exploring the Intermediates of Cycloisomerization Reactions

As explained in the **General Introduction** of this manuscript, cycloisomerization of enynes has gained great attraction for the construction of complex carbon skeletons under mild conditions.[28] Particularly representative is the stereospecific cycloisomerization of aryl 1,6-enynes **57** that undergo a formal [4+2] cycloaddition reaction in the presence of a gold(I) catalyst leading to tricyclic scaffolds **58** (Scheme 14). The reaction commences with the formation of cyclopropyl gold(I) carbene **Int2** via a 5-*exo*-dig pathway that can open to form the aryl stabilized cation **Int3**. Then, Friedel-Crafts-type reaction takes place to give **Int5**, which upon re-aromatization and protodemetalation yields to the formation of tricyclic derivatives **58**.[29]
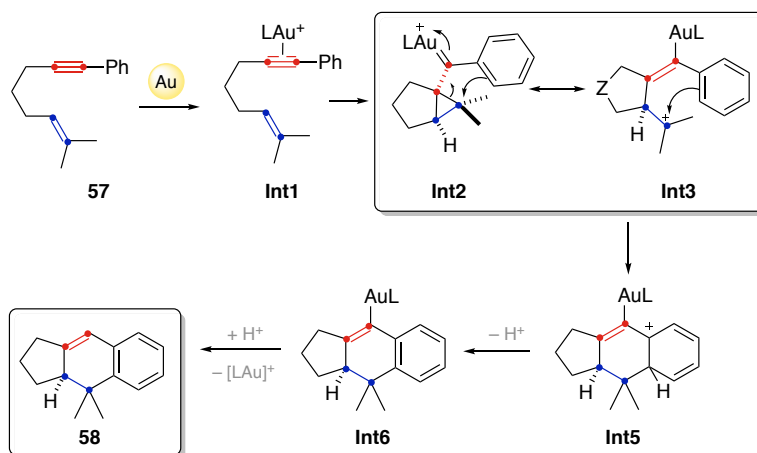
Scheme 14. Mechanistic proposal for the intramolecular [4+2] cycloaddition reaction of aryl-substituted 1,6-enynes type **57**.

According to previous DFT calculations by our group (Scheme 15),[29] this reaction proceeds stepwise through intermediates **IXb** and **IXb'** that were formed in an almost thermoneutral process (these intermediates correspond to our **Int2** and **Int3** in Scheme 14). Although cyclopropyl gold carbene **IXb** (in Scheme 14, **Int2**) opened to aryl stabilized carbocation **IX'b** (in Scheme 14, **Int3**), no transition state connecting these two intermediates was located. Despite the difference in energy between these intermediates was small, these two species were considered to be stationary points in the reaction coordinate with different angles and bond lengths and not resonance forms. At the B3LYP/6-31G(d) (C, H, P),

---

28   (a) Jiménez-Núñez, E.; Echavarren, A. M. *Chem. Rev.* **2008**, *108*, 3326–3350. (b) Obradors, C.; Echavarren, A. M. *Acc. Chem. Res.* **2014**, *47*, 902–912. (c) Dorel, R.; Echavarren, A. M. *Chem. Rev.* **2015**, *115*, 9028–9072. (d) Pflästerer, D.; Hashmi, A. S. K. *Chem. Soc. Rev.* **2016**, *45*, 1331–1367.

29   (a) Nieto-Oberhuber, C.; Pérez-Galán, P.; Herrero-Gómez, E.; Lauterbach, T.; Rodríguez, C.; López, S.; Bour, C.; Rosellón, A.; Cárdenas, D. J.; Echavarren, A. M. *J. Am. Chem. Soc.* **2008**, *130*, 269–279. (b) Check the supporting information of (29a) for further details.

UNIVERSITAT ROVIRA I VIRGILI
COMPUTATIONAL MECHANISTIC STUDIES IN GOLD(I) CATALYSIS AND DESIGN OF NEW CHIRAL LIGANDS
Immaculada Escofet Miquel

Chapter I

LANL2DZ (Au) level of theory, ΔG was found to be 3.7 kcal/mol, whereas using larger basis set (B3LYP/6-311+G(d,p) (C, H, P), LANL2DZ (Au)) the energies difference was smaller (2.0 kcal/mol).[29b] Moreover, formation of Wheland intermediate **Xb** (in Scheme 14, **Int5**) took place in an exergonic process *via* **TS$_{IX'b-Xb}$** and was the most favored pathway since the alternative skeletal rearrangement through **TS$_{IXb-XIb}$**, required higher activation energy (9.3 kcal/mol).
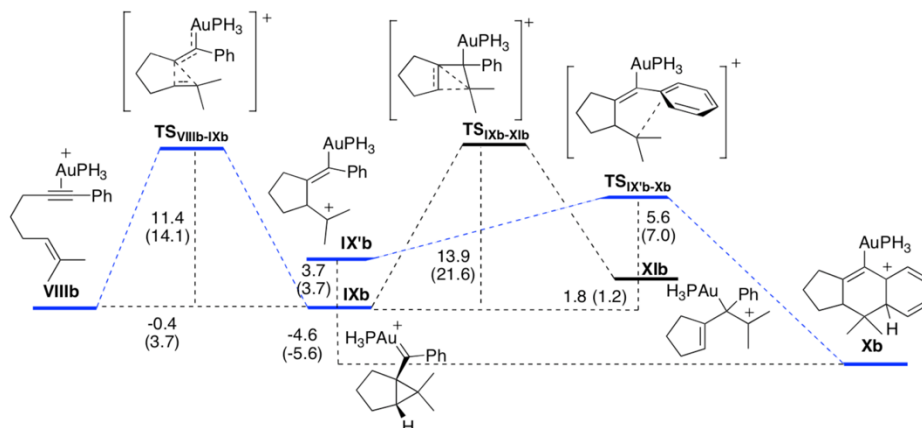
Scheme 15. Reaction pathway and energies for the *exo*-cycloaddtion of **VIIIb** to intermediate **Xb** calculated at B3LYP-D3/6-31G(d) (C, H, P), LANL2DZ (Au) level of theory. (+ ZPE-corrected electronic energies are given in kcal/mol; ΔG in brackets).

This mechanistic puzzle attracted our attention since we were designing new efficient chiral ligands for the development of the enantioselective version of these transformations (See **Chapter III**). We promptly realized that a more complete computational study on cycloisomeritzation reactions catalyzed by gold(I) was still needed. Therefore, we started our investigations towards the aforementioned gold(I) catalyzed intramolecular reaction of 1,6-enynes **57**, in collaboration with Dr. Maria Besora.

Density Functional Theory (DFT) was the method of choice since it has been successfully applied to similar studies. As already mentioned, we aimed to further study this system for the development of its efficient enantioselective version. Thus, BP86 was chosen as a hybrid functional due to is efficiency proved in other studies of enantioselective gold(I) catalysis[30] and for consistency with the previous computational work that we have done in our group in this field (See **Chapter III**).[31]

As expected, we observed the formation of both species, cyclopropyl gold(I) carbene **Int2** together with stabilized open carbocation **Int3**. Interestingly, these two species were found to be in equilibrium through **TS$_{2-3}$**. For our simple model substrate, formation of

30   (a) Kang, R.; Chen, H.; Shaik, S.; Yao, J. *J. Chem. Theory Comput.* **2011**, *7*, 4002−4011. (b) Ciancaleoni, G.; Rampino, S.; Zuccaccia, D.; Tarantelli, F.; Belanzoni, P.; Belpassi, L. *J. Chem. Theory Comput.* **2014**, *10*, 1021−1034.

31   García-Morales, C.; Ranieri, B.; Escofet, I.; López-Suarez, L.; Obradors, C.; Konovalov, A. I.; Echavarren, A. M. *J. Am. Chem. Soc.* **2017**, *139*, 13628−13631.

UNIVERSITAT ROVIRA I VIRGILI
COMPUTATIONAL MECHANISTIC STUDIES IN GOLD(I) CATALYSIS AND DESIGN OF NEW CHIRAL LIGANDS
Immaculada Escofet Miquel

Chapter I

cyclopropyl gold carbene **Int2** was favored by 1.1 kcal/mol *via* **TS₁₋₂**. Moreover, a very low activation energy was observed for the transformation of **Int3** into **Int2** (Scheme 16).
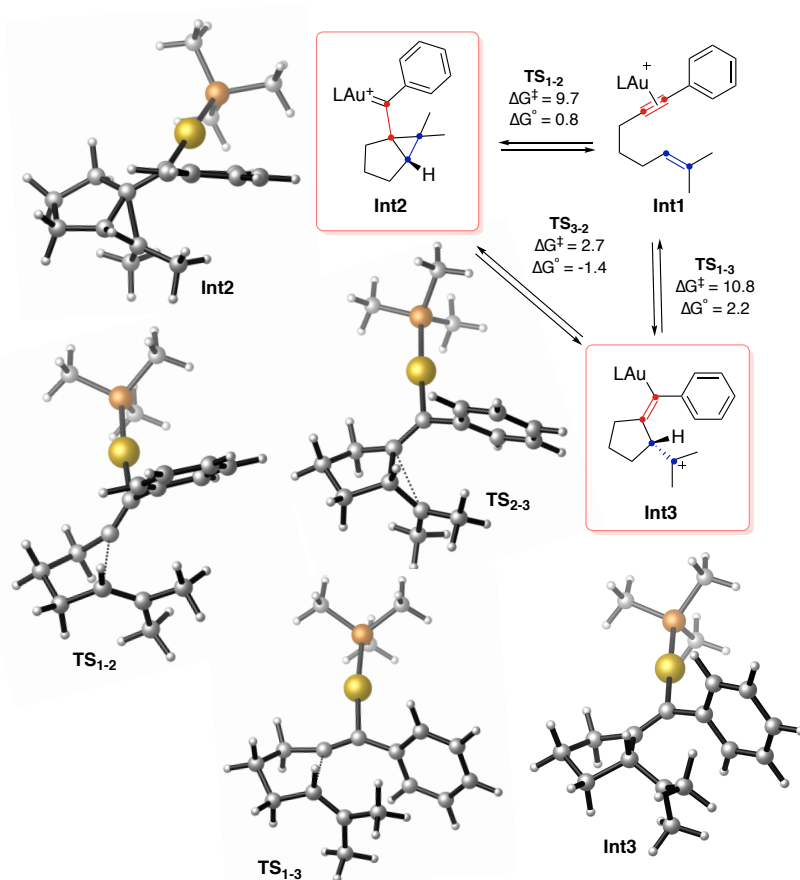
Scheme 16. Calculated formation of cyclopropyl gold(I) carbene **Int2** and open carbocation **Int3**. L=PMe₃. DFT calculations performed with BP86-D3/6-31G(d) (C, H, P) and SDD (Au) in CH₂Cl₂ (PCM). Free energies in kcal/mol.

These key intermediates will be crucial for the enantioinduction (see **Chapter III**) since the chirality of the sp³ carbon will be defined during this step giving rise to (*R* or *S*) tricyclic compound **58**. Since formation of **Int2** and **Int3** is the enantiodetermining step of the transformation, we decided to further study the differences between these two species.

Different angles and bond lengths were observed when comparing **Int2** with **Int3** (Table 2). Remarkably, the angle between (C₂-C₃-C₄) is 115.9º for **Int3** whereas at **Int2** is 69.6º. A longer distance between (C₂-C₄) was also observed for open carbocation species **Int3** 2.584 Å *vs* 1.734 Å for **Int2**. Interestingly, the cationic or carbenic character of gold(I) carbenes was also clear when comparing the (C₁-C₂) distances being 1.417 Å for **Int2** and 1.351 Å for **Int3**.

UNIVERSITAT ROVIRA I VIRGILI
COMPUTATIONAL MECHANISTIC STUDIES IN GOLD(I) CATALYSIS AND DESIGN OF NEW CHIRAL LIGANDS
Immaculada Escofet Miquel

Chapter I

Int2   Int3
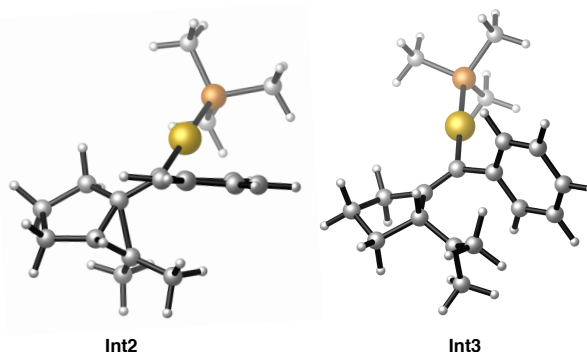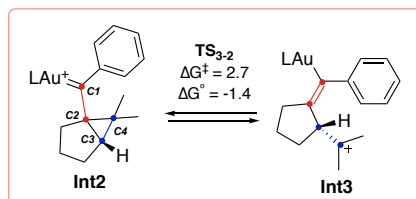
	d(C_1-C_2)	d(C_2-C_3)	d(C_3-C_4)	d(C_2-C_4)	angle(C_2-C_3-C_4)
Int2	1.417	1.552	1.487	1.734	69.6
Int3	1.351	1.575	1.474	2.584	115.9

Table 2. Calculated bond distances and angles of **Int2** and **Int3** by DFT at the BP86-D3/6-31G(d) (C, H, P) and SDD (Au) level in CH_2Cl_2 (PCM). Distances expressed in Å and angles in degrees.

Benchmark of Density Functional Theory Methods

These results prompted us to compute these intermediates and TSs using different DFT functionals and basis sets. In order to discard any artifact associated to the DFT method of choice, we performed a benchmark of DFT functionals.[32] Hence, we compared the performance of twelve different functionals on the intermediates and TSs mentioned before. In addition, we used larger basis sets for this benchmark to increase accuracy.

Very similar computed energies were obtained when changing the basis set from 6-31G* to the larger 6-311+G** (Table 3). Although the relative energies changed depending on the method used, no dramatical effect was detected when using pure methods B97D-D3,[33] BP86-D3,[34] TPSS-D3,[35] PBE-D3[36]. However, when using Grimme's B97D-D3, **Int1** is destabilized with respect to the other pure functionals, thus, same energy (6.2 kcal/mol) was observed for **Int2** and **Int3** in this case. Similarly, hybrid functionals B3LYP-D3,[37]

32   (a) Goerigk, L.; Grimme, S. *Phys. Chem. Chem. Phys.* **2011**, *13*, 6670−6688. (b) Goerigk, L.; Kruse, H.; Grimme, S. *ChemPhysChem.* **2011**, *12*, 3421−3433. (c) Evers, F. O.; Formalik, F.; Olejniczak, A.; Fischer, M. *Theor. Chem. Acc.* **2016**, *135*, 257. (d) Dohm, S.; Hansen, A.; Steinmetz, M.; Grimme, S.; Checinski, M. P. *J. Chem. Theory Comput.* **2018**, *14*, 2596−2608.

33   Grimme, S. *J. Comput. Chem.* **2006**, *27*, 1787–1799.

34   (a) Becke, A. D. *Phys. Rev. A.* **1988**, *38*, 3098–3100. (b) Perdew, J. P. *Phys. Rev. B.* **1986**, *33*, 8822–8824.

35   Tao, J.; Perdew, J. P. *Phys. Rev. Lett.* **2003**, *91*, 146401.

36   Perdew, J. P.; Burke, K.; Ernzerhof, M. *Phys. Rev. Lett.* **1996**, 77, 3865–3868.

37   Becke, A. D. *J. Chem. Phys.* **1993**, *98*, 5648–5652.

UNIVERSITAT ROVIRA I VIRGILI
COMPUTATIONAL MECHANISTIC STUDIES IN GOLD(I) CATALYSIS AND DESIGN OF NEW CHIRAL LIGANDS
Immaculada Escofet Miquel

Chapter I

B3PW91-D3,[37] BMK-D3,[38] or Minnesota functionals[39] do not show many differences, despite slightly higher barriers were found with respect to the initial BP86 functional. Likewise, comparing energies obtained from Minnesota functionals (M06, M06L, M062X, M06HF), similar energies were obtained with all of them including the technically pure, and non-hybrid, M06L.[40]

In addition, we used domain pair natural orbital method, DLPNO-CCSD(T),[41] that allow us to obtain high accurate energies in the faster and easier way. This method has recently been used as calibration for benchmark studies of the performance of density functionals[32d,42] and thus, to select the most appropriate functional for the system we studied. We calculated the energies for **Int1**, **Int2**, **Int3**, **TS$_{1-2}$**, **TS$_{1-3}$, and TS$_{2-3}$** by using ORCA (Table 3, last row).[43]

	Int1	Int2	Int3	TS$_{1-2}$	TS$_{1-3}$	TS$_{2-3}$
BP86	0.0	1.7	2.7	10.3	12.9	4.5
B3LYP	0.0	7.5	9.2	13.5	16.5	9.8
B3PW91	0.0	1.2	4.6	12.8	16.1	5.9
B97D	0.0	6.2	6.2	10.5	13.0	7.6
BMK	0.0	1.4	6.9	16.6	20.7	7.5
TPSS	0.0	1.7	4.9	10.8	13.6	6.4
M062X	0.0	5.5	11.5	15.9	19.4	11.8
M06HF	0.0	4.5	8.7	14.7	19.7	9.8
M06	0.0	3.4	8.4	14.8	18.0	9.4
M06L	0.0	4.1	9.9	14.8	17.3	10.9
PBE0	0.0	-1.8	3.3	12.3	15.6	4.1
PBE	0.0	-0.6	2.0	9.6	12.0	3.3
DLPNO-CCSD(T)	0.0	3.4	8.2	14.3	18.1	8.4

Table 3. DFT functional benchmark regarding **Int1**, **Int2**, **Int3**, **TS$_{1-2}$**, **TS$_{1-3}$, and TS$_{2-3}$**. L=PMe$_3$. Dispersion GD3 was included in all the cases. Energies of single points related to **Int1** in kcal/mol, (6-311+G**) basis set and SDD (Au) level in CH$_2$Cl$_2$ (PCM). Single points calculations in DLPNO-CCSD(T) for BP86-D3 optimized calculation.

The averages of the differences between each single point energy and the one obtained with DLPNO-CCSD(T) method (ORCA) show that, considering this most reliable method, the most appropriated functionals for this system are B3LYP-D3, M06-D3 or BMK-D3. Thus, due to these results, we chose to use M06-D3 and B3LYP-D3 throughout the study based on our experience with these methods (see **Chapter II**). Interestingly, better results were observed when using the hybrid version of PBE, PBE0.[44]

Then, we optimized the intermediates and TSs at M06-D3/6-31G(d) (C, H, P) and SDD (Au) level in order to compare them with the single points (Table 4). Very similar energies

38   Boese, A. D.; Martin, J. M. *J. Chem. Phys.* **2004**, *121*, 3405–3416.
39   Zhao, Y.; Truhlar, D. G. *Theor. Chem. Account.* **2008**, *120*, 215–241.
40   Zhao, Y.; Truhlar, D. G. *J. Chem. Phys.* **2006**, *125*, 194101.
41   Riplinger, C.; Sandhoefer, B.; Hansen, A; Neese, F. *J. Chem. Phys.* **2013**, *139*, 134101.
42   Iron, M. A.; Janes, T. *J. Phys. Chem.* **2019**, *123*, 3761–3781.
43   Neese, F. *WIREs Comput. Mol. Sci.* **2018**, *8*, e1327.
44   Adamo, C. *J. Chem. Phys.* **1999**, *110*, 6158–6170.

UNIVERSITAT ROVIRA I VIRGILI
COMPUTATIONAL MECHANISTIC STUDIES IN GOLD(I) CATALYSIS AND DESIGN OF NEW CHIRAL LIGANDS
Immaculada Escofet Miquel

Chapter I

were obtained for both cases, although lower activation barriers were observed for the new optimizations than for single point calculations.

Method	Int1	Int2	Int3	TS$_{1-2}$	TS$_{1-3}$	TS$_{2-3}$
M06-D3/6-311+G****	0.0	3.4	8.4	14.8	18.0	9.4
M06-D3/6-31-G***	0.0	2.4	7.0	13.1	14.8	8.5

Table 4. Free energies related to **Int1** in kcal/mol.

Substrate Effect on the Carbenic or Cationic Character of the Intermediates

Moreover, we decided to further investigate how the nature of the substrate could influence in the formation of **Int2**, **Int3** and **Int4**. Thus, seven different enynes bearing substituents at the alkyne or alkene moiety were tested (Table 5).
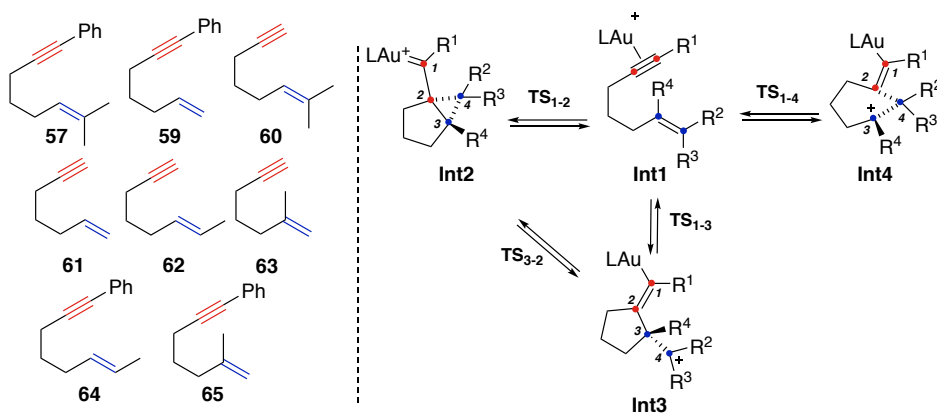
Enyne	Method	Species	d(C$_1$-C$_2$)	d(C$_2$-C$_3$)	d(C$_2$-C$_4$)	A(C$_2$-C$_3$-C$_4$)	ΔG‡	ΔG$^{\circ}$
57	BP86-D3	**57-Int2**	1.417	1.552	1.734	69.6	9.7	0.8
57	BP86-D3	**57-Int3**	1.651	1.575	2.584	115.9	10.8	2.8
57	M06-D3	**57-Int2**	1.413	1.536	1.652	66.5	13.1	2.4
57	M06-D3	**57-Int3**	1.338	1.555	2.549	115.4	14.8	7.0
59	BP86-D3	**59-Int4**	1.424	1.688	1.540	57.7	7.6	-7.4
59	M06-D3	**59-Int4**	1.416	1.632	1.527	58.8	13.9	-5.6
60	BP86-D3	**60-Int2**	1.387	1.727	1.645	61.5	-	-7.9
60	BP86-D3	**60-Int3**	1.372	1.618	1.915	77.0	-	-5.8
60	M06-D3	**60-Int2**	1.375	1.667	1.636	62.9	5.2	-6.1
60	M06-D3	**60-Int3**	1.338	1.590	2.353	101.8	8.0	-1.0
61	BP86-D3	**61-Int4**	1.398	1.747	1.541	56.4	3.8	-9.1
61	M06-D3	**61-Int4**	1.385	1.674	1.531	58.1	13.0	-7.4
62	BP86-D3	**62-Int4**	1.395	1.746	1.565	57.5	2.4	-7.3
62	M06-D3	**62-Int4**	1.382	1.678	1.559	59.2	7.1	-8.5
63	BP86-D3	**63-Int4**	1.377	1.948	1.568	52.5	3.9	-9.0
63	M06-D3	**63-Int4**	1.372	1.758	1.561	57.4	8.9	-7.0
64	BP86-D3	**64-Int2**	1.414	1.608	1.672	65.8	8.1	-2.4
64	BP86-D3	**64-Int3**	-	-	-	-	-	-
64	M06-D3	**64-Int2**	1.404	1.589	1.630	64.7	13.5	-2.6
64	M06-D3	**64-Int3**	1.335	1.552	2.534	115.3	-	-0.7

UNIVERSITAT ROVIRA I VIRGILI
COMPUTATIONAL MECHANISTIC STUDIES IN GOLD(I) CATALYSIS AND DESIGN OF NEW CHIRAL LIGANDS
Immaculada Escofet Miquel

Chapter I

| 65 | BP86-D3 | 65-Int4 | 1.413 | 1.795 | 1.545 | 55.3 | 6.6 | -6.6 |
| 65 | M06-D3 | 65-Int4 | 1.409 | 1.667 | 1.534 | 57.9 | 8.8 | -6.8 |

Table 5. Calculated bond distances and angles of optimized **Int2**, **Int3**, **Int4**, **TS$_{1-2}$**, **TS$_{1-3}$** and **TS$_{1-4}$** by DFT at the BP86-D3 nand M06-D3L=PMe$_3$. Free energies in kcal/mol and referred to **Int1**. Distances expressed in Å and angles in degrees.

For those enynes having a terminal alkene moiety (R^2 and R^3 = H, enynes **59**, **61**, **63**, **65**), only intermediate **Int4** was observed. Similar results were obtained when using BP86-D3 and M06-D3, although higher computed activation energies and higher angles (C$_2$-C$_3$-C$_4$) were observed for M06-D3 functional. Some transition states were not found when using BP86-D3, probably due to the low activation energy of these systems.

Despite all these substrates delivered the same intermediate **Int4**, some structural differences were observed depending on the R^1 and R^4 substituents. Hence, for R^1 = Ph (enynes **59**, **65**), the distance between C1–C2 is longer than in the case of R^1 = H (enynes **61**, **63**) due to conjugation of phenyl ring. Likewise, having a methyl substituent as R^4 (enynes **63**, **65**) leads to higher distances between C2–C3.

On the other hand, we observed the formation of both **Int2** and **Int3** for enyne **60** that has a disubstituted alkene moiety (R^2 and R^3 = Me). Very similar structures to those observed for our first studied enyne **57** were found. For both substrates, **Int3** showed a clearly larger angle (C$_2$-C$_3$-C$_4$) corresponding to a stabilized carbocation species. However, for substrate **60** that has a terminal alkyne, this angle is smaller (101.8º *vs* 115.4º).

Finally, for monosubstituted alkenes (R^2 = Me and R^3 = H, enynes **62**, **64**), the alkyne moiety was found to determine the formation of **Int2**, **Int3** or **Int4**. Thus, terminal alkyne **62** (R^1 = H) delivered **Int4**, whereas enyne **64** (R^1 = Ph) led to the formation of **Int2** together with **Int3**. It is important to highlight that for substrate **64** no transition state was found to connect **64-Int1** with **64-Int3** either with M06-D3 or BP86-D3. However, an alternative pathway was encountered that connects directly **64-Int1** with the Wheland intermediate **64-Int5** (Table 6).
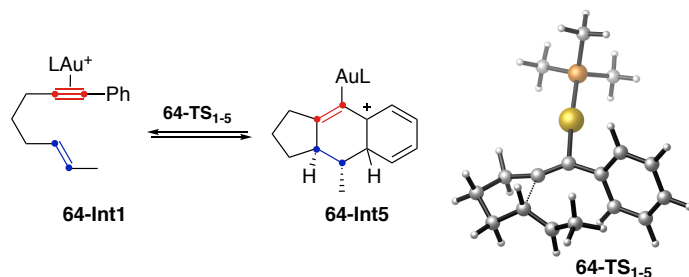
Method	Int1	Int5	TS$_{1-5}$
BP86-D3	0.0	-10.1	11.2
M06-D3	0.0	-7.0	17.4

Table 6. Computed free energies for the formation of Wheland intermediate **64-Int5** and transition states by DFT at the BP86-D3 and M06-D3. L=PMe$_3$. Free energies in kcal/mol respect to **Int1**.

UNIVERSITAT ROVIRA I VIRGILI
COMPUTATIONAL MECHANISTIC STUDIES IN GOLD(I) CATALYSIS AND DESIGN OF NEW CHIRAL LIGANDS
Immaculada Escofet Miquel

Chapter I

NBO analysis

A natural bond orbital (NBO) population analysis[45] was carried out in order to confirm the carbenic or cationic character of **Int2**, **Int3**, and **Int4**.

NBO analysis is based on Natural Orbitals (NO), which are used to calculate the distribution electron density in atoms and bonds.[45] In NBO analysis, the input atomic orbital basis set is transformed through Natural Atomic Orbitals (NAOs) and Natural Hybrid Orbitals (NHOs) into Natural Bond Orbitals (NBOs). The NBOs obtained in this fashion corresponds to the chemist's Lewis picture, in which two-center bonds and lone pairs are localized. Moreover, NBO analysis also shows the atomic charge distribution, so-called Natural Population Analysis Charges (NPA). NPA charges are obtained by resting the nuclear charge and the summed natural population of NAOs on the atom.

Interestingly, NPA charges of intermediates **Int2**, **Int3**, and **Int4** are different for gold and for carbons depending on the studied structure. Au NPA charge was 0.19267 for **57-Int2**, 0.1886 for **57-Int3** and 0.18461 for **63-Int4**, being higher for cyclopropyl gold(I) carbene species of type **Int2**, as expected. Moreover, NPA charges of carbons connected to the gold atom are also slightly different for each system. For **57-Int3** and **63-Int4**, positive charges are clearly delocalized and, for that reason charges on the carbon-carbon double bond are more negative than for **57-Int2**. Thus, the carbenic or cationic character of intermediates type **Int2**, **Int3**, and **Int4** was confirmed by NBO analysis (Table 7).
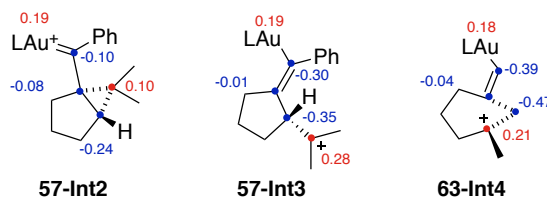
Table 7. Summary of Natural Population Analysis (NPA charges) by NBO of **57-Int2, 57-Int3** and **64-Int3**, optimized at the BP86-D3. Positive charges in red and negative charges in blue.

Quantum Theory Atoms in Molecules

With the aim of further prove the structures of **Int2**, **Int3**, **Int4**, we carried out Quantum Theory Atoms in Molecules (QTAIM)[46] analysis with Multiwfn software[47] (Schemes 17-19). The bond critical points (BCPs) and the ring critical points (RCPs) were located and analyzed using Laplacian maps.

45   (a) Landis, C. R.; Weinhold, F. *Cambridge University Press*, **2005**. (b) Landis, C. R.; Weinhold, F. *J. Am. Chem. Soc.* **2006**, *128*, 7335–7345. (c) http://cup.uni-muenchen.de/ch/compchem
46   (a) Bader, R. F. W. *Clarendon Press*, **1994**. (b) Bader, R. F. W. *Chem. Eur. J.* **2006**, *12*, 7769–7772.
47   Lu, T.; Chen, F. *J. Comput. Chem.* **2012**, *33*, 580–592.

UNIVERSITAT ROVIRA I VIRGILI
COMPUTATIONAL MECHANISTIC STUDIES IN GOLD(I) CATALYSIS AND DESIGN OF NEW CHIRAL LIGANDS
Immaculada Escofet Miquel

Chapter I

We can see in Scheme 17b that we have been able to locate the two ring critical points (RCPs) that can also be observed in Scheme 17c and 17e. For the Laplacian map with electron density contour of atoms **1**–**6**–**3** (Scheme 17d), two bonds do not appear due to the fact that they are out of the plane. However, they can be seen in the topological analysis graph (Scheme 17b).

Regarding the analysis of **Int3** (Scheme 18), we can clearly see that there is no bond between atoms C_8–C_1. Likewise, the ring critical bond was not observed, and the Laplacian clearly indicates the absence of this bond. Also, in this system, in the Laplacian map with electron density contour of atoms **1**–**6**–**3** (Scheme 18d), two bonds do not appear due to the fact that they are out of the plane. However, they can be found in the topological analysis graph (Scheme 18b).

Finally, only one ring critical point was observed in the case of **Int4** (Scheme 19) as a consequence of the semi-opened ring system present in this intermediate. Hence, QTAIM theory confirms that the molecular representation in **17a**, **18a**, and **19a** is accurate.

UNIVERSITAT ROVIRA I VIRGILI
COMPUTATIONAL MECHANISTIC STUDIES IN GOLD(I) CATALYSIS AND DESIGN OF NEW CHIRAL LIGANDS
Immaculada Escofet Miquel

Chapter I
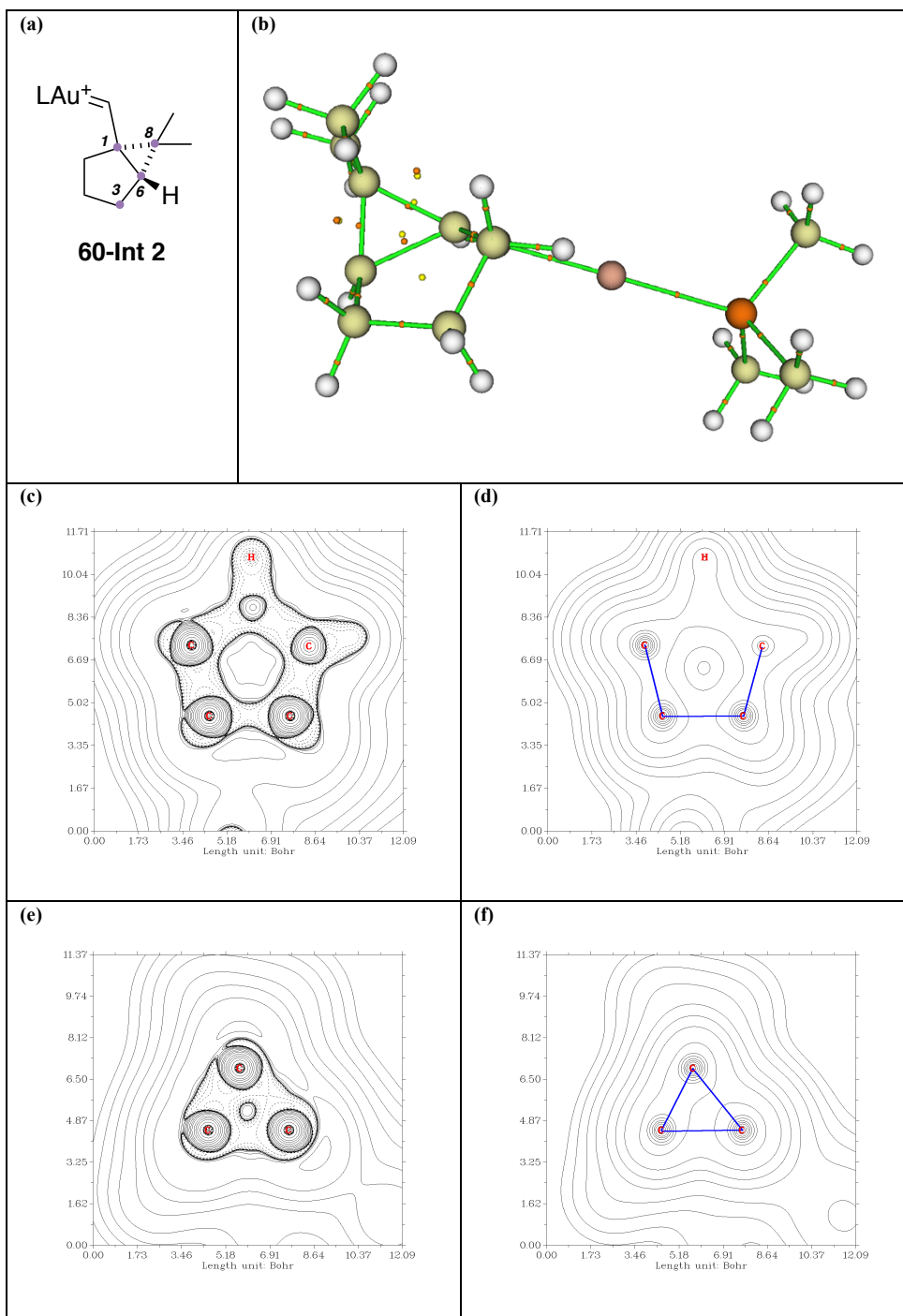
Scheme 17. (a) Molecular structure of **Int2** for enyne **60**. **(b)** Quantum theory of atoms in molecules (QTAIM) Topological Analysis graph with bond critical points (BCPs) in red and ring critical points (RCPs) in yellow. **(c-d)** Laplacian map with electron density contour of atoms **1-6-3**, bonds depicted in blue. **(e-f)** Laplacian map with electron density contour of atoms **1-6-8**, bonds depicted in blue.

UNIVERSITAT ROVIRA I VIRGILI
COMPUTATIONAL MECHANISTIC STUDIES IN GOLD(I) CATALYSIS AND DESIGN OF NEW CHIRAL LIGANDS
Immaculada Escofet Miquel

Chapter I
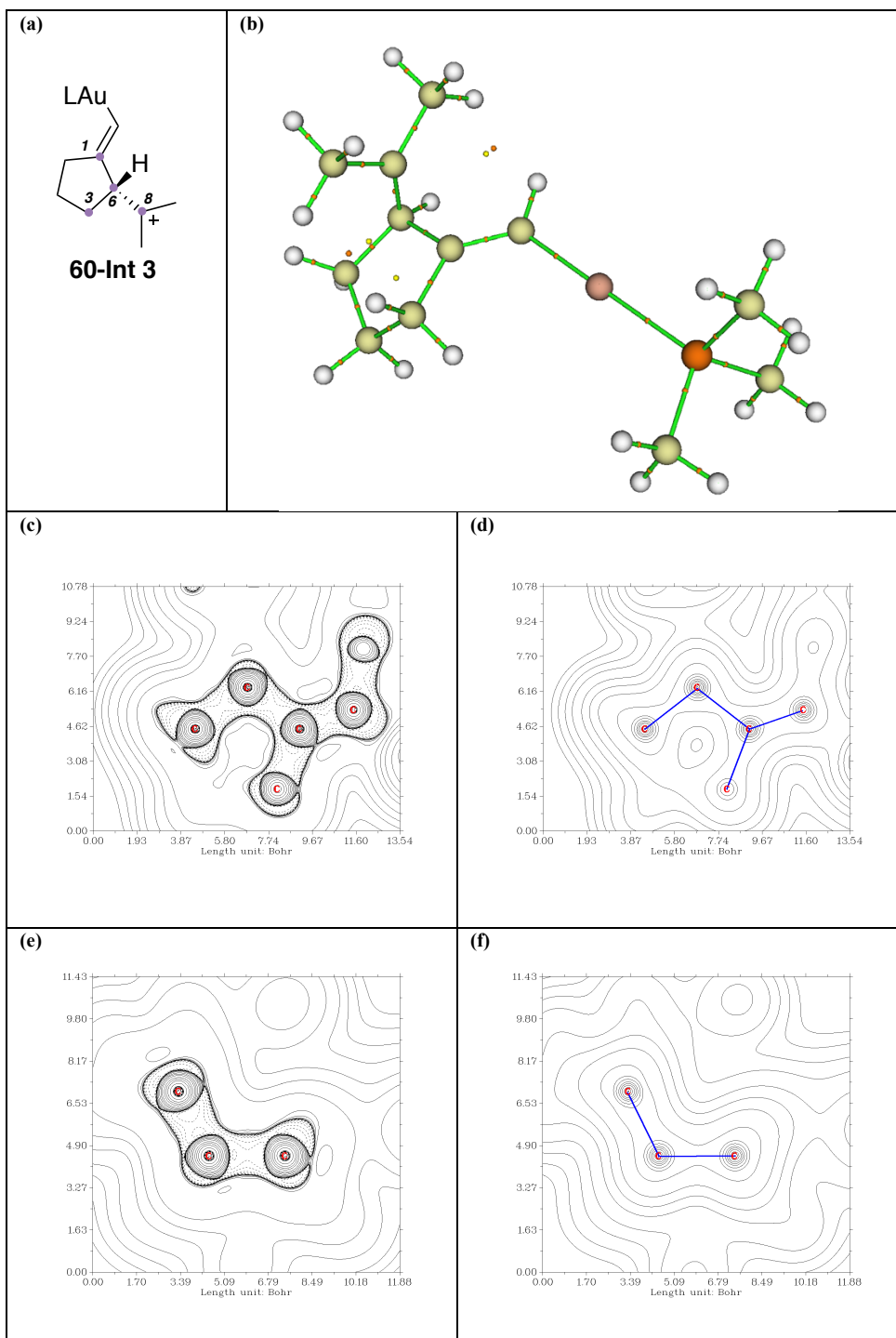
Scheme 18. (a) Molecular structure of **Int3** for enyne **60**. **(b)** Quantum theory of atoms in molecules (QTAIM) Topological Analysis graph with bond critical points (BCPs) in red and ring critical points (RCPs) in yellow. **(c-d)** Laplacian map with electron density contour of atoms **1-6-3**, bonds depicted in blue. **(e-f)** Laplacian map with electron density contour of atoms **1-6-8**, bonds depicted in blue.

UNIVERSITAT ROVIRA I VIRGILI
COMPUTATIONAL MECHANISTIC STUDIES IN GOLD(I) CATALYSIS AND DESIGN OF NEW CHIRAL LIGANDS
Immaculada Escofet Miquel

Chapter I
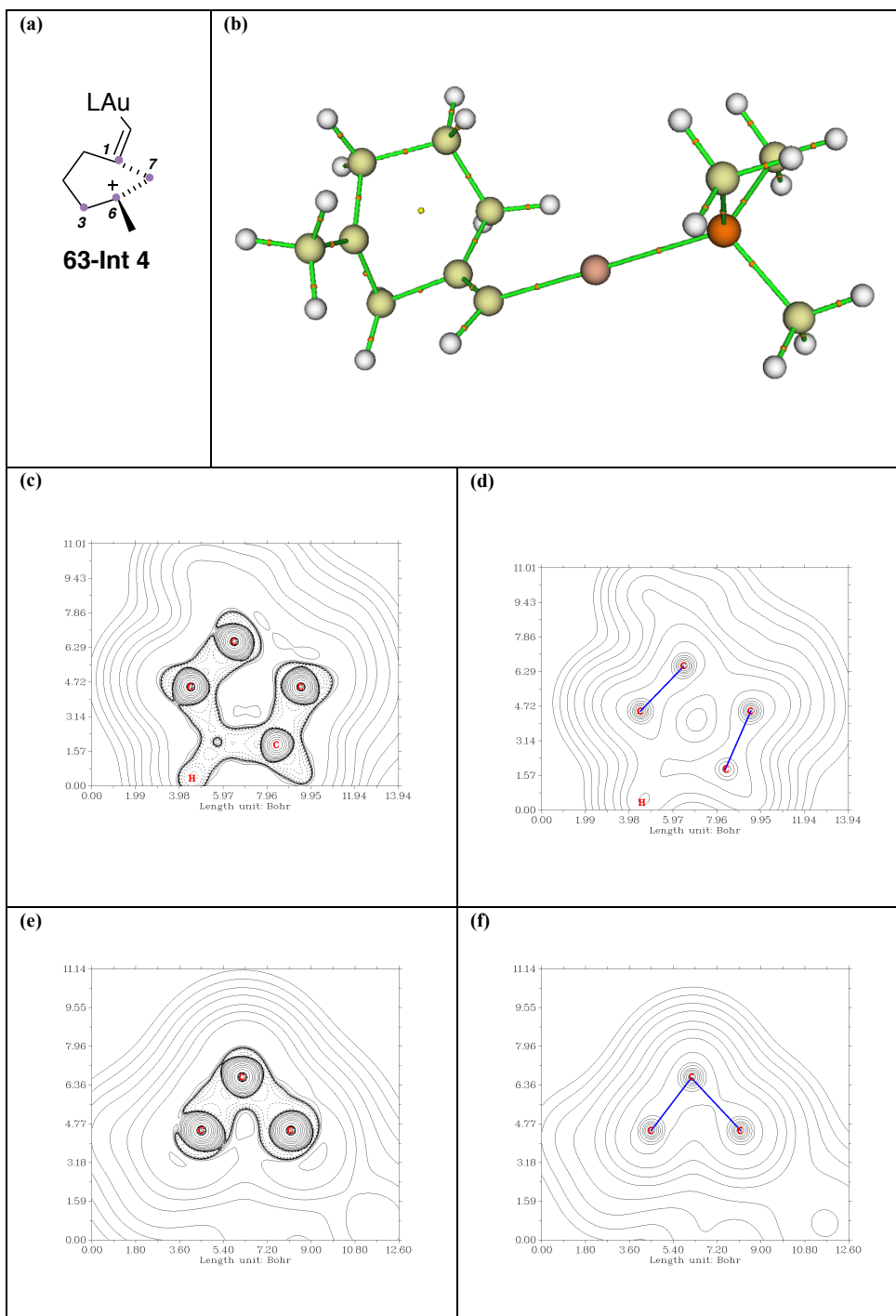
Scheme 19. (a) Molecular structure of **Int4** for enyne **63**. **(b)** Quantum theory of atoms in molecules (QTAIM) Topological Analysis graph with bond critical points (BCPs) in red and ring critical points (RCPs) in yellow. **(c-d)** Laplacian map with electron density contour of atoms **1-6-3**, bonds depicted in blue. **(e-f)** Laplacian map with electron density contour of atoms **1-6-7**, bonds depicted in blue.

UNIVERSITAT ROVIRA I VIRGILI
COMPUTATIONAL MECHANISTIC STUDIES IN GOLD(I) CATALYSIS AND DESIGN OF NEW CHIRAL LIGANDS
Immaculada Escofet Miquel

Chapter I

Indium-catalyzed Cycloisomerizations of 1,6-enynes

Recent mechanistic studies on indium-catalyzed cycloisomerizations of 1,6-enynes have proposed that the key intermediates are of type **Int4**.[48] Therefore, we were curious about the possible existence of the intermediates related to **Int2** and **Int3** in these systems that use $InCl_3$ as catalyst. Thus, we performed DFT calculations to locate the different possible cyclopropyl indium-carbenes formed. We choose M06-D3/6-31G(d) (C, H) and LANL2DZ (In, Cl) level of theory in CH_2Cl_2 (PCM).

Upon the activation of the alkyne moiety of enyne **57**, we observed the formation of both intermediates **In-Int2** and **In-Int3**, whereas in the case of enyne **63** only **In-Int4** was found (Scheme 20).
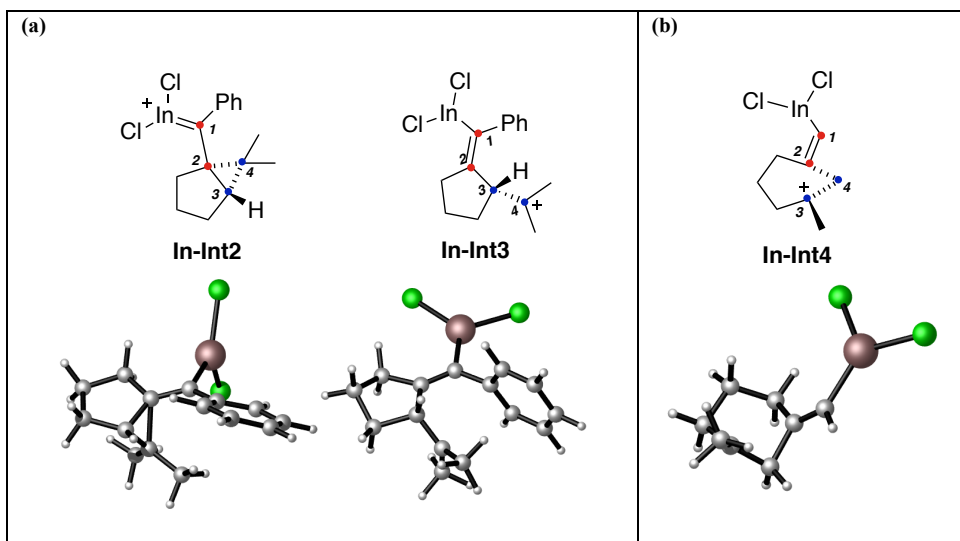
Scheme 20. (a) Optimized geometries of **In-Int2** and **In-Int3** for enyne **57** using $InCl_3$ as catalyst. **(b)** Optimized geometries of **Int4** for enyne **63**, using $InCl_3$ as catalyst. DFT calculations performed with M06-D3. Free energies in kcal/mol.

Therefore, remarkably, the same three intermediates were obtained when switching gold(I) for indium(III) for substrates **57** and **63**. However, slight structural differences were observed when comparing these intermediates (**In-Int2** and **In-Int3**) with the ones obtained previously with gold(I) (**Int2**, **Int3**). In the case of cyclopropyl carbene **In-Int2**, longer distances were observed between C2–C4, indicating a less strained cyclopropane ring than for the gold(I) intermediate. Moreover, the angle (C2-C3-C4) was larger (72º) than for the gold(I)-carbene **Int2** (66.5º). Intermediate **In-Int3** was found to be very similar to **Int3**. Nonetheless, for enyne **63** we observed the formation of a more opened system (longer distances between C2–C3) that presents the smallest angle observed in this study (44.9º) (Table 8).

---

48   Zhuo, L.-G.; Zhang, J.-J. Yu, Z.-Z. *J. Org. Chem*. **2014**, *79*, 3809–3820.

UNIVERSITAT ROVIRA I VIRGILI
COMPUTATIONAL MECHANISTIC STUDIES IN GOLD(I) CATALYSIS AND DESIGN OF NEW CHIRAL LIGANDS
Immaculada Escofet Miquel

Chapter I

Enyne	Species	d(C_1-C_2)	d(C_2-C_3)	d(C_2-C_4)	^(C_2-C_3-C_4)
57	Int2	1.413	1.536	1.652	66.5
57	Int3	1.338	1.555	2.549	115.4
57	In-Int2	1.385	1.542	1.768	72.0
57	In-Int3	1.340	1.538	2.548	115.9
63	Int4	1.372	1.758	1.561	57.4
63	In-Int4	1.338	2.213	1.566	44.9

Table 8. Comparative list of calculated bond distances and angles of **Int2, Int3** (enyne **57**) and **Int4** (enyne **63**) by DFT at the M06-D3/6-31G(d) (C, H, P) and SDD (Au) level in CH_2Cl_2 (PCM) with the ones obtained at the M06-D3/6-31G(d) (C, H) and LANL2DZ (In, Cl) level in CH_2Cl_2 (PCM) (**In-Int2**, **In-Int3**, **In-Int4**). Distances expressed in Å and angles in degrees.

Finally, we compared the computed free energies of the optimized geometries of **Int2, Int3** and **In-Int2**, **In-Int3**. Also, we calculated the difference between **Int2** and **Int3** for each case. Interestingly, **In-Int3** is the favored species formed when using indium catalyst. However, in the case of gold(I), cyclopropyl gold carbene **Int2** was the preferred intermediate (Table 9).

Enyne	Species	Int2-Int3
57	Int2	0.0
57	Int3	7.6
57	In-Int2	0.0
57	In-Int3	-4.4

Table 9. Differences between free energies of (**Int2**, **Int3**) and (**In-Int2**, **In-Int3**) by DFT at the M06-D3 expressed in kcal/mol.

Trans-fused Cyclopropanes by Gold(I)-catalyzed Cyclization Cascade

As mentioned in the **Introduction** of this chapter, we were intrigued both by the selective formation of *trans*-fused cyclopropane **34** and the different selectivity of (*E*)-/(*Z*)-dienynes in the new gold(I)-catalyzed cyclization cascade reactions. Hence, we decided to study the mechanistic pathways of this transformation by means of DFT calculations. Likewise, we aimed to prove the need of an external nucleophile for the selective formation of **34**, as observed in the control experiments (Scheme 13).
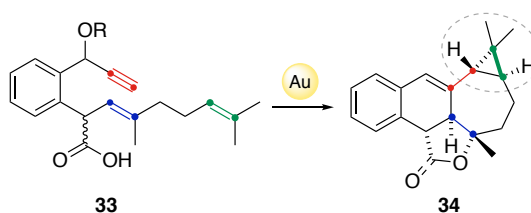
Scheme 13. Gold(I)-catalyzed cyclization of functionalized dienyne **33**, towards jatrophalactone **35**.

We started computing the simpler enynes **66** instead of a dienyne. Moreover, since this substrate does not contain an internal nucleophile such in substrates **33**, **39**, and **40**, we will later compute these other systems in order to compare the reaction pathways and to

UNIVERSITAT ROVIRA I VIRGILI
COMPUTATIONAL MECHANISTIC STUDIES IN GOLD(I) CATALYSIS AND DESIGN OF NEW CHIRAL LIGANDS
Immaculada Escofet Miquel

Chapter I

computationally confirm that the formation of the fused tetrahydrofuran ring plays a crucial role in the final cyclopropanation step.

Thus, we performed DFT calculations using PMe₃ as simplified ligand for gold(I). B3LYP has been chosen as a hybrid functional for this system based on our previous computational studies on gold-catalyzed cyclopropanation reactions.[13] Two possible cyclopropyl gold carbenes could be formed when using enyne **66** as substrate, depending on the orientation of the alkene moiety. Thus, one possible intermediate would have the hydrogen in *syn* to the methoxy group and the other one in *anti*. Interestingly, we observed the formation of both **Int2** and **Int3** types of intermediates (Scheme 21). Hence, when the hydrogen and methoxy group are in *syn*, formation of cyclopropylgold(I) carbene **66-Int2** was observed. In contrast, opened carbocation species **66-Int3** were preferentially formed when the methoxy group and the hydrogen are in *anti*-position. This fact is probably due to steric hindrance, since the alkene is placed very close to the methoxy group and the closed carbene (type of **Int2**) is not that favorable. Noteworthy, in the absence of the alkyl chain tethered to the alkene, formation of cyclopropyl gold carbene **66-Int2** is 3.7 kcal/mol more favorable than formation of the opened carbocation species **66-Int3**.
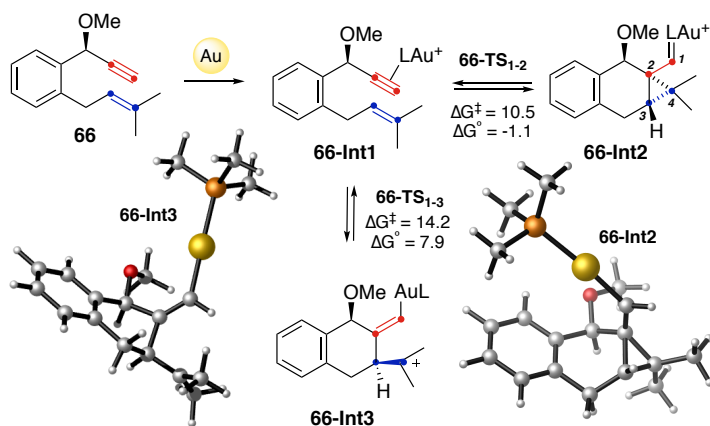
Scheme 21. Calculated formation of cyclopropyl gold(I) carbene **66-Int2** and open carbocation **66-Int3** for enyne **66**. L=PMe₃. DFT calculations performed with B3LYP-D3/6-31G(d) (C, H, O, P) and SDD (Au) in CH₂Cl₂ (PCM). Free energies in kcal/mol.

Although B3LYP was the method of choice for this system, we decided to compute the same pathways using the best alternative functionals found in the aforementioned DFT benchmark. Also, we wanted to proof the existence of these intermediates when using other methods and thus, discard possible computational artifacts (Table 10). Both **66-Int2** and **66-Int3** were found as minima when BP86-D3 and M06-D3 were used. In three cases, **66-Int2** is more stable than **66-Int3** (Scheme 21 and Table 10). The same tendency was observed for enyne **66** than with the previously studied substrate **57**. Thus, formation of **66-Int2** was always favored over **66-Int3** and **66-TS₁₋₂** was lower than **66-TS₁₋₃** for all the cases. Computed results using BP86-D3 were lower in energy for TSs and intermediates than B3LYP-D3 and M06-D3.

UNIVERSITAT ROVIRA I VIRGILI
COMPUTATIONAL MECHANISTIC STUDIES IN GOLD(I) CATALYSIS AND DESIGN OF NEW CHIRAL LIGANDS
Immaculada Escofet Miquel

Chapter I

Likewise, results obtained with M06-D3 are the highest than the other two functionals studied whereas BP86-D3, are the lowest. Hence, we decided to use B3LYP-D3 as functional for the rest of computational studies of this project.

Method	66-Int1	66-Int2	66-Int3	66-TS$_{1-2}$	66-TS$_{1-3}$
BP86-D3	0.0	-6.0	2.2	7.5	11.1
M06-D3	0.0	-6.2	6.2	11.9	16.7

Table 10. Computed free energies of **66-Int2**, **66-Int3**, **66-TS$_{1-2}$**, **66-TS$_{1-3}$**, related to **66-Int1**. DFT calculations performed with BP86-D3 or M06-D3. Free energies in kcal/mol. L=PMe$_3$.

Enyne **67** was then studied under gold(I) catalysis. Furthermore, since this substrate contains an internal nucleophile like in **33**, **39**, and **40**, we will be able to confirm the role of the formation of tetrahydrofuran ring in the final cyclopropanation step. Thus, enyne **67** was explored taking into account the two possible diastereomers (**67a** and **67b**), which upon coordination to gold(I) would give **Int1a-c**, considering different conformers resulting from different orientation of the alkenes (Scheme 22).
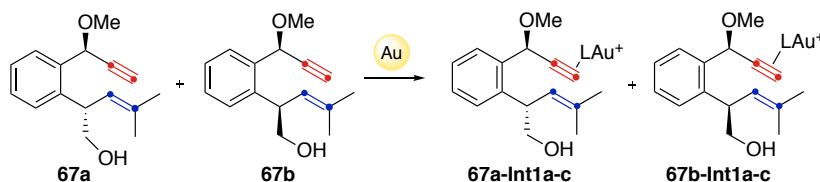
Scheme 22. Formation of **Int1a-c** of enyne **67** (mixture of diastereomers **67a** and **67b**) in the presence of gold(I) catalyst.

A similar energy profile was observed for both diastereomers (**67a** and **67b**). Thus, formation of cyclopropyl gold(I) carbenes **67a-Int2** and **67b-Int2** (with hydrogen in *syn* to the methoxy group) have the lowest energy barriers, although the corresponding intermediates **67a-Int1c** and **67b-Int1c** are the less favored ones. In the case of the opened carbocation intermediates, formation of **67a-Int3** and **67b-Int3** pathways have the highest computed energy barriers. Hence, formation of cyclopropyl gold carbenes of type **Int2** is also favored for substrate **67**. However, alternative pathways were found to directly connect **67a-Int1a** and **67b-Int1a** with tetrahydrofuran products **67a-Int7** and **67b-Int7** *via* **67a-TS$_{1a-7}$** and **67b-TS$_{1a-7}$**, respectively. It is worth mentioning that no transition state was found between cyclopropyl gold carbenes **67a-Int2** and **67a-Int7** nor from **67b-Int3** to **67b-Int7**. This is probably due to the fact that the alcohol moiety is oriented far away from the site of the attack to form tetrahydrofuran rings (Scheme 23). Furthermore, **67b-Int7** can also be obtained *via* **67b-TS$_{2-7}$**.

With these results we conclude that **67a-Int1a**, **67b-Int1a** and **67b-Int2** form cyclized tetrahydrofuran intermediates **67a-Int7** and **67b-Int7**. Also, the presence of an external nucleophile was confirmed to be crucial for the selectivity of the transformation since products of type **Int7** are only obtained when alcohol moiety is present in the *anti*-position with respect to the cyclopropyl.

UNIVERSITAT ROVIRA I VIRGILI
COMPUTATIONAL MECHANISTIC STUDIES IN GOLD(I) CATALYSIS AND DESIGN OF NEW CHIRAL LIGANDS
Immaculada Escofet Miquel

Chapter I
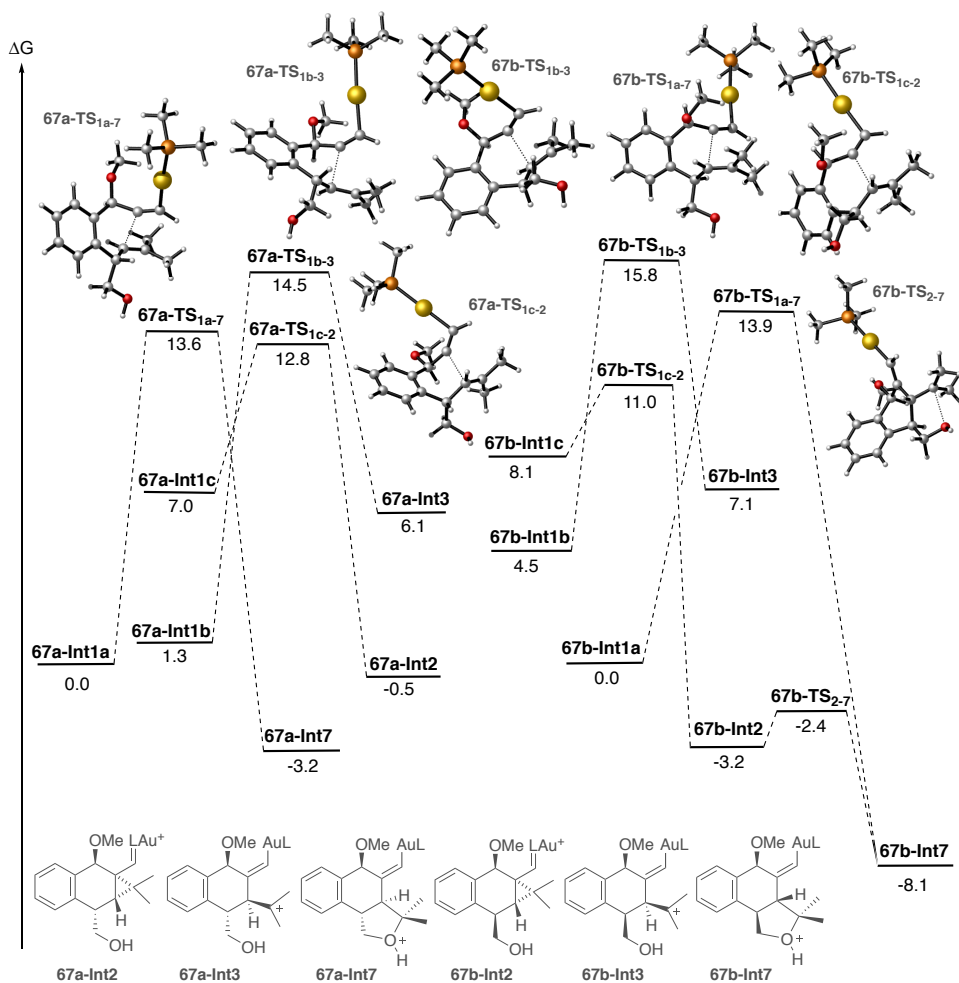
Scheme 23. Calculated formation of intermediates **Int2, Int3 and Int7** for enyne **67**. L=PMe₃. DFT calculations performed with B3LYP-D3/6-31G(d) (C, H, O, P) and SDD (Au) in CH₂Cl₂ (PCM). Free energies in kcal/mol respect to **67a-Int1a** and **67b-Int1a**.
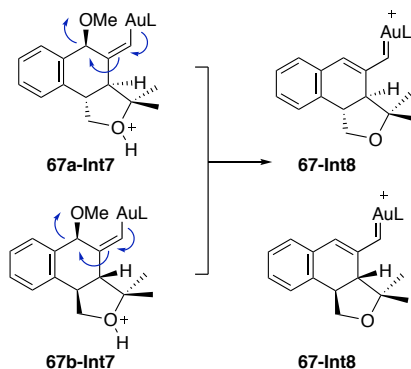
Scheme 24. Formation of intermediates **Int8** for enyne **67**.

UNIVERSITAT ROVIRA I VIRGILI
COMPUTATIONAL MECHANISTIC STUDIES IN GOLD(I) CATALYSIS AND DESIGN OF NEW CHIRAL LIGANDS
Immaculada Escofet Miquel

Chapter I

It is important to note that both **67a-Int7** and **67b-Int7** would give rise to the same intermediate, **67-Int8**, after the elimination of methoxy group (Scheme 24).

Next, we studied (*E*)-configured dienynes **39a**, containing a free hydroxy group and a chain in the alkene moiety, which afford *trans*-fused cyclopropane **41** as a single diastereomer, along with byproduct **42**. Likewise, the analogous diastereomeric mixture of (*Z*)-configured **39b** led to an inseparable mixture of isomers **43** and **44**, together with (*Z*)-**42** (Scheme 25). Furthermore, when the two isomers of **39b** were separated by semi-preparative chromatography and exposed to gold(I)-catalysis, the same mixture of **43** and **44** was obtained, although the reaction was much cleaner for one of the diastereoisomers. According with this last experiment, we envisioned that during reaction mechanism both diastereomers of **39b** would converge into a common intermediate (like we observed for products **67** and **67-Int8**) that would finally deliver the cyclopropanation product with the same *cis*/*trans* ratio.[49]
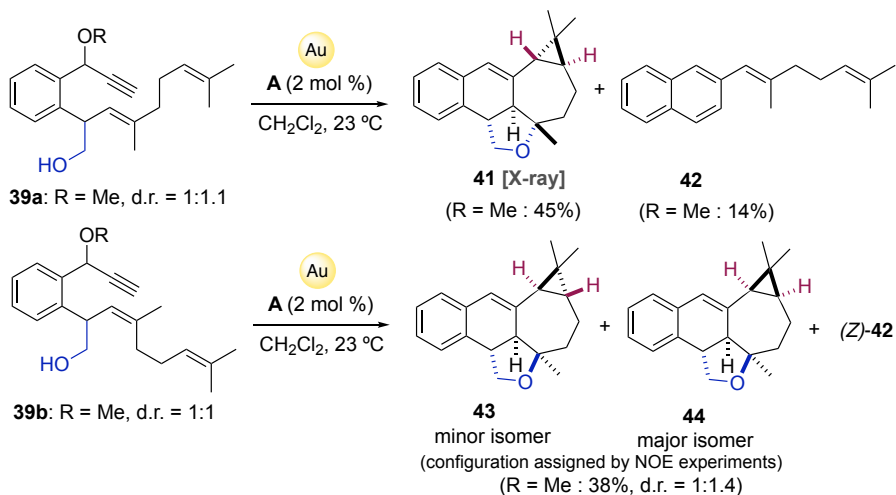
Scheme 25. Gold(I) catalyzed cyclization cascade reactions of **33a**, **39a-b** and **40a-b**.

In order to better understand these experimental results, we computed the system for (*E*)-configured dienyne **39a** and for (*Z*)-configured dienyne **39b**. Four possible diastereomers (**39aa** and **39ab**) and **39b** (**39ba** and **39bb**) were studied under gold(I) catalysis, using PMe$_3$ as simplified ligand for gold. Thus, upon the activation of the alkyne moiety, three conformers of **Int1** were detected in all the cases, as found before for substrate **67**, differing on the orientation of the alkene (**39aa-Int1a-c**, **39ab-Int1a-c**, **39ba-Int1a-c**, and **39bb-Int1a-c**) (Scheme 26).

---

[49] The experimental part of this project has been performed by Dr. Hanna Bruss and Helena Armengol i Relats.

UNIVERSITAT ROVIRA I VIRGILI
COMPUTATIONAL MECHANISTIC STUDIES IN GOLD(I) CATALYSIS AND DESIGN OF NEW CHIRAL LIGANDS
Immaculada Escofet Miquel

Chapter I
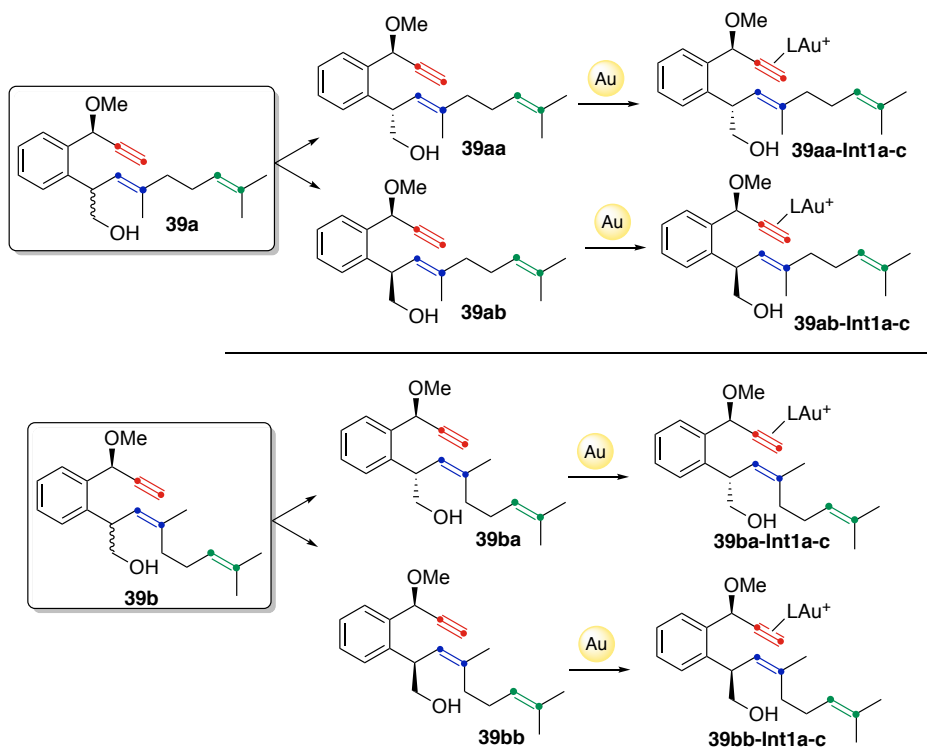
Scheme 26. Gold(I)-catalyzed formation of **Int1a-c** of dienyne **39** ((*E*)-configured **39a** and (*Z*)-configured **39b**). Each one in a 1:1.1 diastereomeric mixture (**39a** (**a** and **b**)) and (**39b** (**a** and **b**)).

Firstly, we investigated the mixture of diastereomers **39aa** and **39ab** (Scheme 27). In this case, six possible conformers of **Int1** (**39aa-Int1a-c**, **39ab-Int1a-c**) were found to have very similar energy. However, very different scenarios were observed for each diastereomer. For **39aa**, the three possible pathways have very similar energy barrier, differing only by 0.5 kcal/mol, being **39aa-Int3** the most favored. Direct formation of **39aa-Int7** *via* **39aa-TS$_{1a-7}$** was also observed. On the other hand, for **39ab**, formation of cyclopropyl gold(I)carbene **39ab-Int2** is more favored than **39ab-Int3** by at least 4.5 kcal/mol. Intermediate **39ab-Int2** would later give rise to **39ab-Int7** *via* **39ab-TS$_{2-7}$**, that has a very low energy barrier, 2.8 kcal/mol. Furthermore, direct formation of **39ab-Int7** was also observed from **39ab-Int1a** through **39ab-TS$_{1a-7}$**. Therefore, we conclude that for **39a**, isomer **39ab** reacts much more selectively than **39aa**. Thus, **39ab** would mainly give rise to **39ab-Int7**, whereas **39aa** would form a mixture of **39aa-Int7** and **39aa-Int2**.

For those intermediates having the alcohol moiety in *anti*-position with respect to the cyclopropyl (**39aa-Int2** and **39ab-Int3**), closure of the tetrahydrofuran ring has not been observed. This can be rationalized by the long distance between the hydroxy group and the site of the attack to the cyclopropyl. These intermediates could instead lead to the formation of naphthalene derivative side products **42**, by a loss of a molecule of formaldehyde and a single cleavage rearrangement (Scheme 25 and 28).

UNIVERSITAT ROVIRA I VIRGILI
COMPUTATIONAL MECHANISTIC STUDIES IN GOLD(I) CATALYSIS AND DESIGN OF NEW CHIRAL LIGANDS
Immaculada Escofet Miquel

Chapter I
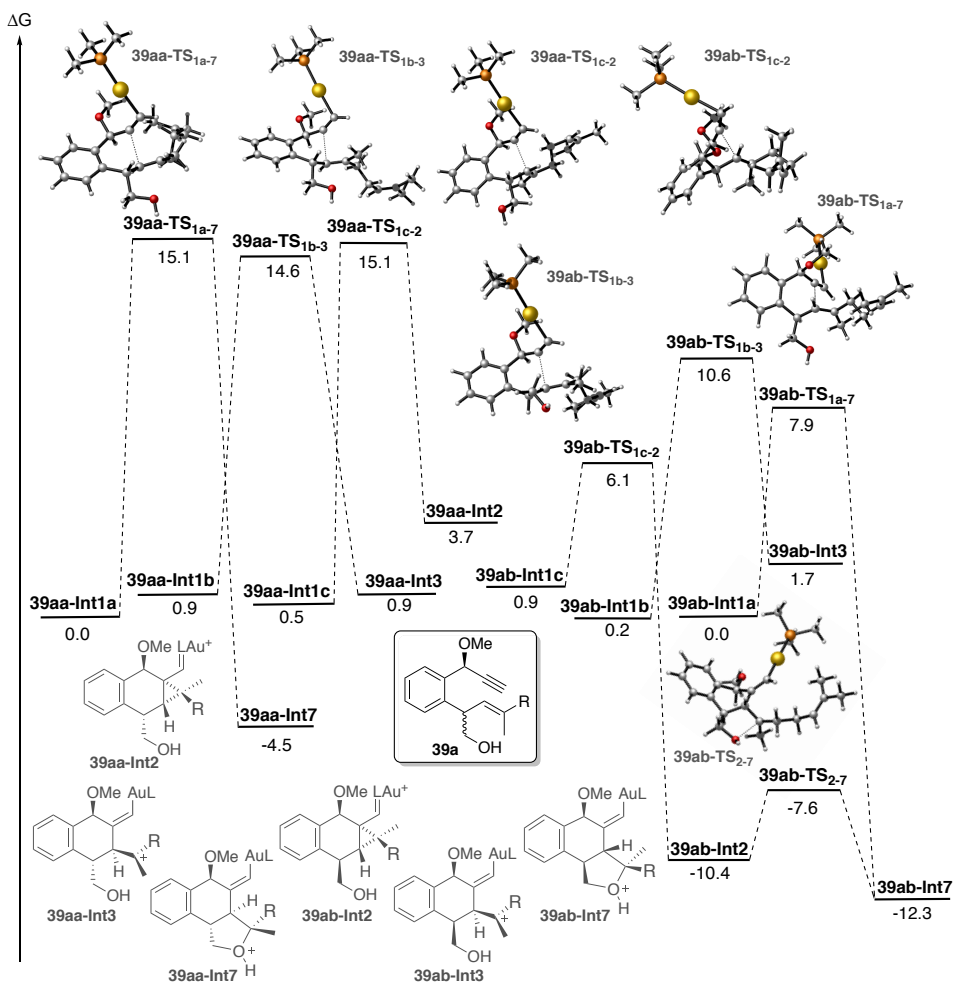
Scheme 27. Computed formation of intermediates type **Int2, Int3 and Int7** for enyne **39a**. L=PMe₃. DFT calculations performed with B3LYP-D3/6-31G(d) (C, H, O, P) and SDD (Au) in CH₂Cl₂ (PCM). Free energies in kcal/mol respect to **Int1a**.
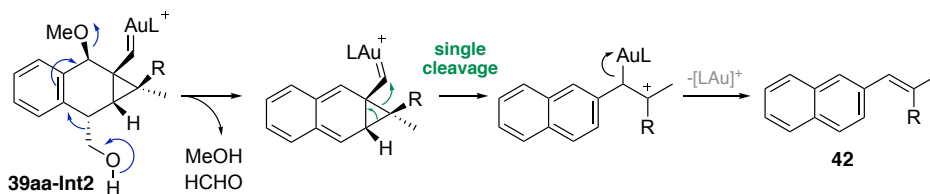
Scheme 28. Formation of side product **42** from **39aa-Int2** intermediate.

UNIVERSITAT ROVIRA I VIRGILI
COMPUTATIONAL MECHANISTIC STUDIES IN GOLD(I) CATALYSIS AND DESIGN OF NEW CHIRAL LIGANDS
Immaculada Escofet Miquel

Chapter I
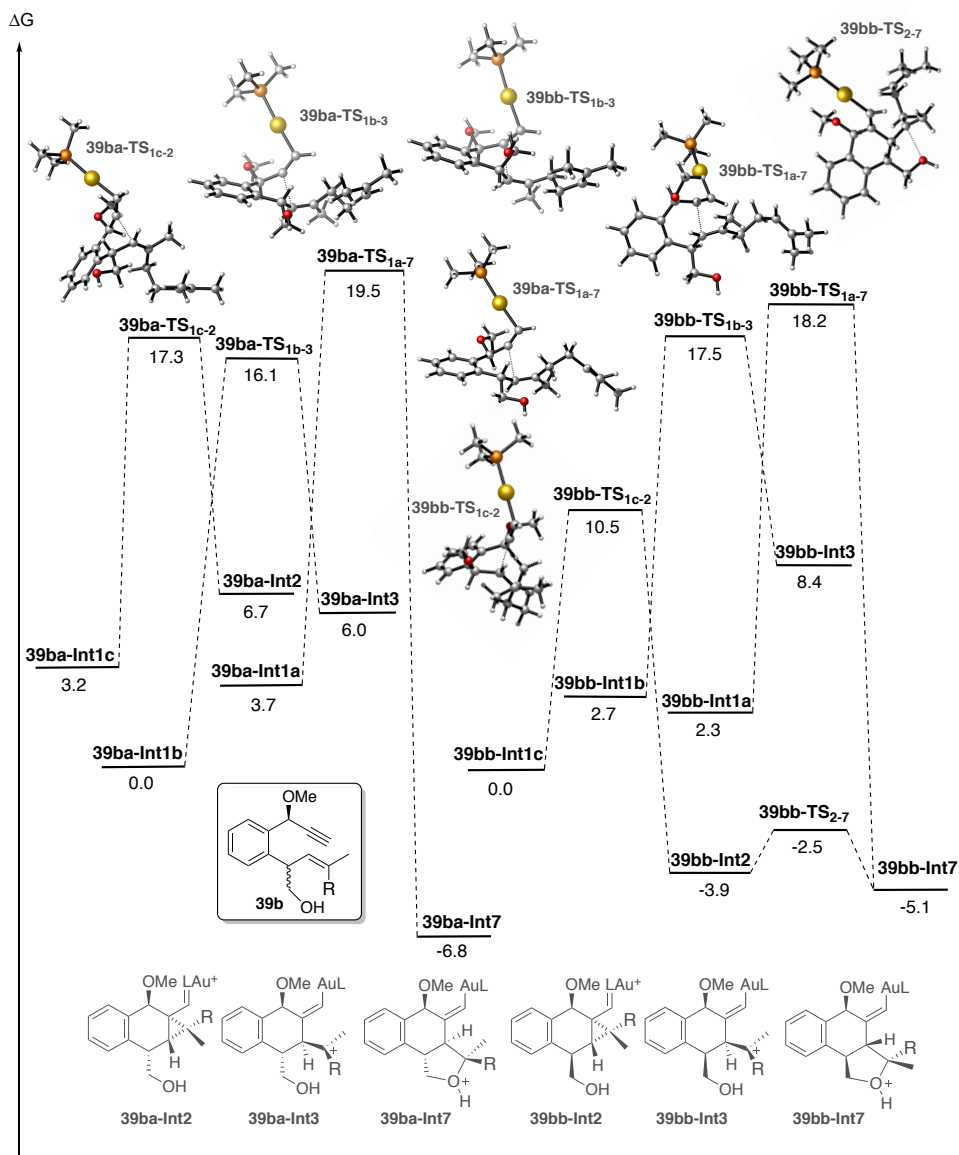
Scheme 29. Computed formation of intermediates type **Int2, Int3 and Int7** for enyne **39b**. L=PMe₃. DFT calculations performed with B3LYP-D3/6-31G(d) (C, H, O, P) and SDD (Au) in CH₂Cl₂ (PCM). Free energies in kcal/mol respect to **Int1a**.

Similarly, computed pathways for diastereomer **39ba** have very similar energy barriers leading to a mixture of products **39ba-Int2** and **39ba-Int7**, like in the case of **39aa**. Contrarily, for **39bb** the predominant pathway by at least 7 kcal/mol is the formation of cyclopropyl gold carbene **39bb-Int2** *via* **39bb-TS₁c-₂**, which would immediately give rise to **39bb-Int7** through **39bb-TS₂-₇**. Again, as it happened for **39aa-Int2**, the formation of tetrahydrofuran product type **Int7** was not observed from **39ba-Int2**. We assumed that this intermediate would also lead to the formation of corresponding (*Z*)-configured side product

UNIVERSITAT ROVIRA I VIRGILI
COMPUTATIONAL MECHANISTIC STUDIES IN GOLD(I) CATALYSIS AND DESIGN OF NEW CHIRAL LIGANDS
Immaculada Escofet Miquel

Chapter I

42 (Scheme 28). Hence, **39bb** would selectively lead to the formation of **39bb-Int7**, in good agreement with the experimental results. For this reason, when the reaction was attempted separately (**39ba** and **39bb**), both diastereomers delivered the same product **39b-Int8** (Scheme 30), although the reaction is much cleaner for **39bb** since no formation of side product **42** was observed.

For both substrates, **39a** and **39b**, the two possible intermediates would lead to the formation of same intermediates **39a-Int8** and **39b-Int8** by loosing the methoxy group (Scheme 30).
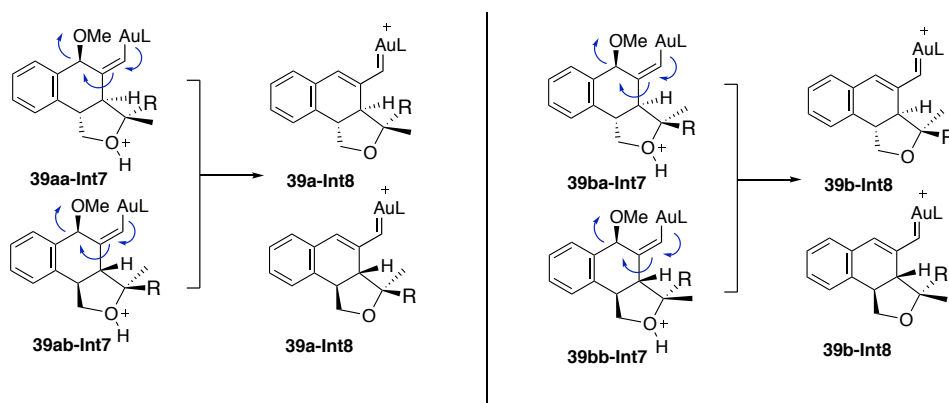
Scheme 30. Formation of intermediates **39a-Int8** and **39b-Int8** for substrates **39a** and **39b**.

To understand the selective formation of *trans*-fused rings **41** and **43** from **39a** and **39b** (Scheme 25), the last cyclopropanation step was computed from intermediates **39a-Int8** and **39b-Int8** (Scheme 31). For substrate **39a** with (*E*)-configured alkene, intermediate **39-Int8** can react further to form **39a-Int9a** *via* **39a-TS$_{8-9a}$** or **39a-Intb9b** through **39a-TS$_{8-9b}$**, respectively. Since these two possible pathways differ in 10.3 kcal/mol, formation of **39a-Int9a,** which leads to *trans*-fused cyclopropane **39-Int9a** (product **41**), is much more favorable than formation of **39a-Intb**, in agreement with our experimental results. However, for (*Z*)-alkene **39b**, two possible pathways compete to form **39b-Int9a** *via* **39b-TS$_{8-9a}$** or **39b-Intb9b** through **39b-TS$_{8-9b}$** giving rise to a mixture of *cis/trans*-cyclopropane products, *cis*-**44** (from **39b-Int9a**) being the major product and *trans*-**43** the minor one (from **39b-Intb9b**), as observed experimentally.

UNIVERSITAT ROVIRA I VIRGILI
COMPUTATIONAL MECHANISTIC STUDIES IN GOLD(I) CATALYSIS AND DESIGN OF NEW CHIRAL LIGANDS
Immaculada Escofet Miquel

Chapter I
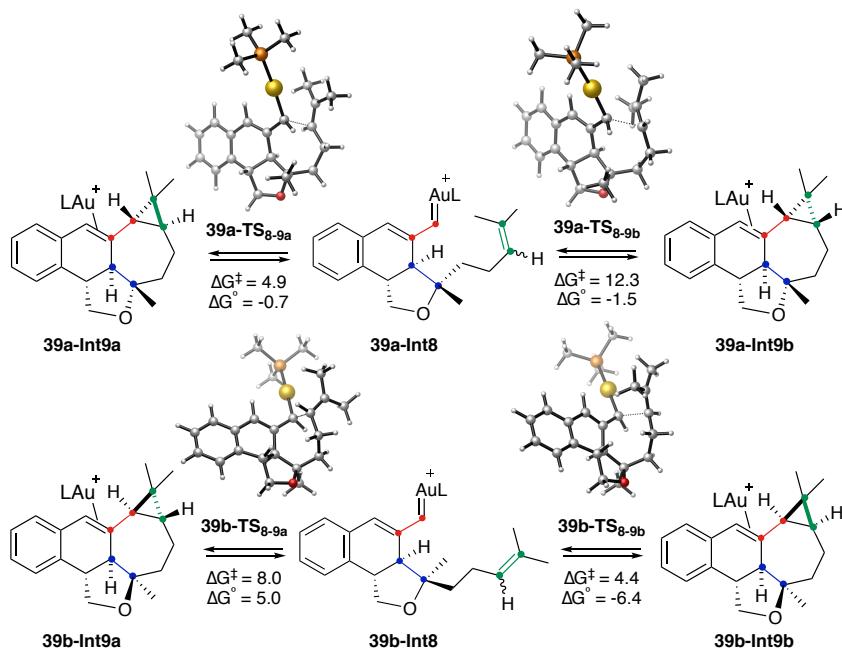
Scheme 31. Different mechanistic pathways for cyclopropanation reactions of intermediates **39a-Int8** and **39b-Int8**. L=PMe$_3$. DFT calculations performed with B3LYP-D3/6-31G(d) (C, H, O, P) and SDD (Au) in CH$_2$Cl$_2$ (PCM). Free energies in kcal/mol.

UNIVERSITAT ROVIRA I VIRGILI
COMPUTATIONAL MECHANISTIC STUDIES IN GOLD(I) CATALYSIS AND DESIGN OF NEW CHIRAL LIGANDS
Immaculada Escofet Miquel

Chapter I

Conclusions

A detailed computational study on the structure of cyclopropyl gold(I) carbenes and their isomeric forms has been performed for different 1,6-enynes (Scheme 32).
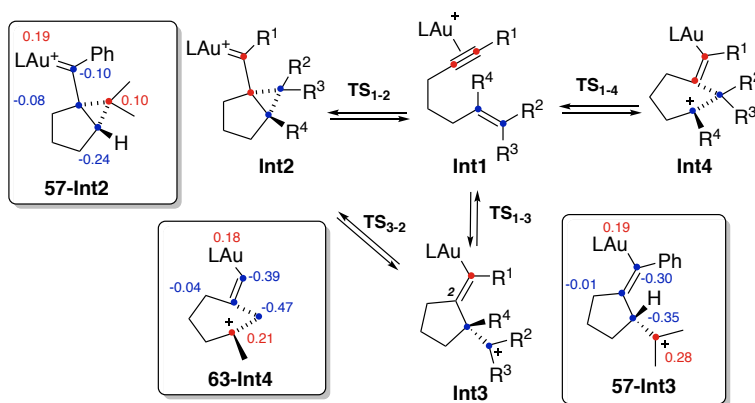
Scheme 32. Different possible pathways for the formation of carbene **Int2**, open carbocation **Int3** and **Int4**. Summary of Natural Population Analysis (NPA charges) by NBO analysis of **57-Int2**, **57-Int3** and **64-Int3** optimized at the BP86. Positive charges in red and negative charges in blue.

For terminal alkenes ($R^2 = R^3 = H$), **Int4** was the only intermediate formed whereas both cyclopropyl gold carbene **Int2** and open carbocation **Int3** were observed for those enynes having disubstituted alkenes ($R^2 = R^3 = Me$). These two species were found to be connected through **TS$_{3-2}$**. However, formation of **Int2**, **Int3** or **Int4** for enynes having monosubstituted alkenes ($R^2 = Me$, $R^3 = H$) depends on the substitution of the alkyne moiety. Thus, enynes containing a terminal alkyne lead to the formation of **Int4**, whereas when $R^1 = Ph$, formation of both **Int2** and **Int3** was observed.

The nature of these different intermediates was further studied by benchmark of DFT methods that confirm the presence of the three species **Int2**, **Int3** or **Int4** for all functionals tested. Moreover, different angles and distances together with QTAIM theory confirmed that the molecular representation of these species was accurate. NBO analysis were also performed, and NPA charges were clearly delocalized confirming the carbenic or cationic character of these species.

Remarkably, the same three intermediates were obtained when switching from gold(I) to indium(III). Thus, we computed the system using InCl$_3$ as catalyst and **Int3** was found to be the favored species, in contrast to results obtained for gold(I) systems, where **Int2** was the preferred intermediate.

UNIVERSITAT ROVIRA I VIRGILI
COMPUTATIONAL MECHANISTIC STUDIES IN GOLD(I) CATALYSIS AND DESIGN OF NEW CHIRAL LIGANDS
Immaculada Escofet Miquel

Chapter I

Furthermore, in our studies towards the total synthesis of jatrophalactone (**35**), we discovered a new gold(I)-catalyzed cyclization cascade of functionalized 7,11-dien-1-ynes that leads to the selective formation of unexpected *trans*-fused cyclopropanes, depending on the dienyne geometry. DFT calculations showed that this specific selectivity was directed by the rigidity of the system in the final cyclopropanation step. Likewise, computed pathways help us to rationalize the role of the formation of the fused tetrahydrofuran ring into the selective final cyclopropanation step. Hence, *(E)*-configured dienynes **39a** afforded *trans*-fused cyclopropane **41** as single diastereomer upon cyclopropanation of **39a-Int8** intermediate *via* **39a-TS8-9a**. The analogous diastereomeric mixture of (Z)-configured **39b** led to an inseparable mixture of isomers **43** and **44** through the competing pathways **39b-TS8-9a** and **39b-TS8-9b**, being this last one 3.4 kcal/mol more favorable (Scheme 33). Noteworthy, formation of both types of intermediates **Int2** and **Int3** were observed for these systems.
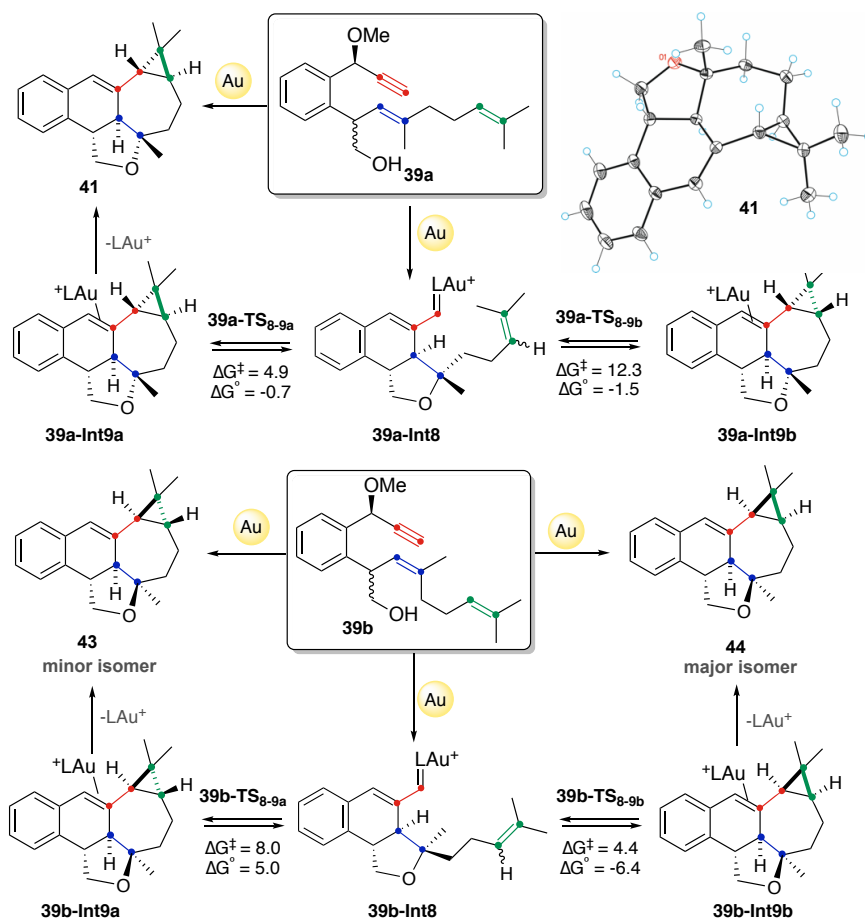
Scheme 33. Proposed mechanism for the formation of carbene products **41**, **43** and **44**. ORTEP representation of **41** with 50% probability of the thermal ellipsoids.

UNIVERSITAT ROVIRA I VIRGILI
COMPUTATIONAL MECHANISTIC STUDIES IN GOLD(I) CATALYSIS AND DESIGN OF NEW CHIRAL LIGANDS
Immaculada Escofet Miquel

Chapter I

Computational Methods

Calculations were performed by means of the Gaussian 09 suite of programs.[50] DFT was applied using B3LYP-D3,[37] M06-D3,[39] and BP86-D3[34] functionals. The SDD basis set and ECP was used to describe Au.[51] The LANL2DZ basis set[52] was utilized to describe In and Cl with ECP and addition polarization function ($\zeta d = 0.143$ for In, $\zeta d = 0.640$ for Cl).[53] The 6-31G(d) basis set[54] was employed for all remaining atoms (C, H, P, and O). Full geometry optimizations were carried out in dichloromethane, through an implicit polarizable continuum model (PCM) as implemented in Gaussian 09.[55] The stationary points were characterized by vibrational analysis. Transition states were identified by the presence of one imaginary frequency while minima by a full set of real frequencies. The connectivity of the transition states was confirmed by the relaxation of each transition state towards both the reactant and the product. Reported energies are potential energies (E) and free energies (G) in solution, computed at 298 K and 1 atm.

50   Gaussian 09, Revision B.1, Frisch, M. J.; Trucks, G. W.; Schlegel, H. B.; Scuseria, G. E.; Robb, M. A.; Cheeseman, J. R.; Scalmani, G.; Barone, V.; Mennucci, B.; Petersson, G. A.; Nakatsuji, H.; Caricato, M.; Li, X.; Hratchian, H. P.; Izmaylov, A. F.; Bloino, J.; Zheng, G.; Sonnenberg, J. L.; Hada, M.; Ehara, M.; Toyota, K.; Fukuda, R.; Hasegawa, J.; Ishida, M.; Nakajima, T.; Honda, Y.; Kitao, O.; Nakai, H.; Vreven, T.; Montgomery, J. A.; Peralta, Jr. J. E.; Ogliaro, F.; Bearpark, M.; Heyd, J. J.; Brothers, E.; Kudin, K. N.; Staroverov, V. N.; Kobayashi, R.; Normand, J.; Raghavachari, K.; Rendell, A.; Burant, J. C.; Iyengar, S. S.; Tomasi, J.; Cossi, M.; Rega, N.; Millam, J. M.; Klene, M.; Knox, J. E.; Cross, J. B.; Bakken, V.; Adamo, C.; Jaramillo, J.; Gomperts, R.; Stratmann, R. E.; Yazyev, O.; Austin, A. J.; Cammi, R.; Pomelli, C.; Ochterski, J. W.; Martin, R. L.; Morokuma, K.; Zakrzewski, V. G.; Voth, G. A.; Salvador, P.; Dannenberg, J. J.; Dapprich, S.; Daniels, A. D.; Farkas, Ö.; Foresman, J. B.; Ortiz, J. V.; Cioslowski, J.; Fox, D. J. Gaussian, Inc., Wallingford CT **2009**.
51   Andrae, D.; Haussermann, U.; Dolg, M.; Stoll, H.; Preuss, H. *Theor. Chim. Acta.* **1990**, *77*, 123–141.
52   Hay, P. J.; Wadt, W. R. *J. Chem. Phys.* **1985**, *82*, 270–283.
53   Höllwarth, A.; Böhme, M.; Dapprich, S.; Ehlers, A. W.; Gobbi, A.; Jonas, V.; Köhler, K. F.; Stegmann, R.; Veldkamp, A.; Frenking, G. *Chem. Phys. Lett.* **1993**, *208*, 237–240.
54   Hehre, W. J.; Ditchfield, R.; Pople, J. A. *J. Chem. Phys.* **1972**, *56*, 2257–2261.
55   Cancès, M. T.; Mennucci, B. B.; Tomasi, J. *J. Chem. Phys.* **1997**, *107*, 3032−3041.

UNIVERSITAT ROVIRA I VIRGILI
COMPUTATIONAL MECHANISTIC STUDIES IN GOLD(I) CATALYSIS AND DESIGN OF NEW CHIRAL LIGANDS
Immaculada Escofet Miquel

Chapter I

Computed Structures and Energies (M06-D3, B3LYP-D3 and BP86-D3)

57-Int1
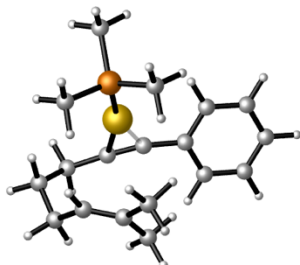
E = - 1179.30316221 Hartrees
G = -1178.968694 Hartrees

57-TS$_{1-3}$
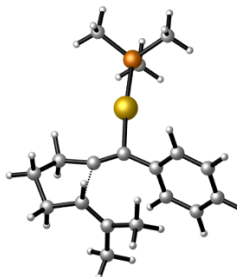
E = - 1179.28460928 Hartrees
G = -1178.951557 Hartrees

57-Int2
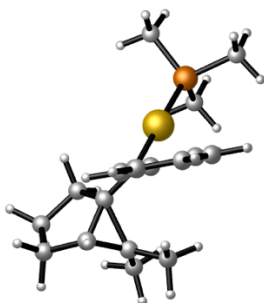
E = -1179.30573929 Hartrees
G = -1178.967494 Hartrees

57-TS$_{1-2}$
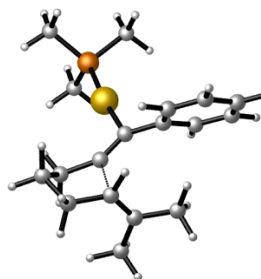
E = -1179.28834677 Hartrees
G = -1178.953159 Hartrees

57-Int3
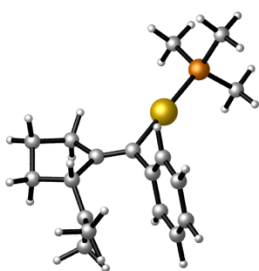
E = -1179.30322281 Hartrees
E = -1178.965207 Hartrees

57-TS$_{3-2}$
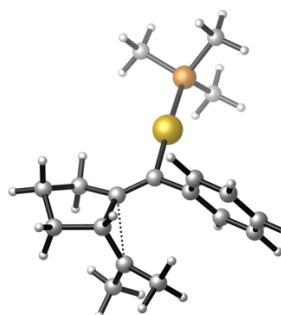
E = -1179.29900272 Hartrees
E = -1178.960965 Hartrees

UNIVERSITAT ROVIRA I VIRGILI
COMPUTATIONAL MECHANISTIC STUDIES IN GOLD(I) CATALYSIS AND DESIGN OF NEW CHIRAL LIGANDS
Immaculada Escofet Miquel

Chapter I
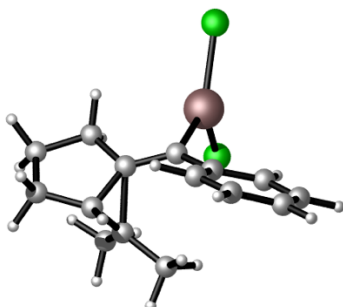
57-In-Int2

E = -613.609319868 Hartrees
E = -613.368953 Hartrees

57-In-Int3
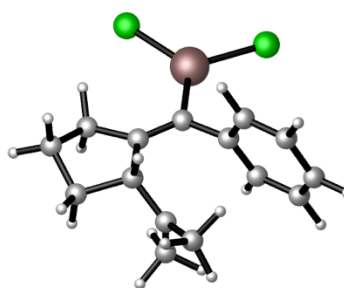
E = -613.619052439 Hartrees
E = -613.381060 Hartrees

63-In-Int4
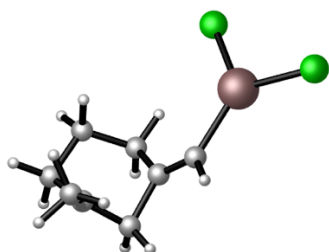
E = -343.460852054 Hartrees
G = -343.323227 Hartrees

63-Int4
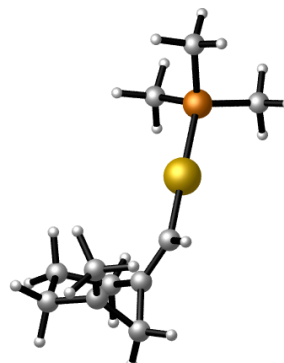
E = -908.382142047 Hartrees
G = -908.135865 Hartrees

64-TS$_{1-5}$
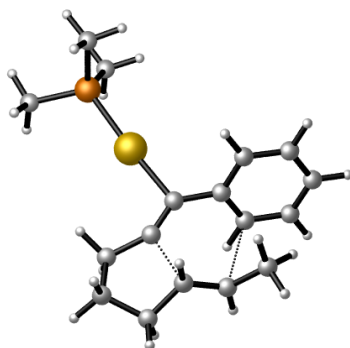
E = -1139.21816081 Hartrees
G = -1138.902158 Hartrees

64-Int1
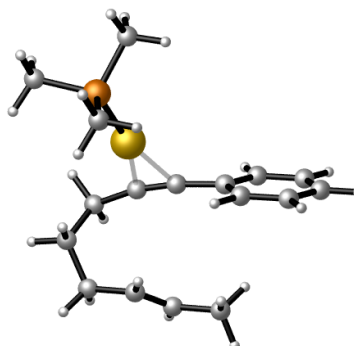
E = -1139.24482632 Hartrees
G = -1138.929412 Hartrees

UNIVERSITAT ROVIRA I VIRGILI
COMPUTATIONAL MECHANISTIC STUDIES IN GOLD(I) CATALYSIS AND DESIGN OF NEW CHIRAL LIGANDS
Immaculada Escofet Miquel

Chapter I

64-Int5
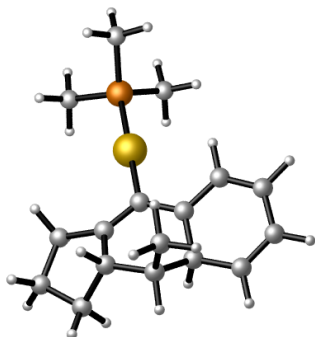
E = -1139.26531603 Hartrees
G = -1138.941015 Hartrees

66-Int1
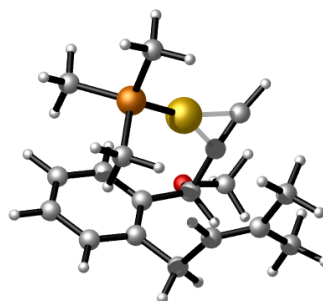
E = -1254.40405230 Hartrees
G = -1254.054442 Hartrees

66-TS$_{1-2}$
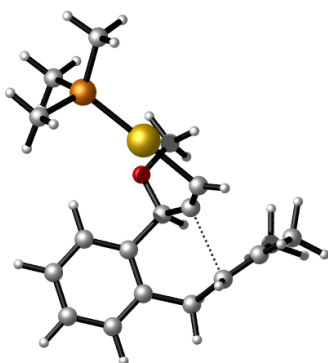
E = -1254.38829242 Hartrees
G = -1254.037760 Hartrees

66-Int3
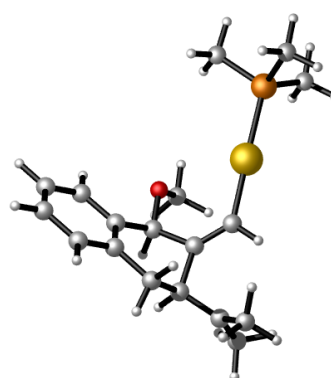
E = -1254.39282795 Hartrees
G = -1254.041865 Hartrees

66-Int2
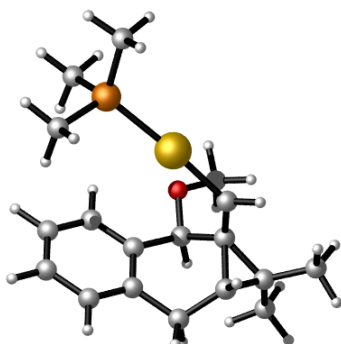
E = -1254.41262414 Hartrees
G = -1254.056248 Hartrees

LAu
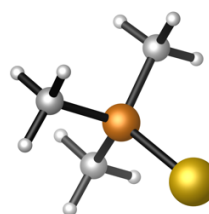
E = -596.765373204 Hartrees
G = -596.683236 Hartrees

UNIVERSITAT ROVIRA I VIRGILI
COMPUTATIONAL MECHANISTIC STUDIES IN GOLD(I) CATALYSIS AND DESIGN OF NEW CHIRAL LIGANDS
Immaculada Escofet Miquel

Chapter I

66-TS₁₋₃
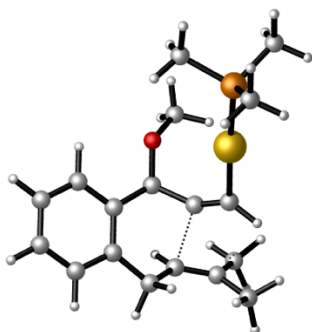
E = -1254.38026719 Hartrees
G = -1254.031808 Hartrees

67a-Int1a
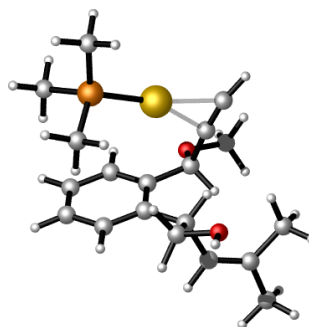
E = -1368.92317945 Hartrees
G = -1368.545726 Hartrees

67a-Int7
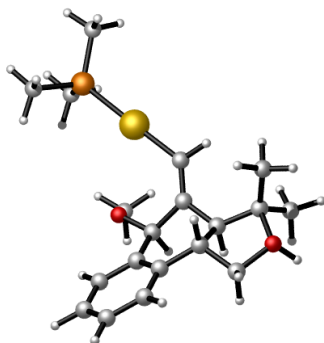
E = -1368.94024197 Hartrees
G = -1368.550787 Hartrees

67a-TS₁ₐ₋₇
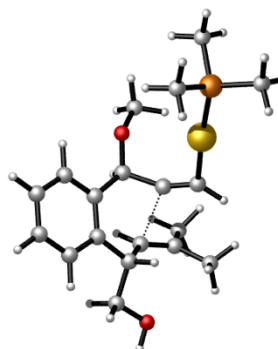
E = -1368.90193066 Hartrees
G = -1368.524121 Hartrees

67a-Int3
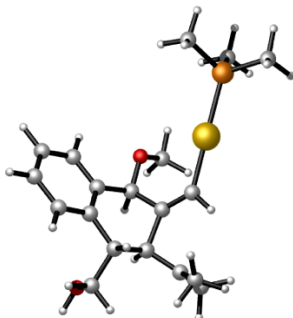
E = -1368.91701766 Hartrees
G = -1368.536022 Hartrees

67a-Int1b
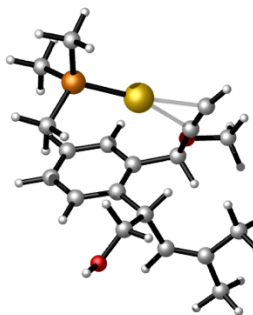
E = -1368.92324624 Hartrees
G = -1368.543656 Hartrees

UNIVERSITAT ROVIRA I VIRGILI
COMPUTATIONAL MECHANISTIC STUDIES IN GOLD(I) CATALYSIS AND DESIGN OF NEW CHIRAL LIGANDS
Immaculada Escofet Miquel

Chapter I
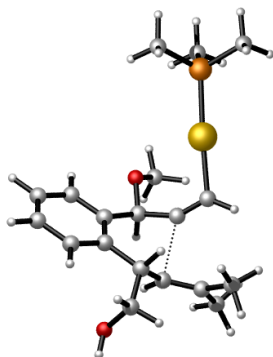
67a-TS1b-3

67a-Int2

E = -1368.90151312 Hartrees
G = -1368.522662 Hartrees
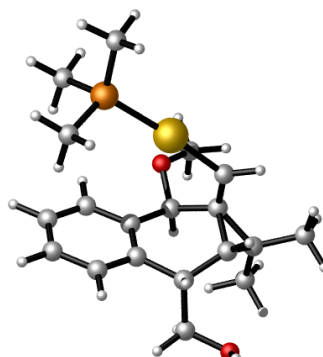
E = -1368.93360849 Hartrees
G = -1368.546537 Hartrees

67a-Int1c
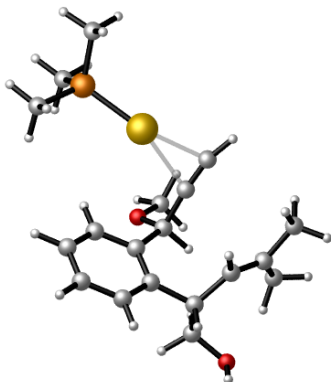
67a-TS$_{1c-2}$

E = -1368.91397062 Hartrees
G = -1368.534565 Hartrees
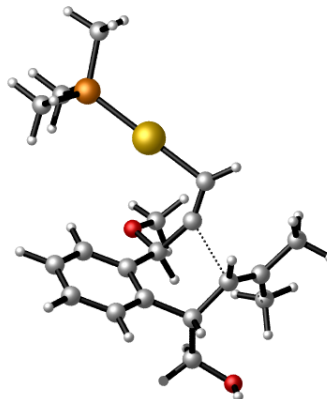
E = -1368.90600042 Hartrees
G = -1368.525282 Hartrees

67b-Int1a
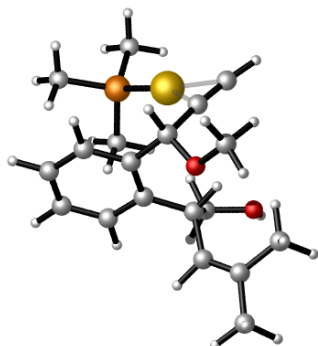
67b-Int7

E = -1368.92306171 Hartrees
G = -1368.545266 Hartrees
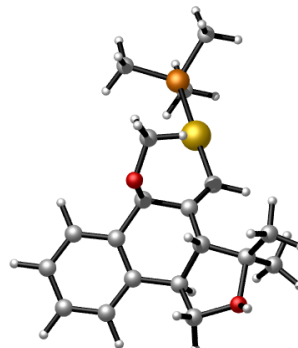
E = -1368.94611390 Hartrees
G = -1368.558095 Hartrees

UNIVERSITAT ROVIRA I VIRGILI
COMPUTATIONAL MECHANISTIC STUDIES IN GOLD(I) CATALYSIS AND DESIGN OF NEW CHIRAL LIGANDS
Immaculada Escofet Miquel

Chapter I
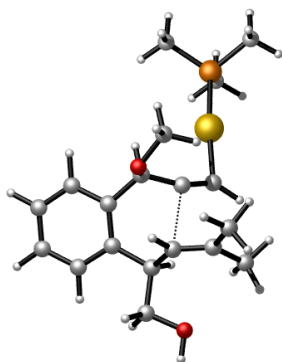
67b-TS₁ₐ₋₇

E = -1368.90119474 Hartrees
G = -1368.523143 Hartrees

67b-Int3
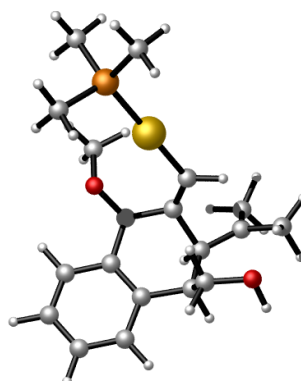
E = -1368.91603181 Hartrees
G = -1368.533997 Hartrees

67b-Int1b
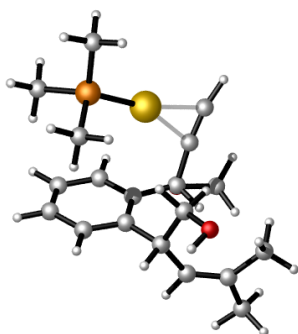
E = -1368.91778045 Hartrees
G = -1368.538029 Hartrees

67b-TS1b-3
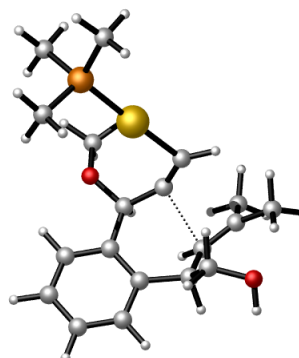
E = -1368.89989606 Hartrees
G = -1368.520042 Hartrees

67b-Int2
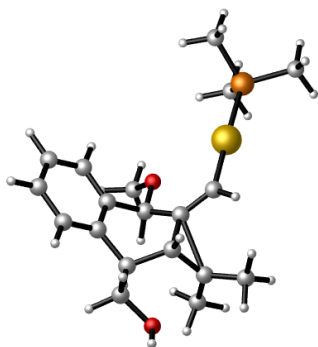
E = -1368.93355617 Hartrees
G = -1368.550308 Hartrees

67b-Int1c
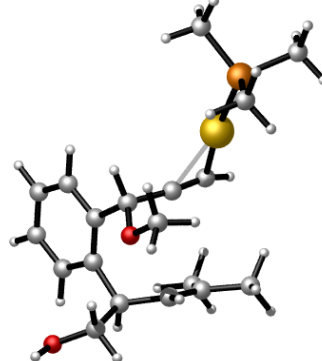
E = -1368.90989075 Hartrees
G = -1368.532370 Hartrees

UNIVERSITAT ROVIRA I VIRGILI
COMPUTATIONAL MECHANISTIC STUDIES IN GOLD(I) CATALYSIS AND DESIGN OF NEW CHIRAL LIGANDS
Immaculada Escofet Miquel

Chapter I

67b-TS$_{1c-2}$
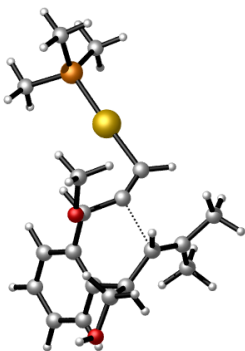
E = -1368.90529544 Hartrees
G = -1368.527754 Hartrees

67b-TS$_{2-7}$
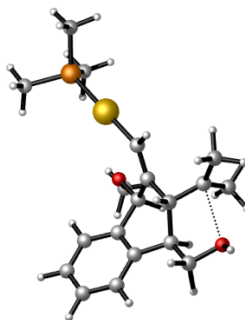
E = -1368.91778045 Hartrees
G = -1368.538029 Hartrees

39a-Int9b
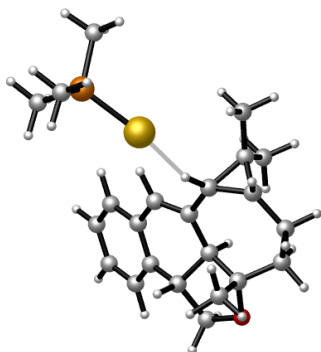
E = -1448.58561868 Hartrees
G = -1448.136303 Hartrees

39a-TS$_{8-9b}$
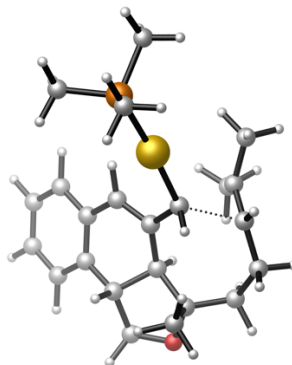
E = -1448.56561761 Hartrees
G = -1448.114332 Hartrees

39a-Int8
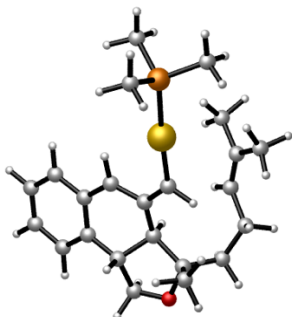
E = -1448.58726727 Hartrees
G = -1448.138627 Hartrees

39a-Int9a
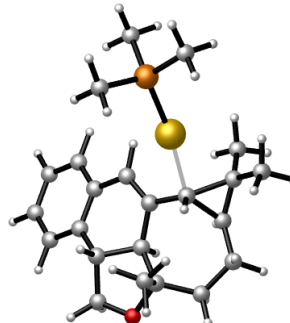
E = -1448.59199111 Hartrees
G = -1448.139731 Hartrees

UNIVERSITAT ROVIRA I VIRGILI
COMPUTATIONAL MECHANISTIC STUDIES IN GOLD(I) CATALYSIS AND DESIGN OF NEW CHIRAL LIGANDS
Immaculada Escofet Miquel

Chapter I

39a-TS$_{8-9a}$
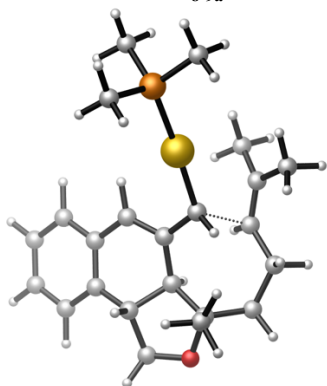
E = -1448.58026045 Hartrees
G = -1448.130782 Hartrees

39aa-Int7
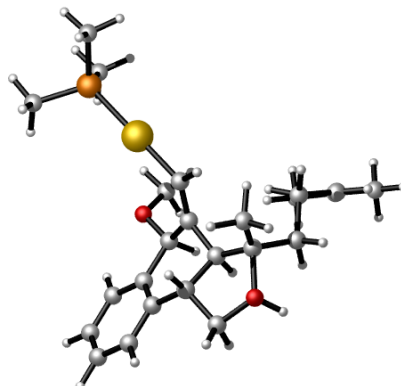
E = -1564.29165613 Hartrees
G = -1563.794700 Hartrees

39aa-TS$_{1a-7}$
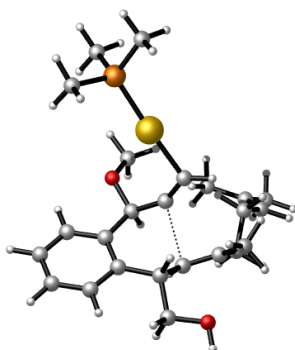
E = -1564.25358617 Hartrees
G = -1563.763505 Hartrees

39aa-Int1a
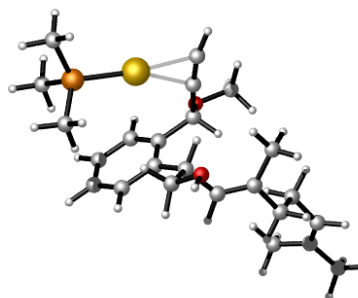
E = -1564.27304488 Hartrees
G = -1563.787559 Hartrees

39aa-TS$_{1b-3}$
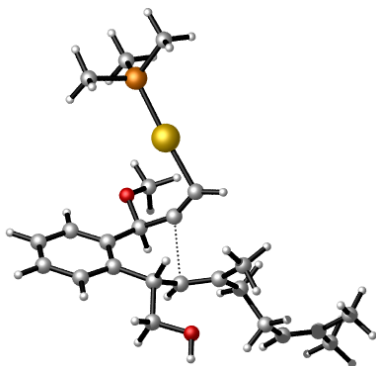
E = -1564.25172581 Hartrees
G = -1563.764369 Hartrees

39aa-Int3
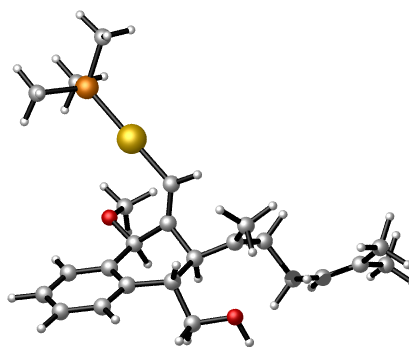
E = -1564.27825180 Hartrees
G = -1563.786203 Hartrees

UNIVERSITAT ROVIRA I VIRGILI
COMPUTATIONAL MECHANISTIC STUDIES IN GOLD(I) CATALYSIS AND DESIGN OF NEW CHIRAL LIGANDS
Immaculada Escofet Miquel

Chapter I
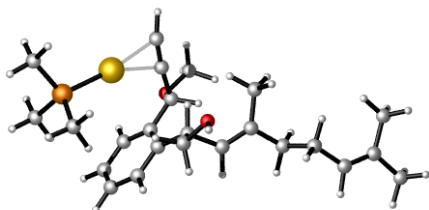
39aa-Int1b

E = -1564.27204468 Hartrees
G = -1563.786146 Hartrees

39aa-TS₁c-₂
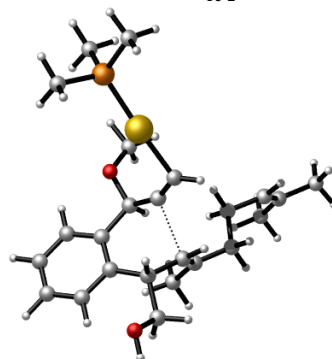
E = -1564.25159275 Hartrees
G = -1563.763481 Hartrees

39aa-Int2
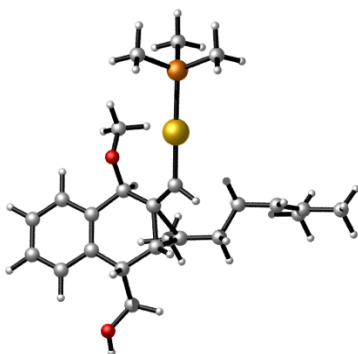
E = -1564.27609729 Hartrees
G = -1563.781710 Hartrees

39aa-Int1c
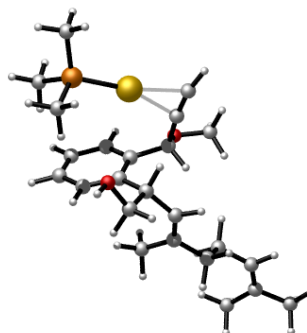
E = -1564.27345491 Hartrees
G = -1563.786711 Hartrees

39ab-Int7
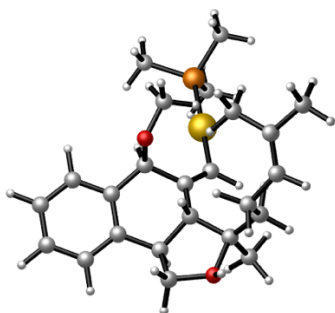
E = -1564.29627700 Hartrees
G = -1563.797108 Hartrees

39ab-TS₁a-₇
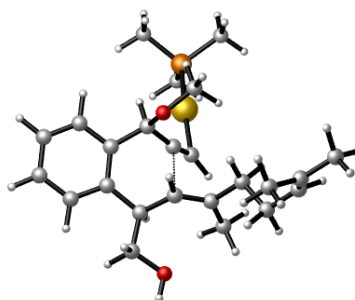
E = -1564.25087812 Hartrees
G = -1563.764848 Hartrees

UNIVERSITAT ROVIRA I VIRGILI
COMPUTATIONAL MECHANISTIC STUDIES IN GOLD(I) CATALYSIS AND DESIGN OF NEW CHIRAL LIGANDS
Immaculada Escofet Miquel

Chapter I
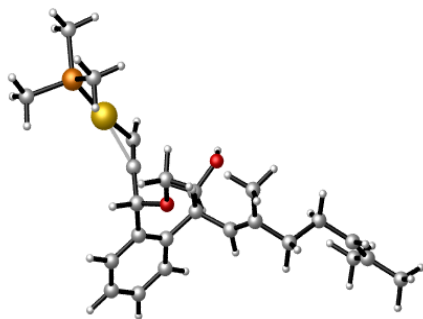
39ab-Int1a

E = -1564.26158377 Hartrees
G = -1563.776581 Hartrees

39ab-TS₁ᵦ₋₃
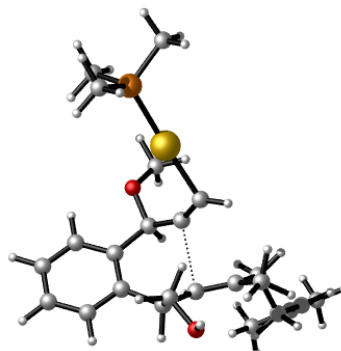
E = -1564.24870522 Hartrees
G = -1563.760591 Hartrees

39ab-Int3
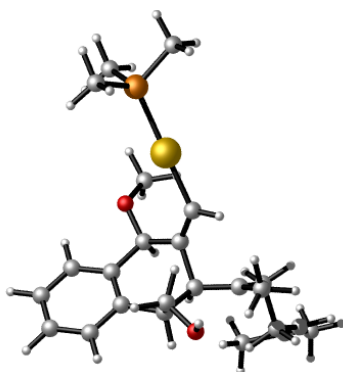
E = -1564.26822499 Hartrees
G = -1563.774696 Hartrees

39ab-Int1b
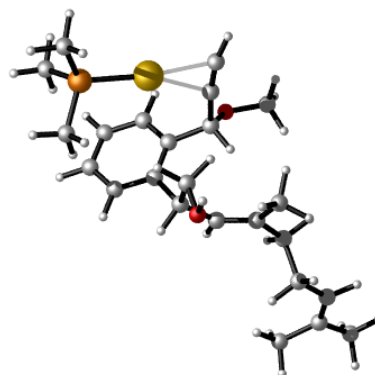
E = -1564.26611105 Hartrees
G = -1563.777769 Hartrees

39ab-TS₁ᵪ₋₂
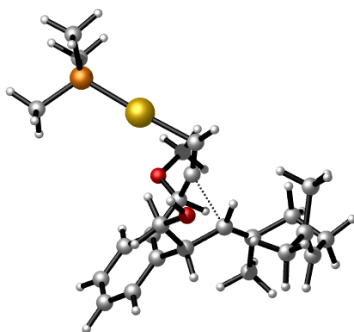
E = -1564.25648322 Hartrees
G = -1563.767707 Hartrees

39ab-Int2
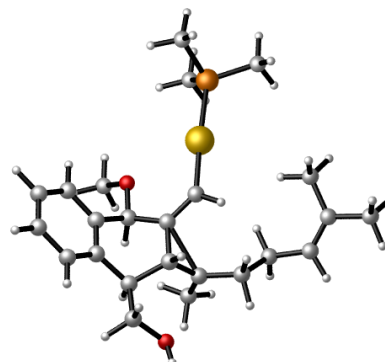
E = -1564.28730302 Hartrees
G = -1563.794081 Hartrees

UNIVERSITAT ROVIRA I VIRGILI
COMPUTATIONAL MECHANISTIC STUDIES IN GOLD(I) CATALYSIS AND DESIGN OF NEW CHIRAL LIGANDS
Immaculada Escofet Miquel

Chapter I

39ab-Int1c
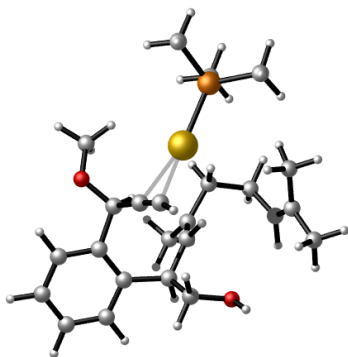
E = -1564.26731024 Hartrees
G = -1563.776094 Hartrees

39ab-TS$_{2-7}$
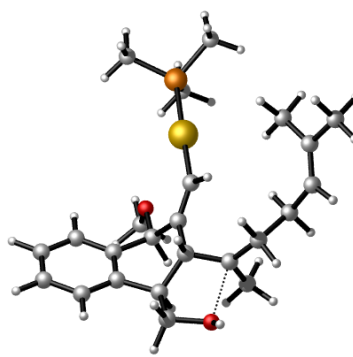
E = -1564.28489795 Hartrees
G = -1563.789574 Hartrees

39b-Int9b
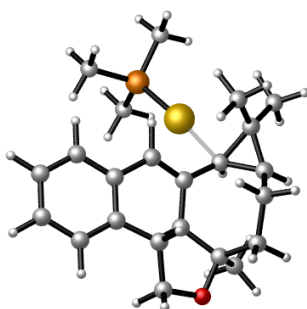
E = -1448.59953985 Hartrees
G = -1448.145193 Hartrees

39b-Int8
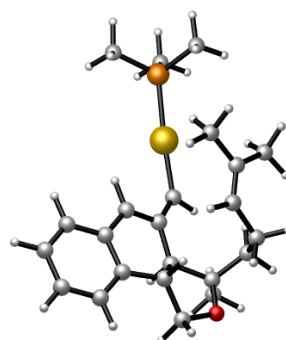
E = -1448.58346222 Hartrees
G = -1448.134787 Hartrees

39b-TS$_{8-9b}$
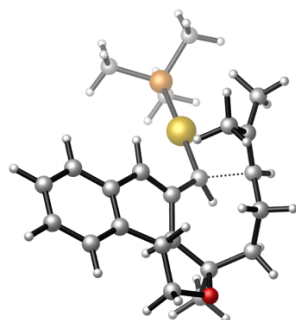
E = -1448.57804943 Hartrees
G = -1448.127928 Hartrees

39b-Int9a
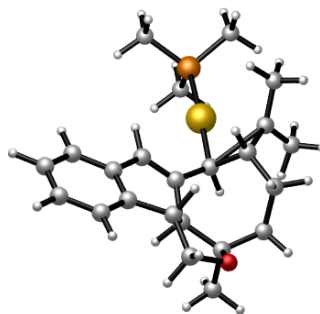
E = -1448.57750726 Hartrees
G = -1448.124763 Hartrees

UNIVERSITAT ROVIRA I VIRGILI
COMPUTATIONAL MECHANISTIC STUDIES IN GOLD(I) CATALYSIS AND DESIGN OF NEW CHIRAL LIGANDS
Immaculada Escofet Miquel

Chapter I

39b-TS$_{8-9a}$
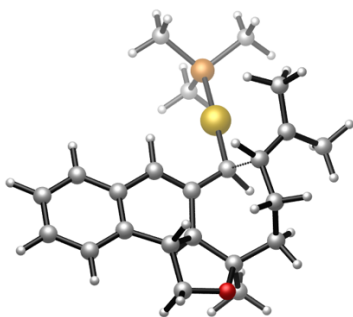
E = -1448.57198018 Hartrees
G = -1448.120759 Hartrees

39ba-Int7
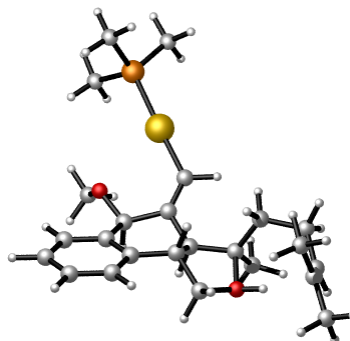
E = -1564.29916745 Hartrees
G = -1563.800204 Hartrees

39ba-TS$_{1a-7}$
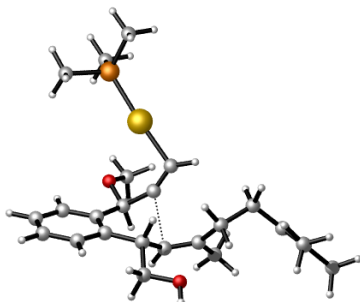
E = -1564.24784951 Hartrees
G = -1563.758383 Hartrees

39ba-Int1a
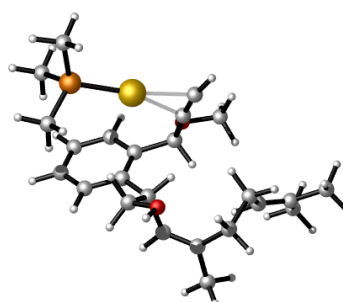
E = -1564.27378225 Hartrees
G = -1563.783491 Hartrees

39ba-TS$_{1b-3}$
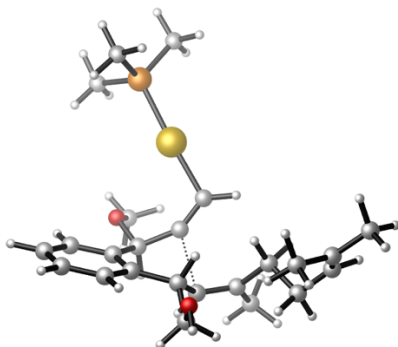
E = -1564.25496360 Hartrees
G = -1563.763850 Hartrees

39ba-Int3
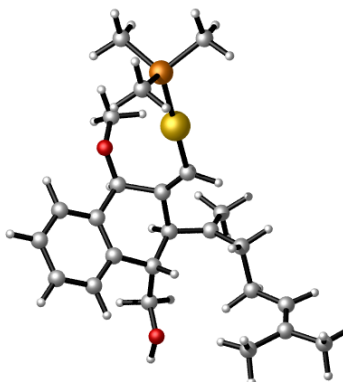
E = -1564.27137108 Hartrees
G = -1563.779811 Hartrees

UNIVERSITAT ROVIRA I VIRGILI
COMPUTATIONAL MECHANISTIC STUDIES IN GOLD(I) CATALYSIS AND DESIGN OF NEW CHIRAL LIGANDS
Immaculada Escofet Miquel

Chapter I
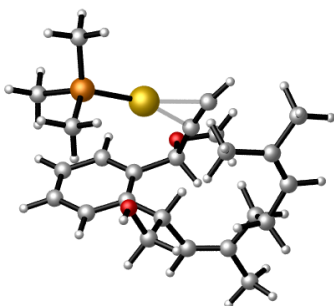
39ba-Int1b

E = -1564.28235145 Hartrees
G = -1563.789428 Hartrees

39ba-TS₁c-₂
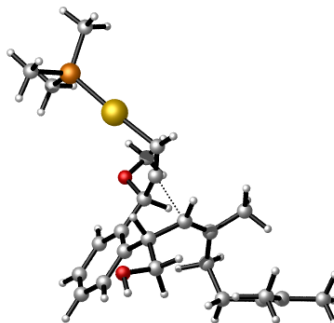
E = -1564.25179227 Hartrees
G = -1563.761877 Hartrees

39ba-Int2
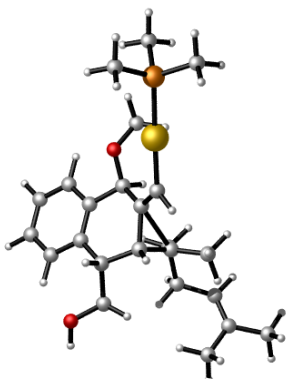
E = -1564.27412822 Hartrees
G = -1563.778697 Hartrees

39ba-Int1c
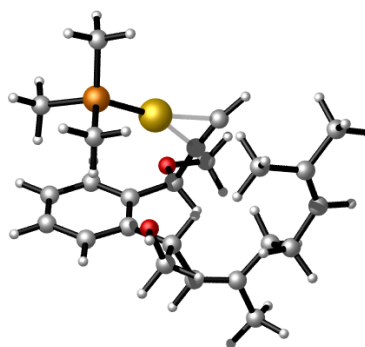
E = -1564.27486872 Hartrees
G = -1563.784277 Hartrees

39bb-Int7
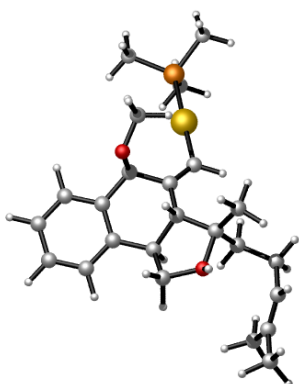
E = -1564.29084246 Hartrees
G = -1563.794540 Hartrees

39bb-TS₁a-₇
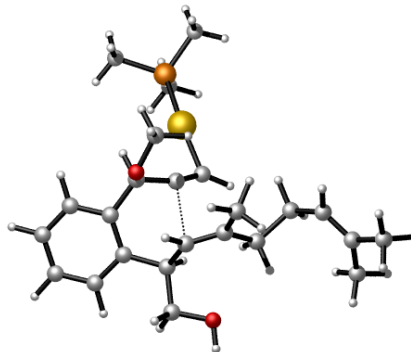
E = -1564.24652057 Hartrees
G = -1563.757227 Hartrees

UNIVERSITAT ROVIRA I VIRGILI
COMPUTATIONAL MECHANISTIC STUDIES IN GOLD(I) CATALYSIS AND DESIGN OF NEW CHIRAL LIGANDS
Immaculada Escofet Miquel

Chapter I

39bb-Int1a
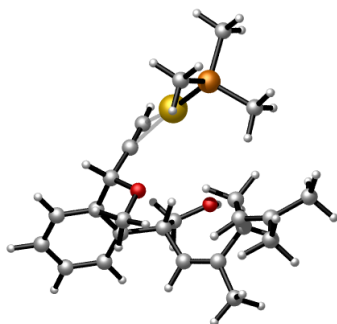
39bb-TS$_{1b-3}$

E = -1564.27317825 Hartrees
G = -1563.782591 Hartrees
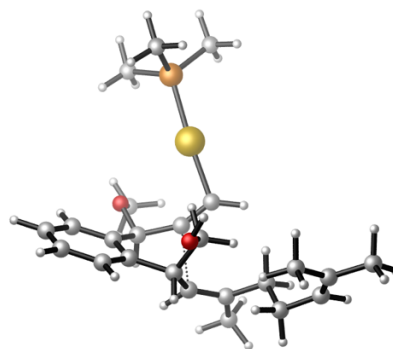
E = -1564.24880489 Hartrees
G = -1563.758370 Hartrees

39bb-Int3
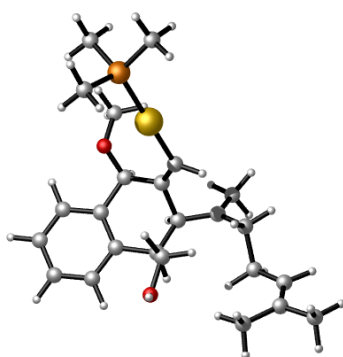
39bb-Int1b

E = -1564.26625952 Hartrees
G = -1563.772765 Hartrees
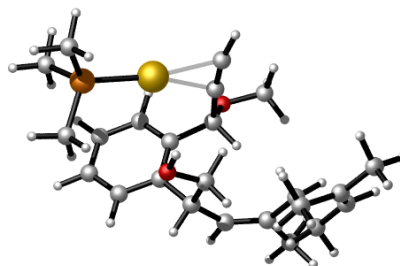
E = -1564.27242276 Hartrees
G = -1563.781873 Hartrees

39bb-TS$_{1c-2}$
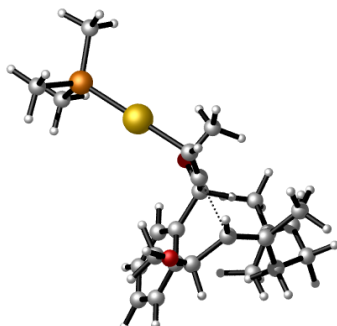
39bb-Int2

E = -1564.26056720 Hartrees
G = -1563.769491 Hartrees
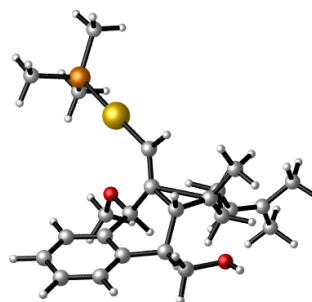
E = -1564.28566898 Hartrees
G = -1563.792408 Hartrees

UNIVERSITAT ROVIRA I VIRGILI
COMPUTATIONAL MECHANISTIC STUDIES IN GOLD(I) CATALYSIS AND DESIGN OF NEW CHIRAL LIGANDS
Immaculada Escofet Miquel

Chapter I

39bb-Int1c
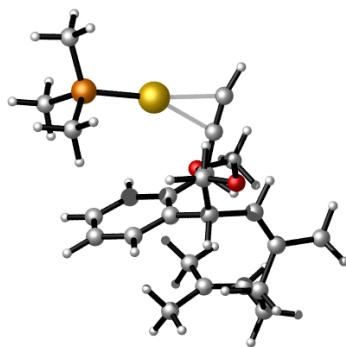
39bb-TS$_{2-7}$

E = -1564.27668737 Hartrees
G = -1563.786229 Hartrees
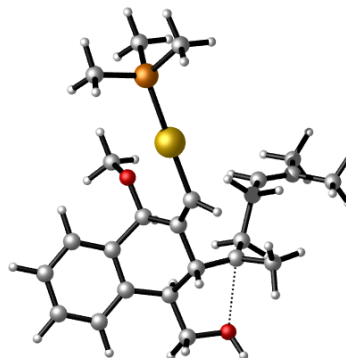
E = -1564.28466804 Hartrees
G = -1563.790183 Hartrees

UNIVERSITAT ROVIRA I VIRGILI
COMPUTATIONAL MECHANISTIC STUDIES IN GOLD(I) CATALYSIS AND DESIGN OF NEW CHIRAL LIGANDS
Immaculada Escofet Miquel

UNIVERSITAT ROVIRA I VIRGILI
COMPUTATIONAL MECHANISTIC STUDIES IN GOLD(I) CATALYSIS AND DESIGN OF NEW CHIRAL LIGANDS
Immaculada Escofet Miquel

Chapter II: Computational Study of the Gold(I)-Catalyzed Activation of Acetylene

UNIVERSITAT ROVIRA I VIRGILI
COMPUTATIONAL MECHANISTIC STUDIES IN GOLD(I) CATALYSIS AND DESIGN OF NEW CHIRAL LIGANDS
Immaculada Escofet Miquel

UNIVERSITAT ROVIRA I VIRGILI
COMPUTATIONAL MECHANISTIC STUDIES IN GOLD(I) CATALYSIS AND DESIGN OF NEW CHIRAL LIGANDS
Immaculada Escofet Miquel

Chapter II

Introduction

As was stated in the **General Introduction**, the last decade has witnessed the impact of gold(I) catalysis for the construction of molecular complexity,[1] particularly in the field of the total synthesis of natural products.[2] Despite these major advances, intermolecular gold(I)-catalyzed transformations have been shown to be more challenging than intramolecular versions.[3] Both unsaturated substrates involved in the reaction (alkynes and alkenes) can compete for binding gold(I) center and, thus, decreasing the concentration of the active (η^2-alkyne)gold(I) complexes.[4] Furthermore, inherently acidic gold catalysts can promote the polymerization of alkenes *via* cationic mechanisms.[5]
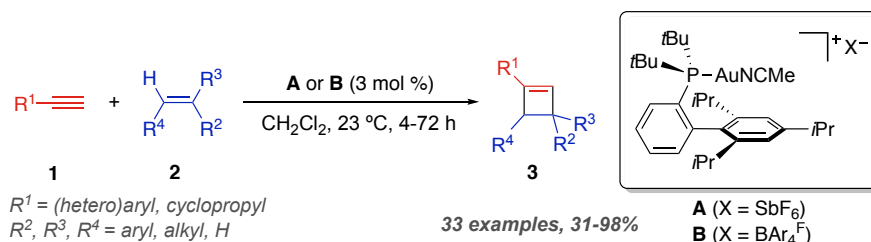
Scheme 1. Gold(I)-catalyzed [2+2] cycloaddition of terminal alkynes with alkenes.

Nevertheless, our group demonstrated that the intermolecular reaction between terminal alkynes **1** and alkenes **2** leads to cyclobutenes **3** in a regioselective manner (Scheme 1).[6] The use of gold(I) complex **A** bearing the sterically hindered *t*BuXPhos ligand was found to be key for the success of these transformations, in which the counterion also plays an important role. Thus, replacing SbF_6^- counterion for softer BAr_4^{F-}, using catonic complex **B**, led to a significant increase (10-30%) in the yield in most cases.[7] Aryl and cyclopropyl alkynes are required to ensure high reactivities. Electron-rich alkenes, preferentially being bi- and tri-substituted, are the best reaction counterparts for the most efficient cycloaddition. Therefore, terminal electron-rich alkynes were found to react with alkenes by [2+2] gold(I)-catalyzed cycloaddition to afford cyclobutenes **3**. On the other hand, electron-deficient alkynes furnished 1,3-butadienes **4** by stereospecific cross metathesis or lactones **5** *via*

1   (a) Fürstner, A. *Chem. Soc. Rev.* **2009**, *38*, 3208–3221. (b) Fensterbank, L.; Malacria, M. *Acc. Chem. Res.* **2014**, *47*, 953–965. (c) Dorel, R.; Echavarren, A. M. *Chem. Rev.* **2015**, *115*, 9028–9072. (d) Echavarren, A. M.; Muratore; M. E.; López-Carrillo, V.; Escribano-Cuesta, A.; Huguet, N.; Obradors, C. *Org. React.* **2017**, *92*, 1–288. (e) Boyle, J. W.; Zhao, Y.; Chan, P. W. H. *Synthesis* **2018**, *50*, 1402–1416.

2   (a) Pflästerer, D.; Hashmi, A. S. K. *Chem. Soc. Rev.* **2016**, *45*, 1331–1367. (b) Stathakis, C. I.; Gkizis, P. L.; Zografos, A. L. *Nat. Prod. Rep.* **2016**, *33*, 1093–1117. (c) Quach, R.; Furkert, D. P.; Brimble, M. A. *Org. Biomol. Chem.* **2017**, *15*, 3098–3104. (d) Mayans, J. G.; Armengol-Relats, H.; Calleja, P.; Echavarren, A. M. *Isr. J. Chem.* **2018**, *58*, 639–658.

3   (a) Muratore, M. E.; Homs, A.; Obradors, C.; Echavarren, A. M. *Chem. Asian. J.* **2014**, *9*, 3066–3082. (b) García-Morales, C.; Echavarren, A. M. *Synlett* **2018**, *29*, 2225–2237.

4   (a) Brown, T. J.; Dickens, M. G.; Widenhoefer, R. A. *J. Am. Chem. Soc.* **2009**, *131*, 6350–6351. (b) Brown, T. J.; Widenhoefer, R. A. *J. Organomet. Chem.* **2011**, *696*, 1216–1220. (c) Brooner, R. E. M.; Widenhoefer, R. A. *Angew. Chem. Int. Ed.* **2013**, *52*, 11714–11724.

5   (a) Urbano, J.; Hormigo, A. J.; de Frémont, P.; Nolan, P.S.; Díaz-Requejo, M. M.; Pérez, P. J. *Chem. Commun.* **2008**, 759–761. (b) Brown, T. J.; Dickens, M. G.; Widenhoefer, R. A. *Chem. Commun.* **2009**, 6451–6453.

6   López-Carrillo, V.; Echavarren, A. M. *J. Am. Chem. Soc.* **2010**, *132*, 9292–9294.

7   Homs, A.; Obradors, C.; Leboeuf, D.; Echavarren, A. M. *Adv. Synth. Catal.* **2014**, *356*, 221–228.

UNIVERSITAT ROVIRA I VIRGILI
COMPUTATIONAL MECHANISTIC STUDIES IN GOLD(I) CATALYSIS AND DESIGN OF NEW CHIRAL LIGANDS
Immaculada Escofet Miquel

Chapter II

formal (4+1) annulation, respectively, in the presence of gold(I) complex **C** and a silver(I) salt (Scheme 2).[8]
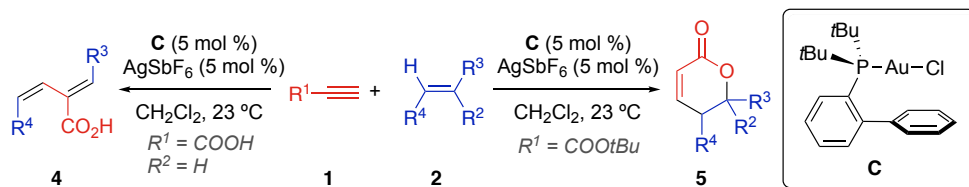
Scheme 2. Different outcomes obtained in gold(I)-catalyzed cycloaddition reactions of alkynes with alkenes depending on the nature of the substrates.

Interestingly, 1,3-dienes type **6** can be formed upon the reaction of alkenes with electron-rich alkynes bearing *ortho*-substituents, in a mixture with cyclobutenes **3** (Scheme 3a).[9] In contrast, we discovered that less sterically demanding 1,3-butadiynes **7**[9] and 1,3-enynes **9**[10] react with alkenes to form exclusively cyclobutenes **8** and **10**, respectively (Scheme 3b and 3c). With regards to 1,3-dienes **12**, selective cycloaddition of the most electron-rich double bond yielded only cyclobutenes **13** (Scheme 3d).[10]
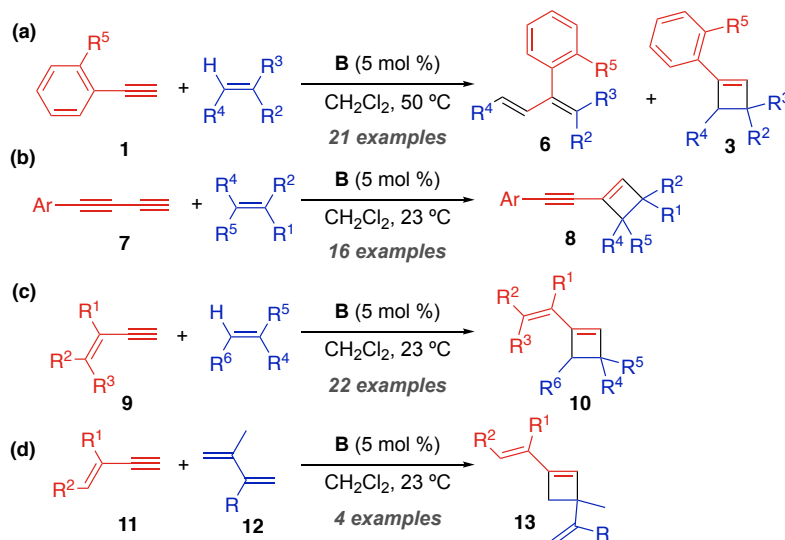
Scheme 3. (a) Cycloaddition *vs*. rearrangement of *ortho*-substituted aryl alkynes. **(b)** Gold(I)-catalyzed cycloaddition of 1,3-butadiynes **7**. **(c)** Reaction of 1,3-enynes **9** with alkenes that lead to 1-vinylcyclobutenes **10**. **(d)** Formation of 3-vinylcyclobutenes **13** from 1,3-dienes **12** using gold(I).

Mechanistic studies revealed that the associative ligand exchange between (η^2-alkene)gold(I) complex **I** and phenylacetylene **1a** to form (η^2-alkyne)gold(I) intermediate **II** is the rate-determining step of the catalytic cycle (Scheme 4).[7] These species **II** enter the catalytic cycle *via* nucleophilic attack of **2a** to **I** generating the key intermediate,

8   Yeom, H.-S.; Koo, J.; Park, H.-S.; Wang, Y.; Liang, Y.; Yu, Z.-X.; Shin, S. *J. Am. Chem. Soc.* **2012**, *134*, 208–211.

9   de Orbe, M. E.; Amenós, L.; Kirillova, M. S.; Wang, Y.; López-Carrillo, V.; Maseras, F.; Echavarren, A. M. *J. Am. Chem. Soc.* **2017**, *139*, 10302–10311.

10   de Orbe, M. E.; Echavarren, A. M. Eur. *J. Org. Chem.* **2018**, *22*, 2740–2752.

UNIVERSITAT ROVIRA I VIRGILI
COMPUTATIONAL MECHANISTIC STUDIES IN GOLD(I) CATALYSIS AND DESIGN OF NEW CHIRAL LIGANDS
Immaculada Escofet Miquel

Chapter II

cyclopropylgold(I) carbene **III,** followed by ring expansion (**IV**) and demetallation (**V**). Then, a final associative ligand exchange closes the catalytic cycle releasing product **3a**. Simultaneously, unreactive σ,π-digold(I) alkyne complexes **E** could be formed as a minor byproduct of the deprotonation of intermediate (η^2-phenylacetylene)gold(I) **II**, which is in equilibrium with **D**. Complex **D** can react with another molecule of active complexes **A-B** to form non-catalytically active species **E**, which are dead-ends outside the catalytic cycle. According to NMR studies, the only two long-living species were **I** and **E**. The generation of unreactive σ,π-digold(I) alkyne **E** was less favored when complex initially used contains softer counterion, BAr$_4$^F- (complex **B**) instead of the more basic counterion SbF$_6^-$ (complex **A**). Thus, cationic complex **B**, bearing *t*BuXPhos ligand and bulky counterion BAr$_4$^F-, was selected as the best catalyst for these transformations.
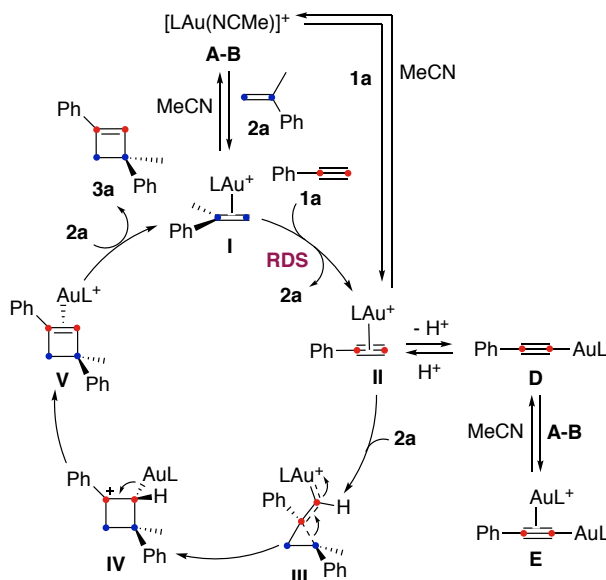
Scheme 4. Proposed catalytic cycle for [2+2] cycloaddition between phenylacetylene **1a** and α-methylstyrene **2a** catalayzed by gold(I).

Different possible pathways for the formation of cyclobutenes **3** and 1,3-dienes **6** were studied in detail by means of DFT calculations using PMe$_3$ as the simplified ligand for gold(I) and M06/6-31G(d) (C, H, P), SDD (Au) in CH$_2$Cl$_2$ (SMD) (Scheme 5).[9] The reaction begins with the associative ligand exchange of (η^2-alkene)gold(I) complexes **I** leading to the moderately less stable (η^2-alkyne)gold(I) complexes **II**, which was followed by the attack of the alkene **2a** in a *anti* or *syn* manner to form intermediates **III** and **III-b**. Both cyclopropyl gold(I) carbenes are in equilibrium due to C3–C4 bond rotation *via* ring opened gold(I) complex **VI**. Interestingly, the evolution of intermediate **III** proceed through lower computed energy barriers than those of **III-b**. Therefore, cyclopropyl gold(I) carbene **III** evolves to complex **V** to afford cyclobutenes type **3** after formal deauration. For *ortho*-substituted alkynes, 1,3 migration of *C4* can also take place giving rise to intermediate **VII** that would lead 1,3-dienes **6**, upon ring opening. Noteworthy, very similar activation energies were observed for rearrangements of intermediate **III**. Thus, in accordance with

UNIVERSITAT ROVIRA I VIRGILI
COMPUTATIONAL MECHANISTIC STUDIES IN GOLD(I) CATALYSIS AND DESIGN OF NEW CHIRAL LIGANDS
Immaculada Escofet Miquel

Chapter II

the experimental results, different reaction outcomes can be obtained depending on the substitution patterns of the substrates.
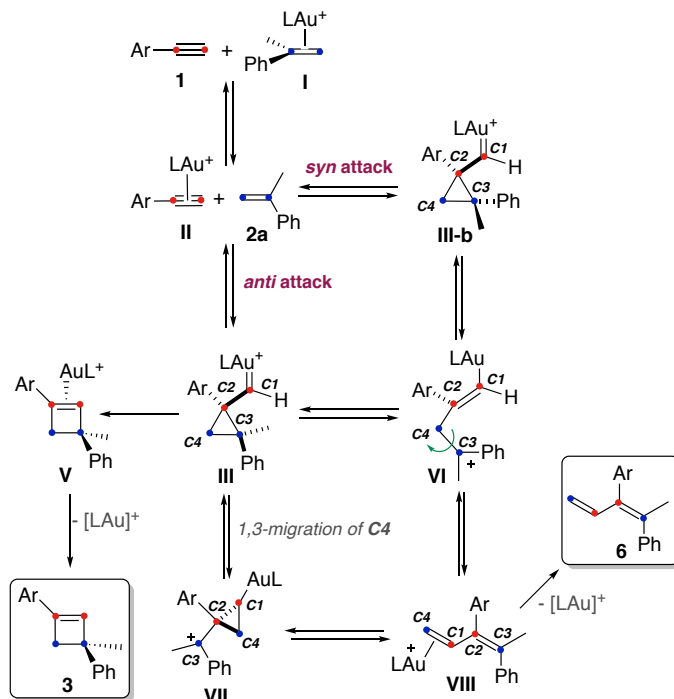
Scheme 5. Different pathways for the formation of 1,3-dienes **6** and cyclobutenes **3**.

Gold(I)-catalyzed cycloadditions of ynamides with alkenes have been reported recently (Scheme 6).[11] Thus, 1,3,5-trisubstituted cyclohexenes **16** could be obtained stereoselectively when mixing terminal ynamides **14** with enol ethers **15**. In this reaction, the intermediate cyclopropyl gold(I) carbenes are intermolecularly attacked by another enol ether that is in excess in the reaction mixture.
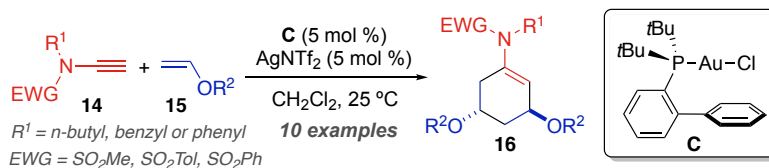
Scheme 6. Intermolecular [2+2+2] cycloadditions of ynamides **14** and alkenes.

Subsequently, an intermolecular gold(I)-catalyzed [2+2] cycloaddition reaction using aryl chloroalkynes **17** instead of terminal aryl alkynes **1** has been disclosed.[12] Interestingly, cyclobutenes **19** were synthesized by using unactivated mono- and disubstituted alkenes **18** in the presence of catalyst **F** (Scheme 7).

---

11   Dateer, R. B.; Shaibu, B. S.; Liu, R.-S. *Angew. Chem. Int. Ed.* **2012**, *51*, 113–117.
12   Bai, Y.-B.; Luo, Z.; Wang, Y.; Gao, J.-M.; Zhang, L. *J. Am. Chem. Soc.* **2018**, *140*, 5860–5865.

UNIVERSITAT ROVIRA I VIRGILI
COMPUTATIONAL MECHANISTIC STUDIES IN GOLD(I) CATALYSIS AND DESIGN OF NEW CHIRAL LIGANDS
Immaculada Escofet Miquel

Chapter II
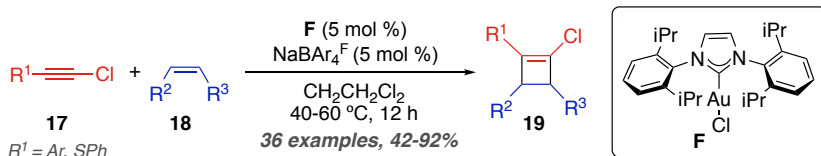
Scheme 7. Gold(I)-catalyzed intermolecular [2+2] cycloadditions of aryl chloroalkynes.

On the other hand, our group discovered that gold(I) carbenes could be formed by retro Buchner reaction of 7-substituted 1,3,5-cycloheptatrienes **20** releasing a molecule of benzene (Scheme 8).[13] Thus, retrocylopropanation of norcaradiene **21**, valence tautomer of **20**, takes place at relatively high temperatures followed by a formal decarbenation. As an example, *(Z,Z)*-diene **23** was obtained selectively when cycloheptatriene **22** was used as a reagent. Hence, upon the formation of cyclopropylgold(I) carbene **IX**, the most favored pathway through transition state **X** gives rise to *(Z,Z)*-**23** by 1,3-shift of a CHPh fragment. Interestingly, the formation of *(E,E)*-**23** that would have proceeded by ring expansion of cyclobutene **IX**, was not observed.
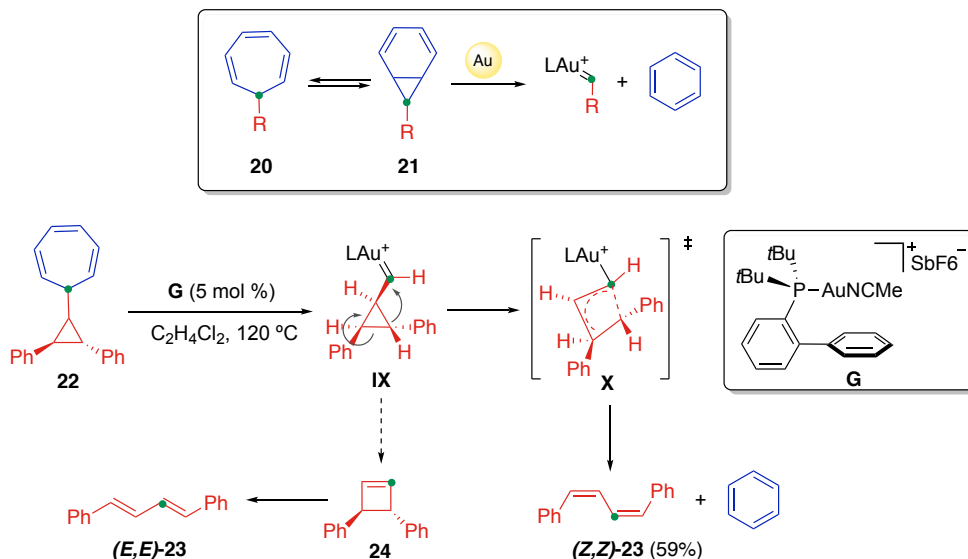
Scheme 8. Generation and evolution of carbene **IX** by Retro-Buchner reaction of **22**.

Despite the fact that cyclopropyl gold carbenes of type **IX** formally correspond to those that would be generated by gold(I)-catalyzed intermolecular reaction of acetylene with *trans*-stilbene, to date, very few experiments have been performed using this commodity feedstock as reagent in homogeneous gold(I) catalysis. Although acetylene is used for the production of vinyl chloride,[14] among a wide range of industrial applications, so far, it has not been used for the preparation of cyclobutenes **3** or dienes **6**. Due to its flammability and

---

13   (a) Solorio-Alvarado, C. R.; Echavarren, A. M. *J. Am. Chem. Soc.* **2010**, *132*, 11881–11883. (b) Solorio-Alvarado, C. R.; Wang, Y.; Echavarren, A. M. *J. Am. Chem. Soc.* **2011**, *133*, 11952–11955.

14   Trotuş, I.-T.; Zimmermann, T.; Schüth, F. *Chem. Rev.* **2014**, *114*, 1761–1782.

UNIVERSITAT ROVIRA I VIRGILI
COMPUTATIONAL MECHANISTIC STUDIES IN GOLD(I) CATALYSIS AND DESIGN OF NEW CHIRAL LIGANDS
Immaculada Escofet Miquel

Chapter II

explosion risk, handling acetylene requires special safety precautions, particularly when working with high pressure cylinders. However, a more convenient procedure to produce acetylene *in situ* has been reported recently that involves the use of safer calcium carbide and water[15] and a Y-shaped two-chamber flask.[16] At this point, our group pioneered the use of acetylene as a dicarbene equivalent for gold(I) catalysis.[17] Thus, based on our expertise on intermolecular gold(I) catalysis, we reported a methodology in which acetylene was generated *in situ* and reacted with alkenes (Scheme 9). Initial experiments using calcium carbide (7.8 equiv) and H_2O (28 equiv) in $CHCl_3$ at 23 ºC and 5 mol% of gold(I) catalyst **G** in the presence of alkene **25** (1 equiv) for 24h led to the formation of both 1,3-diene **26** (24 %) and biscyclopropane **27** (11 %).[18] Later, several gold(I) catalyst were tested and complex **B**, bearing a *t*BuXPhos ligand, was found to deliver selectively (*Z,Z*)-diene **26** whereas IPr gold(I) complex **H** favored the selective formation of **27**. After further optimization, we expanded the scope for both transformations. The low to moderate yields observed in the formation of **26** result from the competing reaction between acetylene with the 1,3-dienes leading to oligomerization which was detected by MALDI analysis of the crude reaction mixtures.
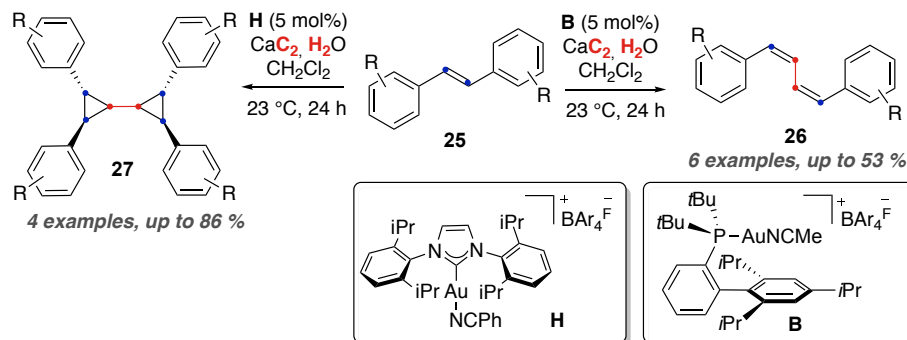
Scheme 9. Synthesis of dienes **26** and biscyclopropyl compounds type **27** from acetylene generated *in situ* and stilbenes **25** catalyzed by gold(I).

Regarding the formation of biscyclopropanes **27**, only one diastereomer was observed by NMR, chiral supercritical fluid chromatography and reverse phase ultra-high-performance liquid chromatography. The relative configuration of one example of these biscyclopropanes was confirmed by X-ray diffraction.

Furthermore, reaction of 1,5 dienes **28** with acetylene gave rise to tricyclo[5.1.0.0²,⁴]octanes **29** as single diastereomers in the presence of catalyst **B** (Scheme 10). The relative configuration of these products was also assigned by X-ray diffraction. Finally, this

15   Rodygin, K. S.; Werner, G.; Kucherov, F. A.; Ananikov, V. P. *Chem. Asian J.* **2016**, *11*, 965–976.
16   Voronin, V. V.; Ledovskaya, M. S.; Gordeev, E. G.; Rodygin, K. S.; Ananikov, V. P. *J. Org. Chem.* **2018**, *83*, 3819–3828.
17   Scharnagel, D.; Escofet, I.; Armengol-Relats, H.; de Orbe, M. E.; Korber, J. N.; Echavarren, A. M. *Angew. Chem. Int. Ed.* **2020**, *59*, 4888–4891.
18   Experimental part of this project was carried out by: Dr. Dagmar Scharnagel, Helena Armengol i Relats, M. Elena de Orbe and J. Nepomuk Korber. All the experimental details can be found in the supporting information of (17).

UNIVERSITAT ROVIRA I VIRGILI
COMPUTATIONAL MECHANISTIC STUDIES IN GOLD(I) CATALYSIS AND DESIGN OF NEW CHIRAL LIGANDS
Immaculada Escofet Miquel

Chapter II

biscyclopropanation was applied for the one step total synthesis of waitzacuminone (**31**),[19] a sesquiterpene isolated from the aerial parts of an annual herb native to Australia (*Waitza acuminata*) starting from geranyl acetone **30**. The relative configuration was confirmed by X-ray of its crystalline derivative hydrazone **32**.[20]
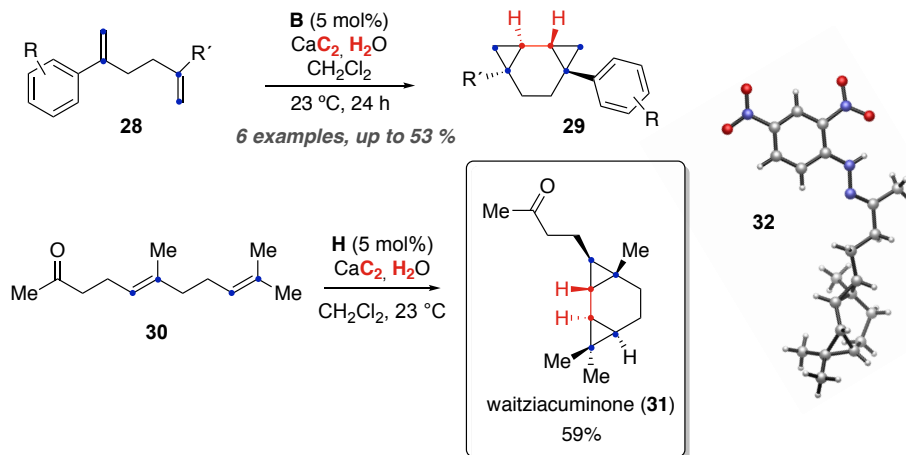
Scheme 10. Biscyclopropanation of 1,5-dienes **28**, its application for the total synthesis of waitzacuminone **31** and X-ray crystal structure of it 2,4-dinitrophenylhydrazone **32**.

Isotopic labelling experiments previously done in our group also confirmed the stereospecificity in the formation of biscyclopropanes.[6] Thus, phenylacetylene reacted with deuterated 1,5-diene **33** in the presence of catalyst **A** to afford a 1:1 mixture of products **34** and **35** (Scheme 11). Noteworthy, biscyclopropyl derivatives **34** were obtained with an *anti*-relative configuration *via* intramolecular cyclopropanantion, whereas ring expansion of the cyclopropyl gold(I) carbene intermediate gave rise to cyclobutenes **35**, as mentioned before.
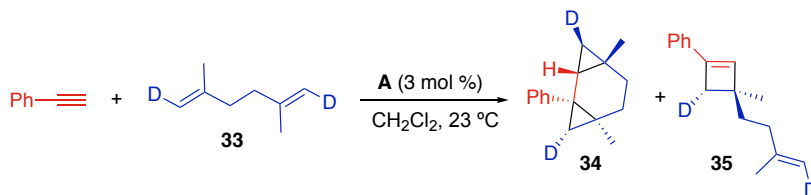
Scheme 11. Isotopic labelling experiment for the intermolecular gold(I)-catalyzed reaction of phenylacetylene with 1,5-dienes-*d₂* **33**.

19   (a) Jakupovic, J.; Schuster, A.; Bohlmann, F.; King, R. M.; Haegi, L. *Phytochemistry* **1989**, *28*, 1943–1948. (b) Reuss, S. H. von.; Wu, C.-L.; Muhle, H.; König, W. A. *Phytochemistry* **2004**, *65*, 2277–2291.
20   See the supporting information of (17) for details.

UNIVERSITAT ROVIRA I VIRGILI
COMPUTATIONAL MECHANISTIC STUDIES IN GOLD(I) CATALYSIS AND DESIGN OF NEW CHIRAL LIGANDS
Immaculada Escofet Miquel

Chapter II

Objectives

Our group has recently reported the use of acetylene as a dicarbene equivalent for intermolecular gold(I)-catalyzed transformations. This novel methodology uses a Y-shaped reactor for the *in situ* generation of acetylene gas, which reacts with several alkenes type **36** leading to the formation of (*Z,Z*)-1,4-disubstituted 1,3-butadienes **37**, biscyclopropranes **38** and tricyclo[5.1.0.0^{2,4}]octanes **39**. Noteworthy, the latter transformation was applied for the first total synthesis of waitziacuminone in only one step by the stereoselective formation of four C–C bonds and three rings.
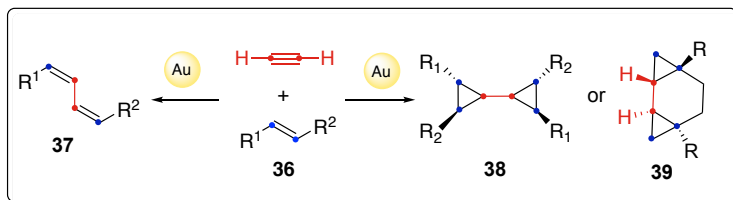
Scheme 12. Examples on the Au(I)-catalyzed activation of acetylene.

We decided to provide a rational for the high selectivity on these transformations by means of a DFT stydy of the mechanisms that are involved in these processes.

UNIVERSITAT ROVIRA I VIRGILI
COMPUTATIONAL MECHANISTIC STUDIES IN GOLD(I) CATALYSIS AND DESIGN OF NEW CHIRAL LIGANDS
Immaculada Escofet Miquel

Chapter II

Results and Discussion

We focused our investigations on the aforementioned gold(I) catalyzed intermolecular reactions between acetylene gas with alkenes that give rise to the formation of (*Z,Z*)-1,4-disubstituted 1,3-butadienes **37**, biscyclopropranes **38** and tricyclo[5.1.0.0²,⁴]octanes **39** (Scheme 12).

Density Functional Theory (DFT) was the method of choice since it has been successfully applied to similar studies. In line with the previous computational work that has been carried out in our group on the intermolecular gold(I) catalyzed transformations,[9] M06 has been chosen as a hybrid functional.
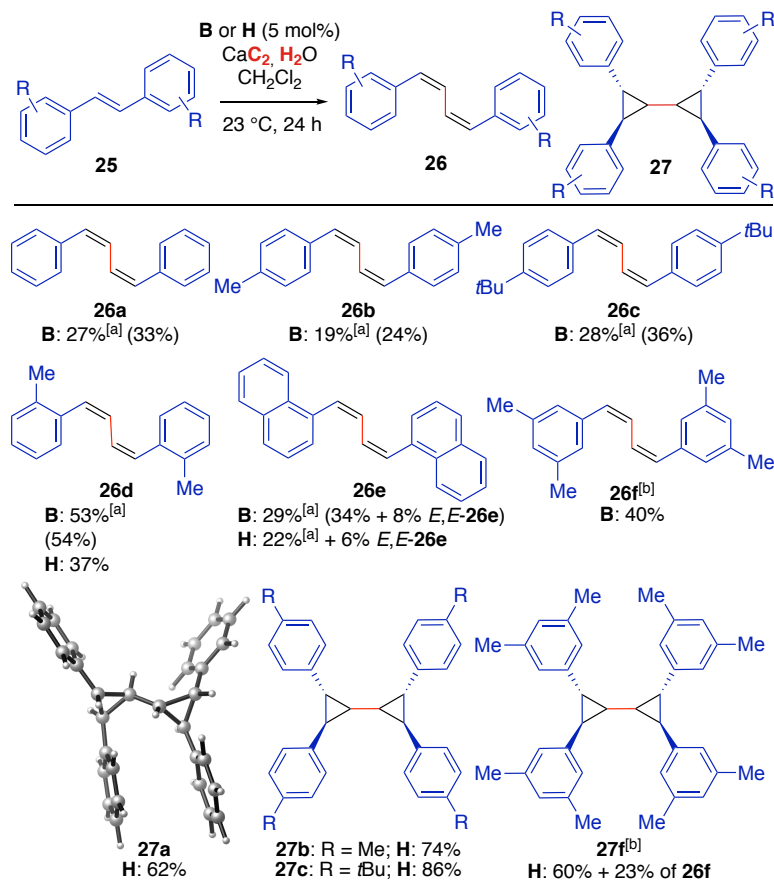
Scheme 13. Synthesis of dienes **26** and biscyclopropyl compounds **27** from acetylene and stilbenes **25a-f**. Isolated yields (yields determined by ¹H NMR using diacetyl benzene as internal standard in parenthesis); **27a** is shown as a CYLlview depiction of the X-ray crystal structure. [a] Isolated as a mixture with starting material. [b] Reaction carried out in chloroform, at 40 ºC.

UNIVERSITAT ROVIRA I VIRGILI
COMPUTATIONAL MECHANISTIC STUDIES IN GOLD(I) CATALYSIS AND DESIGN OF NEW CHIRAL LIGANDS
Immaculada Escofet Miquel

Chapter II

First of all, we aim to fully understand the high selectivity observed on the formation of *meso*-biscyclopropyl products **27** when treating alkenes **25** with acetylene gas, generated *in situ* (Figure 1), in the presence of gold(I) catalyst **H**. It is important to remark that, under these conditions, the reaction was found to undergo biscyclopropanantion to afford **27** selectively, whereas using *t*BuXPhos catalyst **B** preferentially afforded dienes **26** (Scheme 13).

first vessel: CaC₂, solvent

second vessel: substrate, catalyst, solvent
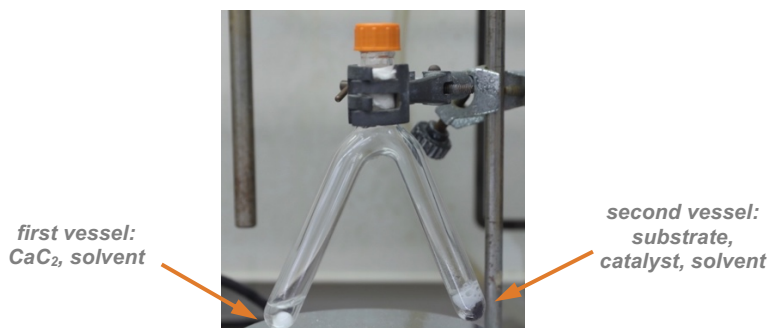
Figure 1. Design of the two-chamber reactor and loading of the two vessels.

The relative configuration of **27a** was determined by X-ray diffraction as meso (Scheme 13). Therefore, we decided to compute the reaction between *trans*-stilbene (**25a**) and (η^2-alkyne)gold(I) complex **Int1a** using PMe₃ as simplified ligand for gold(I) (Scheme 14). As we have shown before,[9] cyclopropyl gold carbene **Int2a** is formed in an exergonic process ($\Delta G° = -8.0$ kcal/mol), upon the nucleophilic attack of alkene **25a** to the active (η^2-alkyne)gold(I) complex **Int1a**.
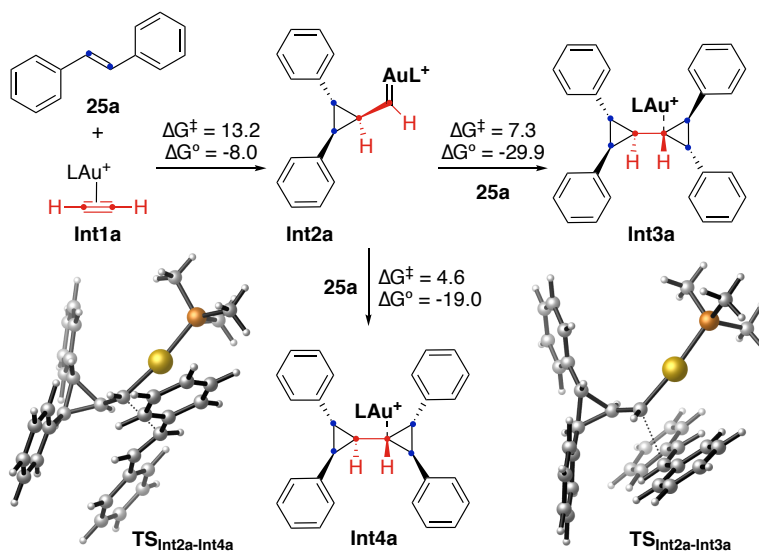
Scheme 14. Calculated formation of different diastereomers of biscyclopropyl **27** products. L=PMe₃. DFT calculations performed with M06-D3/6-31G(d) (C, H, P) and SDD (Au) in CH₂Cl₂ (SMD). Free energies in kcal/mol.

UNIVERSITAT ROVIRA I VIRGILI
COMPUTATIONAL MECHANISTIC STUDIES IN GOLD(I) CATALYSIS AND DESIGN OF NEW CHIRAL LIGANDS
Immaculada Escofet Miquel

Chapter II

Then, intermediate **Int2a** can react further with a second molecule of *trans*-stilbene **25a** to form **Int3a** via **TS_Int2a-Int3a** or **Int4a** through **TS_Int2a-Int4a**, respectively. Since these two possible pathways for the formation of different diastereomers of biscyclopropyl compounds type **27** differ in 2.7 kcal/mol, formation of **Int4a,** which leads to *meso*-**27a**, is more favorable than formation of **Int3a**. These computed results are in good agreement with what was observed in our experiments.
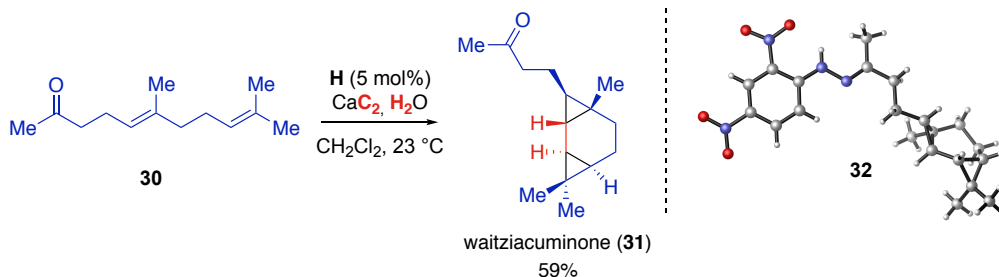
Scheme 15. One step total synthesis of waitzacuminone (**31**) and X-ray crystal sutrucure of its derivative **32**, right (CYLview depiction).

On the other hand, we were curious about the stereoselectivity on the aforementioned biscyclopropanation reaction between geranyl acetone (**30**) and acetylene in the presence of IPr catalyst **H** (Scheme 15). Hence, we carried out DFT studies on the total synthesis of waitzacuminone product **31** which involves the formation of four C–C bonds and three rings, creating five stereocenters, in only one step. Thus, four possible cyclopropyl gold carbenes can be formed by the reaction of both alkene moieties of **30** with the active (η^2-alkyne)gold(I) complex **Int1a** (Scheme 16). Although very similar energy barriers were found for the formation of the four gold(I) carbenes, the most favorable one gives **Int6a** *via* **TS_30-Int6a**. Moreover, **Int6a** immediately undergoes a second cyclopropanation reaction through **TS_Int6a-Int7a** to form **Int7a**, and finally waitziacuminone (**31**) (Scheme 17). This pathway could also compete with the initial cyclopropanation of the internal alkene of **30** leading to **Int5a** *via* **TS_30-Int5a**, which would similarly undergo an intramolecular cyclopropanation to form **Int7a** through **TS_Int5a-Int7a**. In contrast, the two other alternative pathways have slightly higher activation energies (0.9 and 1.2 kcal/mol) and the corresponding cyclopropyl gold carbenes **Int5b** and **Int6b** would be unproductive, since the second cyclopropanation reaction would generate a highly strained tricyclo[5.1.0.0^{2,4}]octane bearing *trans*-fused cyclopropane **Int7b** (Scheme 18), as shown by the high activation energies found for these endergonic processes (for **TS_Int5b-Int7b**, $\Delta G°$ = 27.8 kcal/mol and for **TS_Int6b-Int7b**, $\Delta G°$ = 26.5 kcal/mol). These computational results also support the stereoselective formation of biscyclopropanes already confirmed by deuterium labelled experiments performed earlier by our group (Scheme 11).[6] Hence, the *anti*-relative configuration and *cis*-fused cyclopropanes were preferentially obtained as a product in these transformations.

UNIVERSITAT ROVIRA I VIRGILI
COMPUTATIONAL MECHANISTIC STUDIES IN GOLD(I) CATALYSIS AND DESIGN OF NEW CHIRAL LIGANDS
Immaculada Escofet Miquel

Chapter II
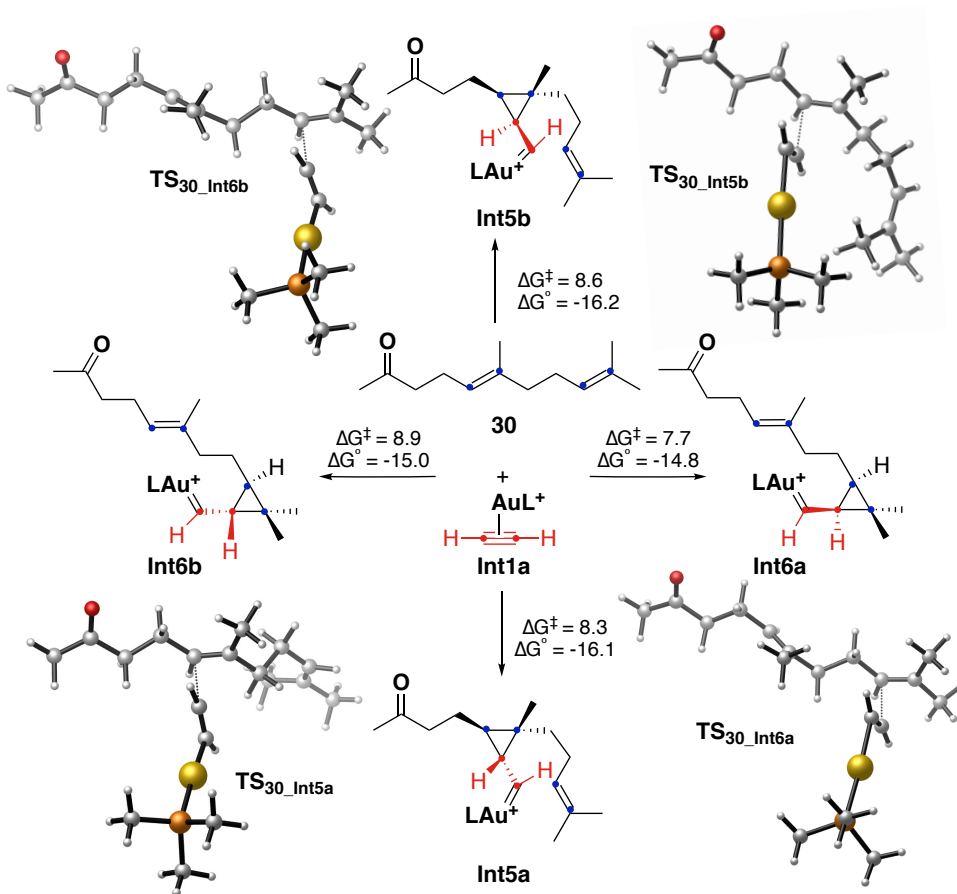
Scheme 16. Four possible pathways to form cyclopropyl gold gold carbenes **Int5a,b** or **Int6a,b** from substrate **30** in the presence of **Int1a**. L=PMe$_3$. DFT calculations performed with M06-D3/6-31G(d) (C, H, P, O) and SDD (Au) in CH$_2$Cl$_2$ (SMD). Free energies in kcal/mol.

126

UNIVERSITAT ROVIRA I VIRGILI
COMPUTATIONAL MECHANISTIC STUDIES IN GOLD(I) CATALYSIS AND DESIGN OF NEW CHIRAL LIGANDS
Immaculada Escofet Miquel

Chapter II
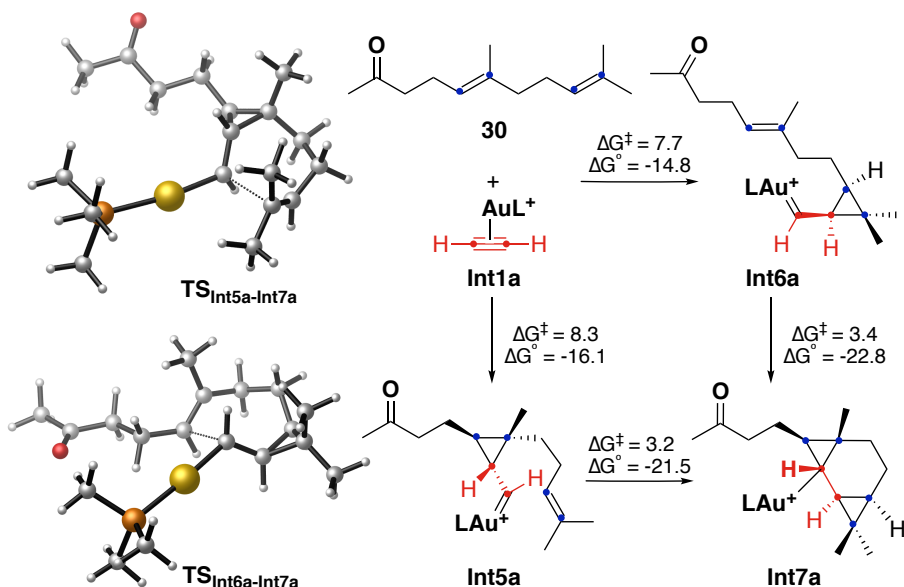
Scheme 17. Different mechanistic pathways to form **Int7a** by double cyclopropanation reactions of substrate **30** in the presence of **Int1a**. L=PMe₃. DFT calculations performed with M06-D3/6-31G(d) (C, H, P, O) and SDD (Au) in CH₂Cl₂ (SMD). Free energies in kcal/mol.
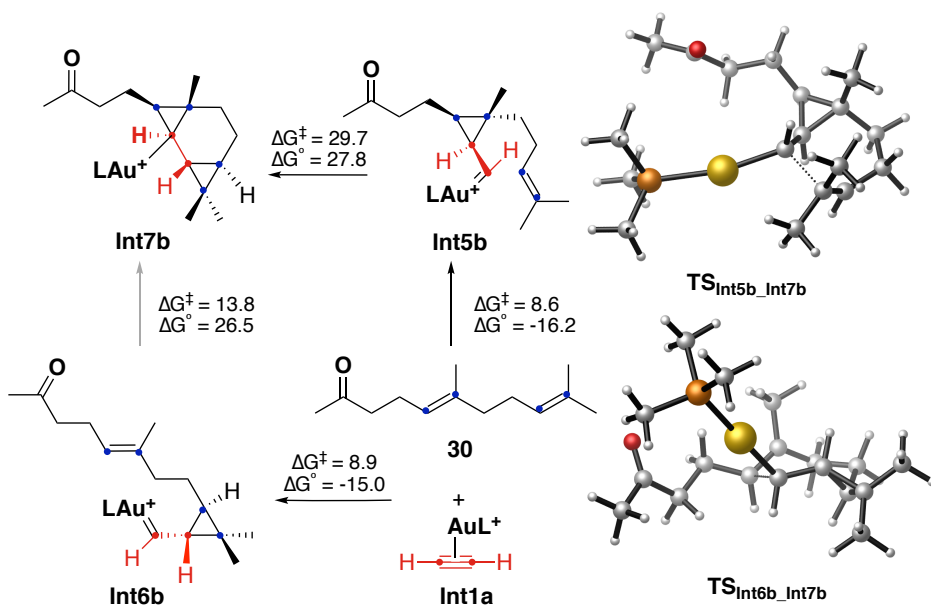
Scheme 18. Different mechanistic pathways to form **Int7b** by double cyclopropanation reactions of substrate **30** in the presence of **Int1a**. L=PMe₃. DFT calculations performed with M06-D3/6-31G(d) (C, H, P, O) and SDD (Au) in CH₂Cl₂ (SMD). Free energies in kcal/mol.

UNIVERSITAT ROVIRA I VIRGILI
COMPUTATIONAL MECHANISTIC STUDIES IN GOLD(I) CATALYSIS AND DESIGN OF NEW CHIRAL LIGANDS
Immaculada Escofet Miquel

Chapter II

Conclusions

Our group has developed catalytic systems for the incorporation of acetylene gas into complex frameworks by means of gold(I) catalysis. Acetylene gets activated by gold(I) as a dicarbene equivalent that allows for the stereoselective formation of (*Z,Z*)-dienes, biscyclopropanes and tricyclo[5.1.0.0^{2,4}]octanes.

Formation of only one diastereomer of the biscyclopropanes when mixing *trans*-stilbene with acetylene, conveniently generated *in situ* in a user-friendly procedure, under gold(I) catalysis has been rationalized by means of DFT calculations. Thus, the formation of cyclopropyl gold carbene **Int2a** by activation of acetylene with gold(I) is followed preferentially by the intermolecular attack of the styrene molecule leading to the formation of *meso*-biscyclopropanes selectively in good agreement with the experimental results.

According to our computational studies, the formation **Int7a** is much more favored since the two other alternative pathways have slightly higher activation energies. Moreover, the second cyclopropanation reactions present very high activation energies and are endergonic processes. Intermediates **Int5b** and **Int6b** would be unproductive since they would lead to strained *trans*-fused cyclopropane bearing **Int7b**. Thus, waitziacuminone was selectively formed through the most favorable intermediate **Int7a**, bearing *cis* cycloproprane.

UNIVERSITAT ROVIRA I VIRGILI
COMPUTATIONAL MECHANISTIC STUDIES IN GOLD(I) CATALYSIS AND DESIGN OF NEW CHIRAL LIGANDS
Immaculada Escofet Miquel

Chapter II

Computational Methods

As indicated in the **Introduction** of this chapter, the experimental work of this project has been performed by Dr. Dagmar Scharnagel, Helena Armengol i Relats, M. Elena de Orbe and J. Nepomuk Korber.[18]

Calculations were performed by means of the Gaussian 09 suite of programs.[21] DFT was applied using M06-D3.[22] The SDD basis set and ECP was used to describe Au.[23] The 6-31G(d) basis set[24] was employed for all remaining atoms (C, H, P and O). Full geometry optimizations were carried out in dichloromethane, through an implicit solvent SMD.[25] The stationary points were characterized by vibrational analysis. Transition states were identified by the presence of one imaginary frequency while minima by a full set of real frequencies. The connectivity of the transition states was confirmed by the relaxation of each transition state towards both the reactant and the product or, in some cases, by IRC[26] calculations. Reported energies are potential energies (E) and free energies (G) in solution, computed at 298 K and 1 atm.

A dataset collection of computational results of this chapter is available in the ioChen-BD[27] repository and can be accessed through doi:10.19061/iochem-bd-1-148.

21   Gaussian 09, Revision B.1, Frisch, M. J.; Trucks, G. W.; Schlegel, H. B.; Scuseria, G. E.; Robb, M. A.; Cheeseman, J. R.; Scalmani, G.; Barone, V.; Mennucci, B.; Petersson, G. A.; Nakatsuji, H.; Caricato, M.; Li, X.; Hratchian, H. P.; Izmaylov, A. F.; Bloino, J.; Zheng, G.; Sonnenberg, J. L.; Hada, M.; Ehara, M.; Toyota, K.; Fukuda, R.; Hasegawa, J.; Ishida, M.; Nakajima, T.; Honda, Y.; Kitao, O.; Nakai, H.; Vreven, T.; Montgomery, J. A.; Peralta, Jr. J. E.; Ogliaro, F.; Bearpark, M.; Heyd, J. J.; Brothers, E.; Kudin, K. N.; Staroverov, V. N.; Kobayashi, R.; Normand, J.; Raghavachari, K.; Rendell, A.; Burant, J. C.; Iyengar, S. S.; Tomasi, J.; Cossi, M.; Rega, N.; Millam, J. M.; Klene, M.; Knox, J. E.; Cross, J. B.; Bakken, V.; Adamo, C.; Jaramillo, J.; Gomperts, R.; Stratmann, R. E.; Yazyev, O.; Austin, A. J.; Cammi, R.; Pomelli, C.; Ochterski, J. W.; Martin, R. L.; Morokuma, K.; Zakrzewski, V. G.; Voth, G. A.; Salvador, P.; Dannenberg, J. J.; Dapprich, S.; Daniels, A. D.; Farkas, Ö.; Foresman, J. B.; Ortiz, J. V.; Cioslowski, J.; Fox, D. J. Gaussian, Inc., Wallingford CT **2009**.
22   Zhao, Y.; Truhlar, D. G. *Theor. Chem. Acc.* **2008**, *120*, 215–241.
23   Andrae, D.; Haussermann, U.; Dolg, M.; Stoll, H.; Preuss, H. *Theor. Chim. Acta.* **1990**, *77*, 123–141.
24   Hehre, W. J.; Ditchfield, R.; Pople, J. A. *J. Chem. Phys.* **1972**, *56*, 2257–2261.
25   Marenich, A. V.; Cramer, C. J.; Truhlar, D. G. *J. Phys. Chem. B.* **2009**, *113*, 6378–6396.
26   Gonzalez, C.; Schlegel, H. B. *J. Phys. Chem.* **1990**, *94*, 5523–5527.
27   Álvarez-Moreno, M.; de Graaf, C.; Lopez, N.; Maseras, F.; Poblet, J. M.; Bo, C. *J. Chem. Inf. Model.* **2015**, *55*, 95−103

UNIVERSITAT ROVIRA I VIRGILI
COMPUTATIONAL MECHANISTIC STUDIES IN GOLD(I) CATALYSIS AND DESIGN OF NEW CHIRAL LIGANDS
Immaculada Escofet Miquel

Chapter II

Computed Structures and Energies (M06-D3)

25a
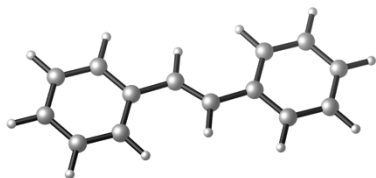
E = - 540.276142 Hartrees
G = - 540.098925 Hartrees

30
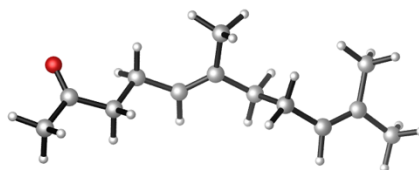
E = - 583.384583717 Hartrees
G = - 583.110799 Hartrees

Int2a
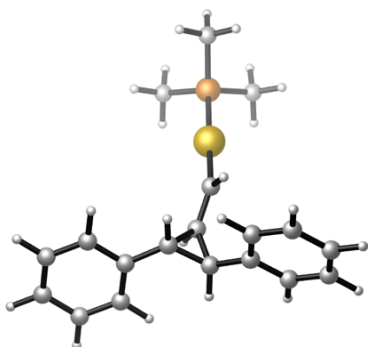
E = - 1754.52088294 Hartrees
G = - 1754.010248 Hartrees

Int3a
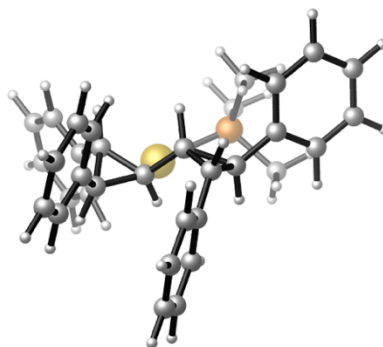
E = - 1754.57308100 Hartrees
G = - 1754.057943 Hartrees

Int4a
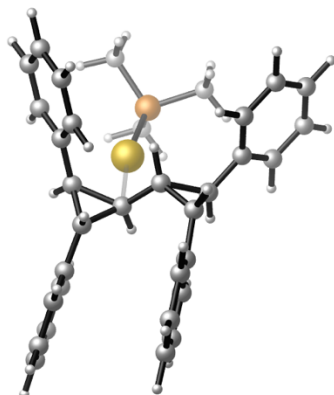
E = - 1754.55848972 Hartrees
G = - 1754.040464 Hartrees

Int5a
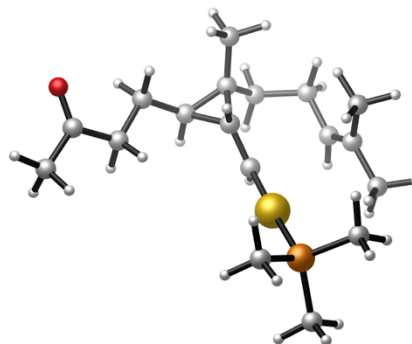
E = - 1257.34591021 Hartrees
G = - 1256.936110 Hartrees

UNIVERSITAT ROVIRA I VIRGILI
COMPUTATIONAL MECHANISTIC STUDIES IN GOLD(I) CATALYSIS AND DESIGN OF NEW CHIRAL LIGANDS
Immaculada Escofet Miquel

Chapter II

Int5b
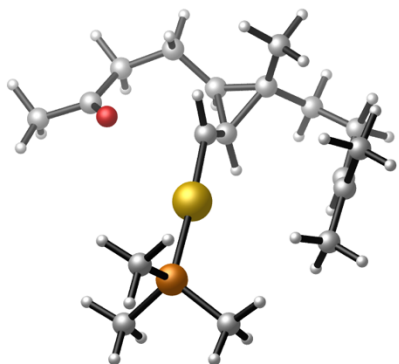
E = - 1257.34800879 Hartrees
G = - 1256.936370 Hartrees

Int6a
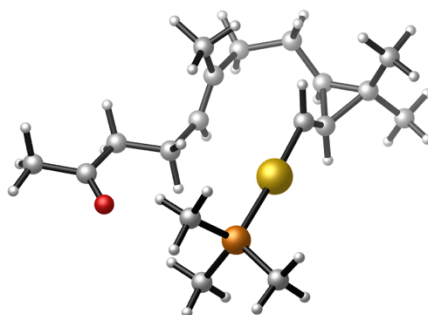
E = - 1257.34675345 Hartrees
G = - 1256.934134 Hartrees

Int6b
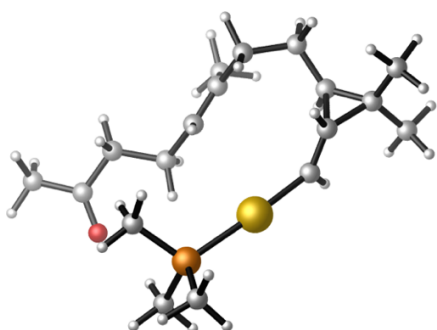
E = - 1257.34519211 Hartrees
G = - 1256.934361 Hartrees

Int7a
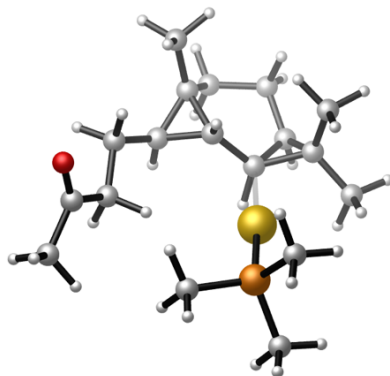
E = - 1257.38633291 Hartrees
G = - 1256.970419 Hartrees

Int7b
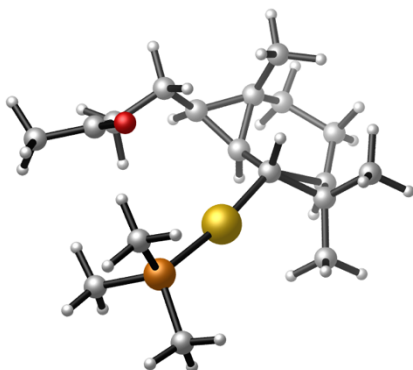
E = - 1257.30804510 Hartrees
G = - 1256.892113 Hartrees

TS25a_Int2a
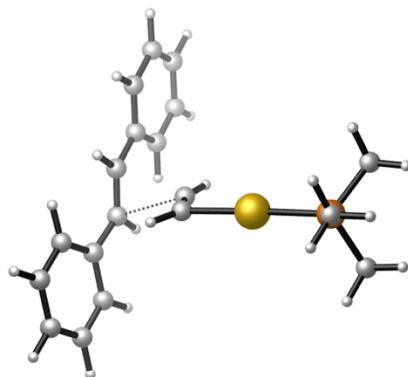
E = - 1214.17912493 Hartrees
G = - 1213.877563 Hartrees

UNIVERSITAT ROVIRA I VIRGILI
COMPUTATIONAL MECHANISTIC STUDIES IN GOLD(I) CATALYSIS AND DESIGN OF NEW CHIRAL LIGANDS
Immaculada Escofet Miquel

Chapter II
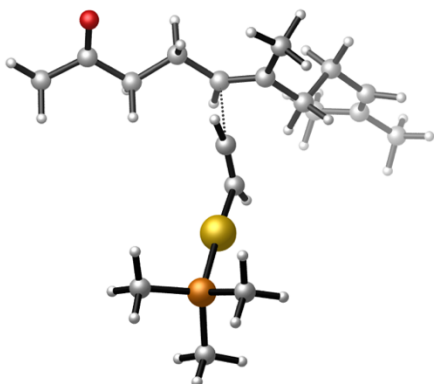
TS30_Int5a

E = - 1257.29332129 Hartrees
G = - 1256.897313 Hartrees

TS30_Int5b
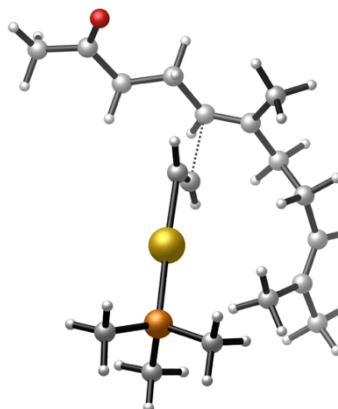
E = - 1257.29721106 Hartrees
G = - 1256.896750 Hartrees

TS30_Int6a
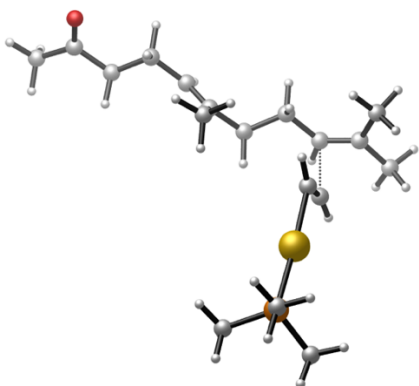
E = - 1257.29458794 Hartrees
G = - 1256.898199 Hartrees

TS30_Int6b
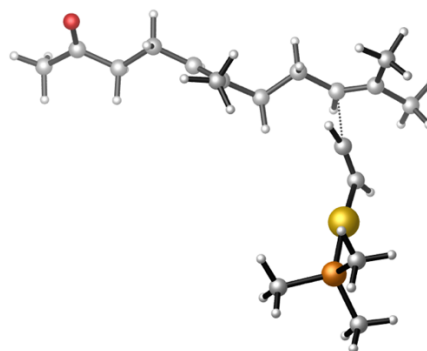
E = - 1257.29292376 Hartrees
G = - 1256.896267 Hartrees

Int1a
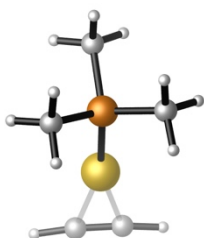
E = - 673.904179606 Hartrees
G = - 673.799679 Hartrees

LAu
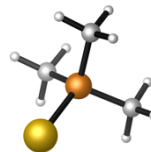
E = - 596.603072 Hartrees
G = - 596.523751 Hartrees

UNIVERSITAT ROVIRA I VIRGILI
COMPUTATIONAL MECHANISTIC STUDIES IN GOLD(I) CATALYSIS AND DESIGN OF NEW CHIRAL LIGANDS
Immaculada Escofet Miquel

Chapter II
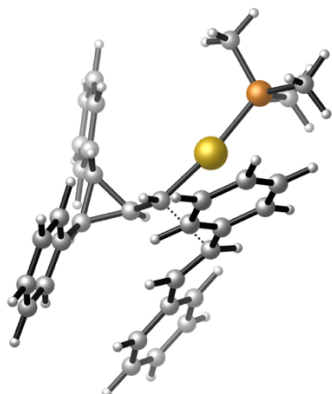
TSInt2a_Int3a

E = - 1754.51094917 Hartrees
G = - 1753.998576 Hartrees

TSInt2a_Int4a
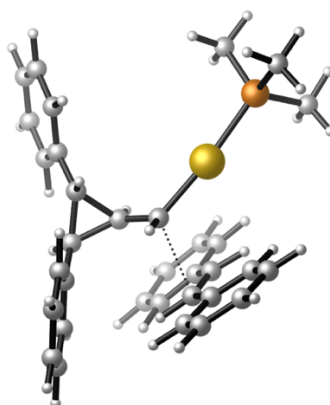
E = - 1754.51479281 Hartrees
G = - 1754.002938 Hartrees

TSInt5a_Int7a
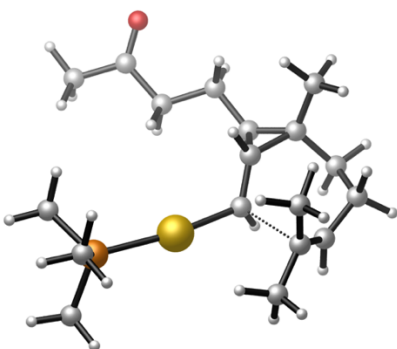
E = - 1257.34398625 Hartrees
G = - 1256.931031 Hartrees

TSInt5b_Int7b
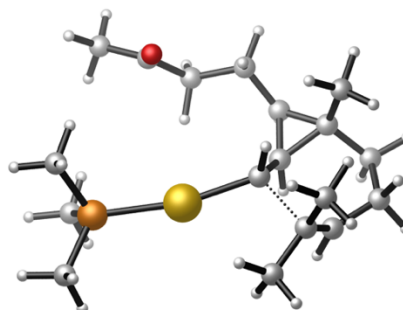
E = - 1257.30510119 Hartrees
G = - 1256.889017 Hartrees

TSInt6a_Int7a
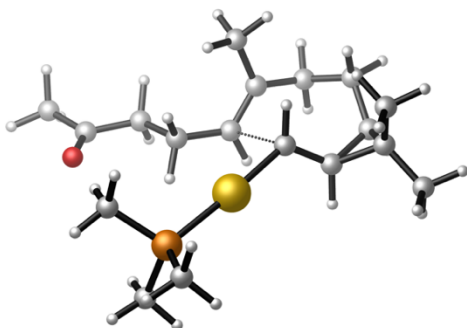
E = - 1257.34252725 Hartrees
G = - 1256.928789 Hartrees

TSInt6b_Int7b
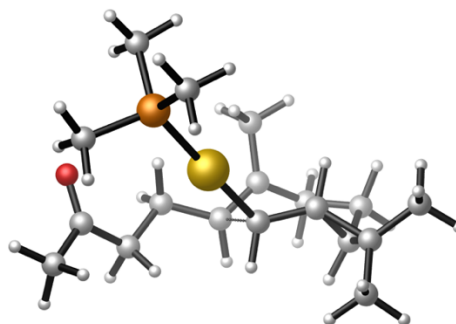
E = - 1257.32802350 Hartrees
G = - 1256.912383 Hartrees

UNIVERSITAT ROVIRA I VIRGILI
COMPUTATIONAL MECHANISTIC STUDIES IN GOLD(I) CATALYSIS AND DESIGN OF NEW CHIRAL LIGANDS
Immaculada Escofet Miquel

Chapter III: Enantioselective Gold(I) Catalysis

UNIVERSITAT ROVIRA I VIRGILI
COMPUTATIONAL MECHANISTIC STUDIES IN GOLD(I) CATALYSIS AND DESIGN OF NEW CHIRAL LIGANDS
Immaculada Escofet Miquel

UNIVERSITAT ROVIRA I VIRGILI
COMPUTATIONAL MECHANISTIC STUDIES IN GOLD(I) CATALYSIS AND DESIGN OF NEW CHIRAL LIGANDS
Immaculada Escofet Miquel

Chapter III

Introduction

Origin of the Enantioselectivity in Gold(I) Catalysis

As explained in the **General Introduction**, much of the progress in asymmetric gold(I) catalysis has been achieved over the last decade and has mainly involved intramolecular reactions. However, broad scope intermolecular enantioselective transformations are still relatively scarce.[1] This slow development can be rationalized by the preferred linear dicoordination adopted by gold(I) in which the chiral ligand (L*) is placed far away from the reaction center, resulting in poor enantioinduction. The problem due to the distance between the substrate and the ligand is further heighten by the outer-sphere attack of the nucleophiles (Figure 1).[2]

Main Challenges for Asymmetric Au(I) catalysis:

- Linear coordination geometry adopted by Au(I)

- Outer-sphere attack of the nucleophile in the enantiodetermining step
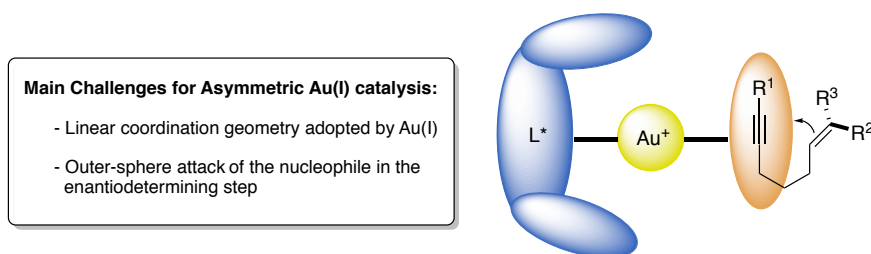
Figure 1. General coordination mode and main challenges for asymmetric Au(I) catalysis.

One of the most common strategies to face this challenge is based on the use of axially chiral digold complexes.[3,4] However, the working mode of theses catalysts can be ambiguous since the second gold center can also play an importat role in the enantiodiscrimination. Therefore, fully understanding the origin of enantioselectivity is often puzzling. On the other hand, monogold complexes based on phosphoroamidite ligands have also been used in several examples of enantioselective gold(I) reactions.[5]

1   (a) Fairlamb, I. J. S *Angew. Chem. Int. Ed.* **2004**, 43, 1048–1052. (b) Bongers, N.; Krause, N. *Angew. Chem. Int. Ed.* **2008**, *47*, 2178–2181. (c) Widenhoefer, R. A. *Chem. Eur. J.* **2008**, *14*, 5382–5391. (d) Sengupta, S.; Shi, X. *ChemCatChem.* **2010**, *2*, 609–619. (e) Lee, A.-L. *Annu. Rep. Prog. Chem.,* Sect. B, **2010**, *106*, 428–446. (f) Shapiro, N. D.; Toste, F. D. *Synlett* **2010**, 2010, 675–691. (g) Pradal, A.; Toullec, P. Y.; Michelet, V. *Synthesis* **2011**, 1501–1514. (h) Wang, Y. M.; Lackner, A. D.; Toste, F. D. *Acc. Chem. Res.* **2014**, *47*, 889–901. (i) Li, Y.; Li, W.; Zhang, J. *Chem. Eur. J.* **2017**, *23*, 467–512.

2   Zi, W.; Toste, F. D. *Chem. Soc. Rev.* **2016**, *45*, 4567–4589.

3   (a) Muñoz, M. P.; Adrio, J.; Carretero, J. C.; Echavarren, A. M. *Organometallics.* **2005**, *24*, 1293–1300. (b) Johansson, M. J.; Gorin, D. J.; Staben, S. T.; Toste, F. D. *J. Am. Chem. Soc.* **2005**, *127*, 18002–18003. (c) LaLonde, R. L.; Sherry, B. D.; Kang, E. J.; Toste, F. D. *J. Am. Chem. Soc.* **2007**, *129*, 2452–2453.

4   (a) Zhang, Z.; Liu, C.; Kinder, R. E.; Han, X.; Qian, H.; Widenhoefer, R. A. J. *J. Am. Chem. Soc.* **2006**, *128*, 9066–9073. (b) Luzung, M. R.; Mauleón, P.; Toste, F. D. *J. Am. Chem. Soc.* **2007**, *129*, 12402–12403. (c) Zhang, Z.; Widenhoefer, R. A. *Angew. Chem. Int. Ed.* **2007**, *46*, 283–285. (d) Zhang, Z.; Bender, C. F.; Widenhoefer, R. A. *Org. Lett.* **2007**, *9*, 2887–2889.

5   (a) Alonso, I.; Trillo, B.; López, F.; Montserrat, S.; Ujaque, G.; Castedo, L.; Lledós, A.; Mascareñas, J. L. *J. Am. Chem. Soc.* **2009**, *131*, 13020–13030. (b) González, A. Z.; Toste, F. D. *Org. Lett.* **2009**, *12*, 200–203. (c) González, A. Z.; Benitez, D.; Tkatchouk, E.; Goddard, W. A.; Toste, F. D. *J. Am. Chem. Soc.* **2011**, *133*, 5500–5507.

UNIVERSITAT ROVIRA I VIRGILI
COMPUTATIONAL MECHANISTIC STUDIES IN GOLD(I) CATALYSIS AND DESIGN OF NEW CHIRAL LIGANDS
Immaculada Escofet Miquel

Chapter III

In 2007, the group of Gagné reported an asymmetric gold(I)-catalyzed cyloisomerization of eneallenes type of **1** using gold complexes based on BINAP ligands.[6] Vinylcyclohexanes **2** and **3** were obtained in good yields and modest enantioselectivities (Scheme 1). Both regioselectivity and enantioselectivity were found to depend on the solvent and the counterion. When using AgOTs instead of AgOTf as chloride scavenger, the enantiomeric excess dropped, although product **2** was obtained in higher regioselectivity (50% *ee*, and 10:1 *r.r.*). The counterion acted as a weak base in the β-elimination step giving rise to vinylcyclohexanes. Moreover, X-ray crystallography showed a well-defined chiral environment for catalyst **A** due to key π-π interactions between two P-bound aryl groups. These non-covalent interactions (3.7 Å) provided a degree of rigidity, resulting high enantioinduction.
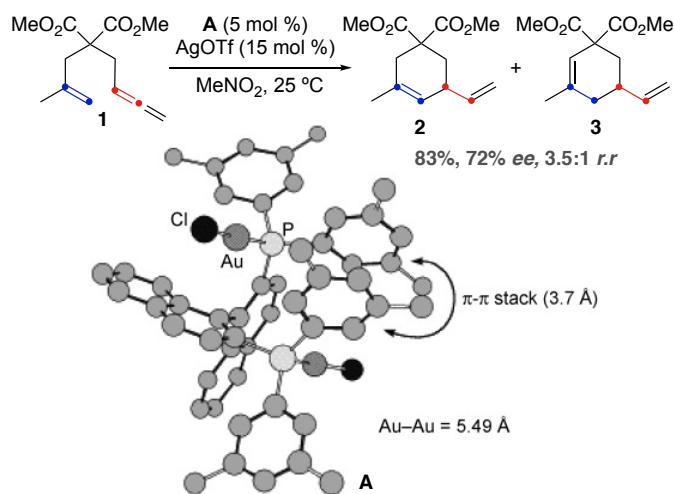
Scheme 1. Enantioselective gold(I)-catalyzed eneallenes **1** cyclization and X-ray structure of catalyst **A** highlighting key interactions.

Eneallenes **4** can undergo [2+2] cycloaddition using TADDOL-derived phosphoroamidites as chiral ligands, catalysts **B-G** (Scheme 2).[7] High enantiomeric ratios were obtained when using electron rich catalysts (**B** and **C**), whereas phenyl groups containing electron poor aryl groups (**D** and **E**) led to lower enantioinduction. The enantioselective formation of cycloadducts **5** was claimed to be driven by electrostatic interactions in the chiral pocket of the catalyst. These results can be rationalized by a through-space interaction between the arenes and the electron deficient gold center of the catalyst (3.2–3.9 Å). Thus, electron rich aromatic rings would tighten the chiral pocket with a stronger arene-gold cationic interaction and thereby would afford cycloadducts **5** in higher enantioselectivities. In order to strengthen these interactions, new phosphoroamidite ligands were prepared with acyclic TADDOL backbones (**F-G**) that enhance enantioselectivity (Scheme 2).

6   Tarselli, M. A.; Chianese, A. R.; Lee, S. L.; Gagné, M. R. *Angew. Chem. Int. Ed.* **2007**, *46*, 6670–6673.
7   Teller, H.; Flügge, S.; Goddard, R.; Fürstner, A. *Angew. Chem. Int. Ed.* **2010**, *49*, 1949–1953.

UNIVERSITAT ROVIRA I VIRGILI
COMPUTATIONAL MECHANISTIC STUDIES IN GOLD(I) CATALYSIS AND DESIGN OF NEW CHIRAL LIGANDS
Immaculada Escofet Miquel

Chapter III
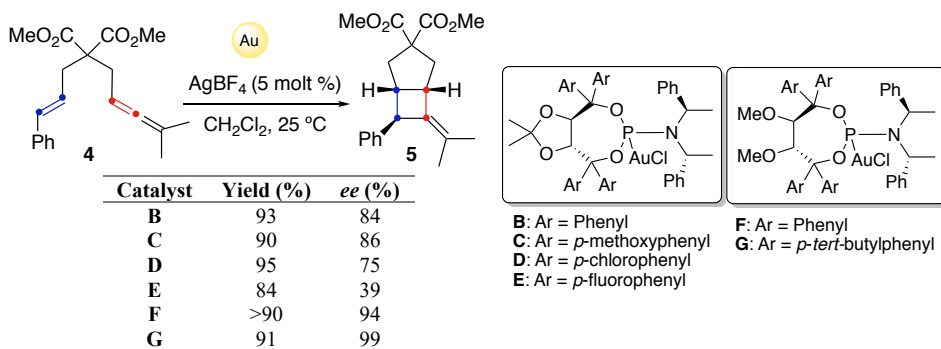
Scheme 2. Enantioselective [2+2] cycloaddition of **4** catalyzed by gold(I) complexes **B-G**.

Novel asymmetric gold(I)-catalyzed polyene cyclization reactions were reported by Toste and co-workers (Scheme 3).[8] Good yields and high enantioselectivities were achieved by using monocationic diphosphine-gold complex based on DTB-MeOBIPHEP ligands **H**. Thus, 1,6-enyne **6** is converted to polycyclic compounds such as **7** whose configuration is consistent with the Stork-Eschenmoser postulate, *via* transition state **I**. Interestingly, only one equivalent of silver salt has been used, while the other Au-Cl moiety has an important role for the high enantioinduction. This methodology was applied for the construction of other carbo- and heterocyclic structures (Scheme 3).
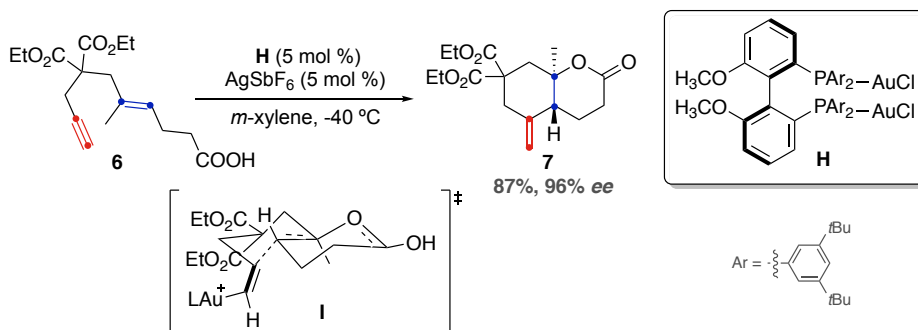
Scheme 3. Enantioselective gold(I)-catalyzed polycyclization of enyne **6**.

In addition, the synthesis of tricyclic compounds **9** was reported from arylenynes **8** in excellent yields and 93% *ee* when using similar bimetallic gold(I) complexes **I** based on MeOBIPHEP ligand. Products **9** could be obtained in 92% *ee*, albeit in moderate yields, when the aryl ring is substituted with a *para*-methoxy group (Scheme 4).[9] This result confirmed the possibility of further developing efficient enantioselective gold(I)-catalyzed transformations of enynes.

8   Sethofer, S. G.; Mayer, T.; Toste, F. D. *J. Am. Chem. Soc.* **2010**, *132*, 8276–8277.
9   Chao, C.-M.; Vitale, M. R.; Toullec, P. Y.; Genêt, J.-P.; Michelet, V. *Chem. Eur. J.* **2009**, *15*, 1319–1323.

UNIVERSITAT ROVIRA I VIRGILI
COMPUTATIONAL MECHANISTIC STUDIES IN GOLD(I) CATALYSIS AND DESIGN OF NEW CHIRAL LIGANDS
Immaculada Escofet Miquel

Chapter III
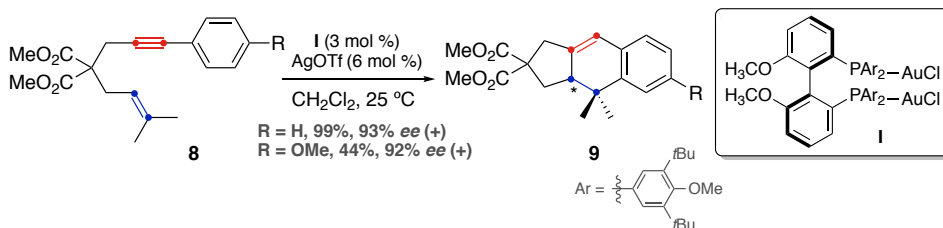
Scheme 4. Asymmetric gold(I)-catalyzed cyclization of arylenynes **8**.

Very recent progress relies on the design of new ligands such as monodentate helically chiral phosphine ligands with embedded phosphole units. This crucial structural feature was found to promote cycloisomerizations of *N*-tethered 1,6-enynes **10** to afford the corresponding azabicyclo[4.1.0]heptanes **11** (Scheme 5).[10a] Interestingly, these gold(I) complexes have also been used for the formal [4+2] cyclization of 1,6-enynes of type **8** (Scheme 4) giving rise to dihydro-cyclopenta[*b*]napththalene derivates **9** in excellent yields and with up to 91% *ee*.[10b]
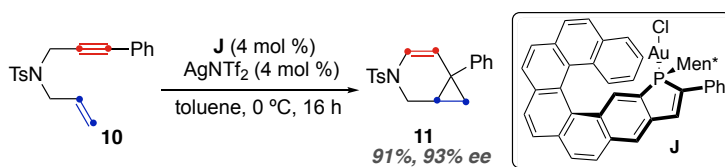
Scheme 5. Asymmetric gold(I)-catalyzed cyclization of enynes **10**.

Other strategies rely on the use of sulfinamide monophosphines, so-called PC-Phos, which were designed combining Ming-Phos and Xant-Phos moieties.[11] This new geometry broadens the space and change the angle between the phosphine and the sulfinamide (Scheme 6).
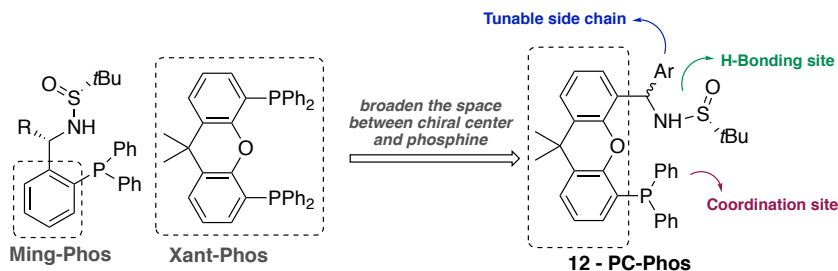
Scheme 6. Novel sulfonamide monophosphine ligand design.

10   (a) Yavari, K.; Aillard, P.; Zhang, Y.; Nuter, F.; Retailleau, P.; Voituriez, A.; Marinetti, A. *Angew. Chem., Int. Ed.* **2014**, *53*, 861−865. (b) Aillard, P.; Dova, D.; Magne, V.; Retailleau, P.; Cauteruccio, S.; Licandro, E.; Voituriez, A.; Marinetti, A. *Chem. Commun.* **2016**, *52*, 10984−10987.

11   Wang, Y.; Zhang, P.; Di, X.; Dai, Q.; Zhang, Z.-M.; Zhang, J. *Angew. Chem., Int. Ed.* **2017**, *56*, 15905−15909.

UNIVERSITAT ROVIRA I VIRGILI
COMPUTATIONAL MECHANISTIC STUDIES IN GOLD(I) CATALYSIS AND DESIGN OF NEW CHIRAL LIGANDS
Immaculada Escofet Miquel

Chapter III

PC-Phos is an effective ligand in the gold(I)-catalyzed cyclization of *N*-allenamides **13** giving enantioenriched tetrahydrocarbolines **14** in excellent yields and enantioselectivities (Scheme 7). In this transformation, the sulfonyl group forms a hydrogen bond with the hydrogen atom of the catalyst. Hence, the *Si* face of allenamide becomes shielded by the ligand and the indole group preferentially attacks at the *Re* face, leading to enantioenriched product **14**.
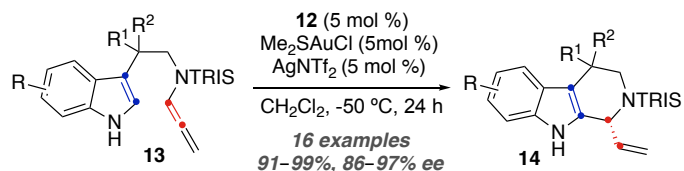
Scheme 7. Asymmetric synthesis of tetrahydrocarbolines **14** catalyzed by gold(I) PC-Phos complex.

In a different approach, the group of Liming Zhang has recently introduced the use of axially chiral monodentate phosphine ligands with a remote cooperative functionality.[12] Gold(I) complexes (**K-L**) based on these bifunctional ligands enable the synthesis of 2-vinyltetrahydrofuranes **16** and 2,5-dihydrofuranes **18** in high enantioselectivities (Scheme 8). Key for the cyclization of **15** was the use of catalyst **K** whose amide group acts a general base catalyst and selectively pre-orientates the substrate for the nucleophilic attack into one of the prochiral allene faces. Consequently, very low catalyst loadings are necessary due to the accelerative nature of the catalysis. Similarly, in the presence of catalyst **L**, enantioselective tandem isomerization/cyclization of propargylic alcohol **17** give rise to product **18**.
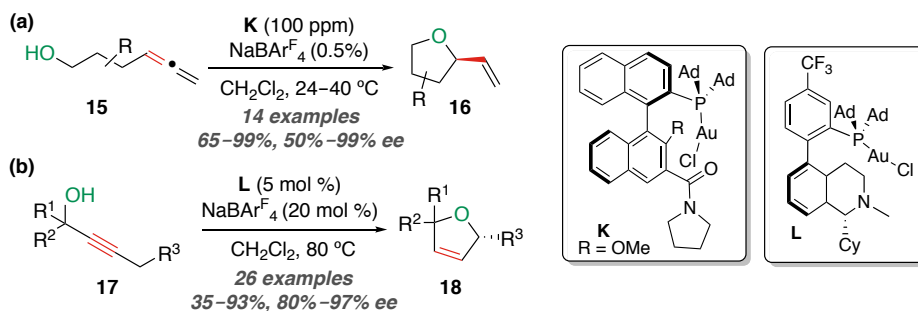
Scheme 8. Application of chiral biarylphosphine ligands with remote functionality in gold(I)-catalyzed synthesis of **16** and **18**.

---

12   (a) Wang, Z.; Nicolini, C.; Hervieu, C.; Wong, Y.-F.; Zanoni, G.; Zhang, L. *J. Am. Chem. Soc.* **2017**, *139*, 16064–16067. (b) Cheng, X.; Wang, Z.; Quintanilla, C. D.; Zhang, L. *J. Am. Chem. Soc.* **2019**, *141*, 3787–3791.

UNIVERSITAT ROVIRA I VIRGILI
COMPUTATIONAL MECHANISTIC STUDIES IN GOLD(I) CATALYSIS AND DESIGN OF NEW CHIRAL LIGANDS
Immaculada Escofet Miquel

Chapter III

Asymmetric Synthesis of Cyclobutenes

Cyclobutenes are important structural motifs occurring in many natural products and in biologically relevant compounds (Scheme 9).[13] Their high reactivity can be attributed to the four-membered ring strain and the presence of double carbon-carbon bond. Therefore, these carbocycles have been used as building blocks to access a diversity of scaffolds,[14] such as cyclobutanes and cyclopropanes.[15]
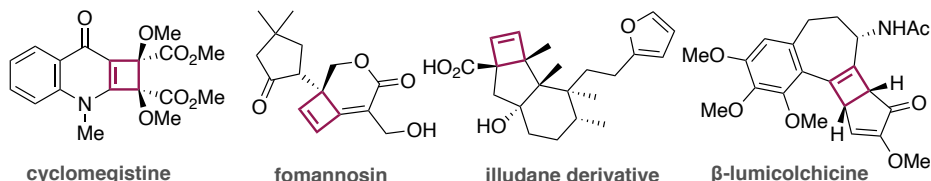
Scheme 9. Selected natural products containing cyclobutenes.

Several strategies have been designed for the efficient preparation of cyclobutenes using Lewis acids,[16] transition metals,[17] and photochemical processes.[18] Among these strategies, the [2+2] cycloaddition of alkynes with alkenes is one of the most straightforward methodologies.

As highlighted in **Chapter II**, our group demonstrated that the intermolecular reaction between terminal alkynes **19** and alkenes **20** leads regioselectively to cyclobutenes **21** (Scheme 10).[19]

13   (a) Chapman, O. L.; Smith, H. G.; King R. W. *J. Am. Chem. Soc.* **1963**, *85*, 803–806. (b) Fokialakis, N.; Magiatis, P.; Terzis, A.; Tillequin, F.; Skaltsounis, A.-L. *Tetrahedron Lett.* **2001**, *42*, 5323–5325. (c) Dembitsky, V. M. *J. Nat. Med.* **2008**, *62*, 1–33. (d) Bohlmann, F.; Grenz, M.; Wegner, P.; Jakupóvic, J. Liebigs. *Ann. Chem.* **1983**, 2008–2020. (e) Sittiwong, W.; Zinniel, D. K.; Fenton, R. J.; Marshall, D. D.; Story, C. B.; Kim, B.; Lee, J.-Y.; Powers, R.; Barletta, R.G.; Dussault, P. H. *ChemMedChem.* **2014**, 9, 1838–1849.

14   (a) Arichi, N.; Yamada, K.; Yamaoka, Y.; Takasu, K. *J. Am. Chem. Soc.* **2015**, *137*, 9579–9582. (b) Misale, A., Niyomchon, S.; Maulide, N. *Acc. Chem. Res.* **2016**, *49*, 2444–2458.

15   (a) Namyslo, C. J.; Kaufmann, D. E. *Chem. Rev.* **2003**, *103*, 1485−1537. (b) Lukin, K.; Kishore, V.; Gordon, T. *Org. Process Res. Dev.* **2013**, *17*, 666–671. (c) Kallemeyn, J. M.; Ku, Y.-Y.; Mulhern, M. M.; Bishop, R.; Pal, A.; Jacob, L. *Org. Process Res. Dev.* **2014**, *18*, 191–197. (d) Guisán-Ceinos, M.; Parra, A.; Martín-Heras, V.; Tortosa, M. *Angew. Chem. Int. Ed.* **2016**, *55*, 6969–6972. (e) Roy, S. R.; Eijsberg, H.; Bruffaerts, J.; Marek, I. *Chem. Sci.* **2017**, *8*, 334–339.

16   (a) Snider, B. B. *Acc. Chem. Res.* **1980**, *13*, 426–432. (b) Clark, R. D.; Untch, K. G. *J. Org. Chem.* **1979**, *44*, 248–255. (c) Fienemann, H.; Hoffmann, H. M. R. *J. Org. Chem.* **1979**, *44*, 2802–2804. (d) Snider, B. B.; Rodini, D. J.; Conn, R. S. E.; Sealfon, S. *J. Am. Chem. Soc.* **1979**, *101*, 5283–5293. (e) Quendo, A.; Rousseau, G. *Tetrahedron Lett.* **1988**, *29*, 6443–6446. (f) Franck-Neumann, M.; Miesch, M.; Gross, L. *Tetrahedron Lett.* **1992**, *33*, 3879–3882. (g) Sweis, R. F.; Schramm, M. P.; Kozmin, S. A. *J. Am. Chem. Soc.* **2004**, *126*, 7442–7443. (h) Okamoto, K.; Shimbayashi, T.; Tamura, E.; Ohe, K. *Org. Lett.* **2015**, *17*, 5843–5845.

17   (a) Lautens, M.; Klute, W.; Tam, W. *Chem. Rev.* **1996**, *96*, 49–92. (b) Sakari, K.; Kochi, T.; Kakiuchi, F. *Org. Lett.* **2013**, *15*, 1024–1027. (c) Fructos, M. R.; Prieto, A. *Tetrahedron* **2016**, *72*, 355–369.

18   (a) Lee-Ruff, E.; Mladenova, G. *Chem. Rev.* **2003**, *103*, 1449–1484. (b) Yang, C.; Inoue, Y. *Chem. Soc. Rev.* **2014**, *43*, 4123−4143. (c) Xu, Y.; Conner, M. L.; Brown, M. K. *Angew. Chem Int. Ed.* **2015**, *54*, 11918−11928. (d) Blum, T. R.; Miller, Z. D.; Bates, D. M.; Guzei, I. A.; Yoon, T. P. *Science* **2016**, *354*, 1391–1395. (e) Poplata, S.; Tröster, A.; Zou, Y.-Q.; Bach, T. *Chem. Rev.* **2016**, *116*, 9748–9815.

19   López-Carrillo, V.; Echavarren, A. M. *J. Am. Chem. Soc.* **2010**, *132*, 9292–9294.

UNIVERSITAT ROVIRA I VIRGILI
COMPUTATIONAL MECHANISTIC STUDIES IN GOLD(I) CATALYSIS AND DESIGN OF NEW CHIRAL LIGANDS
Immaculada Escofet Miquel

Chapter III

The use of gold(I) complex **M**, with bulky *t*BuXPhos ligand, was found to be key for the success of these transformations, in which the counterion plays an important role.[20]
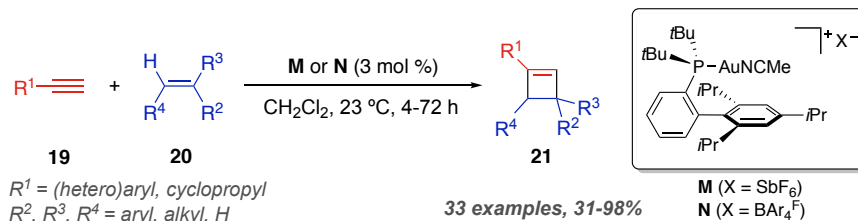
Scheme 10. Gold(I)-catalyzed [2+2] cycloaddition of terminal alkynes with alkenes.

Nevertheless, the development of efficient asymmetric transformations has been relatively slow-paced. Indeed, the first chiral Lewis acid-catalyzed enantioselective [2+2] cycloaddition reaction was developed in 2004 and was applied for the total synthesis of (+)-tricycloclavulone.[21] A mixture of copper salt, silver hexafluoroantimonate and chiral bis-pyridine ligand **O** catalyzed the reaction of **22** with **23** to give bicyclic product **24** with 73% *ee* in 67% yield (Scheme 11). This reaction was limited to the use of electron-deficient alkenes and electron-rich alkynes such as thioacetylene **22**. This methodology was later employed for the enantioselective total synthesis of (+)-precapnelladiene.[22]
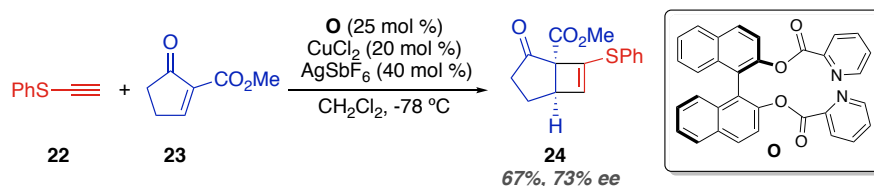
Scheme 11. Copper-catalyzed asymmetric [2+2] cycloaddition reaction of **22** and **23**.

Another interesting example of asymmetric [2+2] cycloaddition catalyzed by Lewis acids is the enantioselective Ficini[23] reaction between ynamides **25** and cyclic enones **26** reported by the group of Mezzetti (Scheme 12).[24]
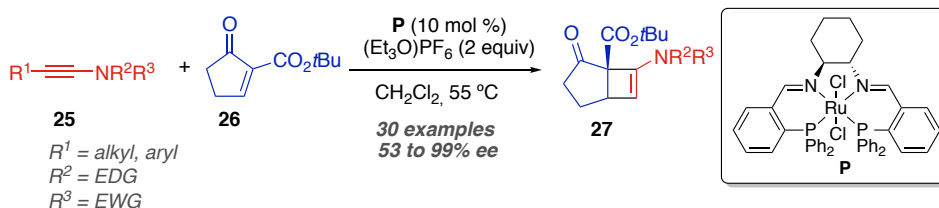
Scheme 12. Ruthenium-catalyzed enantioselective Ficini reaction of ynamides **25** with **26**.

20   Homs, A.; Obradors, C.; Leboeuf, D.; Echavarren, A. M. *Adv. Synth. Catal.* **2014**, *356*, 221–228.
21   Ito, H.; Hasegawa, M.; Takenaka, Y.; Kobayashi, T.; Iguchi, K. *J. Am. Chem. Soc.* **2004**, *126*, 4520–4521.
22   Takenaka, Y.; Ito, H.; Iguchi, K. *Tetrahedron* **2006**, *63*, 510–513.
23   Ficini, J. *Tetrahedron* **1976**, *32*, 1449–1486.
24   Schotes, C.; Mezzetti, A. *Angew. Chem. Int. Ed.* **2011**, *50*, 3072–3074.

UNIVERSITAT ROVIRA I VIRGILI
COMPUTATIONAL MECHANISTIC STUDIES IN GOLD(I) CATALYSIS AND DESIGN OF NEW CHIRAL LIGANDS
Immaculada Escofet Miquel

Chapter III

The advantage of using ynamides instead of ynamines (initially used by Ficini) is that the electron-withdrawing group decreases the alkyne reactivity allowing for the catalytic asymmetric approach. Thus, aminocyclobutenes **24** were obtained in high yields and enantioselectivities under ruthenium catalysis. Noteworthy, Molecular Modeling (MM) calculations show that the ruthenium/PNNP catalyst **P** stabilizes the enolate intermediate, thus increasing the enantioinduction. Similarly, Nakada and co-workers reported the asymmetric copper-catalyzed [2+2] cycloaddition of cyclic α-alkylidene β-oxo imides with ynamides.[25]

Later, a zinc(II) catalyst with chiral *N,N'*-dioxide ligand **Q** was used for the efficient enantioselective [2+2] cycloaddition of electron poor alkynones **28** with electron-rich cyclic enol silyl ethers **29** (Scheme 13). Hence, strained cyclobutenes **30** were obtained with good to excellent enantioselectivities and were further transformed into fused cyclobutane derivatives.[26]
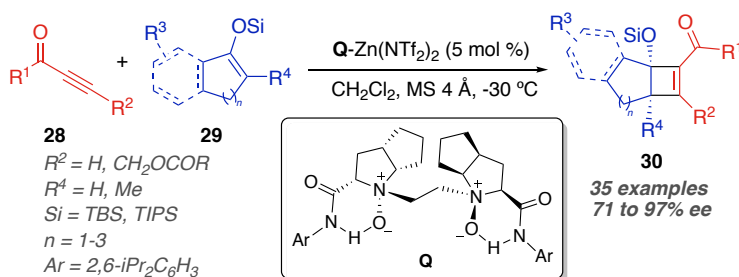
Scheme 13. Enantioselective Zn-catalyzed [2+2] cycloaddition of alkynones **28** and cyclic enol silyl ethers **29**.

On the other hand, several strategies have been reported involving the use of transition metals to promote asymmetric [2+2] cycloadditions (Scheme 14). Nonetheless, most of them only proceed when using strained alkenes such as norbornene derivatives, as found by Shibata in 2006 for the synthesis of chiral cyclobutenes **31** (Scheme 14).[27] Thus, propiolates and norbornene derivatives undergo a [2+2] cycloaddition catalyzed by chiral rhodium complex affording **31** with moderate to excellent enantiomeric ratios. Later, the enantioselective iridium-catalyzed [2+2] cycloaddition of terminal alkynes with oxabicyclic alkenes was reported leading to the formation strained cyclobutenes **32** in high enantioselectivities.[28] In addition, neutral chiral ruthenium(II) catalyst **R**, based on an atrophchiral cyclopentadienyl (Cpˣ) ligand, was found to be active for the asymmetric synthesis of cyclobutenes **33** at very low catalyst loading.[29] Remarkably, a strong counterion

25   Enomoto, K.; Oyama, H.; Nakada, M. *Chem. Eur. J.* **2015**, *21*, 2798–2802.
26   Kang, T.; Ge, S.; Lin, L.; Lu, Y.; Liu, X.; Feng, X. *Angew. Chem. Int. Ed.* **2016**, *55*, 5541–5544.
27   Shibata, T.; Takami, K.; Kawachi, A. *Org. Lett.* **2006**, *8*, 1343–1345.
28   Fan, B.-M.; Li, X.-J.; Peng, F.-Z.; Zhang, H.-B.; Chang, A. S. C.; Shao, Z.-H. *Org. Lett.* **2010**, *12*, 304–306.
29   Kossler, D.; Cramer, N. *Chem. Sci.* **2017**, *8*, 1862–1866.

UNIVERSITAT ROVIRA I VIRGILI
COMPUTATIONAL MECHANISTIC STUDIES IN GOLD(I) CATALYSIS AND DESIGN OF NEW CHIRAL LIGANDS
Immaculada Escofet Miquel

Chapter III

effect of a bound chloride anion transforms the unselective cationic complex into the enantioselective neutral version.

In 2018, the Ni-catalyzed enantioselective [2+2] cycloaddition of hetero-bicyclic strained alkenes with non-activated alkynes was reported.[30] This straightforward protocol leads to the formation of four-membered carbocycles **34** with several stereocenters (Scheme 14).
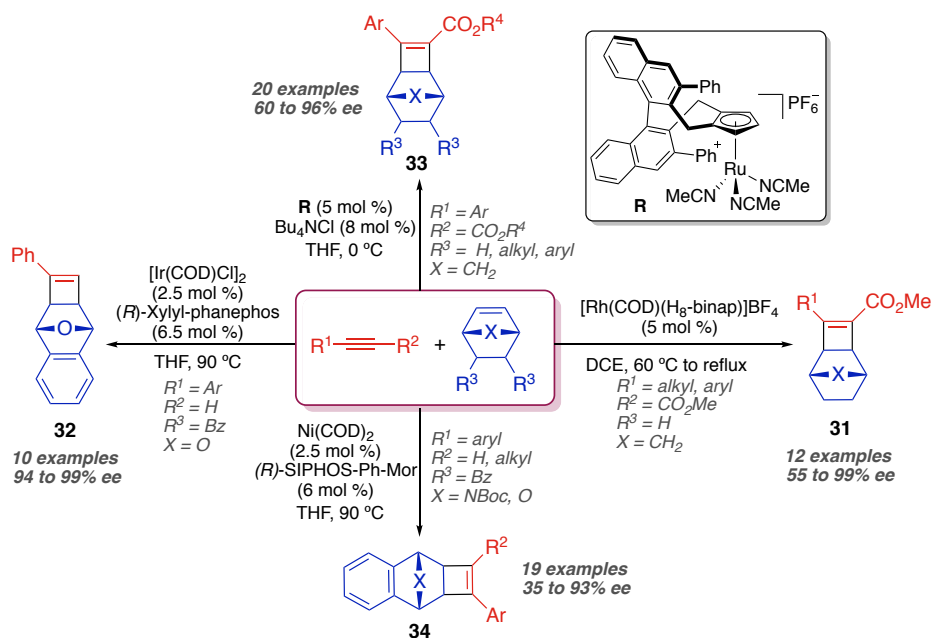
Scheme 14. Enantioselective metal-catalyzed [2+2] cycloaddition of alkynes with strained alkenes.

An alternative route to obtain enantioenriched cyclobutenes by means of cobalt catalysis has recently been reported.[31] This methodology employs phosphino-oxazoline chiral ligands along with cobalt bromide to catalyze the [2+2] cycloaddition of wide variety of alkynes **35** and alkenyl derivatives **36** giving rise to over 50 cyclobutenes **37** with moderate to high enantioselectivities (Scheme 15).

Most of these transition metal-catalyzed asymmetric cycloadditions have been proposed to proceed through coordination of both the alkene and the alkyne to the metal center. These metal dicoordinated species would undergo oxidative cyclometalation leading to metallacycle intermediates followed by reductive elimination to buildup cyclobutene products.

30   Qin, H.; Chen, J.; Li, K.; He, Z.; Zhou, Y.; Fan, B. *Chem. Asian J.* **2018**, *13*, 2431–2434.
31   Parsutkar, M. M.; Vishnu-Pagar, V.; RajanBabu, T. V. *J. Am. Chem. Soc.* **2019**, *141*, 15367–15377.

UNIVERSITAT ROVIRA I VIRGILI
COMPUTATIONAL MECHANISTIC STUDIES IN GOLD(I) CATALYSIS AND DESIGN OF NEW CHIRAL LIGANDS
Immaculada Escofet Miquel

Chapter III
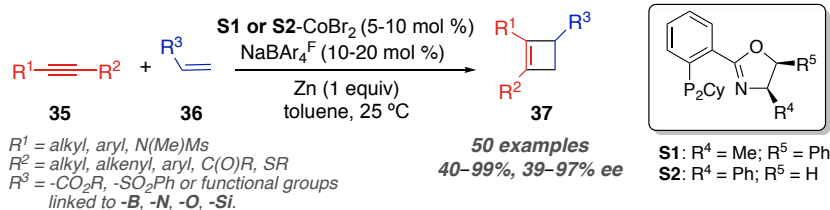
Scheme 15. Co(I)-catalyzed synthesis of enantioenriched cyclobutenes **37** from alkynes **35** and alkenyl derivatives **36**.

It is worth mentioning that most of the recent advances mentioned in this **Introduction** were reported during the course in this Doctoral Thesis. Moreover, previous to the results that we will discuss later[32] (see **Results and Discussion**, **Chapter III**), only one example of Au(I)-catalyzed enantioselective intermolecular [2+2] cycloadditions had been reported for the construction of cyclobutenes type of **21a** in very low enantiomeric ratios.[33] Thus, phenylacetylene **19a** and α-methylstryrene **20a** underwent cycloaddition reaction in the presence of gold(I) complexes (**T** or **U**) based on axially chiral imidazoisoquinolin-2-ylidenes ligands (Scheme 16).
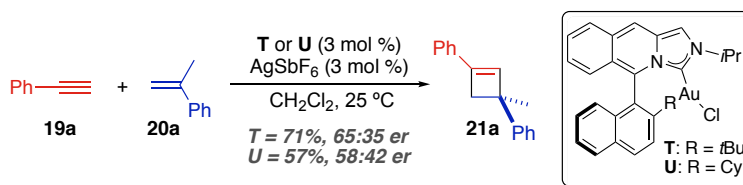
Scheme 16. Enantioselective gold(I)-catalyzed [2+2] cycloaddition of alkyne **19a** and alkenes **20a**.

New Chiral Ligand Design with a Remote C_2-Chiral Element

Due to the ambiguous mode of action of chiral catalysts, to achieve high enantioselectivities in gold(I) catalyzed reactions often requires the screening of many chiral ligands. Furthermore, the activation of alkynes, which are not prochiral, presents a special difficulty in asymmetric gold(I) catalysis. Hence, a system that allows for the rigorous study of the reaction pathway together with the control of the enantioselective folding of enynes is still challenging.

Very recently, our group pioneered the development of a series of chiral catalysts based on a new conceptual design in which the chiral elements, C_2-symmetric *trans*-2,5-diarylpyrrolidines, are in para position of a modified JohnPhos-type ligand.[34] Thus, the

32   García-Morales, C.; Ranieri, B.; Escofet, I.; Obradors, C.; López-Suárez, L.; Konovalov, A. I.; Echavarren, A. M. *J. Am. Chem. Soc.* **2017**, *139*, 13628–13631.

33   Grande-Carmona, F.; Iglesias-Sigüenza, J.; Álvarez, E.; Díez, E.; Fernández, R.; Lassaletta, J. M. *Organometallics* **2015**, *34*, 5073–5080.

34   Zuccarello, G.; Mayans, J. G.; Escofet, I.; Scharnagel, D.; Kirillova, M. S.; Pérez-Jimeno, A. H.; Calleja, P.; Boothe, J. R.; Echavarren, A. M. *J. Am. Chem. Soc.* **2019**, *141*, 11858–11863.

UNIVERSITAT ROVIRA I VIRGILI
COMPUTATIONAL MECHANISTIC STUDIES IN GOLD(I) CATALYSIS AND DESIGN OF NEW CHIRAL LIGANDS
Immaculada Escofet Miquel

Chapter III

bulky substituents on the phosphine prevent rotation around the C_{aryl}-P bond and force the P-Au-Cl axis to be parallel to the biphenyl axis, pointing towards the chiral environment. Moreover, a local C_2-axis is introduced resulting in an unambiguous source of chirality (Figure 2).[35]

These new mononuclear chiral gold(I) complexes are designed for the linear coordination adopted by gold(I), since the substrate gets encapsulated in the chiral pocket. In addition, they are catalytically active in the aforementioned intramolecular [4+2] cycloaddition of 1,6-enynes **8** leading to the formation of cycloadducts **9** in good yields and excellent enantioselectivities (Scheme 17).[36] Upon the screening of these new complexes, the best results were obtained when using *(R,R)*-**V**. The absolute configuration of one example type of **9** was assigned as *R* by single-crystal X-ray diffraction, and those of the remaining cycloadducts were correlated by circular dichroism.[35]
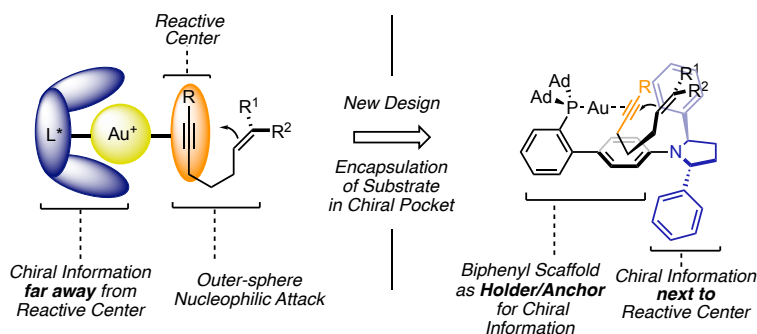
Figure 2. Traditional approach in enantioselective gold(I) catalysis and new catalyst design.

Likewise, we further studied the performance of our designed complexes in the 6-*endo*-dig cyclization[37] of *N*-tethered 1,6-arylenyne **10** catalyzed by gold(I).[38] Hence, in the presence of catalyst **V**, azabicyclo [4.1.0]hept-4-enes **11** were obtained in moderate to good yields and good enantioselectivities. The absolute configuration was assigned by comparison with those previously reported (Scheme 17).[39]

Furthermore, a highly enantioselective 6-*endo*-dig cyclization[40] of 1,6-enynes **38** has allowed to accomplish the first total synthesis of the three members of the carexane family

35   Experimental part of this project was carried out by Giuseppe Zuccarello, Joan G. Mayans, Dr. Dagmar Scharnagel, Dr. Mariia S. Kirillova, Alba H. Pérez-Jimeno, Pilar Calleja and Jordan R. Boothe. All the experimental details can be found in the supporting information of (34).

36   (a) Nieto-Oberhuber, C.; López, S.; Echavarren, A. M. *J. Am. Chem. Soc.* **2005**, *127*, 6178–6179. (b) Nieto-Oberhuber, C.; Pérez-Galán, P.; Herrero-Gómez, E.; Lauterbach, T.; Rodríguez, C.; López, S.; Bour, C.; Rosellón, A.; Cárdenas, D. J.; Echavarren, A. M. *J. Am. Chem. Soc.* **2008**, *130*, 269–279

37   Nieto-Oberhuber, C.; Muñoz, M. P.; López, S.; Jiménez-Núñez, E.; Nevado, C.; Herrero-Gómez, E.; Raducan, M.; Echavarren, A. M. *Chem. Eur. J.* **2006**, *12*, 1677–1693.

38   Fürstner, A.; Szillat, H.; Stelzer, F. *J. Am. Chem. Soc.* **2000**, *122*, 6785–6786.

39   Teller, H.; Corbet, M.; Mantilli, L.; Gopakumar, G.; Goddard, R.; Thiel, W.; Fürstner, A. *J. Am. Chem. Soc.* **2012**, *134*, 15331−15342.

40   Sanjuán, A. M.; Martínez, A.; García-García, P.; Fernández-Rodríguez, M. A.; Sanz, R. *Beilstein J. Org. Chem.* **2013**, *9*, 2242–2249.

UNIVERSITAT ROVIRA I VIRGILI
COMPUTATIONAL MECHANISTIC STUDIES IN GOLD(I) CATALYSIS AND DESIGN OF NEW CHIRAL LIGANDS
Immaculada Escofet Miquel

Chapter III

of natural products.[41] Carexanes are a series of secondary metabolites that have been isolated from leaves of *Carex distachya* and possess antimicrobial activity. Thus, 1,2-dihydronapthalenes **39** were afforded in the presence of water and other external nucleophiles, together with complex **V** (Scheme 17).
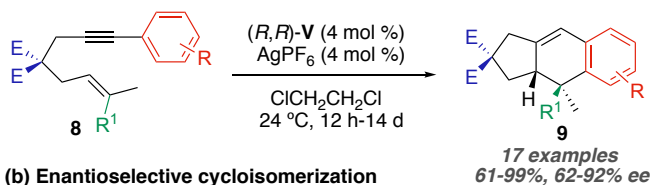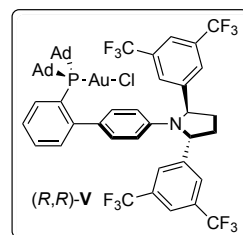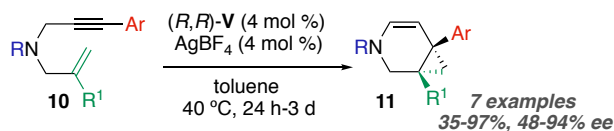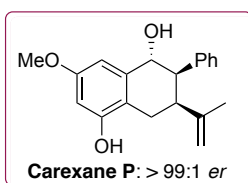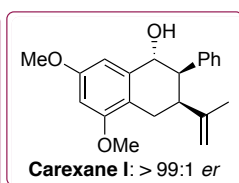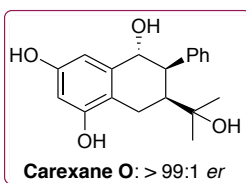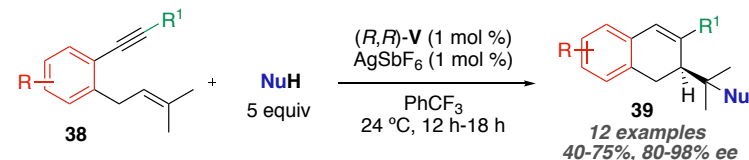
Scheme 17. Applications of chiral complex **V** in catalysis and total synthesis.

It is worth mentioning that before testing these pyrrolidinyl-biphenyl phosphine complexes, we screened 80 chiral ligands from different families at the ICIQ HTE (High Throughput Experimentation) facility. Among them, only the JosiPhos family of ligands gave dihydronaphthalenes **39** in moderate enantioselectivities 80:20 *er*. (Remarkably, this same family of ligands were used in the intermolecular [2+2] cycloaddition of alkynes with alkenes that we will further discuss in the **Results and Discussion** section of this **Chapter III**.

Although the three presumably related cyclizations of 1,6-enynes **8**, **10** and **38** proceed with high enantiomeric ratios, the first two transformations occur with a facial preference for the *Si* face of the alkene, whereas the cyclization of **38** leads to the opposite configuration by

41   (a) D'Abrosca, B.; Fiorentino, A.; Golino, A.; Monaco, P.; Oriano, P.; Pacifico, S. *Tetrahedron Lett.* **2005**, *46*, 5269−5272. (b) Fiorentino, A.; D'Abrosca, B.; Izzo, A.; Pacifico, S.; Monaco, P. *Tetrahedron* **2006**, *62*, 3259−3265. (c) Fiorentino, A.; D'Abrosca, B.; Pacifico, S.; Iacovino, R.; Izzo, A.; Uzzo, P.; Russo, A.; Di Blasio, B.; Monaco, P. *Tetrahedron* **2008**, *64*, 7782−7786.

UNIVERSITAT ROVIRA I VIRGILI
COMPUTATIONAL MECHANISTIC STUDIES IN GOLD(I) CATALYSIS AND DESIGN OF NEW CHIRAL LIGANDS
Immaculada Escofet Miquel

Chapter III

reaction through the *Re* face of the alkene. Therefore, remarkably, two different folding modes occur for this type of substrates and thus, different geometrical arrangements may occur in the chiral pocket. We hypothesized that the aryl tether in enyne **38** directs the stereocontrol of the cyclization, whereas the aryl substituent at carbon C1 in enynes **8** and **10**, is mainly responsible for the recognition in the chiral cavity (Scheme 18).
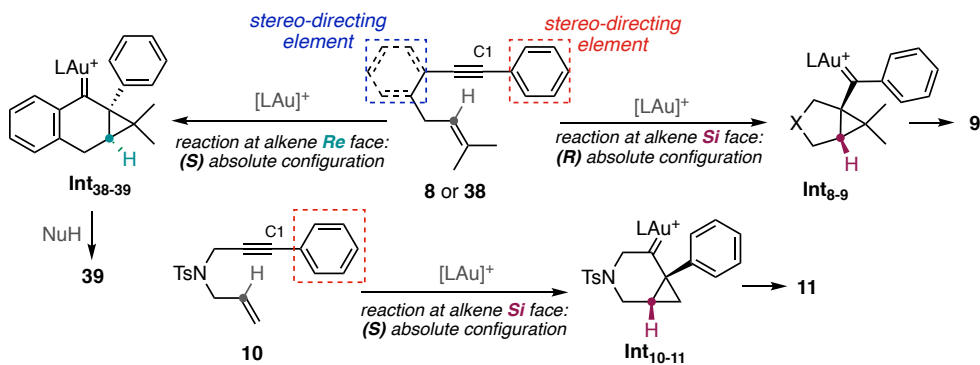
Scheme 18. Stereodirecting moieties in substrates **8**, **10** and **38**.

To probe this hypothesis, control experiments have been performed with substrates **40**, **42** and **44** (Scheme 19). Thus, cycloadduct **41** was obtained with poor enantiomeric ratio since the enyne **40** contains a smaller vinyl group in the aromatic substituent at the alkyne instead of the stereo-directing aryl moiety. Likewise, the hydroxycyclization of terminal alkynes **42**, gave rise to product **43** as a racemic mixture. In contrast, enyne **44**, which contains a cyclohenexyl ring instead of the phenyl at C1, leads to the formation of dihydronaphthalene **45** with essentially the same enantioselectivity observed in the cyclization of enynes **38** to afford **39**.
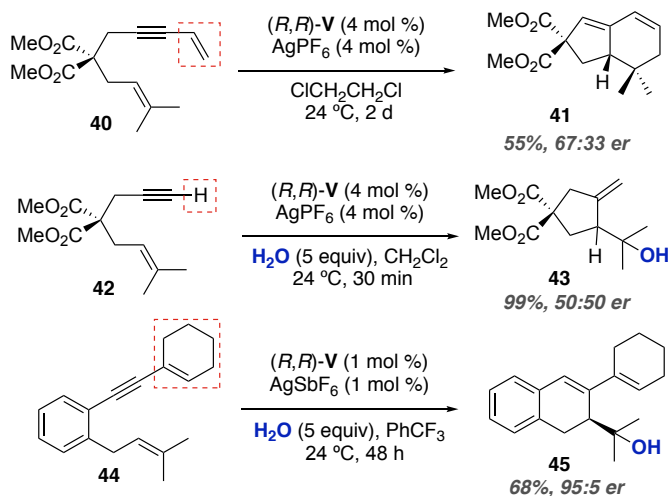
Scheme 19. Control experiments with substrates **40**, **42** and **44**.

UNIVERSITAT ROVIRA I VIRGILI
COMPUTATIONAL MECHANISTIC STUDIES IN GOLD(I) CATALYSIS AND DESIGN OF NEW CHIRAL LIGANDS
Immaculada Escofet Miquel

Chapter III

Objectives

The design and synthesis of novel chiral ligands that can react in a general manner in gold(I) catalytic transformations is still a significant challenge. Therefore, one of the objectives of this Doctoral Thesis was the development of an enantioselective intramolecular [4+2] cycloaddition of 1,6-enyne **8** with new chiral gold(I) phosphite complexes (Scheme 20).
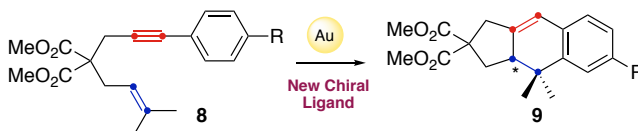
Scheme 20. Enantioselective gold(I)-catalyzed [4+2] cycloaddition of 1,6-enynes **8**.

On the other hand, since enantioenriched cyclobutenes can be used as building blocks, we aimed at developing a general enantioselective synthesis of cyclobutenes **21** by intermolecular gold(I)-catalyzed [2+2] cycloaddition of alkynes **19** with alkenes **21** (Scheme 21).
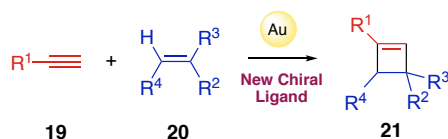
Scheme 21. Enantioselective Au-catalyzed [2+2] cycloaddition of alkynes **19** with alkenes **20**.

Furthermore, intrigued by the different outcomes observed in our recent ligand designed based on a JohnPhos-type ligand with a *trans*-2,5-diarylpyrrolidine at the para position, we decided to study the different mechanistic pathways by means of DFT calculations. Likewise, we aimed to computationally prove our hypothesis on the stereodirecting effect exerted by the different structural elements of the substrates to better understand the working mode of our novel chiral catalysts (Scheme 18).

Scheme 18. Stereodirecting moieties in substrates **8**, **10** and **38**.

UNIVERSITAT ROVIRA I VIRGILI
COMPUTATIONAL MECHANISTIC STUDIES IN GOLD(I) CATALYSIS AND DESIGN OF NEW CHIRAL LIGANDS
Immaculada Escofet Miquel
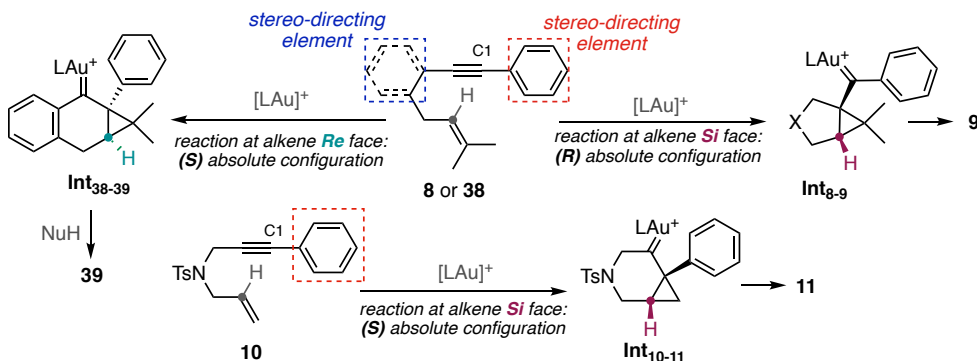
Chapter III

Results and Discussion

This **Chapter III** has been divided in three main parts. First, we will show the experimental results obtained on the synthesis of chiral phosphite monogold(I) complexes easily prepared from BINOL, and its applications in gold(I)-catalyzed transformations. Secondly, broad scope enantioselective synthesis of cyclobutenes will be discussed. Finally, computational study on the mode of action of the new pyrrolidinyl-biphenyl phosphine gold(I) complexes will be presented.

Modular Chiral Gold(I) Phosphite Complexes

Previous work on the enantioselective gold(I)-catalyzed intramolecular [4+2] cycloaddition of arylenynes reported by our group used chiral gold(I) complexes based on commercially available phosphines and phosphoroamidites ligands.[42] These preliminary studies were the starting point in the development of new classes of chiral ligands.
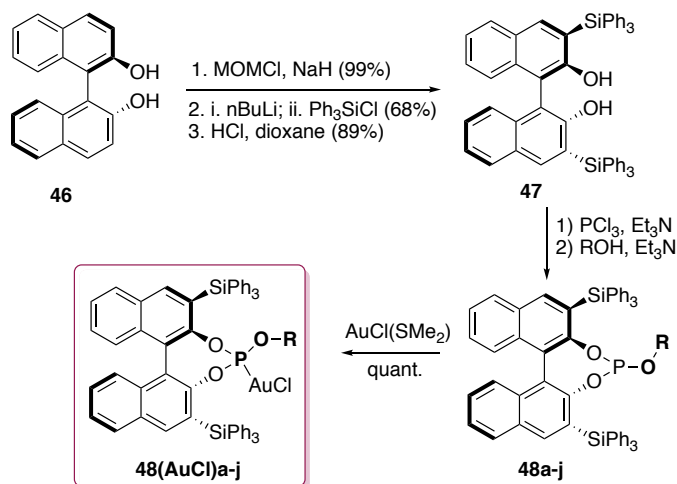
Scheme 22. Synthesis of gold(I) phosphite complexes **48(AuCl)a-j**.

We prepared a series of complexes bearing chiral phosphite ligands **48a-j** based on the BINOL motive (Scheme 22). We used a modular approach starting from commercially available 1,1'-bi-2-napthol.[43] Phosphites were selected over phosphines due to their lower sensitivity to air and other oxidizing agents,[44] and the high reactivity of their resulting complexes towards alkynes.[45]

---

42 Initial studies were performed by Patricia Pérez Galán, Mihai Raducan, Dr. Christophe Bour and Dr. Riccardo Sinisi. Further details on all the complexes tested and synthetic procedures can be found in the supporting information of: *Catal. Sci. Technol.* **2013**, 3, 3007−3012.

43 This work has been done in collaboration with Nicolas Delpont and Dr. Dirk Spiegl.

44 Van Leeuwen, P. W. N. M.; Kamer, P. C. J.; Claver, C.; Pàmies, O.; Diéguez, M. *Chem. Rev.* **2011**, *111*, 2077−2118.

45 (a) Amijs, H. M.; López-Carrillo, V.; Raducan, M.; Pérez-Galán, P.; Ferrer, C.; Echavarren. A. M. *J. Org. Chem.* **2008**, *73*, 7721−7730. (b) Benitez, D.; Shapiro, N. D.; Tkatchouk, E.; Wang, Y.; Goddard III W. A.; Toste, D. F. *Nature Chem.* **2009**, *1*, 482−486.

UNIVERSITAT ROVIRA I VIRGILI
COMPUTATIONAL MECHANISTIC STUDIES IN GOLD(I) CATALYSIS AND DESIGN OF NEW CHIRAL LIGANDS
Immaculada Escofet Miquel

Chapter III
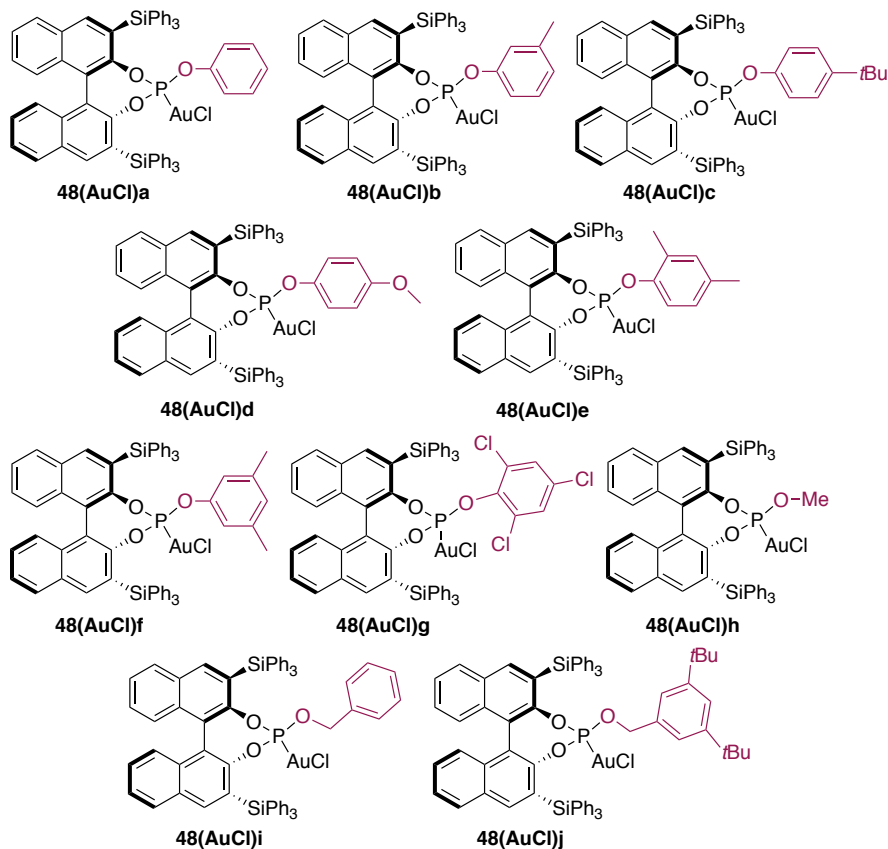
Figure 3. Series of chiral gold(I) phosphite complexes **48(AuCl)a-j**.

The preparation of a series of phosphite ligands **48a-j** with different OR groups was easily carried out using known methods[46] from commercially available (*R*)-BINOL **46**[47] by known procedures *via* BINOL derivative **47**, which is also commercially available (Figure 3). The triphenylsilyl moieties remained unchanged whereas the phenol unit was modified to afford ligands **48a-j** in two steps from a reported procedure.[48] Thus, **47** reacted with PCl$_3$ giving rise to BINOL-derived chlorophosphite, that was trapped *in situ* with different OR groups to give **48a-j** in moderate to good yields.[49] Ligands **48a-j** were purified by chromatography on silica gel under inert atmosphere and the corresponding monogold(I) complexes **48(AuCl)a-j** were prepared in quantitative yields upon the reaction of phosphites **48a-j** with [AuCl(SMe$_2$)].

46   Bedford, R. B.; Chang, Y.-N.; Haddow, M. F.; McMullin, C. L. *Dalton Trans.* **2011**, *40*, 9034–9041.
47   Brunel, J. M. *Chem. Rev.* **2005**, *105*, 4233–4233.
48   Albrow, V. E.; Blake, A. J.; Fryatt, R.; Wilson, C.; Woodward, S. *Eur. J. Org. Chem.*, **2006,** 2549–2557.
49   See the **Experimental Section** at the end of this **Chapter III** for further details.

UNIVERSITAT ROVIRA I VIRGILI
COMPUTATIONAL MECHANISTIC STUDIES IN GOLD(I) CATALYSIS AND DESIGN OF NEW CHIRAL LIGANDS
Immaculada Escofet Miquel

Chapter III

The catalytical activity of these new mononuclear gold(I) phosphite complexes was assayed in the intramolecular formal [4+2] cycloaddition of 1,6-enyne **8a** at 0 °C in CH_2Cl_2 (Table 1).

Table 1. Screening of catalysts **48(AuCl)a-j** in the asymmetric [4+2] cyclization of **8a**.
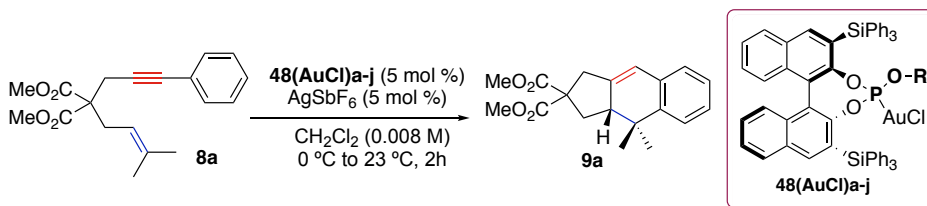
Entry	Catalyst	R	**9a** ee (%)[d]
1	**48(AuCl)a**	Ph	70
2	**48(AuCl)b**	*m*-Tol	72
3	**48(AuCl)c**	4-*t*BuC$_6$H$_4$	82
4[a]	**48(AuCl)c**	4-*t*BuC$_6$H$_4$	88
5	**48(AuCl)d**	4-MeOC$_6$H$_4$	60
6	**48(AuCl)e**	2,4-Me$_2$C$_6$H$_3$	74
7	**48(AuCl)f**	3,5-Me$_2$C$_6$H$_3$	81
8	**48(AuCl)g**	2,4,6-Cl$_3$C$_6$H$_2$	46
9	**48(AuCl)h**	Me	5
10[b]	**48(AuCl)i**	PhCH$_2$	81
11[c]	**48(AuCl)j**	3,5-*t*Bu$_2$C$_6$H$_3$CH$_2$	74

[a] Reaction at -20 °C for 16 h. [b] Reaction at -25 °C for 36 h. [c] Reaction at 0 °C for 7 h.
[d] Enantiomeric excess determined by HPLC, Chiralpack IA.

Under these conditions, **48(AuCl)a** led to cycloadduct **9a** in 70% *ee* (Table 1, entry 1). Interestingly, an increase in enantioselectivity was found using a *p*-alkyl substituted phenol complex (Table 1, entries 3 and 4). Therefore, the best result was achieved with **48(AuCl)c**, performing the reaction at -20 °C. Moreover, satisfactory results were also obtained with precatalysts **48(AuCl)f** and **48(AuCl)i** (Table 1, entries 7 and 10).

Solvent effects were investigated with **48(AuCl)c** (Table 2). The reactions were slower (16–24 h) in 1,2-dichloroethane, diethyl ether or acetone as solvent and gave compound **9a** in moderate enantiomeric ratios (63–82% *ee*) (Table 2, entries 3, 4 and 8), whereas no reaction was observed in toluene or 1,4-dioxane after 1-2 days (Table 2, entries 5 and 7). Furthermore, $MeNO_2$ gave moderate enantioselectivity but loner reaction time (Table 2, entry 6).

UNIVERSITAT ROVIRA I VIRGILI
COMPUTATIONAL MECHANISTIC STUDIES IN GOLD(I) CATALYSIS AND DESIGN OF NEW CHIRAL LIGANDS
Immaculada Escofet Miquel

Chapter III

Table 2. Influence of solvent on the cyclization of **8a** to **9a** catalyzed by **48(AuCl)c**.
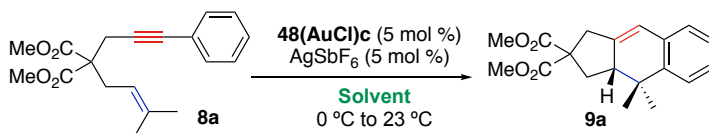
Entry	Solvent	t	**9a** *ee* (%)[a]
1	CH₂Cl₂	2 h	82
2	CDCl₃	1 h	79
3	(CH₂)₂Cl₂	20 h	63
4	Et₂O	20 h	82
5	toluene	2 days	n.r.
6	MeNO₂	16 h	66
7	1,4-dioxane	1 day	n.r.
8	acetone-d₆	1 day	82

[a] Enantiomeric excess determined by HPLC.

The use of different silver salts did not lead to significant improvements. Therefore, changing from AgSbF₆ to AgOTf or AgNTf₂ (Table 3, entries 1, 2 and 5) did not significantly affect the reactivity and enantioinduction. However, slightly lower enantiomeric excesses were observed with AgPF₆ (Table 3, entry 4). No reaction took place when AgOBz was used as chloride scavenger, whereas similar results were obtained with NaBAr₄^F (Table 3, entries 3 and 6). This latter scavenger required longer reaction time to complete.

Table 3. Influence of chloride scavenger on the cyclization of **8a** to **9a** catalyzed by **48(AuCl)c**.
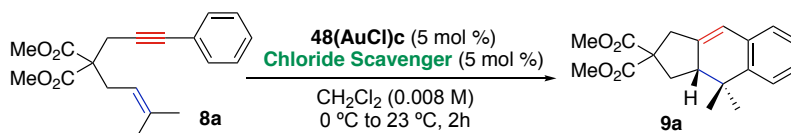
Entry	Solvent	t	**9a** *ee* (%)[a]
1	AgSbF₆	2 h	82
2	AgOTf	2 h	80
3	AgOBz	1 day	n.r.
4	AgPF₆	1 day	72
5	AgNTF₂	2 h	82
6	NaBAr_F	1 day	81

[a] Enantiomeric excess determined by HPLC.

Therefore, AgNTf₂ was finally selected as the chloride scavenger instead of AgSbF₆ since the first one is more stable to air.

UNIVERSITAT ROVIRA I VIRGILI
COMPUTATIONAL MECHANISTIC STUDIES IN GOLD(I) CATALYSIS AND DESIGN OF NEW CHIRAL LIGANDS
Immaculada Escofet Miquel

Chapter III

Moreover, the temperature effect was studied under these conditions and the best results were obtained at –20 ºC, 88% *ee*, in a reasonable reaction time (Table 4, entry 3). The same results were obtained when decreasing the catalyst loading from 5 mol% to 2 mol%.

Table 4. Influence of the temperature on the cyclization of **8a** to **9a** catalyzed by **48(AuCl)c**.
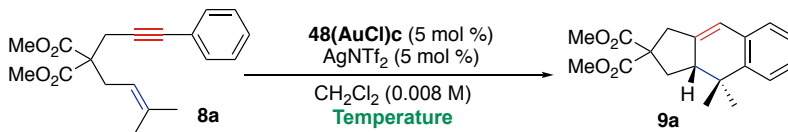
Entry	T (ºC)	t	**9a** *ee* (%)[a]
1	0	2 h	82
2	-10	16 h	85
3	-20	16 h	88
4	-40	25 h	87

[a] Enantiomeric excess determined by HPLC.

Finally, we investigated the substrate scope under the optimized conditions. Different 1,6-enynes **8a-e** with different substituents at the aryl ring were tested using 2 mol% catalyst loadings (Scheme 23). Thus, a methoxy group in para position gave the corresponding cycloadduct **9b** in good yield and enantioselectivity, although a longer reaction time was required (30 h). Good enantioselectivity was also obtained with enyne **8c** bearing a *p*-Me group at –20ºC over 15 h. Sterically more demanding substrate **8d**, could also be cyclized in 70% yield and 79% *ee*. Finally, cyclization of enyne **8e** with strong electron-withdrawing group at the para position of the phenyl ring gave rise to cycloadduct **9e** in 80% yield and 73% *ee*.
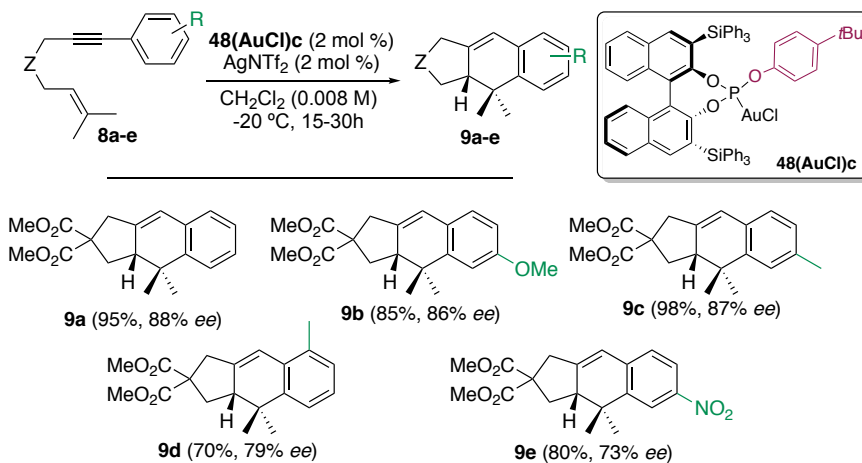
Scheme 23. Gold(I)-catalyzed [4+2] cycloaddition of 1,6-enynes **8a-e** with catalyst **48(AuCl)a-j**.

To better understand the working mode of our chiral monogold(I) phosphite complexes, we analyzed the X-ray structure of **48(AuCl)a** (Figure 4). This complex shows a cone-shaped

UNIVERSITAT ROVIRA I VIRGILI
COMPUTATIONAL MECHANISTIC STUDIES IN GOLD(I) CATALYSIS AND DESIGN OF NEW CHIRAL LIGANDS
Immaculada Escofet Miquel

Chapter III

binding pocket with a closest distance of 3.304 Å between the Au center and a phenyl ring of one of the SiPh$_3$ groups, which is within the range (3.0-3.2 Å) observed in gold(I) complexes in bulky biaryl Buchwald phosphines.[50] These Au-arene interactions can play a crucial role in the transformation by establishing a well-defined chiral environment. Additionally, the steric hindrance from the triphenylsilyl groups forces the phenol ring to point towards the gold center inducing chirality.
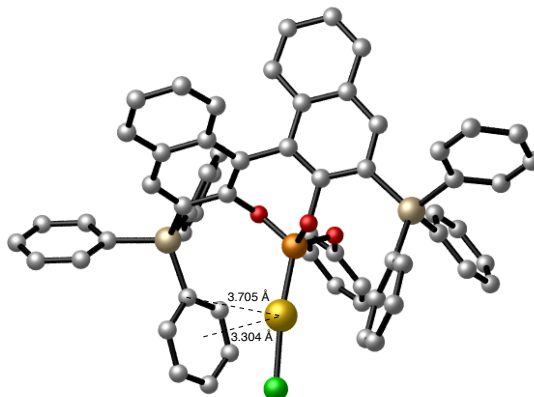
Figure 4. CYLview depiction of the X-ray crystal structure of gold complex **48(AuCl)a**. Hydrogen atoms are omitted for clarity. Distances expressed in Å.

Intermolecular [2+2] Cycloaddition of Alkynes with Alkenes

With the aim of developing a general asymmetric synthesis of cyclobutenes **21**, we studied the performance of our chiral phosphite-supported gold(I) catalysts on the intermolecular [2+2] cycloaddition previously reported by our group.[19] Phenylacetylene **19a** with α-methylstyrene **20a**, were chosen as the model substrates. In collaboration with Dr. Laura López, we screened a series of complexes based on chiral commercially available ligands together with the aforementioned chiral phosphite complexes **48(AuCl)a-j** (Tables 5 and Table 6).

Table 5. Screening of catalysts **48(AuCl)a-j** in the enantioselective Au(I)-catalyzed [2+2] cycloaddition of phenylacetylene **19** with α-methylstyrene **20**.
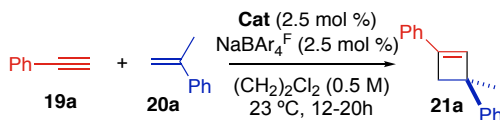
Entry	Catalyst	R	*21a* Yield (%)[a]	*21a* er[b]
1	**48(AuCl)a**	Ph	29	55:45

50   Pérez-Galán, P.; Delpont, N.; Herrero-Gómez, E.; Maseras, F.; Echavarren, A. M. *Chem. Eur. J.* **2010**, *16*, 5324–5332.

UNIVERSITAT ROVIRA I VIRGILI
COMPUTATIONAL MECHANISTIC STUDIES IN GOLD(I) CATALYSIS AND DESIGN OF NEW CHIRAL LIGANDS
Immaculada Escofet Miquel

Chapter III

2	**48(AuCl)b**	*m*-Tol	37	60:40
3	**48(AuCl)c**	4-*t*BuC$_6$H$_4$	22	-[c]
4	**48(AuCl)d**	4-MeOC$_6$H$_4$	24	61:39
5	**48(AuCl)e**	2,4-Me$_2$C$_6$H$_3$	28	64:36
6	**48(AuCl)f**	3,5-Me$_2$C$_6$H$_3$	25	60:40
7	**48(AuCl)g**	2,4,6-Cl$_3$C$_6$H$_2$	29	59:41
8	**48(AuCl)h**	Me	36	65:35
9	**48(AuCl)i**	PhCH$_2$	46	57:43
10	**48(AuCl)j**	3,5-*t*Bu$_2$C$_6$H$_3$CH$_2$	27	61:39

[a] ^{1}H NMR yield using diphenylmethane as internal standard. [b] Enantiomeric ratio determined by UPC2 (Chiralpak ID, CH$_3$CN 15%). [c] Not determined.

Table 6. Screening of catalysts in the enantioselective Au(I)-catalyzed [2+2] cycloaddition of phenylacetylene **19** with α-methylstyrene **20**.

Entry	Catalyst	Structure	21a yield (%)[a]	21a er[b]
1	**L1(AuCl)**		10	-[d]
2	**L2(AuCl)**		30	53:47
3	**L3(AuCl)**		13	<52:48
4	**L4(AuCl)**		18	<52:48
5	**(R)-DMM-Garphos(AuCl)$_2$**		10	50:50
6	**(R)-MeOBiphep(AuCl)$_2$**		32[c]	69:31
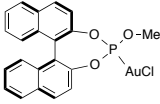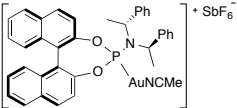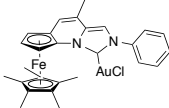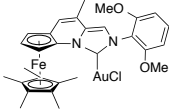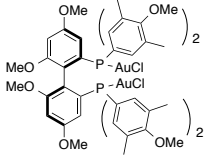
UNIVERSITAT ROVIRA I VIRGILI
COMPUTATIONAL MECHANISTIC STUDIES IN GOLD(I) CATALYSIS AND DESIGN OF NEW CHIRAL LIGANDS
Immaculada Escofet Miquel

Chapter III
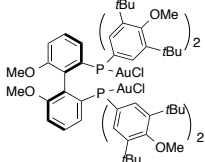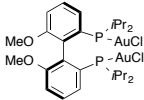
7	**(R)-iPr-MeOBIPHEP(AuCl)₂**		49	<52:48
8	**Ph-Ric(AuCl)**		0	-
9	**tBu-Ric(AuCl)**		42	58:42
10	**L5(AuCl)**		16	51:49
11	**L6(AuCl)**		8	55:45
12	**L7(AuCl)**		15	<52:48
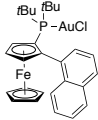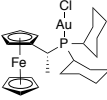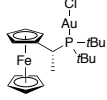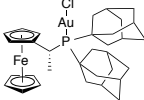
[a] ¹H NMR yield using diphenylmethane as internal standard. [b] Enantiomeric ratio determined by HPLC (Chiralpak IA, 99:1 hexane-iPrOH, 1 mL/min) or UPC2 (Chiralpak ID, CH₃CN 15%). [c] Isolated yield. [d] Not determined.

Disappointedly, the results were observed with the chiral catalyst tested were not satisfactory. Therefore, further ligand screening was performed by HTE (High Throughput Experimentation). Hence, more than 60 chiral ligands were used in the reaction forming the gold(I) chlorides *in situ* by mixing the ligand with (Me₂S)AuCl. After solvent evaporation, the remaining reagents were added to the reaction vials (Scheme 24). All the results of Tables 5, 6 and 7 are summarized in Figure 5.

Moreover, as highlighted in the **General Introduction**, the order of addition of chloride scavenger can play a crucial role in the reactivity.[51] Therefore, unless otherwise stated, a mixture of the neutral complexes with the substrates was firstly prepared, and the chloride scavenger was always added last. Hence, formation of less reactive chloride-bridged complexes would be minimized by using this prococol.

---

51   Homs, A.; Escofet, I.; Echavarren, A. M. *Org. Lett.* **2013**, *15*, 5782–5785.

UNIVERSITAT ROVIRA I VIRGILI
COMPUTATIONAL MECHANISTIC STUDIES IN GOLD(I) CATALYSIS AND DESIGN OF NEW CHIRAL LIGANDS
Immaculada Escofet Miquel

Chapter III
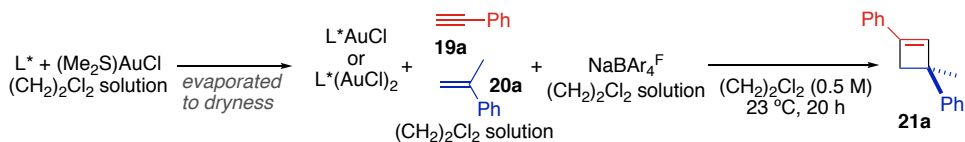
Scheme 24. General HTE procedure used for chiral ligand testing in synthesis of **21a** and image of HTE 96 positions reaction plate.

Table 7. High-throughput ligand screening for the enantioselective synthesis of **21a**.

Entry	Ligand	Structure	er^a
1	**(R,R)-DIPAMP**		-[b]
2	**(R)-FeSulPhos**		-[b]
3	**(R)-BTFM-Garphos**		-[b]
4	**(R)-Ph-Garphos**		-[b]

UNIVERSITAT ROVIRA I VIRGILI
COMPUTATIONAL MECHANISTIC STUDIES IN GOLD(I) CATALYSIS AND DESIGN OF NEW CHIRAL LIGANDS
Immaculada Escofet Miquel

Chapter III
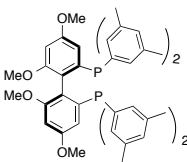
5	**(R)-Xyl-Garphos**		50:50
6	**(R)-DTBM-Garphos**		68:32
7	**(R)-BTFM-Garphos**		_[b]
8	**(R)-C3-TunePhos**		_[b]
9	**(R)-DTBM-Segphos**		52:48
10	**(R)-Segphos**		_[b]
11	**(R)-DM-Segphos**		_[b]
12	**(R)-Difluorophos**		_[b]
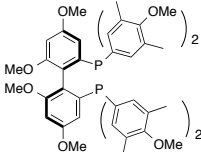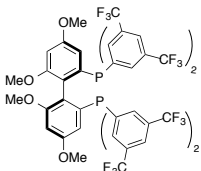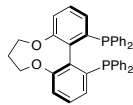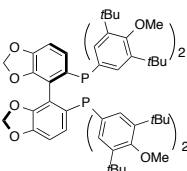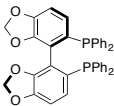
UNIVERSITAT ROVIRA I VIRGILI
COMPUTATIONAL MECHANISTIC STUDIES IN GOLD(I) CATALYSIS AND DESIGN OF NEW CHIRAL LIGANDS
Immaculada Escofet Miquel

Chapter III
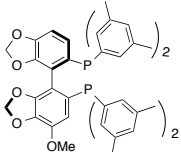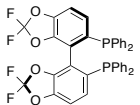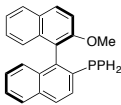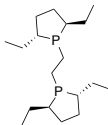
13	**(*R*)-MOP**		50:50
14	**(*R*,*R*)-Et-BPE**		_[b]
15	**(*R*,*R*)-*I*Pr-BPE**		_[b]
16	**(*R*,*S*)-STB-Bn-Siphox**		65:35
17	**(*R*)-MeOBIPHEP**		63:37
18	**(*S*)-3,5-Xylyl-MeoBIPHEP**		_[b]
19	**(*S*)-*p*Tol-MeOBIPHEP**		_[b]
20	**(*S*)-3,5-*t*Bu-MeOBIPHEP**		_[b]
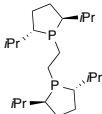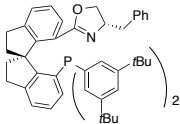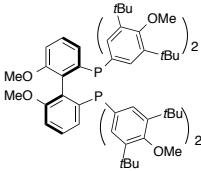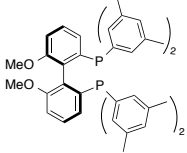
UNIVERSITAT ROVIRA I VIRGILI
COMPUTATIONAL MECHANISTIC STUDIES IN GOLD(I) CATALYSIS AND DESIGN OF NEW CHIRAL LIGANDS
Immaculada Escofet Miquel

Chapter III
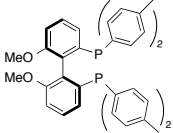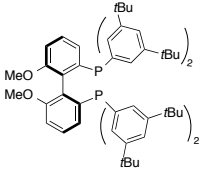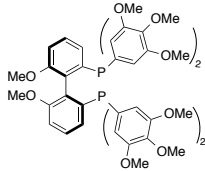
21	**(*S*)-3,4,5-MeO-MeOBIPHEP**		_[b]
22	**(*S*)-3,5-*i*Pr-4-NMe₂-MeOBIPHEP**		_[b]
23	**(*S*)-2-Furyl-MeOBIPHEP**		_[b]
24	**(*R*)-Cl-MeOBIPHEP**		_[b]
25	**(*R*,*R*)-Et-Ferrotane**		_[b]
26	**Kelliphite**		60:40
27	**(*R*,*R*)-Norphos**		_[b]
28	**(*R*)-SDP**		62:38
29	**(*R*)-Synphos**		_[b]
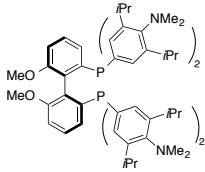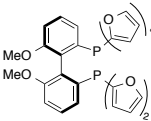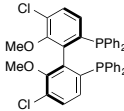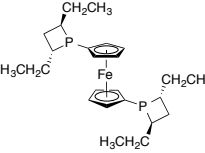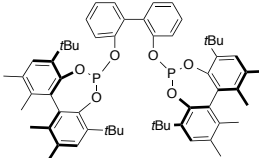
UNIVERSITAT ROVIRA I VIRGILI
COMPUTATIONAL MECHANISTIC STUDIES IN GOLD(I) CATALYSIS AND DESIGN OF NEW CHIRAL LIGANDS
Immaculada Escofet Miquel

Chapter III
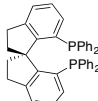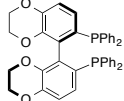
30	**(*R,R*)-Chiraphos**		_[b]
31	**(*R*)-Phanephos**		75:25
32	**(*R*)-Xyl-Binap**		66:34
33	**(*S*)-MonoPhos**		_[b]
34	**(*R,R*)-Monophos-1**		55:45
35	**(*S*)-MonoPhos-2**		_[b]
36	**(S)-Monophos-3**		_[b]
37	**(*S*)-MonoPhos-4**		53:47
38	**(*R,R*)-MonoPhos-5**		_[b]
39	**(*R,R*)-MonoPhos-6**		51:49
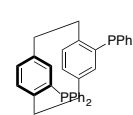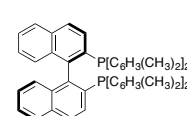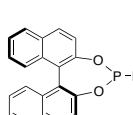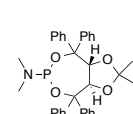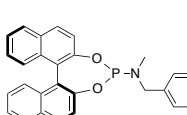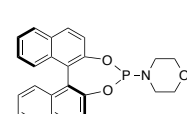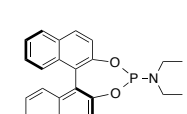
UNIVERSITAT ROVIRA I VIRGILI
COMPUTATIONAL MECHANISTIC STUDIES IN GOLD(I) CATALYSIS AND DESIGN OF NEW CHIRAL LIGANDS
Immaculada Escofet Miquel

Chapter III
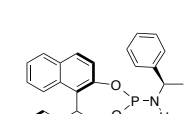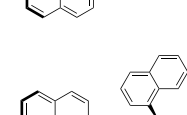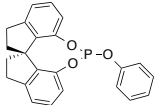
40	**(R)-ShiP**		55:45
41	**(S,S)-Me-DuPhos**		-[b]
42	**(S,S)-Et-DuPhos**		-[b]
43	**(R,R)-iPr-DuPhos**		55:45
44	**(R,R)-BenzP***		-[b]
45	**(R,R)-QUINOXP***		-[b]
46	**(R,R)-DACH-naphtyl-Trost**		-[b]
47	**(R,R)-Chiraphite**		55:45
48	**(R,S_P)-Josiphos-1**		72:28
49	**(R,S_P)-Josiphos-2**		72:28
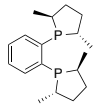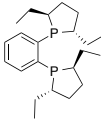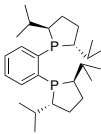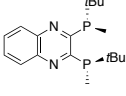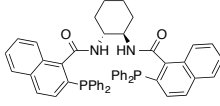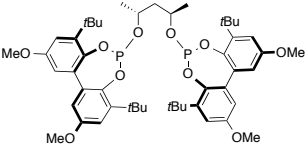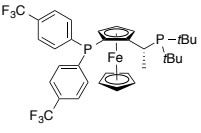
UNIVERSITAT ROVIRA I VIRGILI
COMPUTATIONAL MECHANISTIC STUDIES IN GOLD(I) CATALYSIS AND DESIGN OF NEW CHIRAL LIGANDS
Immaculada Escofet Miquel

Chapter III
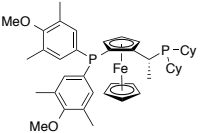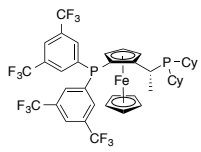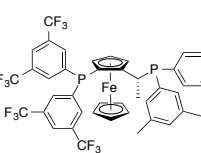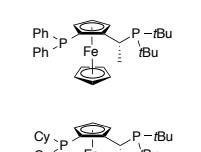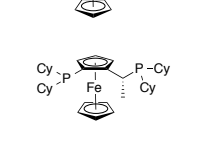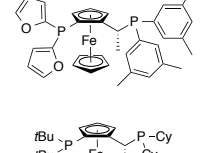
50	**(R,S_P)-Josiphos-3**		71:29
51	**(R,S_P)-Josiphos-4**		_[b]
52	**(R,S_P)-Josiphos-5**		77:23
53	**(R,S_P)-Josiphos-6**		_[b]
54	**(R,S_P)-Josiphos-7**		63:37
55	**(R,S_P)-Josiphos-8**		71:29
56	**(R,S_P)-Josiphos-9**		66:34
57	**(R,S_P)-Josiphos-10**		60:40
58	**(R,S_P)-Josiphos-11**		_[b]
59	**(S,R_P)-Josiphos-12**		85:15
60	**(R,S_P)-Josiphos-13**		76:24
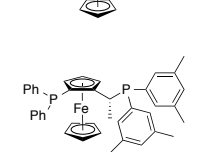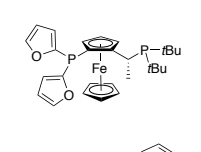
UNIVERSITAT ROVIRA I VIRGILI
COMPUTATIONAL MECHANISTIC STUDIES IN GOLD(I) CATALYSIS AND DESIGN OF NEW CHIRAL LIGANDS
Immaculada Escofet Miquel

Chapter III
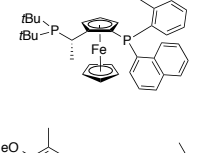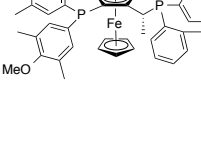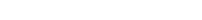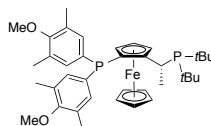
| 61 | **(*R*,*S*~P~)-Josiphos-14** | | 82:18 |

a Enantiomeric ratio determined by UPC2 (Chiralpak ID, CH₃CN 15%). *b* **21a** was not formed in enough amount to determine the enantiomeric ratio.
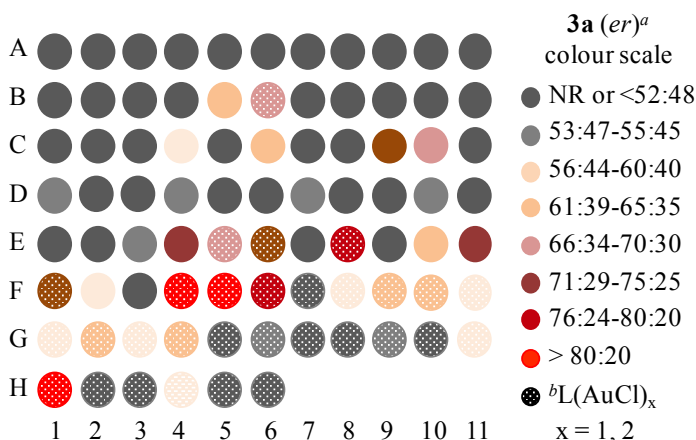
Figure 5. *er* of **21a** determined by HPLC (Chiralpak IA, 99:1 hexane-iPrOH) or by UPC2 (Chiralpak ID, CH₃CN 15%).ᵃ A1 (*R*,*R*)-DIPAMP; A2 (*R*)-FeSulPhos; A3 (*R*)-BTFM-Garphos; A4 (*R*)-Ph-Garphos; A5 (*R*)-Xyl-Garphos; A6 (*R*)-DTBM-Garphos; A7 (*R*)-BTFM-Garphos; A8 (*R*)-C3-TunePhos; A9 (*R*)-DTBM-Segphos; A10 (*R*)-Segphos; A11 (*R*)-DM-Segphos; B1 (*R*)-Difluorophos; B2 (*R*)-MOP; B3 (*R*,*R*)-Et-BPE; B4 (*R*,*R*)-*i*Pr-BPE; B5 (*R*,*S*)-STB-Bn-Siphox; B6 (*R*)-MeOBIPHEP(AuCl)₂; B7 (*S*)-3,5-Xylyl-MeOBIPHEP; B8 (*S*)-*p*Tol-MeOBIPHEP; B9 (*S*)-3,5-*t*Bu-MeOBIPHEP; B10 (*S*)-3,4,5-Meo-MeOBIPHEP; B11 (*S*)-3,5-*i*Pr-NMe₂-MeOBIPHEP; C1 (*S*)-2-Furyl-MeOBIPHEP; C2 (*S*)-Cl-MeOBIPHEP; C3 (*R*,*R*)-Et-Ferrotane; C4 Kelliphite; C5 (*R*,*R*)-Norphos; C6 (*R*)-SDP; C7 (*R*)-Synphos; C8 (*R*,*R*)-Chiraphos; C9 (*R*)-Phanephos; C10 (*R*)-Xyl-Binap; C11 (*S*)-MonoPhos; D1 (*R*,*R*)-MonoPhos-1; D2 (*S*)-MonoPhos-2; D3 (*S*)-MonoPhos-3; D4 (*S*)-MonoPhos-4; D5 (*R*,*R*)-MonoPhos-5; D6 (*R*,*R*)-MonoPhos-6; D7 (*R*)-ShiP; D8 (*S*,*S*)-Me-DuPhos; D9 (*S*,*S*)-EtDuPhos; D10 (*R*,*R*)-*i*Pr-DuPhos; D11 (*R*,*R*)-BenzP*; E1 (*R*,*R*)-QUINOXP*; E2 (*R*,*R*)-DACH-naphtyl-Trost; E3 (*R*,*R*)-Chiraphite; E4 (*R*,*S*~P~)-Josiphos-1; E5 (*R*,*S*~P~)-Josiphos-2(AuCl)₂; E6 (*R*,*S*~P~)-Josiphos-3(AuCl)₂; E7 (*R*,S~P~)-Josiphos-4; E8 **49-(*S*,*R*~P~)-A**, (*R*,*S*~P~)-Josiphos-5(AuCl)₂; E9 (*R*,*S*~P~)-Josiphos-6; E10 (*R*,*S*~P~)-Josiphos-7; E11 (*R*,*S*~P~)-Josiphos-8; F1 (*R*,*S*~P~)-Josiphos-9(AuCl)₂; F2 (*R*,S~P~)-Josiphos-10; F3 (*R*,*S*~P~)-Josiphos-11; F4 **49-(*S*,*R*~P~)-B**, **(*S*,*R*~P~)-Josiphos-12(AuCl)₂**; F5 **49-(*R*,*S*~P~)-C**, **(*R*,*S*~P~)-Josiphos-13(AuCl)₂**; F6 **49-(*R*,*S*~P~)-D**, (*R*,*S*~P~)-Josiphos-14(AuCl)₂; F7 **48(AuCl)a**; F8 **48(AuCl)b**; F9 **48(AuCl)d**; F10 **48(AuCl)e**; F11 **48(AuCl)f**; G1 **48(AuCl)g**; G2 **48(AuCl)h**; G3 **48(AuCl)i**; **G4 48(AuCl)j**; G5 L1(AuCl); G6 L2(AuCl); G7 L3(AuCl); G8 L4(AuCl); G9 (*R*)-*i*Pr-MeOBIPHEP(AuCl)₂; G10 (*R*)-Ph-Ric(AuCl); G11 (*R*)-tBu-Ric(AuCl); H1 **49-(*R*,*S*~P~)-E**, **(*R*,*S*~P~)-Josiphos-15(AuCl)₂**; H2 49-(*S*,*R*~P~)-F, (*R*,*S*~P~)-Josiphos-016(AuCl)₂; H3 L5(AuCl); H4 L6(AuCl); H5 L7(AuCl); H6 (*R*,*S*~P~)-Josiphos-12(AuCl).

Although most chiral ligands led to **21a** with low enantioselectivities, the breakthrough came when using Josiphos ligands family (Figure 5, highlighted in red). Among them, the

UNIVERSITAT ROVIRA I VIRGILI
COMPUTATIONAL MECHANISTIC STUDIES IN GOLD(I) CATALYSIS AND DESIGN OF NEW CHIRAL LIGANDS
Immaculada Escofet Miquel

Chapter III

best result was obtained with ligand (S,R_P)-**Josiphos-12**$(AuCl)_2$ giving cyclobutene **21a** in 85:15 *er*.

We prepared a series of digold(I) catalysts **49** bearing chiral Josiphos ligands, in order to test them at laboratory scale (Figure 6).[49]
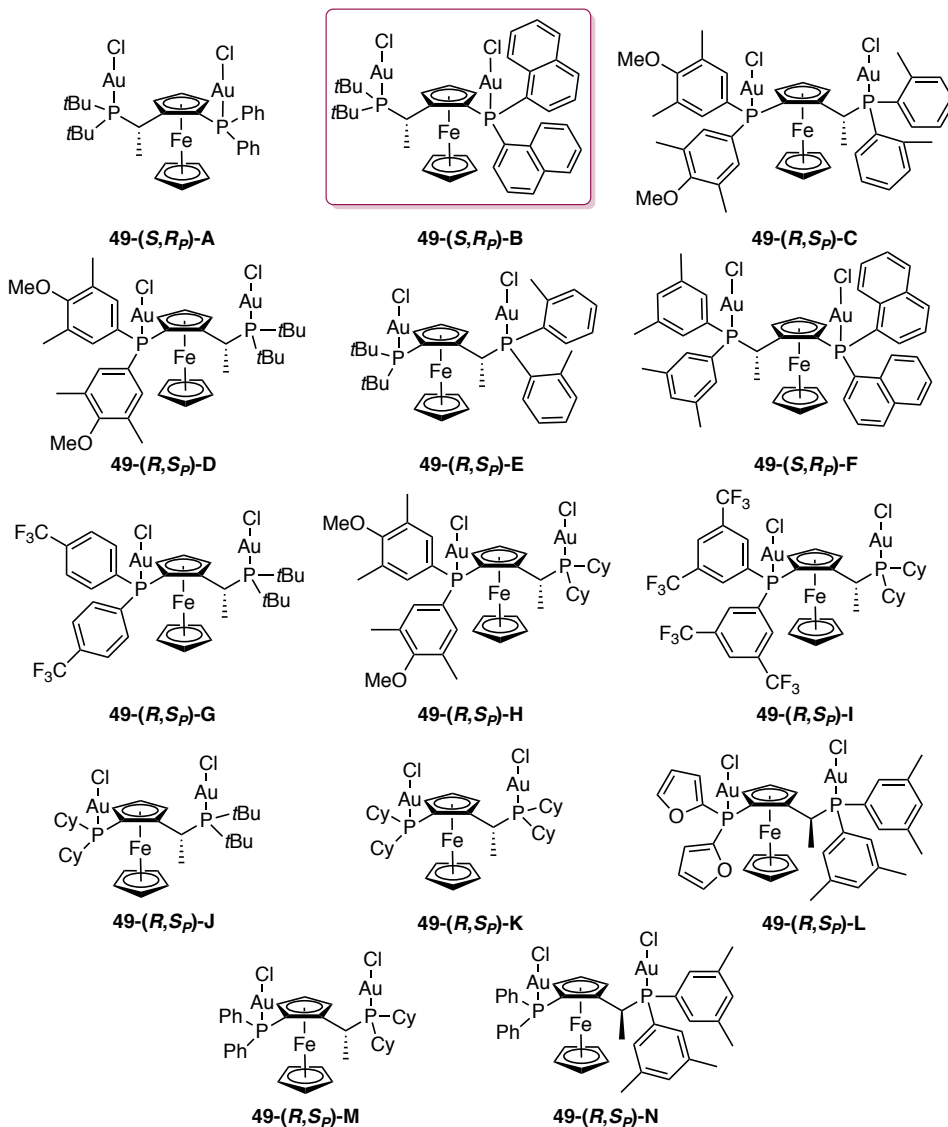
Figure 6. Series of Josiphos digold(I) complexes.

Josiphos ligands are chiral ferrocenyldiphosphine ligands that constitute one of the most versatile and successful ligand families. These ligands were developed by Togni in 1994 at

UNIVERSITAT ROVIRA I VIRGILI
COMPUTATIONAL MECHANISTIC STUDIES IN GOLD(I) CATALYSIS AND DESIGN OF NEW CHIRAL LIGANDS
Immaculada Escofet Miquel

Chapter III

the Ciba-Geigy company (Novartis today).[52] They received the name of the technician who prepared the first one, Josi Puleo. Interestingly, these ligands have been used in several catalyzed transformations involving Rh-, Ir-, Pd- and Ru-catalyzed hydrogenation reactions, and promptly became privileged ligands in asymmetric homogeneous catalysis.[53] Although large variety of Josiphos ligands are commercially available, only the (*R*,*S*P)/(*S*,*R*P) enantiomers are commonly used since they provide higher enantioinduction than the corresponding diastereomers.

For consistency with the previous results obtained in HTE, the screening of precatalysts was performed using dichloroethane as solvent, NaBAr₄F, and 2:1 ratio of reagents **20a**:**19a** (Table 8). Cyclobutene **21a** was afforded in low yields with precatalysts **49-(*S*,*R*P)-A**, **49-(*R*,*S*P)-C**, **49-(*R*,*S*P)-D**, **49-(*R*,*S*P)-E**, **49-(*R*,*S*P)-G**, **49-(*R*,*S*P)-I**, and **49-(*R*,*S*P)-M** (Table 8, entries 1, 3-5, 7, 9, 13), whereas complex **49-(*R*,*S*P)-H** led to **21a** in 45% yield but with low enantiomeric ratio (66:34 *er*). Noteworthy, complexes **49-(*S*,*R*P)-F**, **49-(*R*,*S*P)-J**, **49-(*R*,*S*P)-K**, **49-(*R*,*S*P)-L** and **49-(*R*,*S*P)-N** led to extensive oligomerization of the α-methylstyrene **20a** (Table 8, entries 6, 10-12 and 14). However, promising results were obtained when precatalyst **49-(*S*,*R*P)-B** was employed (Table 8, entry 2), in good agreement with the previous HTE screening. Since no oligomerization of **20a** was observed with complex **49-(*S*,*R*P)-B**, cyclobutene **21a** was obtained in higher yield and promising enantioselectivity, 84:16 *er*.

Table 8. Screening of precatalysts **49-A-N** in the enantioselective formation of **21a**.[a]
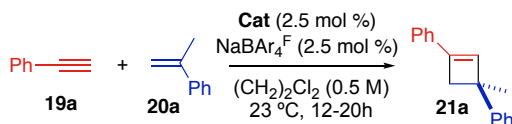
Entry	Catalyst	**21a** Yield (%)[b]	**21a** *er* (%)[c]
1	**49-(*S*,*R*P)-A**	13	78:22
2	**49-(*S*,*R*P)-B**	66	84:16
3	**49-(*R*,*S*P)-C**	10	82:18
4	**49-(*R*,*S*P)-D**	10	80:20
5	**49-(*R*,*S*P)-E**	9	82:18
6	**49-(*S*,*R*P)-F**	0	-
7	**49-(*R*,*S*P)-G**	16	69:31

52   (a) Togni, A.; Breutel, C.; Schnyder, A.; Spindler, F.; Landert, H.; Tijani, A. *J. Am. Chem. Soc.* **1994**, *116*, 4062–4066. (b) Togni, A. *Chimia International Journal for Chemistry*. **1996**, *50*, 86–93.
53   (a) Blaser, H.-U. *Topics Catal.* **2002**, *19*, 1–26. (b) Littke, A. F.; Fu, G. C. *Angew. Chem. Int. Ed.* **2002**, *41*, 4176–4211.

UNIVERSITAT ROVIRA I VIRGILI
COMPUTATIONAL MECHANISTIC STUDIES IN GOLD(I) CATALYSIS AND DESIGN OF NEW CHIRAL LIGANDS
Immaculada Escofet Miquel

Chapter III

8	**49-(R,S$_P$)-H**	45	66:34
9	**49-(R,S$_P$)-I**	13	72:28
10	**49-(R,S$_P$)-J**	0	-
11	**49-(R,S$_P$)-K**	0	-
12	**49-(R,S$_P$)-L**	0	-
13	**49-(R,S$_P$)-M**	19	71:29
14	**49-(R,S$_P$)-N**	0	-

[a] **20a/19a** = 2:1, **19a** (0.1 mmol). [b] Isolated yield. [c] Enantiomeric ratio determined by UPC2 (Chiralpak ID, CH$_3$CN 15%).

With these results in hand, further optimization was carried out with complex **49-(S,R$_P$)-B**. Different chloride scavengers such as silver, sodium and lithium salts were screened (Table 9). Among all silver salts tested, only AgBF$_4$ gave cyclobutene **21a** in good enantioselectivities, however in low yields (Table 9, entry 2). Better results were observed when using less basic bulky counterions BAr$_4$$^{F-}$ which were found to prevent the generation of unreactive σ,π-digold(I) alkyne species (**Chapter II**, Scheme 4). Similarly, a lithium salt with fluorinated boron anion gave rise to a similar outcome (Table 9, entry 10). Finally, no reaction took place when using silver salt containing a chiral counterion (Table 9, entry 11). As we have found before,[20] BAr$_4$$^{F-}$ was the best counterion for these transformations.

Table 9. Different chloride scavengers for the [2+2] cycloaddition between **19a** and **20a**.[a]
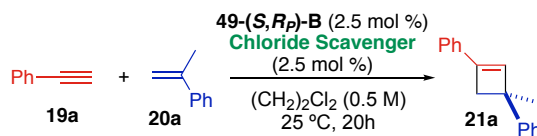
Entry	Chloride Scavenger	**21a** Yield (%)[b]	**21a** er[c]
1	AgSbF$_6$	-[d]	-
2	AgBF$_4$	23	84:16
3	AgPF$_6$	-[d]	-
4	AgNTf$_2$	-[d]	-
5	AgOBz	-[d]	-
6	AgOPNB	-[d]	-

UNIVERSITAT ROVIRA I VIRGILI
COMPUTATIONAL MECHANISTIC STUDIES IN GOLD(I) CATALYSIS AND DESIGN OF NEW CHIRAL LIGANDS
Immaculada Escofet Miquel

Chapter III

7	NaSbF$_6$	-^{d}	-
8	NaBF$_4$	-^{d}	-
9	NaBAr$_4$^{F}	66	84:16
10	Li[B(C$_6$F$_5$)$_4$]	52	84:16
11^f	AgX	-^{d}	-

^{a} **20a/19a** = 2:1, **19a** (0.1 mmol). ^{b} Isolated yield. ^{c} Enantiomeric ratio determined by UPC2. ^{d} No cyclobutene **21a** was formed. ^{f} Chlorobenzene.

X (R = 2,4,6-*i*Pr$_3$-C$_6$H$_2$)
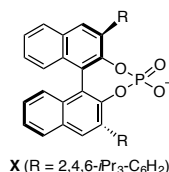
With the aim of developing a practical methodology that would not involve the activation of the precatalysts *in situ*, attempts to synthesize the cationic complexes were carried out. Following the procedures explained in the **General Introduction** (Scheme 3), we used labile ligands such as acetonitrile, benzonitrile or 1,3,5-trimethoxybenzonitrile. However, no coordination to gold(I) center was detected by NMR in any of the cases. Indeed, the same spectra was obtained for these experiments than that obtained upon mixing **49-(S,R$_P$)-B** with NaBAr$_F$^{4} in 1:1 ratio. Furthermore, crystallization of these species was not possible due to their low crystallinity. Thus, we decided to continue with the reaction optimization by generating the monocationic species *in situ* by chloride abstraction.

An extensive screening of solvents was then performed using NaBAr$_F$^{4} (Table 10). The use of highly non-polar solvents afforded cyclobutene **21a** in very low yields and enantiomeric ratios, while no reactivity was observed in coordinating solvents (Table 10, entries 1-4). Chlorinated solvents outperformed fluorinated ones in yield and enantiomeric ratios (Table 10, entries 5-9, 10-11. Thus, using chlorobenzene as solvent and performing the reaction at 0 ºC lead to **21a** in 63% yield and 88:12 *er* (Table 10, entry 14).

Table 10. Solvent optimization for the [2+2] cycloaddition between **19a** and **20a**.^{a}
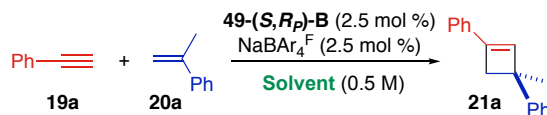
Entry	Solvent	T (ºC)	t (h)	**21a** Yield (%)^b	**21a** *er*^{c}
1	THF	25	20	-	-

UNIVERSITAT ROVIRA I VIRGILI
COMPUTATIONAL MECHANISTIC STUDIES IN GOLD(I) CATALYSIS AND DESIGN OF NEW CHIRAL LIGANDS
Immaculada Escofet Miquel

Chapter III

2	MeOH	25	20	-	-
3	Hexane	25	20	6	52:48
4	Toluene	25	20	10	75:25
5	$(CH_2)_2Cl_2$	25	20	66	84:16
6	$CHCl_3$	25	20	77	86:14
7	Chlorobenzene	25	20	76	86:14
8	1,1,2,2-Tetrachloroethane	25	20	77	83:17
9	1,1,2-Trichloroethane	25	20	71	83:17
10	Perfluorohexane	25	20	40	83:17
11	2,2,2-Trifluoroethanol	25	20	40	80:20
12	1,2-Dichlorobenzene	0	25	61	83:17
13	$(CH_2)_2Cl_2$	0	24	55	88:12
14	Chlorobenzene	0	24	63	88:12
15	$CHCl_3$	0	40	43	87:13
16	1,1,2-Trichloroethane	0	40	76	87:13

[a] **20a/19a** = 2:1, **19a** (0.1 mmol). [b] Isolated yield. [c] Enantiomeric ratio determined by UPC2.

Moreover, the possible effect of other parameters such as concentration, temperature, catalyst loadings and amount of chloride scavenger used was investigated (Table 11). Thus, when doubling the amount of NaBAr4[F], no differences were found (Table 11, entry 2), whereas reaction yields dropped to 59% when doubling the catalyst loading (Table 11, entry 5). Inverse order of addition or more diluted conditions had a negative effect on the reaction yield while the same enantiomeric ratios where obtained (Table 11, entries 3, 4 and 6). Despite the enantioselectivity reached 90:10 *er* by lowering the temperature to –20 ºC (Table 11, entries 10-15), oligomerization of **20a** was found to compete with formation of **21a** at this temperature (Table 11, entry 10). In addition, oligomerization of **20a** was also found when increasing the amount of alkene, the concentration or catalyst loading (Table 11, entries 11-13). This problem was finally solved by slow addition of substrate **20a** over 12 h giving rise to **21a** in 70% yield and 90:10 *er* (Table 11, entry 14).

UNIVERSITAT ROVIRA I VIRGILI
COMPUTATIONAL MECHANISTIC STUDIES IN GOLD(I) CATALYSIS AND DESIGN OF NEW CHIRAL LIGANDS
Immaculada Escofet Miquel

Chapter III

Table 11. Further optimization studies for the formation of **21a** with chlorobenzene as solvent.[a]
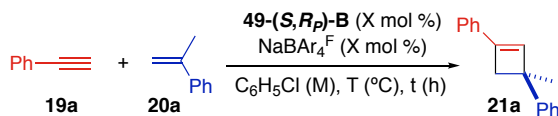
Entry	49-(**R**,**S**ₚ)-**B** (mol %)	NaBAr₄F (mol %)	20a/19a	T (°C)	(M)	t (h)	Yield (%)[b]	er[c]
1	2.5	2.5	2	25	0.5	20	76	84:16
2	2.5	5	2	25	0.5	20	78	84:16
3	2.5	2.5	2	25	0.25	40	66	84:16
4	2.5	2.5	2	25	0.1	72	45	84:16
5	5	5	2	25	0.5	20	59	84:16
6[d]	2.5	2.5	2	25	0.5	48	71	84:16
7	2.5	2.5	2	0	0.5	24	63	88:12
8	2.5	2.5	2	−10	0.5	24	62	89:11
9	2.5	2.5	4	−10	0.5	24	57	89:11
10[e]	2.5	2.5	2	−20	0.5	72	46	90:10
11[e]	2.5	2.5	4	−20	0.5	72	49	90:10
12[e]	5	5	2	−20	0.5	20	37	90:10
13[e]	2.5	2.5	2	−20	1	20	33	90:10
14[f]	2.5	2.5	2	−20	0.5	48	70	90:10

[a] **19a** (0.3 mmol). [b] Isolated yield of **21a**. Average of two runs. [c] er of **21a** determined by UPC2. [d] (49-(**S**,**R**ₚ)-**B** + NaBAr₄F) + (**19a** + **20a**). [e] Oligomerization of **20a**. [f] Slow addition of **20a**.

With these optimal conditions in hand, we expanded the scope of this transformation. Hence, the gold(I)-catalyzed cycloaddition of terminal alkynes **19a-i** with 1,1-disubstituted alkenes **20a-j** led to the formation of enantioenriched cyclobutenes **21a-ac** in moderate to excellent yields and enantiomeric ratios up to 94:6 (Scheme 25). The reaction proceeded satisfactorily with aryl alkynes bearing electron rich substituents in para and meta position (Scheme 25, products **21b**, **21c**, **21d**, **21g** and **21h**). Interestingly, *para*-Cl and *para*-Br substituted alkynes were also well tolerated and afforded cyclobutenes (**21e-f**) with excellent enantiomeric ratios, but moderated yields. 3-Ethynylthiopene also led to the corresponding cyclobutenes **21i**, **21t**, **21v**, and **21aa**. The absolute configuration of **21f** and

UNIVERSITAT ROVIRA I VIRGILI
COMPUTATIONAL MECHANISTIC STUDIES IN GOLD(I) CATALYSIS AND DESIGN OF NEW CHIRAL LIGANDS
Immaculada Escofet Miquel

Chapter III

21v was assigned by X-ray diffraction as *R* and those of the remaining products was assigned by analogy. No oligomerization was observed for *para*-substituted α-methylstyrenes. Consequently, these substrates were added in one pot giving rise **to 21j-o** in good yields and enantioselectivities. However, 1,1-dialkyl substituted alkenes or simple styrenes afforded **21ab** and **21a** in significantly lower *er*.

21a: R = Ph (70%, 90:10 *er*)
21b: R = biphenyl (57%, 91:9 *er*)
21c: R = *p*-Tol (82%, 82:18 *er*)
21d: R = *p*-tBuC$_6$H$_4$ (80%, 87:13 *er*)
21e: R = *p*-ClC$_6$H$_4$ (47%, 93:7 *er*)
21f: R = *p*-BrC$_6$H$_4$ (45%, 93:7 *er*)
21g: R = *m*-Tol (74%, 90:10 *er*)
21h: R = *m*-MeOC$_6$H$_4$ (60%, 91:9 *er*)
21i: R = 3-thienyl (78%, 84:16 *er*)

21j: R = F (72%, 91:9 *er*)
21k: R = Cl (57%, 86:14 *er*)
21l: R = Br (66%, 87:13 *er*)
21m: R = Me (57%, 89:11 *er*)[a]
21n: R = *i*Pr (52%, 88:12 *er*)[a]
21o: R = *t*Bu (89%, 88:12 *er*)

21p: R = *p*-tBuC$_6$H$_4$ (85%, 87:13 *er*)
21q: R = *p*-ClC$_6$H$_4$ (37%, 91:9 *er*)
21r: R = *p*-BrC$_6$H$_4$ (84%, 88:12 *er*)[a]
21s: R = *m*-MeOC$_6$H$_4$ (40%, 89:11 *er*)
21t: R = 3-thienyl (85%, 86:14 *er*)

21w: R = Ph (83%, 83:17 *er*)
21x: R = *p*-ClC$_6$H$_4$ (92%, 88:12 *er*)
21y: R = *p*-BrC$_6$H$_4$ (81%, 85:15 *er*)
21z: R = *m*-MeOC$_6$H$_4$ (88%, 89:11 *er*)
21aa: R = 3-thienyl (87%, 83:17 *er*)

21ab (67%, 64:36 *er*)[a]

21ac (53%, 66:34 *er*)[a]

21u: R = *p*-tBuC$_6$H$_4$ (63%, 89:11 *er*)
21v: R = 3-thienyl (56%, 94:6 *er*)

Scheme 25. Synthesis of cyclobutenes **21a-ac** using 1,1-disubstituted alkenes and complex **49-(S,R$_P$)-B**. [a] 25 ºC.

Moreover, highly enantioenriched biscyclobutenes **21ad-ah** were synthesized from dialkynes and dialkenes as reaction counterparts by 2-fold cycloaddition (Scheme 26). The corresponding meso derivatives were obtained as minor products in these reactions (20–30% yields). Interestingly, at 25 ºC, **21ad-e** were obtained in higher yields but lower enantiomeric ratio.

UNIVERSITAT ROVIRA I VIRGILI
COMPUTATIONAL MECHANISTIC STUDIES IN GOLD(I) CATALYSIS AND DESIGN OF NEW CHIRAL LIGANDS
Immaculada Escofet Miquel

Chapter III

21ad: R = *p*-FC$_6$H$_4$
(32%, 98:2 *er*)
(41%, 97:3 *er*)[a]

21ae: R = *p-t*BuC$_6$H$_4$
(32%, 98:2 *er*)
(60%, 95:5 *er*)[a]

21af: R = *m*-MeC$_6$H$_4$ (45%, 98:2 *er*)
21ag: R = *p-t*BuC$_6$H$_4$ (67%, 96:4 *er*)
21ah: R = 3-thienyl (70%, 96:4 *er*)

X-ray of **21ad**

X-ray of **21ae**
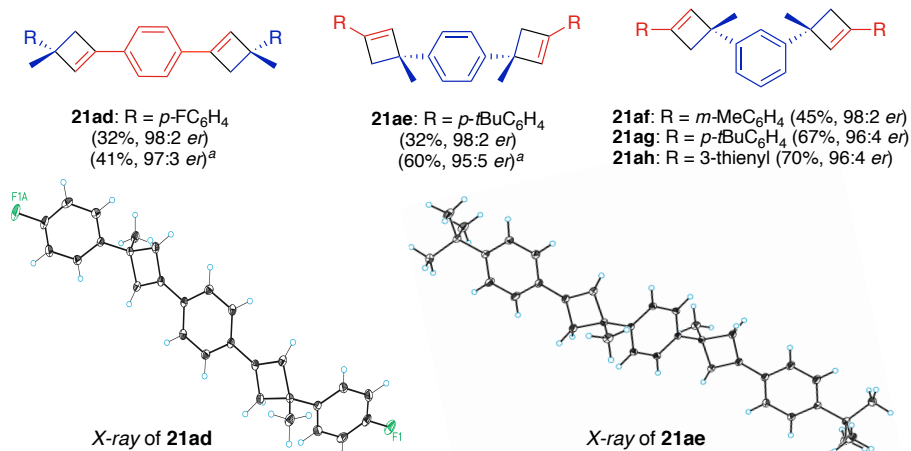
Scheme 26. Synthesis of biscyclobutenes **21ad-ah**. X-ray structures of **21ad** and 2**1ae**. [a] 25 ºC.

The cycloaddition of 1,1,2-trisubstituted alkenes **20l-n** with terminal alkynes was also investigated with the same catalyst **49-(S,R$_P$)-B** (Scheme 27). To our surprise, cyclobutenes **21a-k** were obtained in low enantiomeric and diastereomeric ratios. Nonetheless, catalyst **49-(S,R$_P$)-F**, bearing aryl substituted at phosphorous in the stereogenic center, was found to be more selective than *tert*-butyl substituted catalyst **49-(S,R$_P$)-B**. Thus, cyclobutenes **21ai-k** were obtained in higher regioselectivities and excellent enantiomeric ratios.

21ai
B: 78%, 3:1 *dr*, 67:33 *er*
F: 80%, 3:1 *dr*, 86:14 *er*

21aj
B: 91%, 1.5:1 *dr*, 69:31 *er*
F: 78%, 12:1 *dr*, 89:11 *er*

21ak
B: 78%, 2:1 *dr*, 64:36 *er*
F: 37%, 10:1 *dr*, 83:17 *er*
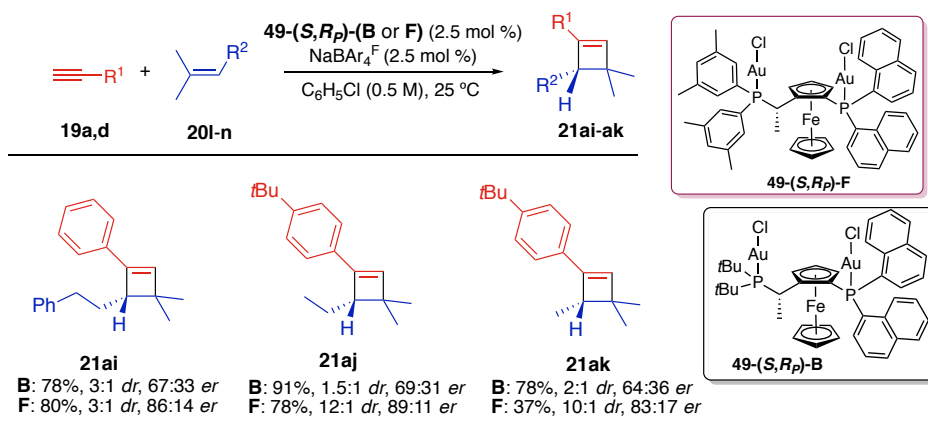
Scheme 27. Synthesis of cyclobutenes **21ai-ak** with catalyst **49-(S,R$_P$)-B** or **49-(S,R$_P$)-F**.

We then performed the cycloaddition of alkenes **20l-o** with terminal alkynes **19a,c-e** by using catalyst **49-(S,R$_P$)-F** at -20 ºC (Scheme 28). Several 1,3,3-tetrasubstituted cyclobutenes **21ai-ap** were obtained in good yields and moderate to excellent regiomeric ratios. 1,2,4,4-Tetrasubstituted cyclobutenes were formed as minor regioisomers in most of the cases. Noteworthy, enantioselectivities were on the same range to those obtained with 1,1-disubstituted alkenes (Scheme 25).

174

UNIVERSITAT ROVIRA I VIRGILI
COMPUTATIONAL MECHANISTIC STUDIES IN GOLD(I) CATALYSIS AND DESIGN OF NEW CHIRAL LIGANDS
Immaculada Escofet Miquel

Chapter III
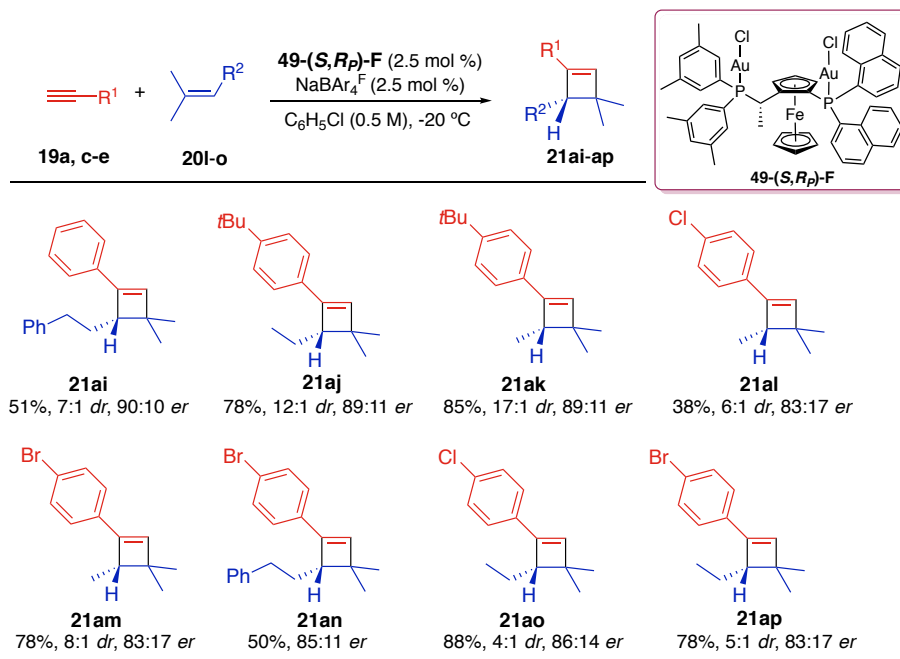
Scheme 28. Synthesis of cyclobutenes **21ai-ap** with catalyst **49-(S,R$_P$)-F**.

Some alkynes were not suitable for the efficient asymmetric synthesis of cyclobutenes. For example, *meta*-substituted aryl alkynes bearing halides or esters lead to cyclobutenes in excellent enantioselectivities but very poor yields (less than 15%). Finally, no reaction was observed when using cyclopropyl alkyne as substrate.

Table 12 summarizes alkenes that did not undergo the cycloaddition reaction with alkynes. Highly electron rich alkenes suffered acid-catalyzed dimerization and oligomerization (Table 12, entry 1), whereas no reaction took place for electron poor substituted aryl alkynes (Table 12, entries 2-3). Complex mixtures were obtained with *o*-bromo-α-methylstyrene (Table 12, entry 4), 1-methylene-1,2,3,4-tetrahydronaphthalene (Table 12, entry 5), alkenes with bulkier alkyl substituents (Table 12, entries 6-7), 1,1-dialkyl alkene, allyl ether and allyl silyl ether (Table 12, entries 8-10).

Table 12. Alkenes that did not give good results in the cycloaddition with phenylacetylene **19a**.

UNIVERSITAT ROVIRA I VIRGILI
COMPUTATIONAL MECHANISTIC STUDIES IN GOLD(I) CATALYSIS AND DESIGN OF NEW CHIRAL LIGANDS
Immaculada Escofet Miquel

Chapter III
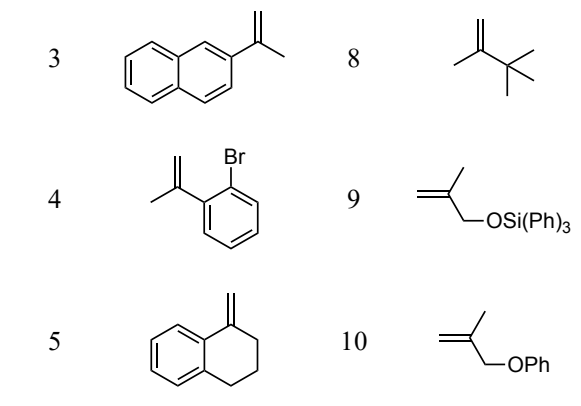
In the case of trisubstituted alkenes, we also found some examples of formation of cyclobutenes **21aq-au** with excellent enantiomeric ratios, yet in only low to moderate yields (Table 13).

Table 13. Unsuccessful examples with trisubstituted alkenes.
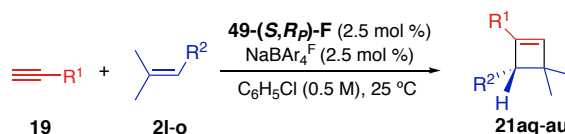
Entry	R^1	R^2	Product	21 Yield (%)^a	21 dr	21 er^b
1	Ph	Ph	**21aq**	17	9:1	85:15
2	p-tBuC$_6$H$_4$	Ph	**21ar**	16	13:1	86:14
3	3-thienyl	Ph	**21as**	26	5:1	85:15
4	m-MeOC$_6$H$_4$	Ph	**21at**	20	7:1	78:22
5	m-MeOC$_6$H$_4$	C$_2$H$_4$Ph	**21au**	72	-	76:24

^{a} Isolated yield. ^{b}er determined by UPC2.

To demonstrate the utility of the asymmetric synthesis of cyclobutenes, a second-generation synthesis of rumphellaone A was developed by Dr. Beatrice Ranieri, Dr. Carla Obradors and Dr. Laura López (Scheme 29).[54] As already mentioned in the **General Introduction** (Scheme 6), gold(I) catalyzed [2+2] macrocyclization was used as the key step in the total

---

54   For further details, see the supporting information of (32).

UNIVERSITAT ROVIRA I VIRGILI
COMPUTATIONAL MECHANISTIC STUDIES IN GOLD(I) CATALYSIS AND DESIGN OF NEW CHIRAL LIGANDS
Immaculada Escofet Miquel

Chapter III

synthesis of rumphellaone A and hushinone.[55] In this new reported enantioselective route, the key [2+2] cycloaddition of **19a** with **20p** furnished cyclobutene **21av** in 70% yield and 91:9 *er*. Finally, cyclobutene **21av** was converted into rumphellaone A in 7 steps.
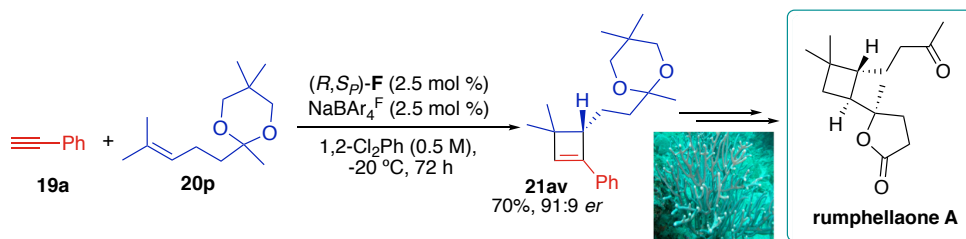
Scheme 29. Enantioselective synthesis of key intermediate **21av** for the enantioselective synthesis of rumphellaone A catalyzed by gold(I).

As already mentioned in the **General Introduction**, cycloaddition of alkenes with alkynes can give rise to lactones. Indeed, the first asymmetric efficient synthesis of lactones has been reported by the group of Shin.[56] (*R*)-DM-Segphos was used as ligand to report a single example of an α,β-unsaturated δ-lactones with 65% *ee*. We envisioned that one of our new Josiphos digold(I) complexes could be an excellent chiral catalyst for the [4+2] annulation of propiolic acids **19j** and alkenes **20m**. Hence, we screened several Josiphos ligands in the HTE for this reaction (Scheme 30).

Scheme 30. General HTE procedure used for Josiphos ligands testing in synthesis of **50**.

Among all the family of ligands tested, it was found that catalyst Josiphos-14, **49-(R,SP)-D** (Figure 6), gave product **50** with 21:79 *er* (Table 14, entry 14).

Table 14. High-throughput ligand screening for the enantioselective synthesis of **50**.

Entry	Ligand	Structure	**50** *er*[a]
1	**(R,SP)-Josiphos-1**		26:74

55   Ranieri, B.; Obradors, C.; Mato, M.; Echavarren, A. M. *Org. Lett.* **2016**, *18*, 1614–1617.
56   Yeom, H.; Koo, J.; Park, H.; Wang, Y.; Liang, Y.; Yu, Z.; Shin, S. *J. Am. Chem. Soc.* **2012**, *134*, 208-211.

UNIVERSITAT ROVIRA I VIRGILI
COMPUTATIONAL MECHANISTIC STUDIES IN GOLD(I) CATALYSIS AND DESIGN OF NEW CHIRAL LIGANDS
Immaculada Escofet Miquel

Chapter III
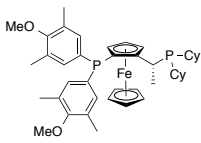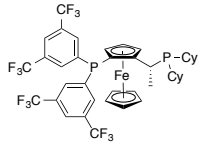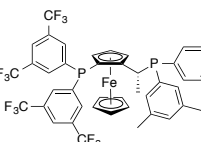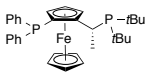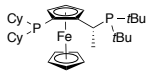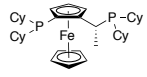
2	**(*R*,*S*P)-Josiphos-2**		26:74
3	**(*R*,*S*P)-Josiphos-3**		31:69
4	**(*R*,*S*P)-Josiphos-4**		28:72
5	**(*R*,*S*P)-Josiphos-5**		30:70
6	**(*R*,*S*P)-Josiphos-6**		32:68
7	**(*R*,*S*P)-Josiphos-7**		32:68
8	**(*R*,*S*P)-Josiphos-8**		30:70
9	**(*R*,*S*P)-Josiphos-9**		29:71
10	**(*R*,*S*P)-Josiphos-10**		27:73
11	**(*R*,*S*P)-Josiphos-11**		35:65
12	**(*S*,*R*P)-Josiphos-12**		26:74
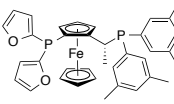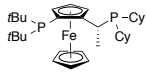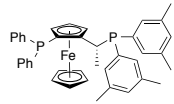
UNIVERSITAT ROVIRA I VIRGILI
COMPUTATIONAL MECHANISTIC STUDIES IN GOLD(I) CATALYSIS AND DESIGN OF NEW CHIRAL LIGANDS
Immaculada Escofet Miquel

Chapter III

| 13 | **(R,S_P)-Josiphos-13** | | 29:71 |
| 14 | **(R,S_P)-Josiphos-14** | | 21:79 |
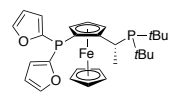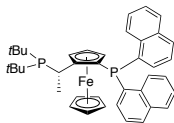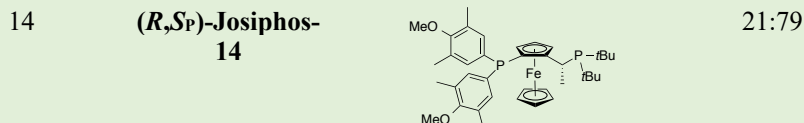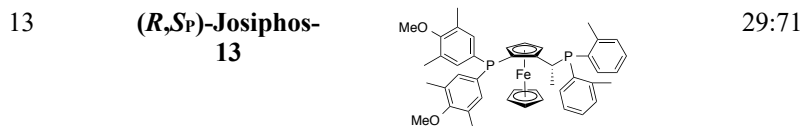
[a] Enantiomeric ratio determined by UPC^2 (Chiralpak IC, EtOH 5%).

Further optimization was carried out in our laboratories with this catalyst **49-(R,S_P)-D**. NaBAr$_4$^{F} (2.5 mol %) was used as chloride scavenger, since the use of silver salts or 5 mol % of NaBAr$_4$ ^{F}, led to a drop in reactivity and enantioselectivity. (Table 15, entries 2-4). Among all the solvents tried, dichloromethane, chloroform and 1,1,2-trichloroethane gave the best enantiomeric ratios at 25 ºC (Table 15, entries 5, 6 and 8). Decreasing the temperature to 10 ºC gave product **50** with slightly better enantiomeric ratios but in poor yields (Table 15, entries 10-12). Optimal conditions were found when using dichloromethane (0.5 M) at 25ºC giving rise to lactone **50** in good yields and moderate enantioselectivity.

Table 15. Solvent screening for the enantioselective synthesis of **50**.
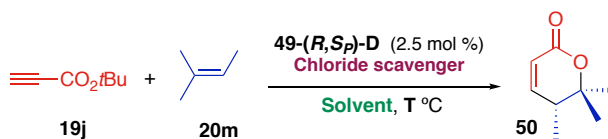
Entry	Chloride Scavenger	Solvent	T (ºC)	**50** Yield[a] (%)	**50** er[b]
1	NaBAr$_4$^{F} (2.5 mol %)	DCE	25	65	19:81
2	NaBAr$_4$^{F} (5 mol %)	DCE	25	63	19:81
3	AgSbF$_6$ (2.5 mol %)	DCE	25	95	24:76
4	AgSbF$_6$ (5 mol %)	DCE	25	95	47:53

UNIVERSITAT ROVIRA I VIRGILI
COMPUTATIONAL MECHANISTIC STUDIES IN GOLD(I) CATALYSIS AND DESIGN OF NEW CHIRAL LIGANDS
Immaculada Escofet Miquel

Chapter III

5	NaBAr$_4$^{F} (2.5 mol %)	DCM	25	86	17:83
6	NaBAr$_4$^{F} (2.5 mol %)	CHCl$_3$	25	75	17:83
7	NaBAr$_4$^{F} (2.5 mol %)	ClPh	25	70	19:81
8	NaBAr$_4$^{F} (2.5 mol %)	1,1,2-Trichloroethane	25	58	17:83
9	NaBAr$_4$^{F} (2.5 mol %)	1,2-Dichlorobenzene	25	26	18:82
10	NaBAr$_4$^{F} (2.5 mol %)	DCM	10	18	16:84
11	NaBAr$_4$^{F} (2.5 mol %)	CHCl$_3$	10	21	16:84
12	NaBAr$_4$^{F} (2.5 mol %)	1,1,2-Trichloroethane	10	15	16:84
13	NaBAr$_4$^{F} (2.5 mol %)	DCM (0.33M) -2h	25	69	16:84
14	NaBAr$_4$^{F} (2.5 mol %)	DCM (0.5M) - 2h	25	80	16:84
15	NaBAr$_4$^{F} (2.5 mol %)	DCM (0.1M)- 2h	25	45	16:84
16	NaBAr$_4$^{F} (2.5 mol %)	DCM (0.5M)- 2h	25	68[c]	16:84

[a] Yield determined by ^{1}H NMR using 1,4-Diacetylbenzene as internal standard. [b] *er* determined by UPC^2 (Chiralpak IC, EtOH 5%). [c] Isolated yields.

UNIVERSITAT ROVIRA I VIRGILI
COMPUTATIONAL MECHANISTIC STUDIES IN GOLD(I) CATALYSIS AND DESIGN OF NEW CHIRAL LIGANDS
Immaculada Escofet Miquel

Chapter III

While these studies were ongoing, a new methodology was disclosed that improved our results.[57] Thus, the asymmetric Au(I)-catalyzed intermolecular [4+2] annulation of *tert*-butyl propiolate **19j** and non-activated alkenes **20** was reported using a bimetallic gold(I) catalyst bearing atropoisomeric bidentate phosphine DM-Segphos to afford enantioenriched lactones **50** (Scheme 31). The use of sodium dodecyl sulphate (SDS) as an anionic surfactant improved the product selectivity.
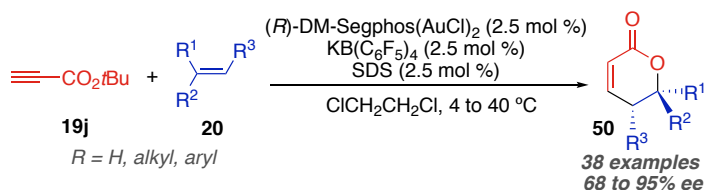
Scheme 31. Asymmetric gold(I)-catalyzed intermolecular [4+2] annulation.

To gain further understanding into the role of both gold centers present in dinuclear precatalyst **49-(S,RP)-B**, we synthesized monogold(I) complex **49-(S,RP)-O** by mixing the same Josiphos ligand with only 1 equivalent of AuCl(Me$_2$S).[49] Thus, gold coordinates the trialkyl phosphine of the ligand, which is the most electron rich center (Scheme 32). We tested this complex in the cycloaddition reaction of phenylacetylene with **20a** and only traces of cyclobutene **21a** were obtained. This result could be attributed to the formation of inactive dimeric species upon chloride abstraction. To exclude the possibility of coordination of the free phosphorous of **49-(S,RP)-O** to the gold after chloride abstraction, the aryl phosphine was protected using BH$_3$.

Hence, catalyst **49-(S,RP)-O·BH₃** was prepared and tested as precatalysts in the formation of cyclobutene **21a** (Scheme 32). Again, only traces of racemic product **21a** were obtained. Moreover, to discard that both catalysts were inactive due to steric issues after forming the cationic species, their reactivity with the cycloisomerizations of 1,6-enyne **42** was also studied. In both cases, enyne **42** reacted and the corresponding products were formed, which excludes the formation of inactive gold(I) dimers. Therefore, with this control experiments conclude that the presence of (naphtyl)$_2$P–AuCl moiety in **49-(S,RP)-B** is crucial to efficiently obtain enantioenriched cyclobutenes type of **21**.

57   Kim, H.; Choi, S. Y.; Shin, S. *Angew. Chem. Int. Ed.* **2018**, *57*, 13130–13134.

UNIVERSITAT ROVIRA I VIRGILI
COMPUTATIONAL MECHANISTIC STUDIES IN GOLD(I) CATALYSIS AND DESIGN OF NEW CHIRAL LIGANDS
Immaculada Escofet Miquel

Chapter III
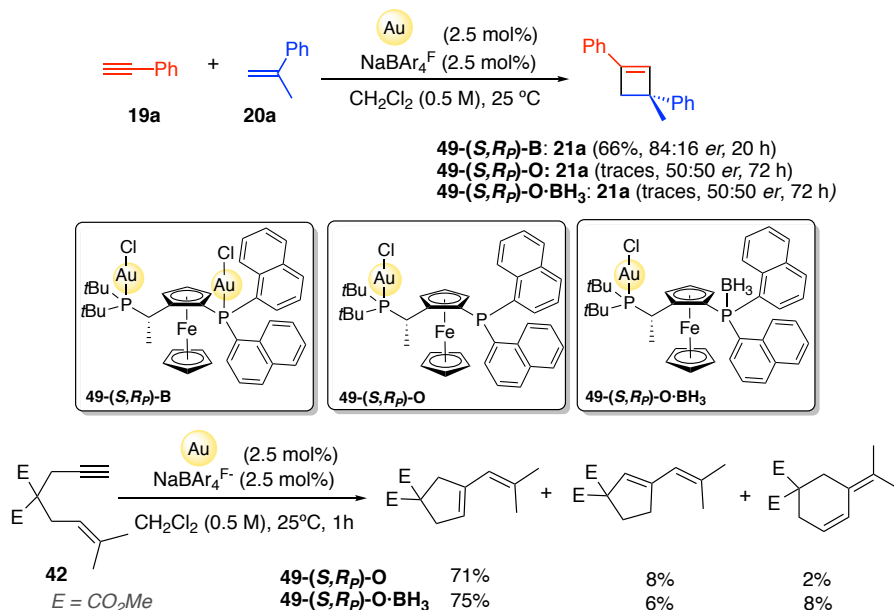
Scheme 32. Reactivity of monogold complexes as precatalysts in cycloaddition of alkenyne **19a** with alkene **20a** and in the cycloisomerization of 1,6-enyne **42**.

Furthermore, kinetic studies were performed by Cristina García-Morales by using initial-rates method. Thus, the reaction of **19a** with **20a** was monitored by ^{1}H NMR (1:1 ratio of NaBAr$_4$[F] and **49-(S,R$_P$)-B**).[58] Therefore, the [2+2] cycloaddition reaction exhibited first-order kinetic dependence on each reactant and the catalyst concentration. With the aim of shedding light into electronic effects in the rate-determining step, Hammett plot studies were performed for a series of *para*-substituted α-methylstyrenes **20a–g,p** (Scheme 33). Interestingly, linear correlations with σ[+] constants were observed for two different sets within the series, one for R = Me, *i*Pr, *t*Bu and cyclopropyl (ρ = +7.05, R^2 = 0.99) and the other one for R = F, H, Cl, and Br (ρ = -2.32, R^2 = 0.97). The abrupt difference in the ρ values is indicative of a change in the catalytic turnover-limiting step as a function of substituents.

---

58   Only the most relevant results are discussed in this chapter. For further details on the kinetic studies check the supporting information of (32).

UNIVERSITAT ROVIRA I VIRGILI
COMPUTATIONAL MECHANISTIC STUDIES IN GOLD(I) CATALYSIS AND DESIGN OF NEW CHIRAL LIGANDS
Immaculada Escofet Miquel

Chapter III
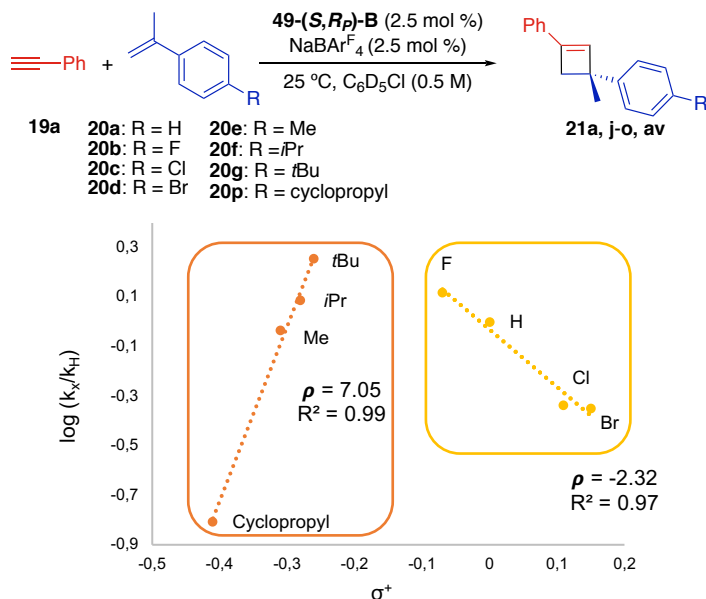
Scheme 33. Hammett plot for the reaction of **19a** and **20a–g,p** using σ^+ values.

The highly positive ρ value for *para*-alkyl substituted alkenes **20e-g,p** suggests the ligand exchange between $[LAu(\eta^2\text{-alkene})]^+$ complex and alkyne **19a** to form $[LAu(\eta^2\text{-alkyne})]^+$ and **21a** is the turnover limiting step (Scheme 34, orange).

Indeed, we have shown before that the associative ligand exchange is the slowest step in the [2+2] cycloaddition reaction with mononuclear gold(I) complexes.[20] For less electron-rich alkenes **20a-d** the formation of $[LAu(\eta^2\text{-alkene})]^+$ complex is less favoured, and therefore the observed negative ρ value is a result of the build-up of positive charge at the most substituted carbon of the alkene in a turn-over limiting Markovnikov-type addition of electrophilic $[LAu(\eta^2\text{-alkyne})]^+$ (Scheme 34, yellow).

UNIVERSITAT ROVIRA I VIRGILI
COMPUTATIONAL MECHANISTIC STUDIES IN GOLD(I) CATALYSIS AND DESIGN OF NEW CHIRAL LIGANDS
Immaculada Escofet Miquel

Chapter III
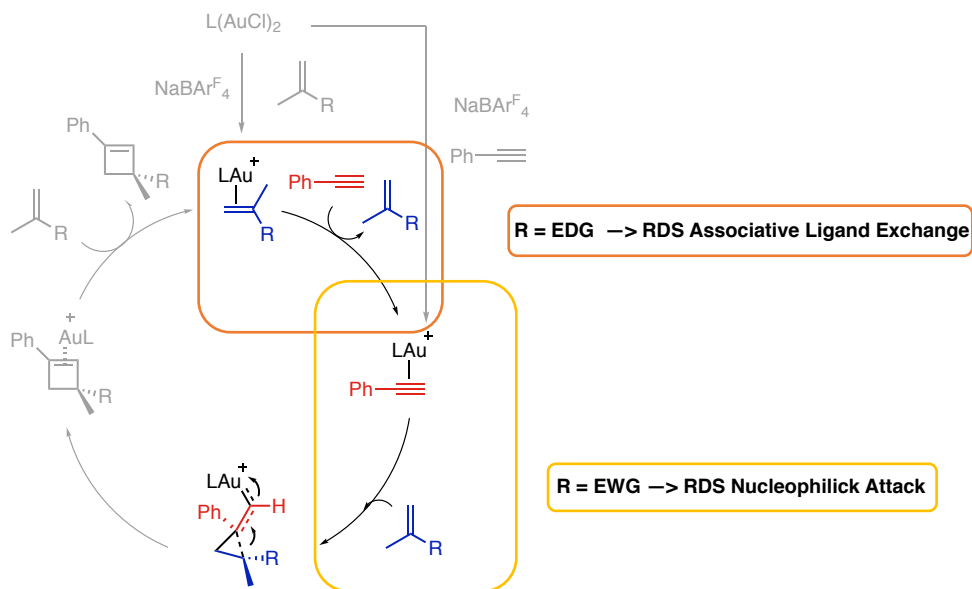
Scheme 34. Mechanistic picture: Two rate-determining steps dependent on the substitution pattern of the reactive alkene in the intermolecular enantioselective gold(I)-catalyzed [2+2] cycloaddition.

Aurophilic interactions have been found to be crucial for chiral transfer for other ferrocenyl diphosphino gold(I) complexes.[59] However, in the solid state, the two gold(I) centers of **49-(S,R_P)-B** and **49-(S,R_P)-F** are *anti*-oriented with respect to each other and aurophilic interactions were not observed (Figure 7).
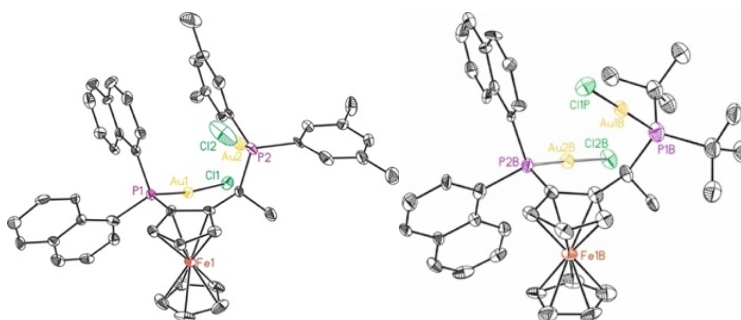
Figure 7. X-ray crystal structures of **49-(S,R_P)-B** (right) and **49-(S,R_P)-F** (left).

With the aim of better rationalize the working mode of our Josiphos precatalyst, DFT calculations were performed by Dr. Andrey I. Konovalov.[60] Calculations provided a model to explain the asymmetric induction in the key attack of α-methylstyrene **20a** at [LAu(η²-alkyne)]⁺ that lead to (R)-**21a**, when complex **49-(S,R_P)-B** is used as the precatalyst. The calculated energy difference between the lowest transition states that lead to (S)- and (R)-

59   Rampazzi, V.; Roger, J.; Amardeil, R.; Penouilh, M.-J.; Richard, P.; Fleurat-Lessard, P.; Hierso, J.-C. *Inorg. Chem.* **2016**, 55, 10907–1092.

60   Calculations were performed at PCM(PhCl)-BP86-D3, SDD(Au, Fe), 6-31G(d) (C, H, P, Cl) level of theory. Only the most relevant computational results will be discussed in this chapter. For further details, check the supporting information of (32).

UNIVERSITAT ROVIRA I VIRGILI
COMPUTATIONAL MECHANISTIC STUDIES IN GOLD(I) CATALYSIS AND DESIGN OF NEW CHIRAL LIGANDS
Immaculada Escofet Miquel

Chapter III

21a $\Delta G^{\ddagger}_{S-R} = 0.7$-$1.1$ kcal·mol^{-1} (depending on the method) were in good agreement with the experimentally value of $\Delta G^{\ddagger}_{S-R} \approx 1$ kcal·mol^{-1} (Figure 8). The lowest transition states were found to be stabilized by π-stacking between two phenyl rings of the substrates (**19a** and **20a**). This face-to-face π-stacking plays an important role in enantiomeric discrimination, which is consistent with the low enantioselectivities found with alkenes substituted with alkyl chains.

To further explore the factors that lead to the relative destabilization of **TS$_S$** *vs.* **TS$_R$**, Hirshfeld surface analysis was performed.[61] In Figure 9, the blue points depict the shape of the intramolecular surface between the ligand framework and the reaction center of the catalytic system in **TS$_S$**, while the red points display the region of elevated electron density, where weak van der Waals forces dominate in the overall interaction energy. Examination of the calculated surface revealed a direct contact between α-methylstyrene **20a** and one of the naphthyl groups of the ligand, which is absent in **TS$_R$** and might be then responsible for the preferred formation of the (*R*)-cyclobutene **21a** (Figure 9).
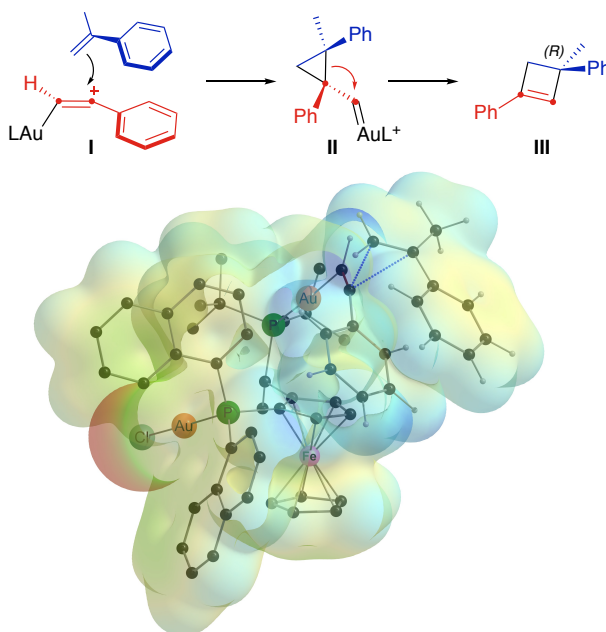
Figure 8. Lowest energy transition state for the reaction of **19a** and **20a** catalyzed by **49-(S,R$_P$)-B**.

61   Spackman, M. A.; Jayatilaka, D. *CrystEngComm* **2009**, *11*, 19−32.

UNIVERSITAT ROVIRA I VIRGILI
COMPUTATIONAL MECHANISTIC STUDIES IN GOLD(I) CATALYSIS AND DESIGN OF NEW CHIRAL LIGANDS
Immaculada Escofet Miquel

Chapter III
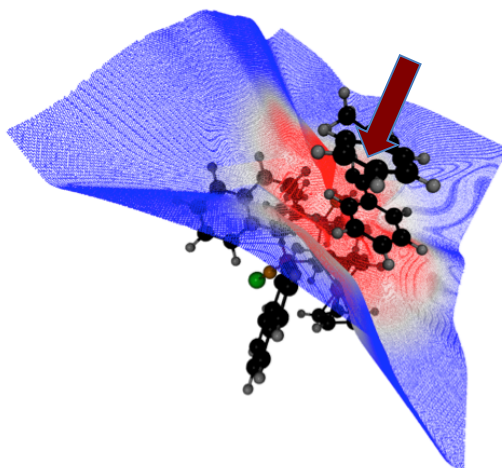
Figure 9. The color mapped Hirshfeld surface for **TS$_S$**. The arrow points to the area of VdW interaction between α-methylstyrene and the naphthyl group.

We further employed the Reduced Density Gradient (RDG) analysis,[62] which allows to distinguish weak interaction types based on the analysis of the residual electron density $\rho(r)$ between molecular fragments. The left plot in Figure 10 shows a significant repulsion between (naphthyl)$_2$P moiety and the reaction center. Analysis of the RDG isosurface also revealed a strong repulsion between (naphthyl)$_2$P–AuCl and the methine hydrogen atom in the α-position to the Cp-ring of the ferrocenyl moiety (Figure 10, right).
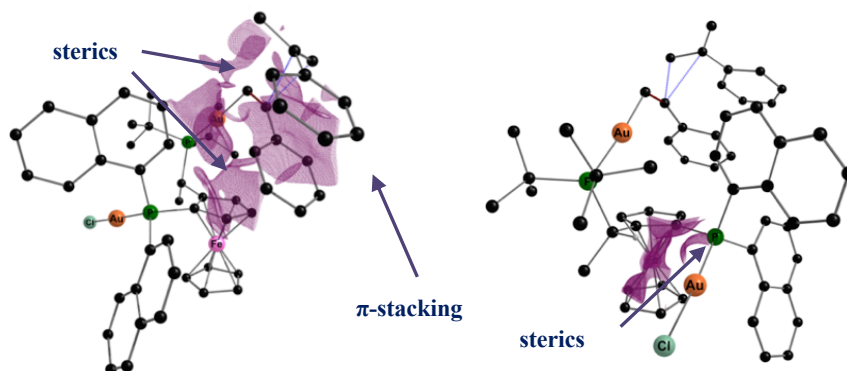
Figure 10. RDG isosurfaces (cut off = 0.6) for TS$_S$. All hydrogen atoms but one which suffers from the steric repulsion coming from AuCl (right) are omitted for clarity.

Noteworthy, the combination of stabilizing π-stacking and unfavorable steric effects between the approaching alkene and the naphthyl rings of the ligand, together with a strong C-H–AuCl repulsion between the (naphthyl)$_2$P-AuCl and the methine hydrogen atom in the

---

62   Johnson, E. R.; Keinan, S.; Mori-Sánchez, P.; Contreras-García, J.; Cohen, A. J.; Yang, W. *J. Am. Chem. Soc.* **2010**, *132*, 6498−6506.

UNIVERSITAT ROVIRA I VIRGILI
COMPUTATIONAL MECHANISTIC STUDIES IN GOLD(I) CATALYSIS AND DESIGN OF NEW CHIRAL LIGANDS
Immaculada Escofet Miquel

Chapter III

α-position to the Cp-ring of the ferrocenyl moiety rise the energy of the TS_S transition state *vs.* TS_R. Moreover, calculations of the corresponding transition states without the second AuCl on (naphthyl)$_2$P led to the complete loss of stereoselectivity, in agreement with the experimental data using complex **49-(S,R$_P$)-O** (Scheme 32), which support the crucial role of the (naphthyl)$_2$PAuCl moiety to induce chirality.

Computational Study of Pyrrolidinyl-Biphenyl Phosphine Gold(I) Catalysts

As mentioned in the **Introduction** of this chapter, our group has recently pioneered the development of a series of chiral catalysts based on a new conceptual design in which the chiral elements, *trans*-2,5-diarylpyrrolidines, are in para position of a modified JohnPhos-type ligand.[34] Thus, the bulky substituents on the phosphine prevent rotation around the C_{aryl}-P bond and force the P-Au-Cl axis to be parallel to the biphenyl axis, pointing towards the chiral environment. Moreover, a local C_2-axis is introduced resulting in a clear source of chirality (Figure 11).[35]
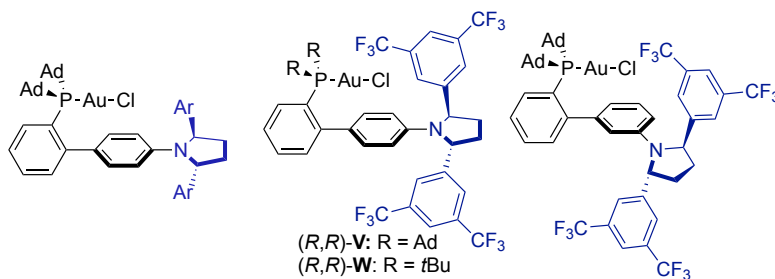
Figure 11. Series of chiral precatalyst synthesized based on JohnPhos-type ligand.

These new mononuclear gold(I) complexes are catalytically active in the intramolecular [4+2] cycloaddition of 1,6-enynes **8a-q** leading to the formation of cycloadducts **9a-q** in good yields and excellent enantioselectivities (Scheme 35). The best enantioselectivities were achieved with catalyst **V**, although similar results were obtained for complex **W** (Figure 11). The absolute configuration of **9o** was assigned as *R* by single-crystal X-ray diffraction, and those of the remaining cycloadducts were correlated by circular dichroism.

UNIVERSITAT ROVIRA I VIRGILI
COMPUTATIONAL MECHANISTIC STUDIES IN GOLD(I) CATALYSIS AND DESIGN OF NEW CHIRAL LIGANDS
Immaculada Escofet Miquel

Chapter III
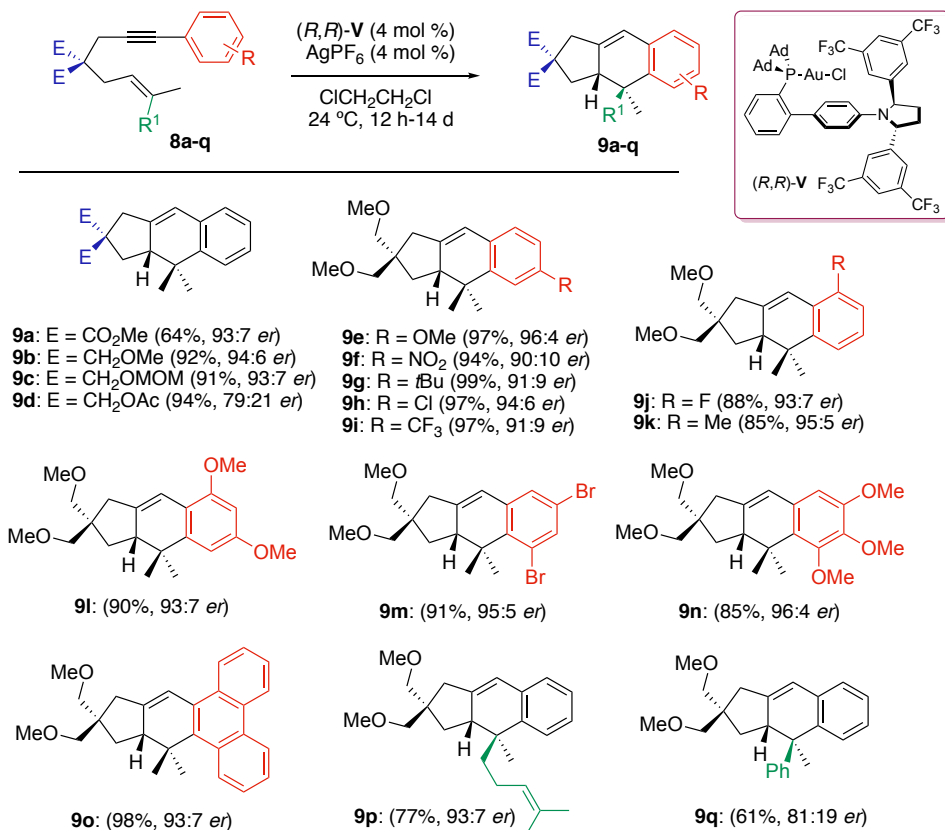
Scheme 35. Scope of the enantioselective cyclization of **8a-q** catalyzed by **V**. Yields determined by ^{1}H NMR using 1,3,5-tribromobenzene as internal standard. *er* measured by chiral HPLC.

A highly enantioselective 6-*endo*-dig cyclization of 1,6-enynes **38** allowed to accomplish the first total synthesis of the three members of the carexanes family of natural products. Thus, 1,2-dihydronapthalenes **39** were afforded in the presence of water and other external nucleophiles, together with catalyst **V** and silver salt (Scheme 36). Carexanes are a series of secondary metabolites that have been isolated from leaves of *Carex distachya*[41] and possess antimicrobial activity. Gratifyingly, precatalysts **V** afforded product **39k** in outstanding enantioselectivities, 99:1 *er*. The absolute configuration of **39k** was assigned by X-ray diffraction as *S* and the remaining ones were correlated by circular dichroism.

UNIVERSITAT ROVIRA I VIRGILI
COMPUTATIONAL MECHANISTIC STUDIES IN GOLD(I) CATALYSIS AND DESIGN OF NEW CHIRAL LIGANDS
Immaculada Escofet Miquel

Chapter III
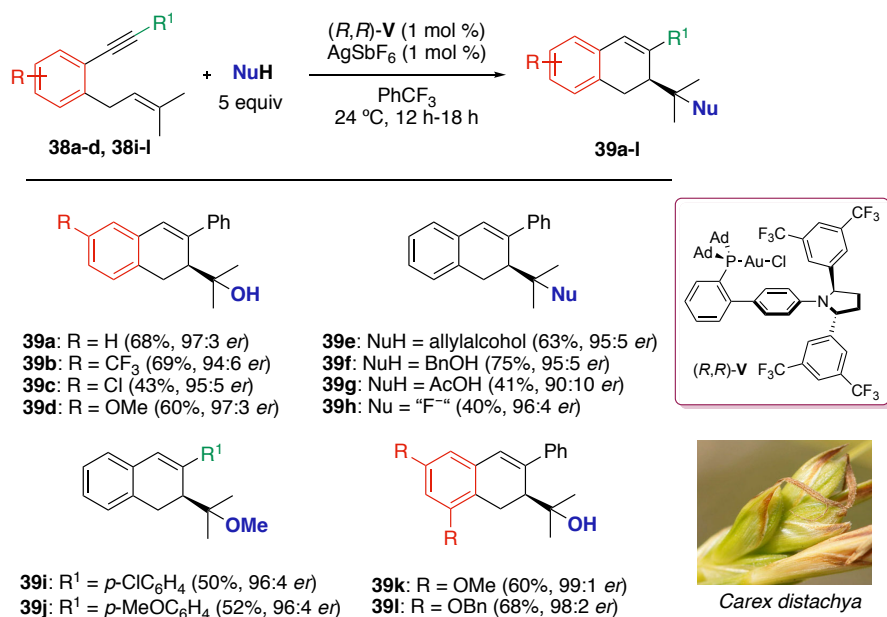
Scheme 36. Scope of asymmetric synthesis of **39a-l** catalyzed by **V** that is applied for the total synthesis of carexanes. *er* measured by chiral HPLC.

Although the three presumably related cyclizations of 1,6-enynes **8**, **10** and **38** proceed with high enantiomeric ratios, the first two transformations occur with a facial preference for the *Si* face of the alkene, whereas the cyclization of **38** leads to the opposite configuration by reaction through the *Re* face of the alkene.

Remarkably, two different folding modes occur for this type of substrates and thus, different geometrical arrangements may occur in the chiral pocket. We hypothesized that the aryl tether in enyne **38** directs the stereocontrol of the cyclization whereas the aryl substituent at carbon C1 in enynes **8** and **10**, is mainly responsible for the recognition in the chiral cavity (Scheme 18).

Scheme 18. Stereodirecting moieties in substrates **8**, **10** and **38**.

UNIVERSITAT ROVIRA I VIRGILI
COMPUTATIONAL MECHANISTIC STUDIES IN GOLD(I) CATALYSIS AND DESIGN OF NEW CHIRAL LIGANDS
Immaculada Escofet Miquel

Chapter III
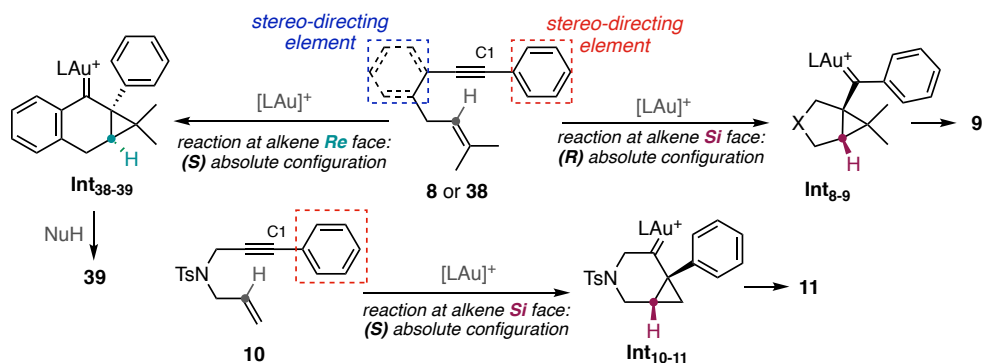
In order to better rationalize these different outcomes *(R or S)* observed for these transformations, we performed DFT calculations. We computed the reaction coordinate for the cyclization of enynes **8b** and **38k**. BP86-D3 has been chosen as a functional due to is efficiency proved in other studies of enantioselective gold(I) catalysis.[63] We used *(R,R)*-**W** as gold(I) catalyst, which is similar but simpler to *(R,R)*-**V**. Our calculations herein center on the nucleophilic attack of the alkene at the $[LAu(\eta^2\text{-alkyne})]^+$ complex as the enantio-determining step.

As detailed in **Chapter I**, for arylenynes such as **8b**, the formation of cyclopropyl gold(I) carbene of type **Int2** was favored over the opened carbocation **Int3** (Scheme 37). Therefore, in the following computational studies with *(R,R)*-**W**, we will only consider the formation of **Int2** and not **Int3** as the formation of the latter is unfavored.
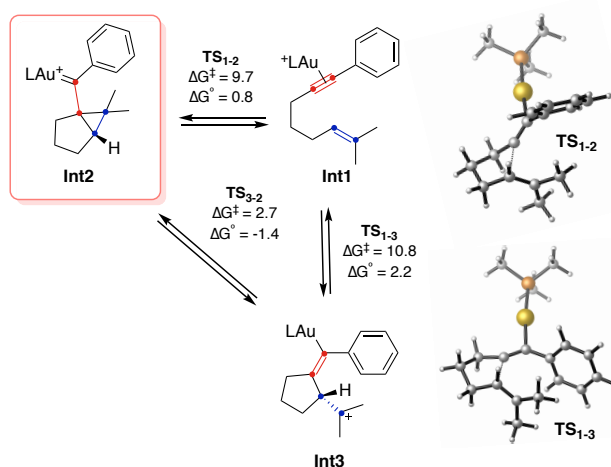
Scheme 37. Calculated formation of cyclopropyl gold(I) carbene **Int2** and open carbocation **Int3**. L=PMe$_3$. DFT calculations performed with BP86-D3/6-31G(d) (C, H, P) and SDD (Au) in CH$_2$Cl$_2$ (PCM). Free energies in kcal/mol.

We first studied the cyclization of **38k** to form racemic product at the same level of theory (BP86-D3/6-31G(d) (C, H, P) and SDD (Au) in CH$_2$Cl$_2$ (PCM), L = PH$_3$) (Scheme 38). We found that 6-*endo*-dig pathways (**TS$_{1\text{-}3a}$**, **TS$_{1\text{-}2a}$**) are more favored than 5-*exo*-dig routes (**TS$_{1\text{-}3b}$**, **TS$_{1\text{-}2b}$**) by at least 0.7 kcal/mol. Similarly, the lowest energy barrier corresponds to the formation of cyclopropyl gold carbene **38k-Int2a**. In addition, as we observed before (**Chapter I**), intermediates of type **Int3** were found to be connected to **Int2** via **TS$_{3\text{-}2}$**.

63   (a) Kang, R.; Chen, H.; Shaik, S.; Yao, J. *J. Chem. Theory Comput.* **2011**, *7*, 4002−4011. (b) Ciancaleoni, G.; Rampino, S.; Zuccaccia, D.; Tarantelli, F.; Belanzoni, P.; Belpassi, L. *J. Chem. Theory Comput.* **2014**, *10*, 1021−1034.

UNIVERSITAT ROVIRA I VIRGILI
COMPUTATIONAL MECHANISTIC STUDIES IN GOLD(I) CATALYSIS AND DESIGN OF NEW CHIRAL LIGANDS
Immaculada Escofet Miquel

Chapter III
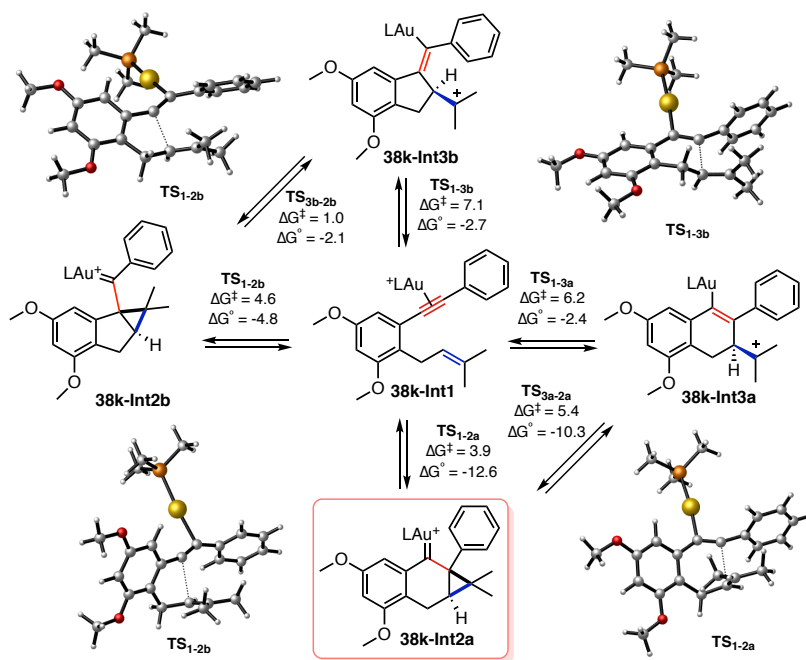
Scheme 38. Calculated formation of cyclopropyl gold(I) carbenes **Int2** and open carbocations **Int3** for the 5-*exo*-dig and the 6-*endo*-dig pathways of enyne **38k**. L=PMe$_3$. DFT calculations performed with BP86-D3/6-31G(d) (C, H, P) and SDD (Au) in CH$_2$Cl$_2$ (PCM). Free energies in kcal/mol.

In the study with complex *(R,R)*-**W**, we calculated four possible minima resulting from two binding orientations (**A and B)** of the substrate coordinated to gold(I) through the alkyne, and the reaction of the two enantiotopic faces of the alkene (Scheme 39 and 40).

In the cyclization of **8b** with catalyst **W**, we examined the evolution of the four possible gold(I)-complexes **Int1a-d** following an exocyclic pathway. The preferred substrate orientation was **B**, being **B-Int1d** the most stable intermediate and the activation energy to reach **B-TS**$_{Int1d-2d}$, lower than other possible pathways by at least 2.5 kcal/mol.

Therefore, in agreement with our experimental results (94:6 *er*), cyclopropyl gold(I) carbene **B-Int2d** with the *R* absolute configuration is preferentially formed (Scheme 39). Attractive non-covalent interactions between the aryl ring of the substrate with the aryl ring of the pyrrolidine (distance 3.62 Å) and with the lower ring of the biphenyl scaffold of the ligand (distance 3.47 Å) as well as aryl-OMe interactions (3.01 Å) play the major role in the chiral folding of the substrate and in the stabilization of the transition state (**B-TS**$_{Int1d-2d}$).

UNIVERSITAT ROVIRA I VIRGILI
COMPUTATIONAL MECHANISTIC STUDIES IN GOLD(I) CATALYSIS AND DESIGN OF NEW CHIRAL LIGANDS
Immaculada Escofet Miquel

Chapter III

Orientation A

Orientation B
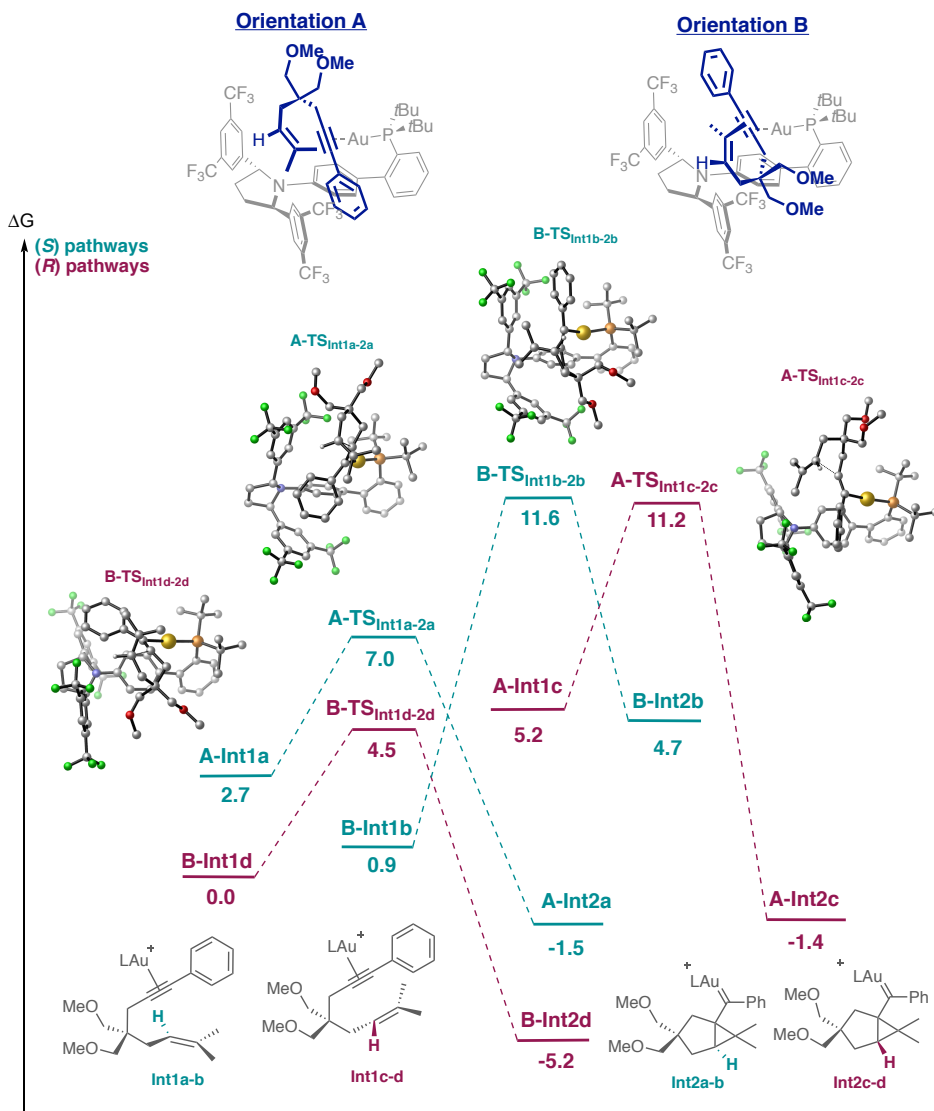
Scheme 39. Free energy profiles for the 5-*exo*-dig enantioselective cyclization reaction of 1,6-enynes **8b** with (*R,R*)-**W**. (*S*) pathways are depicted in green and (*R*) pathways in purple. The energy values are given in kcal/mol and represent the relative free energies. Hydrogen atoms have been omitted for clarity.

However, orientation **A** was found to drive the enantioinduction for enyne **38k** by 6-*endo*-dig pathway of intermediate **A-Int3a**. The strong aryl-aryl interaction of the most electron-rich aromatic ring of the substrate with the aryl group of the pyrrolidine (distance 3.32 Å) favors orientation **A** leading to the *S* enantiomer. Hence, cyclopropyl gold carbene **A-Int4a** is preferentially formed via **A-TS**$_{Int3a-4a}$ that requires 2.5 and 3.7 Kcal/mol less than the competing *R* pathways (**A-TS**$_{Int3c-4c}$, **B-TS**$_{Int3d-4d}$) according with our experimental results (99:1 e*r*) (Scheme 40). In both cases, the lowest energy transitions states were achieved from the most stable orientations (**B** for **8b** and **A** for **38k**).

UNIVERSITAT ROVIRA I VIRGILI
COMPUTATIONAL MECHANISTIC STUDIES IN GOLD(I) CATALYSIS AND DESIGN OF NEW CHIRAL LIGANDS
Immaculada Escofet Miquel

Chapter III
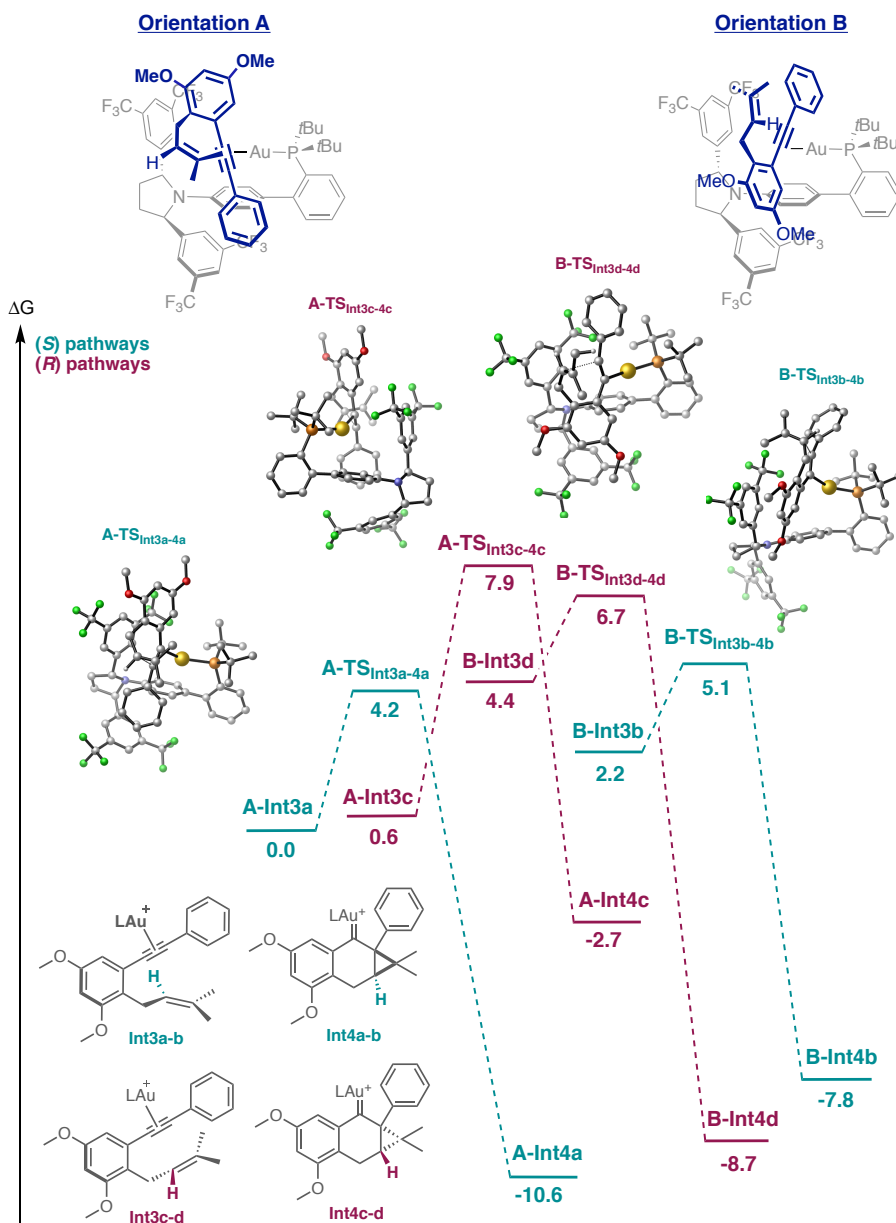
Scheme 40. Free energy profiles for the 6-*endo*-dig enantioselective cyclization reaction of 1,6-enynes **38k** with (R,R)-**W** (S) pathways are depicted in green and (R) pathways in purple. The energy values are given in kcal/mol and represent the relative free energies. Hydrogen atoms have been omitted for clarity.

UNIVERSITAT ROVIRA I VIRGILI
COMPUTATIONAL MECHANISTIC STUDIES IN GOLD(I) CATALYSIS AND DESIGN OF NEW CHIRAL LIGANDS
Immaculada Escofet Miquel

Chapter III

Given the important role that non-covalent interactions could play in the investigated system, we further examined them by NCI analysis.[49] The NCI plots illustrated the size and shape of the surfaces generated from interactions present in the system (Figure 12 and 13). Hence, as revealed by the NCI plots, attractive interactions between the aromatic moieties of the substrates and the aromatic substituents of the pyrrolidine of precatalyst **W**, play the major role in the chiral folding of the substrate and in the stabilization of the corresponding transitions states. Additional stabilization is provided by interactions between the substrates and the biphenyl scaffold of the ligand. In the case of substrate **8b**, attractive aryl-OMe interactions are also stereo-controlling elements that favor reaction through the *Si* face of the alkene in orientation **B** (Figure 12). In the lowest-energy transition states, **B-TS**$_{Int1d-2d}$ and **A-TS**$_{Int3a-4a}$, we observed larger green surfaces, which mainly correspond to aryl-aryl interactions, than in the other possible transition states derived for the other found minima.
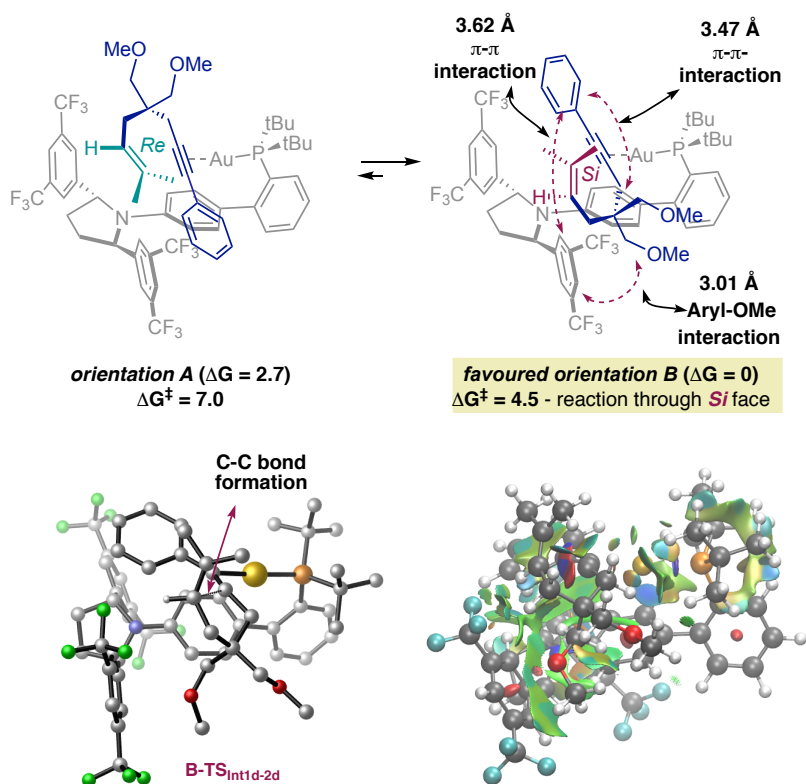
Figure 12. The two most relevant binding orientations (**A** and **B**) of enyne **8b** coordinated to (*R,R*)-**W** and the lowest energy transition states (CYLview representations and NCI plots). Energy values are given in kcal/mol relative to the most stable orientation. Hydrogen atoms are omitted for clarity, with the exception of the stereocenters. Strong attractive interactions are blue (C−C bond formation), weak attractive interactions are green (non-covalent interactions), and strong repulsive interactions are red. Color code: P, orange; Au, yellow; F, cyan; O, red; C, gray; and H, white.

UNIVERSITAT ROVIRA I VIRGILI
COMPUTATIONAL MECHANISTIC STUDIES IN GOLD(I) CATALYSIS AND DESIGN OF NEW CHIRAL LIGANDS
Immaculada Escofet Miquel

Chapter III
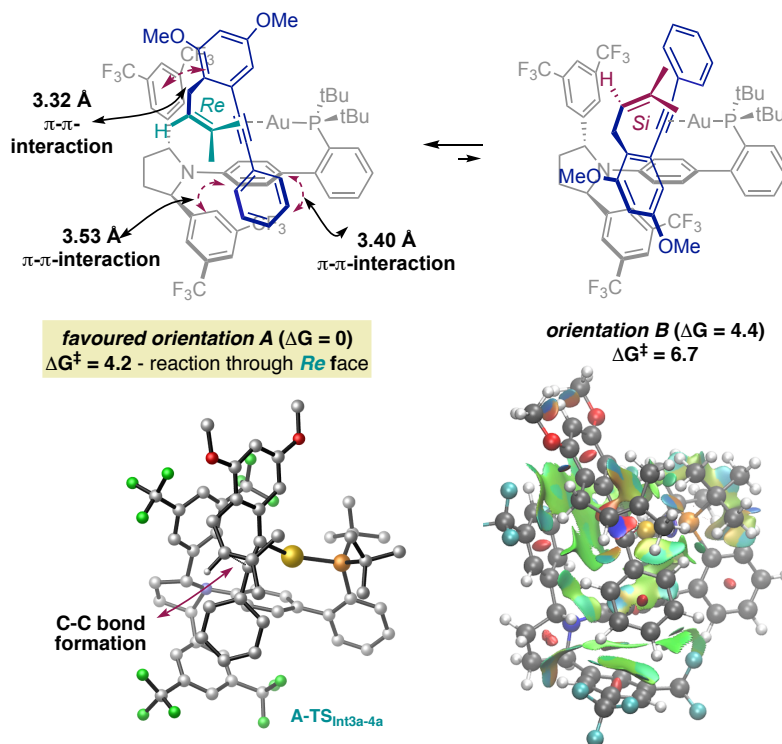
Figure 13. The two most relevant binding orientations (**A** and **B**) of enyne **38k** coordinated to (*R,R*)-**W** and the lowest energy transition states (CYLview representations and NCI plots). Energy values are given in kcal/mol relative to the most stable orientation. Hydrogen atoms are omitted for clarity, with the exception of the stereocenters. Strong attractive interactions are blue (C−C bond formation), weak attractive interactions are green (non-covalent interactions), and strong repulsive interactions are red. Color code: P, orange; Au, yellow; F, cyan; O, red; C, gray; and H, white.

This model is consistent with the lower enantiomeric ratios obtained in the cyclization of enyne **8d** (Scheme 35), in which the non-covalent interactions are probably weaker between diacetate group and the aryl rings of the pyrrolidine. Hence, substrate recognition by the chiral catalysts induces one specific binding orientation via non-covalent interactions leading to the distinct enantioselective folding in the enantioselective cyclization of enynes of type **8**, **10** and **38** (Figure 12 and 13).[64]

Interestingly, negative slopes were obtained when preforming a Hammet study[65] of the reactions of substrates **8e-i** (*er* vs. σ^+_p) and **38a-d** (*er* vs. σ^+_m) with (*R,R*)-**V**. These results confirm the preferred binding of the most electron-rich substrates by the catalyst bearing strongly electron-withdrawing aryl groups (Scheme 41).

64   (a) Neel, A. J.; Hilton, M. J.; Sigman, M. S.; Toste, F. D. *Nature* **2017**, *543*, 637−646. (b) Toste, F. D.; Sigman, M. S.; Miller, S. J. *Acc. Chem. Res.* **2017**, *50*, 609−615.

65   Kinetic studies have been performed by Giuseppe Zuccarello. All the experimental details can be found in the supporting information of (34).

UNIVERSITAT ROVIRA I VIRGILI
COMPUTATIONAL MECHANISTIC STUDIES IN GOLD(I) CATALYSIS AND DESIGN OF NEW CHIRAL LIGANDS
Immaculada Escofet Miquel

Chapter III
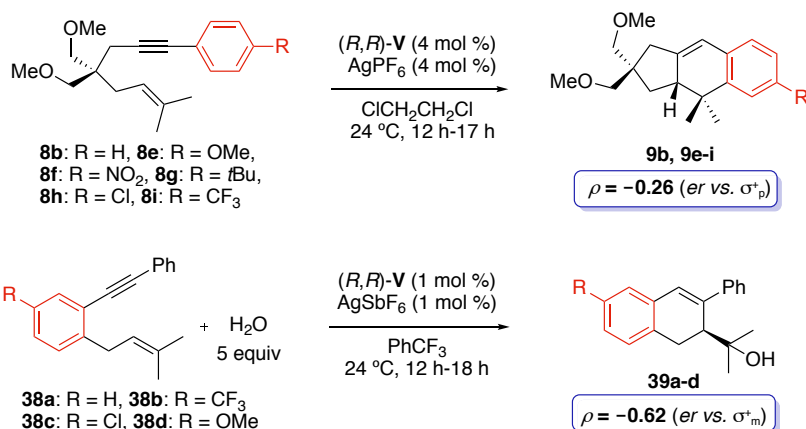
Scheme 41. Hammet study of formal [4+2] cyclization of enynes **8** and **38**.

We further studied the proposed non-covalent interactions using complex (*R,R*)-**X** with chiral 2,5-dicyclohexylpyrrolidine instead of 2,5-diarylpyrrolidine. We expected the formation of **9b** and **39k** in significant lower *er* because the stabilizing aryl-aryl interactions and consequentially the optimal substrate orientation observed with (*R,R*)-**V**/**W** would be disfavored. However, to our surprise, only a small drop in *er* was observed. The absolute configurations of the obtained compounds **9b** (*R*) and **39k** (*S*) were the same (Scheme 42).
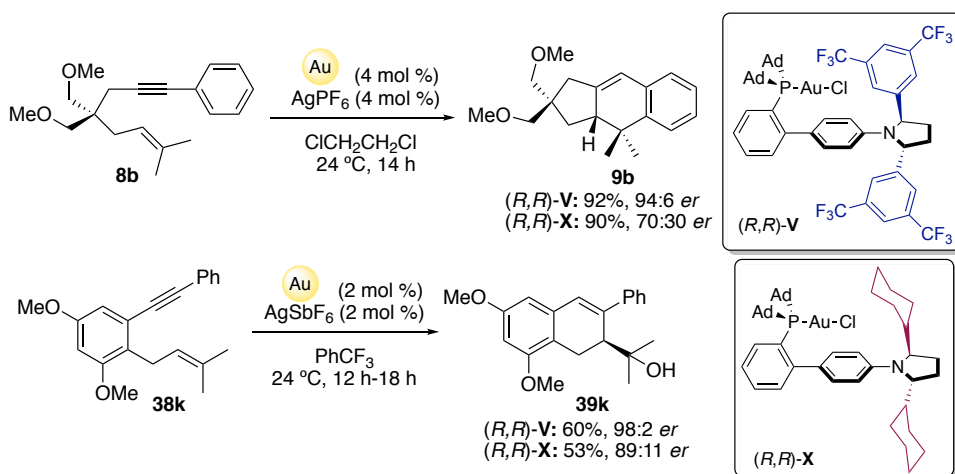
Scheme 42. Performance of (*R,R*)-**X**/**V** in [4+2] cyclization of enynes **8b** and **38k**.

To better rationalize the mode of action of this new chiral complex (*R,R*)-**X**, we calculated the lowest energy transition state for these systems. We computed the reaction coordinates of **8b** and **38k** using simpler complex (*R,R*)-**Y** with di-*tert*-butylphosphine instead of di-adamantyl at the same level of theory (Scheme 43 and 44). Similarly, two possible binding orientations **A** and **B** of the substrate bound to the gold through the alkyne are taken into account along with the two possible prochiral faces of the alkene moiety, *Re* and *Si*.

UNIVERSITAT ROVIRA I VIRGILI
COMPUTATIONAL MECHANISTIC STUDIES IN GOLD(I) CATALYSIS AND DESIGN OF NEW CHIRAL LIGANDS
Immaculada Escofet Miquel

Chapter III

As observed for complex (*R*,*R*)-**W**, cyclization of **8b** evolves *via* the most stable binding orientation **B**, having **B-TS**$_{Int5d-6d}$ the lowest energy barrier that give rise to product **9b** with *R* absolute configuration through the *Si* prochiral face of the alkene by at least 5.2 kcal/mol (Scheme 43).
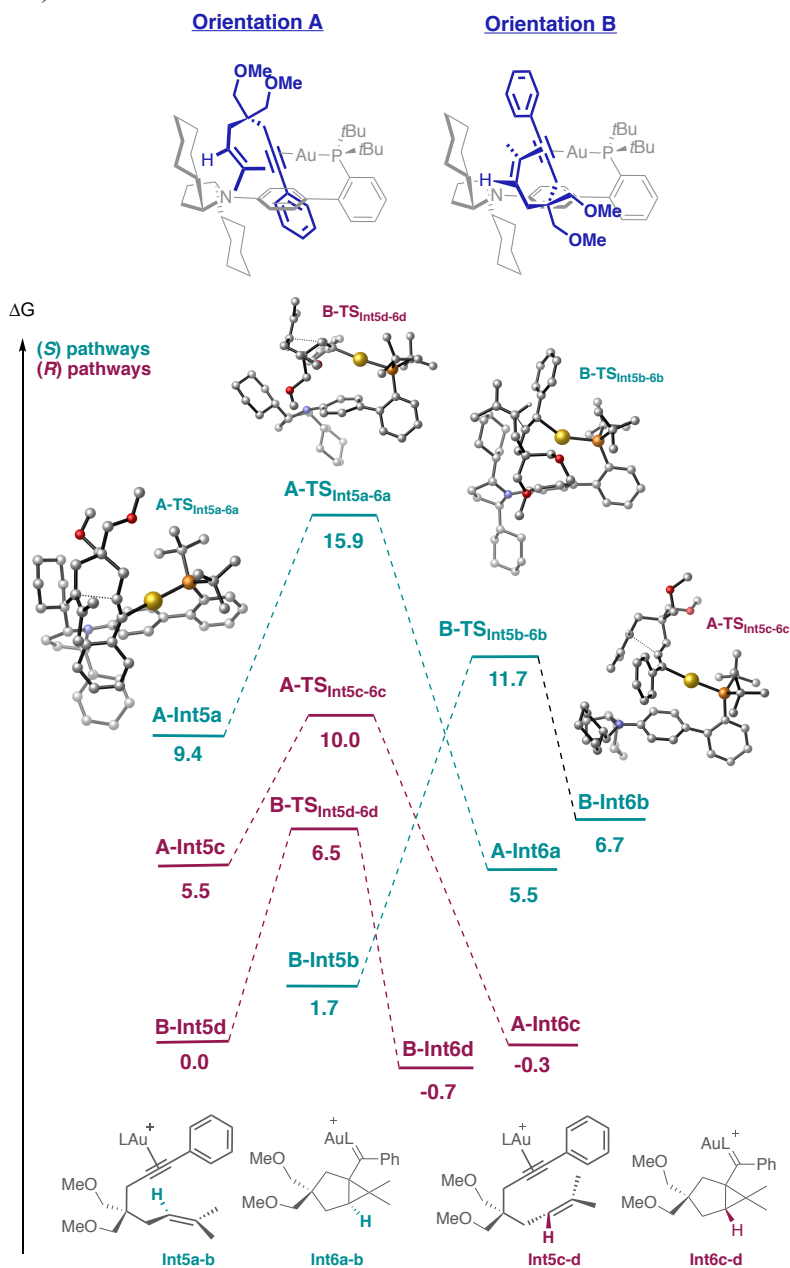
Scheme 43. Free energy profiles for the 5-*exo*-dig enantioselective cyclization reaction of 1,6-enynes **8b** with (*R*,*R*)-**Y**. (*S*) pathways are depicted in green and (*R*) pathways in purple. The energy values are given in kcal/mol and represent the relative free energies. Hydrogen atoms have been omitted for clarity.

UNIVERSITAT ROVIRA I VIRGILI
COMPUTATIONAL MECHANISTIC STUDIES IN GOLD(I) CATALYSIS AND DESIGN OF NEW CHIRAL LIGANDS
Immaculada Escofet Miquel

Chapter III
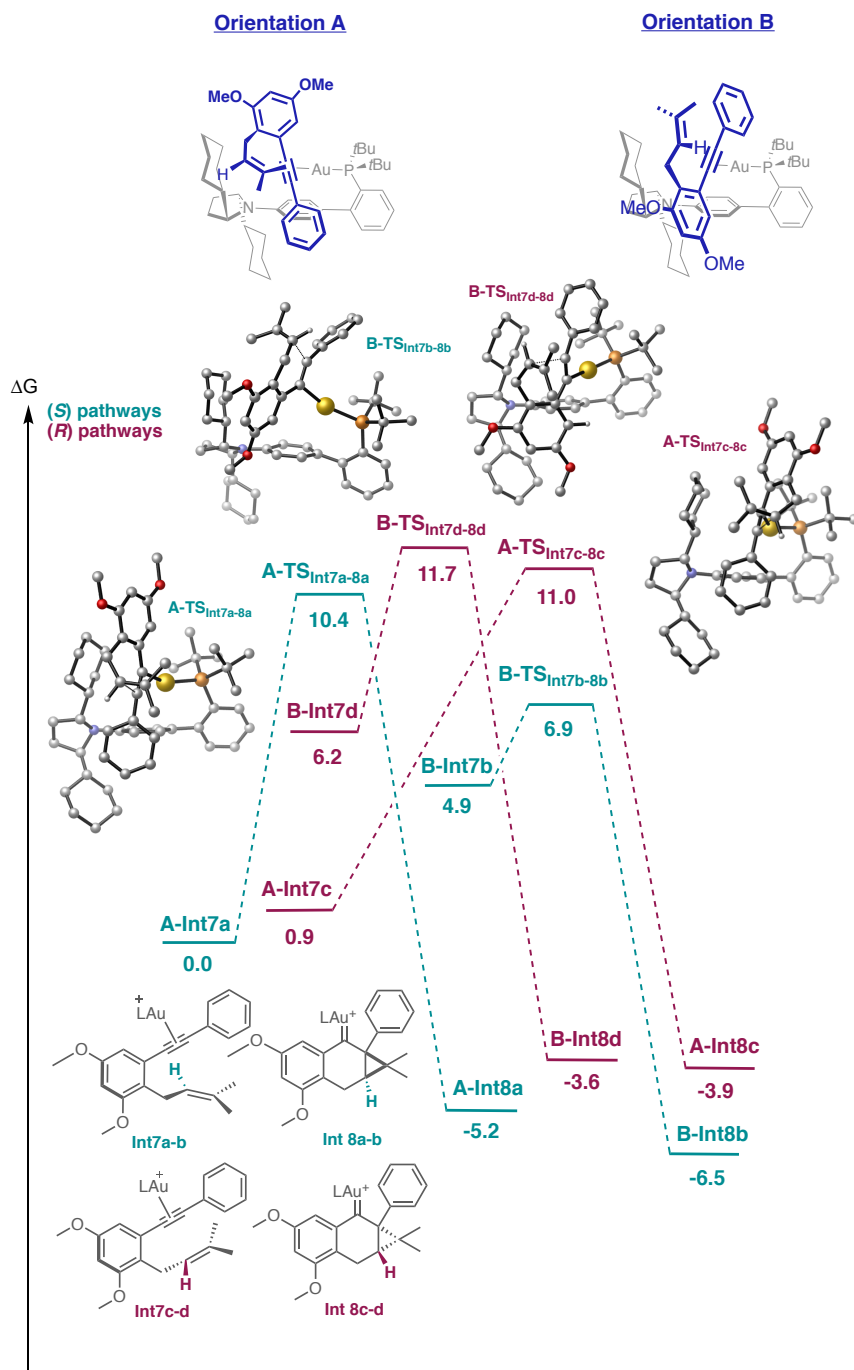
Scheme 44. Free energy profiles for the 6-*endo*-dig enantioselective cyclization reaction of 1,6-enynes **38k** with (*R*,*R*)-**Y**. (*S*) pathways are depicted in green and (*R*) pathways in purple. The energy values are given in kcal/mol and represent the relative free energies. Hydrogen atoms have been omitted for clarity.

UNIVERSITAT ROVIRA I VIRGILI
COMPUTATIONAL MECHANISTIC STUDIES IN GOLD(I) CATALYSIS AND DESIGN OF NEW CHIRAL LIGANDS
Immaculada Escofet Miquel

Chapter III

Surprisingly, the binding orientation adopted by enyne **38k** (**B**) in (*R,R*)-**Y** was found to be the opposite to the case with (*R,R*)-**W**. However, the computed energies suggest that this system is in a Curtin-Hammet scenario where the two possible orientations compete with each other. Although **A-Int7c** is 4 kcal/mol more stable than **B-Int7b**, the major part of the product arises from the latter, **B-TSInt7b-8b**, which is lower in energy than **A-TSInt7c-8c**. Interestingly, there is another pathway that competes with **B-TSInt7b-8b**. Although **A-Int7a** is 4.9 kcal/mol more stable than **B-Int7b**, the same face (*Re*) would be activated for both pathways, leading to the *S* enantiomer (Scheme 44).

In addition to the previously discussed attractive interactions between the aromatic moieties of the substrates and bottom ring of the biphenyl scaffold, NCI plots[49] revealed stabilizing alkyl-OMe interactions as stereo-controlling elements that favor reaction through the *Si* face of the alkene (**B-TS$_{Int5d-6d}$**). Moreover, aryl-alkyl interactions were also observed between the aryl ring of the enyne **8b** and the cyclohexyl of the ligand. In contrast to what we observed using catalyst (*R,R*)-**W**, the competing pathway that would favor the reaction through *Re* face, thus giving product (*S*), is the one that has the same binding orientation, **B** (**B-TS$_{Int5b-6b}$**) (Figure 14).
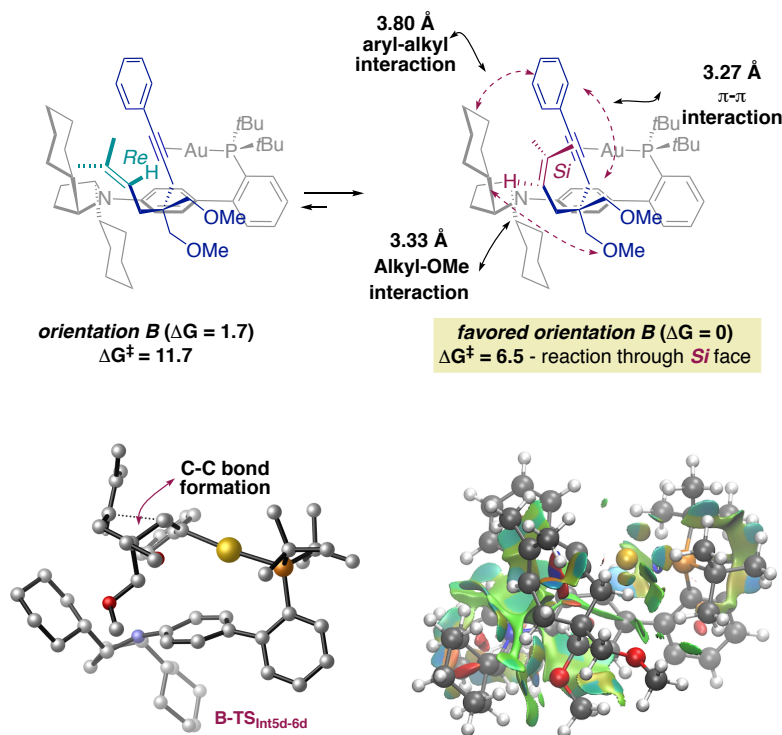
Figure 14. The lowest energy transition states of enyne **8b** coordinated to (*R,R*)-**Y**. (CYLview representations and NCI plots). Energy values are given in kcal/mol relative to the most stable orientation. Hydrogen atoms are omitted for clarity, with the exception of the stereocenters. Strong attractive interactions are blue (C−C bond formation), weak attractive interactions are green (noncovalent interactions), and strong repulsive interactions are red. Color code: P, orange; Au, yellow; F, cyan; O, red; C, gray; and H, white.

UNIVERSITAT ROVIRA I VIRGILI
COMPUTATIONAL MECHANISTIC STUDIES IN GOLD(I) CATALYSIS AND DESIGN OF NEW CHIRAL LIGANDS
Immaculada Escofet Miquel

Chapter III

As suggested by the NCI plots, the lowest-energy transition state for enyne **38k** is stabilized by attractive alkyl-aryl interactions[66] between the cyclohexyl substituent in *(R,R)*-Y and the aromatic tether of **38k** (Figure 15).
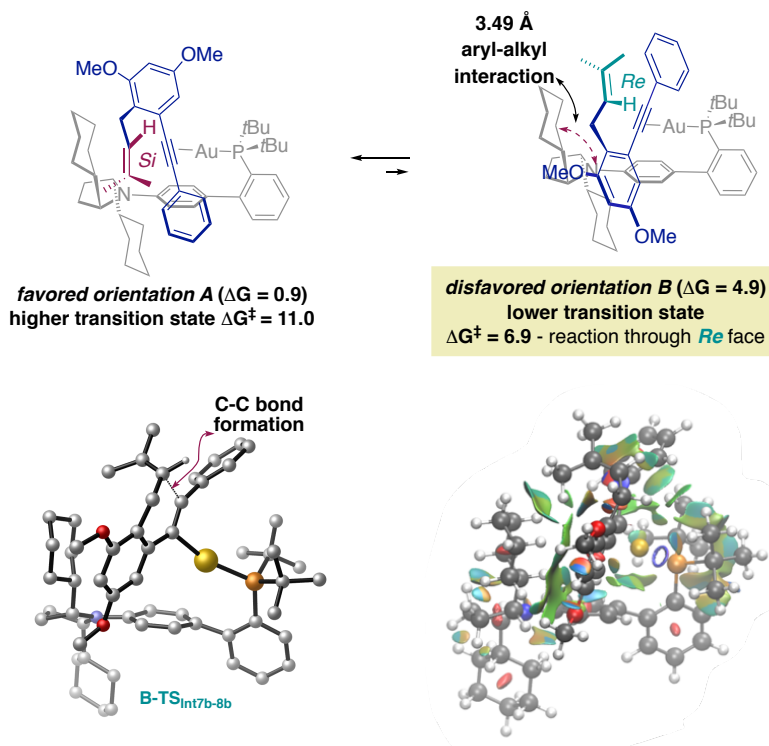
Figure 15. The two most relevant binding orientations (**A** and **B**) of enyne **38k** coordinated to (R,R)-**Y** and the lowest energy transition states (CYLview representations and NCI plots). Energy values are given in kcal/mol relative to the most stable orientation. Hydrogen atoms are omitted for clarity, with the exception of the stereocenters. Strong attractive interactions are blue (C−C bond formation), weak attractive interactions are green (non-covalent interactions), and strong repulsive interactions are red. Color code: P, orange; Au, yellow; F, cyan; O, red; C, gray; and H, white.

66   (a) Ribas, J.; Cubero, E.; Luque, F. J.; Orozco, M. *J. Org. Chem.* **2002**, *67*, 7057–7065. (b) Ninković, D. B.; Vojislavljević-Vasilev, D. Z.; Medaković, V. B.; Hall, M. B.; Brothers, E. N.; Zarić, S. D. *Phys. Chem. Chem. Phys.* **2016**, *18*, 25791−25795. (c) Ninković, D. B.; Blagojević-Filipović, J, P.; Hall, M. B.; Brothers, E. N.; Zarić, S. D. *ACS Cent. Sci.* **2020**, *6*, 420−425.

UNIVERSITAT ROVIRA I VIRGILI
COMPUTATIONAL MECHANISTIC STUDIES IN GOLD(I) CATALYSIS AND DESIGN OF NEW CHIRAL LIGANDS
Immaculada Escofet Miquel

Chapter III

Very recently, these type of alkyl-aryl interactions[66] have been computationally studied by the group of Zarić.[66c] Based on high-level *ab initio* calculations, this group reported that the most stable stacking for benzene-cyclohexane is 17% stronger than that for benzene-benzene. Nonetheless, as these systems are displaced horizontally, the benzene-benzene interaction retains most of its strength. Therefore, at a displacement of 5.0 Å, the benzene-benzene attraction is still ~70% of its maximum strength, while the benzene-cyclohexane attraction has fallen to ~40% of its maximum strength. Therefore, the stronger interaction at large offsets, is the key feature that makes aromatic-aromatic interactions special since two aryl groups can recognize each other over much greater range of distances. However, at short distances, cyclohexane-benzene can form strong electrostatic interactions.

Recently, a series of 2nd generation of complexes have been designed in our laboratories in order to examine the effect of tuning the electronic and steric properties on the enantiodiscrimination. Thus, our ligand design was dissected in three main parts, labeled as the top aryl ring, the bottom aryl ring and the chiral pyrrolidine (Figure 16).
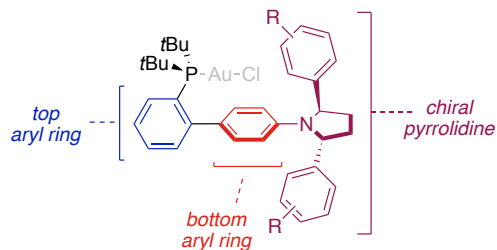
Figure 16. Dissecting the ligand design.

Complexes (*S,S*)-**Z**, (*R,R*)-**AA**, (*R,R*)-**AB** were synthesized and their catalytical activity was tested towards the formal intramolecular [4+2] cycloaddition of enyne **8b** (Table 16). Cycloadduct **9b** was obtained in good yields but essentially as a racemic mixture when complex (*S,S*)-**Z** was used (Table 16, entry 2). Hence, replacing the rigid pyrrolidine ring of (*S,S*)-**V** by an acyclic amine was detrimental for the enantioinduction since the chiral substituents have higher degree of flexibility. On the other hand, functionalization of the top aryl ring with electron withdrawing groups (complexes (*R,R*)-**AA**, (*R,R*)-**AB**) led to product **9b** in comparable enantiomeric ratio to that obtained with (*R,R*)-**V** (Table 16, entry 1) but in reduced reaction times (Table 16, entries 3-4).

UNIVERSITAT ROVIRA I VIRGILI
COMPUTATIONAL MECHANISTIC STUDIES IN GOLD(I) CATALYSIS AND DESIGN OF NEW CHIRAL LIGANDS
Immaculada Escofet Miquel

Chapter III

Table 16. Catalytical activity of 2nd generation complexes in the cycloaddition of **8b**.
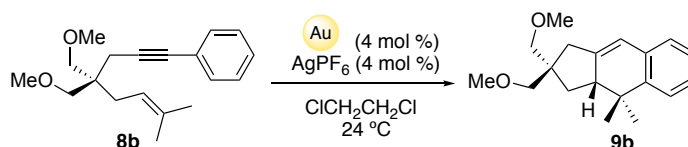
Entry	[Au]	t	**9b** yield (%)[a]	**9b** er[b]
1	(*R,R*)-**V**	16	92	94:6
2	(*S,S*)-**Z**	6	84	51:49
3	(*R,R*)-**AA**	35 min	97	93:7
4	(*R,R*)-**AB**	2	95	93:7

[a] Isolated yields. [b] *er* determined by chiral HPLC.
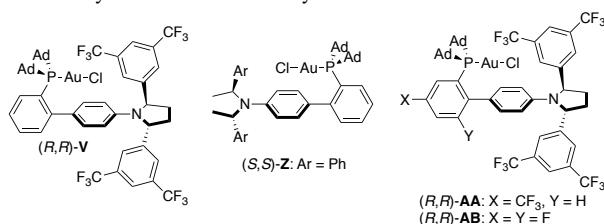
With these results in hand, and to better understand the working mode of these complexes, we decided to computationally study the effect of the substituents on the ligands as a step towards the rational design of a 3rd generation of chiral, more efficient and general catalysts.

Thus, we analyzed a wide variety of substituents (R^1-R^4 at the top aryl ring, and R^5-R^8 at the bottom aryl ring) of (*R,R*)-**Y** towards the formal [4+2] cycloaddition of enyne **8b** (Table 17). Based on the energy profile obtained with enyne **8b** (Scheme 39), we computed competing pathways, **B-TSInt1d** and **A-TSInt1a-2a** for each complex having different substituents in the aromatic rings. Then, we calculated the $\Delta\Delta G$ between the *S* and *R* pathways. Initially, for complex (*R,R*)-**Y** we found that $\Delta\Delta G$ = 2.6 kcal/mol, whereas higher values were obtained when having a bulky CF_3 or CH_3 in R^3 position (Table 17, entries 1, 2 and 4). However, the introduction an electron-withdrawing group F or electron-donating *t*Bu or Ph in R^3 position gave lower energy differences (Table 17, entries 3, 5-6). Replacement of hydrogen for electron withdrawing CF_3 group in R^1 position was key for high computed enantioselectivities. (Table 17, entry 8), while methyl group decreased dramatically the enantiodiscrimination (Table 17, entry 9). Simulations of catalysts (*R,R*)-**AA**, (*R,R*)-**AB**, but containing di-*tert*-butyl phosphines, were in good agreement with the experimental results since slightly smaller enantiomeric ratios were computed (Table 17, entries 10-11). Moreover, promising results were obtained when aryl ring was disubstituted with CF_3 groups in R^2 and R^4 positions (Table 17, entry 12). With regard to the bottom ring, significant effect was observed when changing the aryl substituents R^5-R^8.

UNIVERSITAT ROVIRA I VIRGILI
COMPUTATIONAL MECHANISTIC STUDIES IN GOLD(I) CATALYSIS AND DESIGN OF NEW CHIRAL LIGANDS
Immaculada Escofet Miquel

Chapter III

Hence, according to our calculations, the highest enantiomeric ratios would be obtained when using a complex containing a tetrazine or a tetrafluoraryl ring (Table 17, entries 14-15). Finally, we also computed the system with catalyst (*S,S*)-**Z**, bearing an acyclic *C₂*-symmetric amine ligand, and in agreement with our experimental results (51:49 *er*), the enantioselectivity was calculated to be small ($\Delta\Delta G$ = 0.4 kcal/mol).

Table 17. Computational study on the ligand effect to the enantioselective cycloaddition of **8b**.
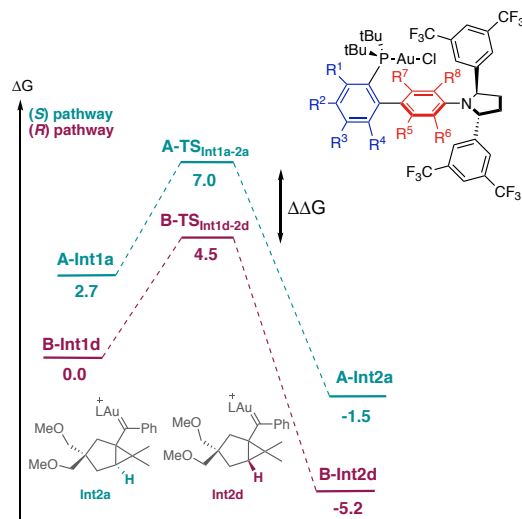
Entry	R^1	R^2	R^3	R^4	R^5	R^6	R^7	R^8	$\Delta\Delta G$
1	H	H	H	H	H	H	H	H	2.6
2	H	H	CF_3	H	H	H	H	H	3.3
3	H	H	F	H	H	H	H	H	2.6
4	H	H	Me	H	H	H	H	H	3.4
5	H	H	*t*Bu	H	H	H	H	H	2.3
6	H	H	Ph	H	H	H	H	H	2.4
7	F	H	H	H	H	H	H	H	2.1
8	CF_3	H	H	H	H	H	H	H	3.5
9	CH_3	H	H	H	H	H	H	H	0.0
10	H	CF_3	H	H	H	H	H	H	2.1
11	H	F	H	F	H	H	H	H	2.1
12	H	CF_3	H	CF_3	H	H	H	H	3.5
13	H	H	H	H	CH_3	H	CH_3	H	2.2
14	H	H	H	H	F	F	F	F	3.6
15	H	H	H	H		tetrazine			6.1

Computed $\Delta\Delta G$ between **B-TSInt1d** and **A-TSInt1a-2a** for each complex. The values are given in kcal/mol. Best results marked in green and worst results in orange.

Further experiments are now ongoing in our laboratories in order to design of a 3ʳᵈ generation of chiral biphenyl phosphine-supported complexes.

UNIVERSITAT ROVIRA I VIRGILI
COMPUTATIONAL MECHANISTIC STUDIES IN GOLD(I) CATALYSIS AND DESIGN OF NEW CHIRAL LIGANDS
Immaculada Escofet Miquel

Chapter III

Conclusions

A series of novel chiral phosphite gold(I) complexes **48(AuCl)a-j** was prepared in a modular manner from BINOL. Cyclization of aryl-substituted 1,6-enynes with these complexes occurs with enantiomeric ratios ranging from 86:14 up to 94:6 (Scheme 45).
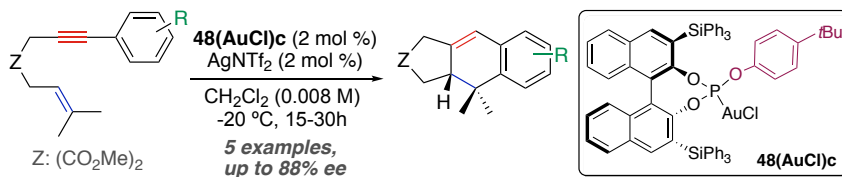
Scheme 45. Asymmetric gold(I)-catalyzed [4+2] cycloaddition of 1,6-enynes **8a-e** with **48(AuCl)c**.

On the other hand, we have discovered that non-C_2 chiral Josiphos digold(I) precatalysts were optimal for the enantioselective [2+2] intermolecular cycloaddition. This methodology was applied to the reaction of aryl alkynes with α-ethyl styrenes, giving rise to cyclobutenes with moderate to good enantiomeric ratios. Alternatively, the use of Josiphos ligand **F**, allowed for the cycloaddition of trisubstituted alkenes (Scheme 46).
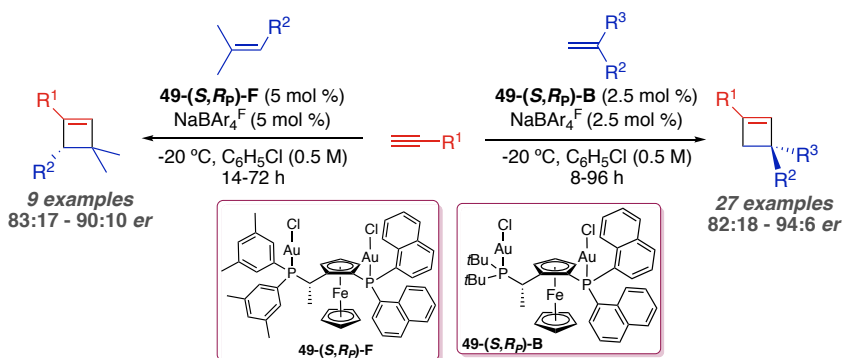
Scheme 46. Enantioselective intermolecular [2+2] cycloaddition.

It has been demonstrated that only one of the gold(I) centers is directly involved in the activation of the alkyne, although the second one is required to induce high enantioselectivity. Our work also reveals that both ligand exchange and electrophilic addition can be turnover-limiting steps in this catalytic cycloaddition. Thus, for moderate electron rich alkenes, the rate determing step is the associative ligand exchange, while for electron poor alkenes the slowest step is the nucleophilic attack.

Furthermore, our group has designed a new class of chiral gold(I) catalysts with monodentate pyrrolidinyl-biphenyl phosphine ligands that promote different enantioselective cyclizations of 1,6-enynes giving rise to corresponding products through 5-*exo*-dig or 6-*endo*-dig pathways. Surprisingly, whereas these seemingly related cyclizations of 1,6-enynes proceed with good to excellent enantiomeric ratios, the first one

UNIVERSITAT ROVIRA I VIRGILI
COMPUTATIONAL MECHANISTIC STUDIES IN GOLD(I) CATALYSIS AND DESIGN OF NEW CHIRAL LIGANDS
Immaculada Escofet Miquel

Chapter III

takes place with a facial preference for the *Si* face of the alkene, while the hydroxycyclization give rise to the opposite configuration by reaction through the *Re* prochiral face of the alkene. Computational studies have identified non-covalent attractive π-π interactions in the chiral pocket of the catalys, which are key to achieve good enantioselectivities. As revealed by NCI plots, non-covalent interactions between the stereodirecting components of the substrates and aryl group of the pyrrolidine induce specific binding orientation inside the catalyst cavity (Scheme 47).
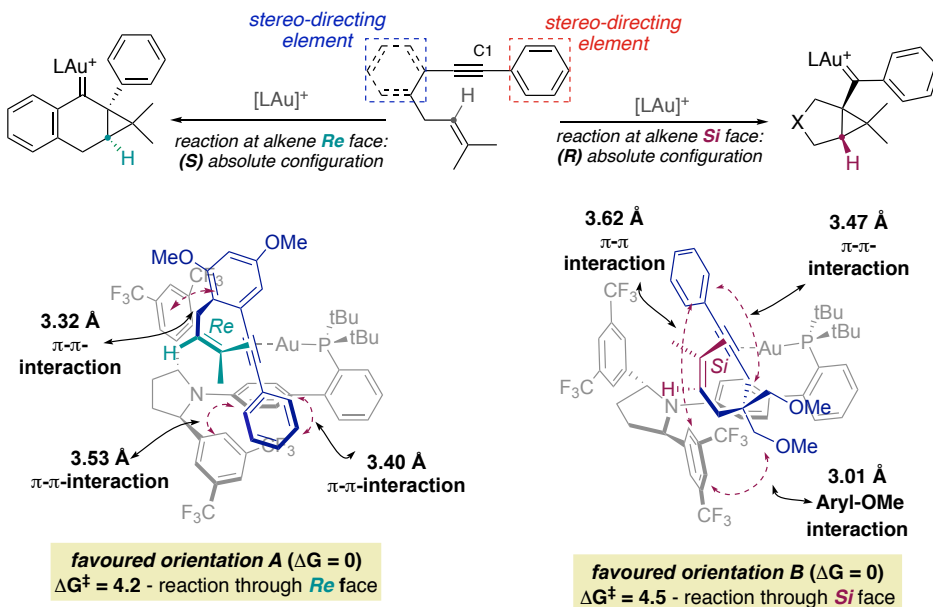
Scheme 47. Mode of enantioinduction for the 5-ex*o*-dig and 6-*endo*-dig cyclizations.

Alkyl-aryl interactions also account to the good enantioselectivities when pyrrolidinyl-biphenyl phosphine ligands bearing cyclohexyl groups at the C_2-chiral pyrrolidine unit.

A 2nd generation of chiral catalysts have been studied in order to determine the role of each component and to predict higher enantioselectivities. These studies set the basis for the rational design of similar modular catalysts with enhanced reactivity and enantioselectivity.

UNIVERSITAT ROVIRA I VIRGILI
COMPUTATIONAL MECHANISTIC STUDIES IN GOLD(I) CATALYSIS AND DESIGN OF NEW CHIRAL LIGANDS
Immaculada Escofet Miquel

Chapter III

Experimental Section

General Methods

The synthesis of gold(I) complexes was carried out under argon using solvents dried by passing through an activated alumina column on a PureSolv™ solvent purification system. The cycloaddition reactions were done using HPLC solvents under air. Thin layer chromatography was carried out using TLC aluminium sheets coated with 0.2 mm of silica gel (Merck GF234) using UV light as the visualizing agent and a solution of vanillin as stain. Reactions were followed using a GCMS apparatus or by TLC. Chromatographic purifications were carried out using flash grade silica gel (SDS Chromatogel 60 ACC, 40-60 µm) or automated flash chromatographer CombiFlash Companion. Preparative TLC was performed on 20 cm × 20 cm silica gel plates (2.0 mm or 1.0 mm thick, Analtech). Commercial grade reagents and solvents were used without further purification. PCl$_3$ was distilled prior to use. [67]

NMR data were recorded in deuterated solvents at 23 ºC on a Bruker Advance 400 Ultra Shield (400 MHz for ^{1}H, 100 MHz for ^{13}C, 162 MHz for ^{31}P and 376 MHz for ^{19}F), Bruker 500 Ultrashield (500 MHz for ^{1}H, 125 MHz for ^{13}C and 202 MHz for ^{31}P) apparatus and Bruker 300 Ultrashield (300 MHz for ^{1}H and 75 MHz for ^{13}C). Chemical shifts (δ) are reported in parts per million (ppm) and referenced to residual solvent or tetramethylsilane. Coupling constants (J) are reported in Hertz (Hz). Mass Spectra were recorded on a Waters LCT Premier Spectrometer (ESI) and Bruker Daltonics Autoflex (MALDI) spectrometers. Specific rotation [α] was determined using a polarimeter Jasco P1030. Elemental analyses were performed on a LECO CHNS 932 micro-analyzer at the Universidad Complutense de Madrid. Melting points were determined using a Büchi melting point apparatus. Single crystal X-ray diffraction data were recorded on a Bruker Kappa APEX II DUO diffractometer equipped with an APPEX 2 4K CCD area detector, a Microsource with Mo$_{ka}$ radiation and an Oxford Cryostream 700 low temperature device (T = −173ºC).

Ligands **L1-L7**, (*R*)-BINOL, (Me$_2$S)AuCl, NaBAr$_4$^{F}, alkynes and alkenes were purchased from commercial sources and used without further purification.

Synthetic Procedures and Analytical Data

BINOL Phosphites 48a-j – General methodology

In a typical procedure,[68] solution of PCl$_3$ (42.7 mg, 374 µmol, 3.0 eq.) in THF (0.5 mL) was added dropwise to a solution of (*R*)-3,3'-bis(triphenylsilyl)-[1,1'-binaphthalene]-2,2'-diol (**3**, 100 mg, 125 µmol, 1.0 eq.) in THF (0.5 mL) at -40 °C. After stirring at -40 °C for 10 min, a solution of NEt$_3$ (63 mg, 623 µmol, 5.0 eq.) was added dropwise. The resulting mixture

67 Amarego, W. L. F.; Chai, C. L. L., *Purification of Laboratory Chemicals* **2003**, 5th edition. Butterworth-Heinemann.

68 (a) Albrow, V. E.; Blake, A. J.; Fryatt, R.; Wilson, C.; Woodward, S. *Eur. J. Org. Chem.* **2006**, *2006*, 2549–2557. (b) Bedford, R. B.; Chang, Y.-N.; Haddow, M. F.; McMullin, C. L. *Dalton Trans.* **2011**, *40*, 9042–9050. (c) Sakakura, A.; Sakuma, M.; Ishihara, K. *Org. Lett.* **2011**, *13*, 3130–3133.

UNIVERSITAT ROVIRA I VIRGILI
COMPUTATIONAL MECHANISTIC STUDIES IN GOLD(I) CATALYSIS AND DESIGN OF NEW CHIRAL LIGANDS
Immaculada Escofet Miquel

Chapter III

was allowed to warm to room temperature and stirred for another 2 h before being filtered through a Celite pad (rinsing with THF). The filtrate was concentrated under reduced pressure and the residue was treated with toluene (1 mL), and evaporated. The obtained solid was redissolved in THF (2 mL) and treated with a solution of NEt₃ (63.0 mg, 623 μmol, 5.0 eq.) in THF (0.5 mL) at RT. A solution of the appropriate phenol or alcohol (249 μmol, 2.0 eq.) in THF (0.5 mL) was added dropwise and the resulting mixture was stirred for 2 h at room temperature. After evaporation of the volatiles under reduced pressure, the residue was purified by column chromatography on silica gel (toluene, Ar) to provide the desired phosphite ligand **48a-j**.

Ligand 48a[68c]
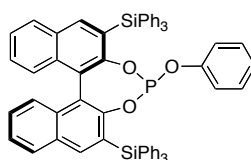
¹H NMR (400 MHz, CDCl₃): δ 8.07 (s, 1H), 7.93 (s, 1H), 7.83 (d, *J*= 8.3 Hz, 1H), 7.77 (d, *J*= 8.3 Hz, 1H), 7.59 (dt, *J*= 6.6, 1.7 Hz, 10 H), 7.54-7.52 (m, 5H), 7.34-7.31 (m, 6H), 7.25-7.21 (m, 10H), 6.82 (dd, *J*= 7.5, 7.1 Hz, 1H), 6.72 (t, *J*=7.8 Hz, 2H), 5.78 (d, *J*= 8.0 Hz, 2H). **¹³C NMR** (126 MHz, CDCl₃) δ 157.46, 137.37, 136.91, 136.89, 136.75, 136.71, 136.66, 136.47, 136.43, 136.25, 134.70, 133.98, 133.02, 129.95, 129.84, 129.55, 129.48, 129.32, 129.18, 128.81, 128.23, 127.93, 127.84, 127.79, 127.75, 127.68, 127.60, 126.99, 125.77, 119.04, 115.69. **³¹P{¹H}-NMR** (162 MHz, CDCl₃): δ 150.5.

Ligand 48b
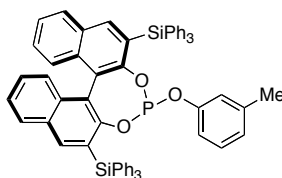
¹H NMR (400 MHz, CDCl₃): δ 8.06 (s, 1H), 7.90 (s, 1H), 7.81 (d, *J* = 8.2 Hz, 1H), 7.74 (d, *J* = 8.1 Hz, 1H), 7.68–7.65 (m, 1H), 7.58 (dd, *J* = 8.0, 1,3 Hz, 6H), 7.54 (dd, *J* = 8.0, 1,3 Hz, 6H), 7.43–7.38 (m, 2H), 7.37–7.28 (m, 10H), 7.24–7.19 (m, 11H), 6.62-6.56 (m, 2H), 5.59 (m, 2H), 1.90 (s, 3H). **¹³C NMR** (126 MHz, CDCl₃) δ 156.61, 139.39, 136.77, 136.57, 136.56, 129.48, 129.31, 129.14, 129.09, 127.84, 127.78, 127.61, 127.57, 120.57, 116.23, 112.54. **³¹P{¹H}-NMR** (162 MHz, CDCl₃): δ 150.8.

UNIVERSITAT ROVIRA I VIRGILI
COMPUTATIONAL MECHANISTIC STUDIES IN GOLD(I) CATALYSIS AND DESIGN OF NEW CHIRAL LIGANDS
Immaculada Escofet Miquel

Chapter III
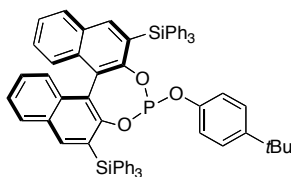
Ligand 48c

¹H NMR (400 MHz, CDCl₃): δ 8.04 (s, 1H), 7.91 (s, 1H), 7.80 (d, J = 8.1 Hz, 1H), 7.75 (d, J = 8.1 Hz, 1H), 7.57 (dd, J = 8.0, 1.3 Hz, 6H), 7.49 (dd, J = 7.9, 1.2 Hz, 6H), 7.42-7.29 (m, 12H), 7.24-7.19 (m, 12H), 6.68 (d, J = 8.7 Hz, 2H), 5.75 (d, J = 8.6 Hz, 2H), 1.21 (s, 9H). **³¹P{¹H}-NMR** (162 MHz, CDCl₃): δ 150.4.
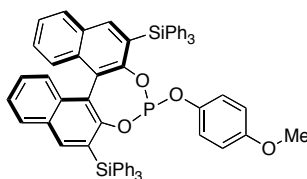
Ligand 48d

¹H NMR (400 MHz, CDCl₃): δ 8.05 (s, 1H), 7.90 (s, 1H), 7.80 (d, J = 8.2 Hz, 1H), 7.75 (d, J = 8.2 Hz, 1H), 7.63–7.68 (m, 1H), 7.58 (dd, J = 8.0, 1,3 Hz, 6H), 7.52 (dd, J = 8.0, 1,3 Hz, 6H), 7.45–7.10 (m, 23H), 6.21 (d, J = 9.1, 2H), 5.68 (d, J = 8.7, 2H), 3.67 (s, 3H). **³¹P{¹H}-NMR** (162 MHz, CDCl₃): δ 150.8.
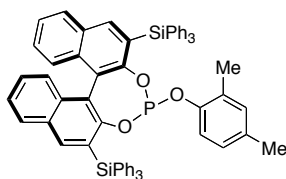
Ligand 48e

¹H NMR (400 MHz, CDCl₃): δ 7.99 (s, 1H), 7.92 (s, 1H), 7.78 (d, J = 8.4 Hz, 1H), 7.75 (d, J = 8.7 Hz, 1H), 7.56 (d, J = 6.7 Hz, 6H), 7.43 (d, J = 6.9 Hz, 6H), 7.39–7.34 (m, 2H), 7.30–7.26 (m, 6H), 7.24-7.12 (m, 16H), 6.58 (s, 1H), 6.31 (d, J = 6.9 Hz, 1H), 5.55 (d, J = 8.1 Hz, 1H), 2.15 (s, 3H), 1.27 (s, 3H). **³¹P{¹H}-NMR** (162 MHz, CDCl₃): δ 149.3.

UNIVERSITAT ROVIRA I VIRGILI
COMPUTATIONAL MECHANISTIC STUDIES IN GOLD(I) CATALYSIS AND DESIGN OF NEW CHIRAL LIGANDS
Immaculada Escofet Miquel

Chapter III
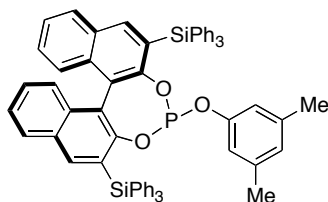
Ligand 48f

¹H NMR (400 MHz, CDCl₃): δ 8.06 (s, 1H), 7.88 (s, 1H), 7.81 (d, J = 8.3 Hz, 1H), 7.73 (d, J = 8.3 Hz, 1H), 7.58 (dd, J = 7.9, 1.1 Hz, 6H), 7.55 (dd, J = 7.9, 1.0 Hz, 6H), 7.42-7.37 (m, 2H), 7.35-7.27 (m, 10H), 7.25-7.19 (m, 12H), 6.44 (s, 1H), 5.42 (s, 2H), 1.85 (s, 6H).
³¹P{¹H}-NMR (162 MHz, CDCl₃): δ 151.3.
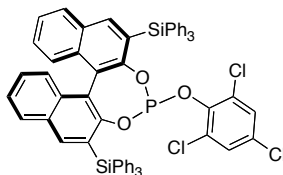
Ligand 48g

¹H NMR (400 MHz, CDCl₃): δ 7.93 (s, 1H), 7.91 (s, 1H), 7.78 (d, J = 2.6 Hz, 1H), 7.76 (d, J = 2.5 Hz, 1H), 7.60–7.58 (m, 6H), 7.48–7.45 (m, 6H), 7.38–7.41 (m, 2H), 7.11–7.32 (m, 22H), 6.83 (s, 2H). **³¹P{¹H}-NMR** (162 MHz, CDCl₃): δ 142.8.
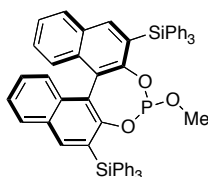
Ligand 48h

¹H NMR (400 MHz, CDCl₃): δ 8.05 (s, 1H), 7.96 (s, 1H), 7.80-7.75 (dd, J = 7.7 Hz, 2H), 7.66–7.63 (m, 1H), 7.62-7.58 (m, 10H), 7.43-7.27 (m, 20H), 7.24-7.14 (m, 5H), 2.37-2.34 (d, J = 10.5Hz, 3H). **³¹P{¹H}-NMR** (162 MHz, CDCl₃): δ 148.7.

UNIVERSITAT ROVIRA I VIRGILI
COMPUTATIONAL MECHANISTIC STUDIES IN GOLD(I) CATALYSIS AND DESIGN OF NEW CHIRAL LIGANDS
Immaculada Escofet Miquel

Chapter III

Ligand 48i
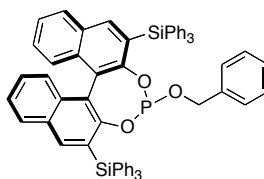
¹H NMR (400 MHz, CDCl₃): δ 8.06 (s, 1H), 7.93 (s, 1H), 7.79 (d, J = 8.2 Hz, 1H), 7.75 (d, J = 8.2 Hz, 1H), 7.65–7.63 (m, 1H), 7.57–7.55 (m, 12H), 7.42–7.32 (m, 10H), 7.31–7.27 (m, 10H), 7.23–7.17 (m, 3H), 7.05 (t, J = 7.4 Hz, 1H), 6.88 (t, J = 7.6 Hz, 2H), 6.50 (d, J = 7.6 Hz, 2H), 3.60 (d, J = 8.5 Hz, 2H). **¹³C NMR** (126 MHz, CDCl₃) δ 140.76, 136.80, 136.73, 136.55, 136.48, 136.44, 136.37, 136.26, 134.67, 134.49, 134.31, 133.84, 130.65, 130.12, 129.95, 129.55, 129.46, 129.43, 128.71, 128.68, 128.35, 128.29, 128.22, 127.98, 127.85, 127.79, 127.66, 127.60, 127.56, 127.26, 126.96, 126.90, 126.79, 126.70, 126.45, 124.71, 124.67. **³¹P{¹H}-NMR** (162 MHz, CDCl₃): δ 151.1.

Ligand 48j
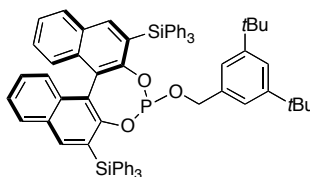
¹H NMR (400 MHz, CDCl₃): δ 8.04 (s, 1H), 7.97 (s, 1H), 7.79 (d, J = 8.2 Hz, 1H), 7.75 (d, J = 8.1 Hz, 1H), 7.65-7.63 (m, 1H), 7.58 (dd, J = 8.0, 1.3 Hz, 6H), 7.51 (dd, J = 7.9, 1.2 Hz, 6H), 7.44-7.27 (m, 14H), 7.24–7.20 (m, 10H), 6.53 (d, J = 1.7 Hz, 2H), 3.87 (dd, J = 12.2, 6.6 Hz, 1H), 3.60 (dd, J = 12.1, 6.6 Hz, 1H), 1.18 (s, 18H). **¹³C NMR** (126 MHz, CDCl₃): δ 150.93, 140.30, 136.75, 136.52, 136.50, 136.46, 136.28, 135.46, 134.70, 134.25, 134.02, 133.06, 129.96, 129.56, 129.54, 129.51, 129.11, 128.24, 127.94, 127.83, 127.81, 127.61, 127.59, 127.56, 127.13, 125.47, 123.86, 122.74, 122.34, 121.55, 121.33, 100.02, 100.00, 65.75, 34.85, 31.49, 31.42, 30.34. **³¹P{¹H}-NMR** (162 MHz, CDCl₃): δ 147.2.

Synthesis of Chiral Au(I) Complexes

In a typical experiment, a solution of the desired ligand (46.3 µmol, 1.0 eq.) in CH₂Cl₂ (0.5 mL) was added dropwise to a suspension of (Me)₂SAuCl (46.3 µmol, 1.0 eq.) in CH₂Cl₂ (0.5 mL) at 0 °C. The resulting clear solution was allowed to warm to room temperature and stirred for another 30 min. The solvent was removed to give the corresponding chiral Au(I) chloride phosphite complex as a white solid (46.3 µmol, quantitative).

UNIVERSITAT ROVIRA I VIRGILI
COMPUTATIONAL MECHANISTIC STUDIES IN GOLD(I) CATALYSIS AND DESIGN OF NEW CHIRAL LIGANDS
Immaculada Escofet Miquel

Chapter III

Complex 48(AuCl)a
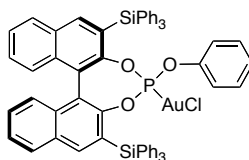
¹H NMR (400 MHz, CDCl₃): δ 8.18 (s, 1H), 8.08 (s, 1H), 7.89 (d, J = 8.3 Hz, 1H), 7.83 (d, J = 8.3 Hz, 1H), 7.59-7.56 (m, 6H), 7.51-7.48 (m, 6H), 7.39-7.30 (m, 12H), 7.26-7.22 (m, 12H), 7.03 (t, J = 7.7 Hz, 1H), 6.90 (t, J = 7.7 Hz, 2H), 6.05 (d, J = 8.2 Hz, 2H). **¹³C NMR** (101 MHz, CDCl₃): δ 156.47, 137.12, 137.03, 136.92, 136.86, 136.82, 136.78, 136.58, 136.55, 136.52, 136.40, 134.64, 134.49, 129.70, 129.67, 129.63, 129.56, 128.37, 128.16, 128.06, 128.00, 127.91, 127.88, 127.81, 127.75, 120.12, 115.58. **³¹P{¹H}-NMR** (162 MHz, CDCl₃): δ 123.7. **HRMS-ESI** m/z calculated for $C_{62}H_{45}AuClO_3PSi_2^+$ [M⁺ -Cl]: 1120.7502 found 1120.7510.

Complex 48(AuCl)b
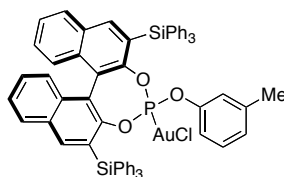
¹H NMR (400 MHz, CDCl₃): δ 8.16 (s, 1H), 8.08 (s, 1H), 7.87 (d, J = 8.0 Hz, 1H), 7.82 (d, J = 8.2 Hz, 1H), 7.68–7.65 (m, 1H), 7.56 (dd, J = 8.0, 1.4 Hz, 6H), 7.51 (dd, J = 8.0, 1.2 Hz, 6H), 7.48–7.27 (m, 16H), 7.25–7.21 (m, 7H), 6.82 (d, J = 7.4 Hz, 1H), 6.77 (t, J = 7.8 Hz, 1H), 5.87 (d, J = 7.8 Hz, 1H), 5.83 (s, 1H), 1.99 (s, 3H). **¹³C NMR** (101 MHz, CDCl₃): δ 156.45, 139.57, 137.10, 136.90, 136.84, 136.80, 136.75, 136.58, 136.54, 136.51, 136.39, 135.29, 134.39, 133.48, 133.25, 130.05, 130.01, 129.91, 129.42, 129.29, 128.33, 128.16, 128.08, 128.05, 127.91, 127.88, 127.79, 120.91, 116.28, 112.57, 21.47. **³¹P{¹H}-NMR** (162 MHz, CDCl₃): δ 123.1. **HRMS-ESI** m/z calculated for $C_{63}H_{47}AuClO_3PSi_2^+$ [M⁺ -Cl]: 1134.7780 found 1134.7764.

Complex 48(AuCl)c
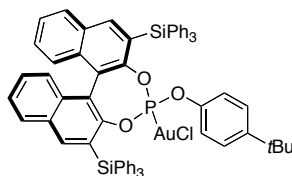
¹H NMR (400 MHz, CDCl₃): δ 8.16 (s, 1H), 8.09 (s, 1H), 7.87 (d, J = 8.0 Hz, 1H), 7.82 (d, J = 8.2 Hz, 1H), 7.59-7.54 (m, 6H), 7.53-7.44 (m, 8H), 7.40–7.26 (m, 15H), 7.24-7.19 (m,

UNIVERSITAT ROVIRA I VIRGILI
COMPUTATIONAL MECHANISTIC STUDIES IN GOLD(I) CATALYSIS AND DESIGN OF NEW CHIRAL LIGANDS
Immaculada Escofet Miquel

Chapter III

7H), 6.88 (d, J = 8.7 Hz, 2H), 6.03 (d, J = 8.5 Hz, 2H), 1.27 (s, 9H). **^{13}C NMR** (126 MHz, CDCl$_3$) ? 136.81, 136.60, 133.58, 133.32, 130.09, 130.05, 128.38, 128.21, 127.97, 126.21, 120.60, 120.56, 34.49, 31.52, 29.86. ^{31}P{^{1}H}-NMR (162 MHz, CDCl$_3$): δ 123.8. **HRMS-ESI** m/z calculated for C$_{63}$H$_{47}$AuClO$_3$PSi$_2^+$ [M$^+$ -Cl]: 1177.2931 found 1177.2927.

Complex 48(AuCl)d
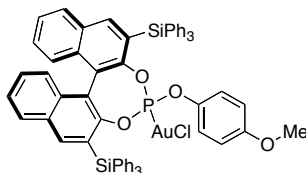
^{1}H NMR (400 MHz, CDCl$_3$): δ 8.17 (s, 1H), 8.07 (s, 1H), 7.87 (d, J = 7.9 Hz, 1H), 7.81 (d, J = 8.1 Hz, 1H), 7.68-7.65 (m, 1H), 7.59-7.57 (m, 6H), 7.51-7.49 (m, 6H), 7.39-7.15 (m, 23H), 6.37 (d, J = 9.1 Hz, 2H), 5.93 (dd, J = 9.0, 1.4 Hz, 2H), 3.73 (s, 3H). **^{13}C NMR** (75 MHz, CDCl$_3$): δ 156.95, 156.92, 151.21, 151.03, 149.83, 142.28, 142.11, 142.05, 141.96, 136.70, 136.61, 136.46, 136.38, 136.08, 134.65, 134.35, 134.08, 133.44, 133.16, 131.29, 130.93, 130.02, 129.98, 129.06, 128.98, 128.90, 128.30, 128.25, 128.11, 127.90, 127.81, 127.75, 126.92, 126.69, 126.25, 126.15, 125.95, 125.86, 125.32, 122.44, 122.40, 122.01, 121.97, 121.82, 121.75, 114.18, 55.61. **^{31}P{^{1}H}-NMR** (162 MHz, CDCl$_3$): δ 124.2. **HRMS-ESI** m/z calculated for C$_{63}$H$_{47}$AuClO$_4$PSi$_2^+$ [M$^+$ -Cl]: 1151.2411 found 1151.2402.

Complex 48(AuCl)e
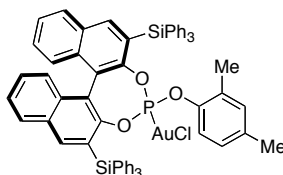
^{1}H NMR (400 MHz, CDCl$_3$): δ 8.15 (s, 1H), 8.09 (s, 1H), 7.87 (d, J = 8.2 Hz, 1H), 7.82 (d, J = 8.1 Hz, 1H), 7.59-7.42 (m, 14H), 7.40-7.20 (m, 16H), 7.19–7.13 (m, 6H), 6.70 (bs, 1H), 6.48 (dd, J = 8.6, 1.9 Hz, 1H), 6.00 (d, J = 8.2 Hz, 1H), 2.23 (s, 3H), 1.37 (s, 3H). **^{13}C NMR** (126 MHz, CDCl$_3$): δ 151.25, 151.15, 149.98, 145.48, 145.42, 142.27, 141.97, 136.70, 136.55, 134.85, 134.41, 134.10, 133.48, 133.25, 131.71, 131.38, 131.00, 130.00, 129.92, 129.24, 129.21, 129.10, 129.05, 128.28, 128.10, 128.01, 127.98, 127.03, 126.72, 126.59, 126.24, 126.21, 126.18, 126.04, 122.72, 122.69, 122.21, 122.19, 120.72, 120.68, 29.85, 20.80, 16.20. **^{31}P{^{1}H}-NMR** (162 MHz, CDCl$_3$): δ 123.2. **HRMS-ESI** m/z calculated for C$_{64}$H$_{49}$AuClO3PSi$_2^+$ [M$^+$ -Cl]: 1149.2618 found 1149.2652.

UNIVERSITAT ROVIRA I VIRGILI
COMPUTATIONAL MECHANISTIC STUDIES IN GOLD(I) CATALYSIS AND DESIGN OF NEW CHIRAL LIGANDS
Immaculada Escofet Miquel

Chapter III

Complex 48(AuCl)f
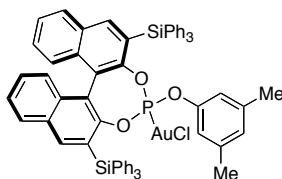
¹H NMR (400 MHz, CDCl₃): δ 8.14 (s, 1H), 8.07 (s, 1H), 7.87 (d, J = 8.2 Hz, 1H), 7.82 (d, J = 8.2 Hz, 1H), 7.58-7.45 (m, 14H), 7.40-7.19 (m, 22H), 6.63 (bs, 1H), 5.68 (bs, 2H), 1.94 (s, 6H). **¹³C NMR** (126 MHz, CDCl₃): δ 151.41, 148.82, 148.77, 142.39, 142.04, 139.06, 136.82, 136.68, 134.43, 134.22, 133.53, 133.34, 131.40, 131.04, 130.06, 130.01, 129.06, 128.35, 128.20, 128.05, 128.01, 127.18, 126.97, 126.79, 126.39, 126.25, 126.07, 118.55, 118.51, 29.85, 21.02. **³¹P{¹H}-NMR** (162 MHz, CDCl₃): δ 122.6. **HRMS-ESI** m/z calculated for $C_{64}H_{49}AuClO3PSi_2^+$ [M⁺ -Cl]: 1149.2618 found 1149.2611.

Complex 48(AuCl)g
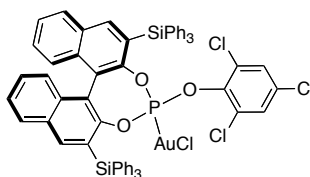
¹H NMR (400 MHz, CDCl₃): δ 8.18 (s, 1H), 8.03 (s, 1H), 7.88 (d, J = 8.1 Hz, 1H), 7.81 (d, J = 8.3 Hz, 1H), 7.64 (dd, J = 7.9, 1.4 Hz, 6H), 7.53-7.47 (m, 2H), 7.45 (dd, J = 8.0, 1.2 Hz, 6H), 7.39-7.14 (m, 22H), 6.89 (s, 2H). **¹³C NMR** (126 MHz, CDCl₃): δ 151.48, 151.37, 149.41, 149.35, 147.06, 142.51, 142.07, 140.68, 140.59, 136.75, 136.33, 134.54, 134.35, 134.34, 133.29, 133.12, 131.48, 131.08, 131.02, 131.01, 129.94, 129.91, 129.16, 129.08, 128.99, 128.66, 128.53, 128.50, 128.36, 128.22, 128.16, 128.07, 128.04, 127.10, 126.70, 126.45, 126.15, 125.82, 125.79, 125.45, 122.69, 122.66, 122.55, 122.52, 121.75. **³¹P{¹H}-NMR** (162 MHz, CDCl₃): δ 124.1. **HRMS-ESI** m/z calculated for $C_{62}H_{42}AuCl_3O_3PSi_2^+$ [M⁺-Cl]: 1223.1136 found 1226.1160.

Complex 48(AuCl)h
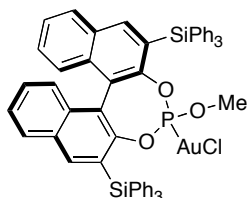
¹H NMR (400 MHz, CDCl₃): δ 8.14 (s, 1H), 8.13 (s, 1H), 7.84 (s, 1H), 7.82 (s, 1H), 7.64-7.59 (m, 12H), 7.49-7.33 (m, 24H), 2.53 (d, J = 15.6 Hz, 3H). **¹³C NMR** (75 MHz, CDCl₃)

UNIVERSITAT ROVIRA I VIRGILI
COMPUTATIONAL MECHANISTIC STUDIES IN GOLD(I) CATALYSIS AND DESIGN OF NEW CHIRAL LIGANDS
Immaculada Escofet Miquel

Chapter III

δ 150.95, 150.78, 149.56, 149.48, 142.22, 141.86, 137.05, 136.68, 136.33, 134.28, 134.07, 133.95, 133.86, 133.42, 131.22, 130.83, 130.12, 129.90, 129.56, 129.06, 128.92, 128.25, 128.16, 127.92, 127.85, 126.84, 126.75, 126.13, 126.08, 125.91, 125.80, 125.33, 122.94, 122.89, 121.85, 121.82, 67.15. **^{31}P{^{1}H}-NMR** (162 MHz, CDCl$_3$): δ 130.5. **HRMS-ESI** m/z calculated for C$_{57}$H$_{43}$AuClO$_3$PSi$_2^+$ [M$^+$-Cl]: 1059.2148 found 1059.2140.

Complex 48(AuCl)i
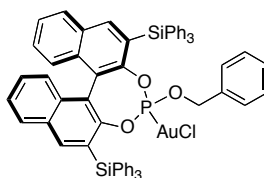
^{1}H NMR (400 MHz, CDCl$_3$): δ 8.13 (d, J = 5.8 Hz, 2H), 7.86 (d, J = 7.7 Hz, 1H), 7.84 (d, J = 7.7 Hz, 1H), 7.66-7.63 (m, 1H), 7.60 (dd, J = 8.0, 1.3 Hz, 6H), 7.49 (dd, J = 8.0, 1.3 Hz, 8H), 7.41-7.32 (m, 10H), 7.29 (dd, J = 7.6, 2.4 Hz, 10H), 7.25-7.18 (m, 2H), 7.14 (t, J = 7.5 Hz, 2H), 6.68 (d, J = 7.2 Hz, 2H), 3.94 (dd, J = 11.8, 9.0 Hz, 1H), 3.70 (dd, J = 11.9, 7.5 Hz, 1H). **^{13}C NMR** (126 MHz, CDCl$_3$): δ 140.76, 136.80, 136.73, 136.55, 136.48, 136.44, 136.37, 136.26, 134.67, 134.49, 134.31, 133.84, 130.65, 130.12, 129.95, 129.55, 129.46, 129.43, 128.71, 128.68, 128.35, 128.29, 128.22, 127.98, 127.85, 127.79, 127.66, 127.60, 127.56, 127.26, 126.96, 126.90, 126.79, 126.70, 126.45, 124.71, 124.67, 99.99, 67.94, 67.26, 65.23, 65.12, 64.82, 45.86. **^{31}P{^{1}H}-NMR** (162 MHz, CDCl$_3$): δ 126.8. **HRMS-ESI** m/z calculated for C$_{63}$H$_{47}$AuClO$_3$PSi$_2^+$ [M$^+$-Cl]: 1134.7673 found 1134.7670.

Complex 48(AuCl)j
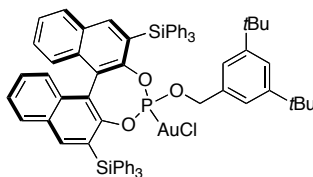
^{1}H NMR (400 MHz, CDCl$_3$): δ 8.13 (d, J = 6.2 Hz, 2H), 7.84 (d, J = 8.4 Hz, 2H), 7.67-7.64 (m, 1H), 7.59 (dd, J = 8.0, 1.3 Hz, 6H), 7.48 (dd, J = 8.0, 1.3 Hz, 6H), 7.52-7.45 (m, 2H), 7.39-7.31 (m, 11H), 7.30-7.26 (m, 5H), 7.25-7.18 (m, 6H), 6.61 (d, J = 1.8 Hz, 2H), 3.93 (dd, J = 11.3, 8.4 Hz, 1H), 3.78 (dd, J = 11.4, 6.9 Hz, 1H), 1.20 (s, 18H). **^{13}C NMR** (75 MHz, CDCl$_3$): δ 152.97, 151.22, 149.85, 149.75, 148.89, 148.81, 142.21, 141.98, 136.62, 136.54, 134.28, 134.07, 133.37, 133.16, 131.28, 130.95, 129.94, 129.87, 128.96, 128.87, 128.21, 128.02, 127.89, 126.93, 126.73, 126.28, 126.15, 126.11, 126.07, 125.94, 122.64, 122.44, 122.09, 122.04, 117.92, 34.64, 31.08, 29.73. **^{31}P{^{1}H}-NMR** (162 MHz, CDCl$_3$): δ 125.6. **HRMS-ESI** m/z calculated for C$_{71}$H$_{63}$AuClO$_3$PSi$_2^+$ [M$^+$-Cl]: 1224.6273 found 1224.6271.

UNIVERSITAT ROVIRA I VIRGILI
COMPUTATIONAL MECHANISTIC STUDIES IN GOLD(I) CATALYSIS AND DESIGN OF NEW CHIRAL LIGANDS
Immaculada Escofet Miquel

Chapter III

*General procedure for the synthesis of enynes **8a-e***

Pd(PPh₃)₂Cl₂ (1 mol %) and copper(I) iodide (2 mol %) were sequentially added to a stirred solution of the terminal alkyne (1.0 equiv) in NEt₃ (0.25 M) under argon at 24 ºC and the mixture was stirred for 10 min. Then, iodoarene (1.2 equiv) was added and the mixture was stirred for the corresponding time. The reaction was quenched with sat. NH₄Cl and extracted with EtOAc (3x). The combined organic phases were washed with brine, dried over Na₂SO₄, and concentrated. The residue was purified by flash column chromatography to yield the desired Sonogashira coupling products.

2-(3-Methyl-but-2-enyl)-2-(3-*o*-tolyl-prop-2-ynyl)-malonic acid dimethyl ester (8e)
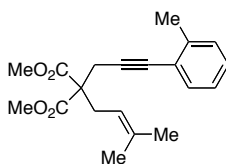
Enyne **8e** prepared in 72 % yield by using 2-methyl-iodobenzene according to the reported procedure.

¹H NMR (400 MHz, CDCl₃): δ 7.33 (d, J = 7.5 Hz, 1H), 7.20-7.06 (m, 3H), 4.97 (t, J = 7.7 Hz, 1H), 3.75 (s, 6H), 3.05 (s, 2H), 2.85 (d, J = 7.7 Hz, 2H), 2.37 (s, 3H), 1.72 (s, 3H), 1.66 (s, 3H). **¹³C-NMR** (101 MHz, CDCl₃): δ 171.3 (CO), 140.7 (C), 137.5 (C), 132.7 (CH), 130.0 (CH), 128.6 (CH), 126.1 (CH), 123.7 (C), 117.8 (CH), 89.2 (C), 82.8 (C), 58.2 (C), 53.3 (CH₃), 31.6 (CH₂), 26.8 (CH₂), 24.3 (CH₃), 21.4 (CH₃), 18.7 (CH₃).

Enantioselective Gold-Catalyzed [4+2] Cycloaddition

In a typical experiment, chiral gold(I) complex **48(AuCl)c** (5mol%) and AgNTf₂ (5 mol%) were weighed in a glove box. CH₂Cl₂ (0.008 M) was added and the resulting solution was stirred for 10 min at 0 °C and further 10 min at room temperature. The obtained catalyst solution was cooled to the indicated temperature followed by dropwise addition of a solution of the desired enyne **8a-e** (1.0 equiv) in CH₂Cl₂ (0.2 M) over 10 min. After complete addition, stirring was continued at the indicated temperature until the starting material was consumed. After quenching with a solution of NEt₃ in hexane (0.1 M, 1 mL), the solids were removed by filtration over silica. Evaporation of the solvent and chromatographic purification on silica (hexanes/EtOAc) provided the title compound. Enantiomeric excess was determined by chiral HPLC.

UNIVERSITAT ROVIRA I VIRGILI
COMPUTATIONAL MECHANISTIC STUDIES IN GOLD(I) CATALYSIS AND DESIGN OF NEW CHIRAL LIGANDS
Immaculada Escofet Miquel

Chapter III

Dimethyl 4,4-Dimethyl-3a,4-dihydro-1*H*-cyclopenta[*b*]naphthalene 2,2(3*H*) dicarboxylate (9a)
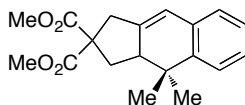
9a was synthesized from **8a** according to the general procedure after stirring at -20 ºC for 18 h (126 mg, 98% yield). Analytical data are in agreement with those reported.[36] $[\alpha]_D^{25} =$ -25.0 ± 2.0 (c = 0.1065, CHCl$_3$). Enantiomeric excess: 88% *ee* (Chiralpak IA 250x4.6mm, 5μm, HEX / IPA 98:2, 1 mL/min).

Dimethyl 6-Methoxy-4,4-dimethyl-3a,4-dihydro-1*H*-cyclopenta[*b*]naphthalene 2,2(3H)-dicarboxylate (9b)
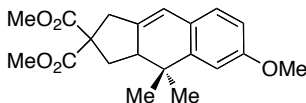
9b was synthesized from **8b** according to the general procedure after stirring at -20 ºC for 30 h (120 mg, 85.5% yield). Analytical data are in agreement with those reported.[36] Enantiomeric excess: 86% *ee* (Chiralpak IC 250x4.6mm, 5μm, Hex / THF 98:2, 1 mL/min).

Dimethyl-4,4,6-trimethyl-3a,4-dihydro-1*H*-cyclopenta[*b*]naphthalene-2,2(3H)-dicarboxylate (9c)
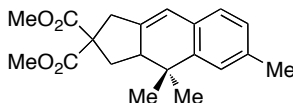
9c was synthesized from **1c** according to the general procedure after stirring at -20 ºC for 15 h (134 mg, 98% yield). Analytical data are in agreement with those reported.[36] Enantiomeric excess: 87% *ee* (Chiralpak IC 250x4.6mm, 5μm, Hex / IPA 99:1, 1 mL/min).

Dimethyl-4,4,8-trimethyl-3a,4-dihydro-1*H*-cyclopenta[*b*]naphthalene-2,2(3H)-dicarboxylate (9d)
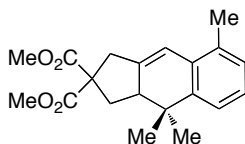
9d was synthesized from **9e** according to the general procedure after stirring at -20 ºC for 30 h (93 mg, 70% yield).

UNIVERSITAT ROVIRA I VIRGILI
COMPUTATIONAL MECHANISTIC STUDIES IN GOLD(I) CATALYSIS AND DESIGN OF NEW CHIRAL LIGANDS
Immaculada Escofet Miquel

Chapter III

¹H NMR (400 MHz, CDCl₃): δ 7.15 (d, J = 7.6 Hz, 1H), 7.06 (t, J = 7.6 Hz, 1H), 6.98 (d, J = 7.4 Hz, 1H), 6.57-6.54 (m, 1H), 3.77 (s, 3H), 3.72 (s, 3H), 3.32 (d, J = 19.2 Hz, 1H), 3.01 (dt, J = 17.9, 3 Hz, 1H), 2.70-2.55 (m, 2H), 2.32 (s, 3H), 2.14 (t, J = 12 Hz, 1H), 1.40 (s, 3H), 0.91 (s, 3H). **¹³C NMR** (100 MHz, CDCl₃) δ 172.3, 172.1, 144.3, 143.1, 133.2, 132.3, 128.3, 126.6, 121.4, 116.2, 59.1, 53.0, 47.9, 39.8, 37.0, 35.0, 26.1, 21.8, 19.8; **HR-APCI-MS** m/z = 351.1 [M+Na]⁺, calc. for $C_{20}H_{24}O_4$ = 328.17.

Enantiomeric excess: 79% *ee* (Chiralpak IC 250x4.6mm, 5μm, Hex / IPA 99:1, 1 mL/min)

Dimethyl 4,4-Dimethyl-6-nitro-3a,4-dihydro-1*H*-cyclopenta[*b*]naphthalene-2,2(3H)-dicarboxylate (9e)
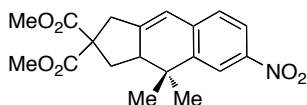
9e was synthesized from **8e** according to the general procedure after stirring at 0 ºC for 15 h (118 mg, 80% yield). Analytical data are in agreement with those reported.[36]

 Enantiomeric excess: 73% *ee* (Chiralpak IB 250x4.6mm, 5μm, HEX / IPA 96:4, 1 mL/min).

General procedure for the synthesis of Josiphos gold(I) chloride complexes

(Me₂S)AuCl was added to a solution of the corresponding phosphine in dry CH₂Cl₂ (0.09 M) under argon at 25 ºC. The solution was left stirring for 1 h and then concentrated under vacuum. The crude product was purified by precipitation adding pentane or Et₂O to a CH₂Cl₂ solution of the crude product or by flash column chromatography on silica gel.

Complex 49-(*S*,*R*ₚ)-A
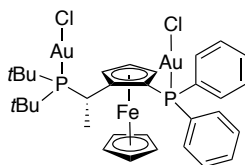
The digold chloride complex was synthesized according to the general procedure from (*S*,*R*ₚ)-Josiphos5 (50 mg, 0.09 mmol) and (Me₂S)AuCl (55 mg, 0.19 mmol). An orange solid was obtained in 72% yield (65 mg, 0.65 mmol) after recrystallization from a solution of CH₂Cl₂ with pentane.

mp 245-247 °C **[α]ᴅ** = −58.2° (*c* = 0.32, 25 ºC), **¹H NMR** (400 MHz, CDCl₃) δ 7.88 – 7.78 (m, 2H), 7.77 – 7.67 (m, 2H), 7.60 – 7.45 (m, 5H), 7.45 – 7.39 (m, 1H), 4.82 (bs, 1H), 4.66 (bs, 1H), 4.38 – 4.21 (m, 1H), 4.16 (bs, 1H), 4.13 (s, 5H), 2.14 (dd, J (¹H-³¹P) = 10.9, J = (¹H-¹H) 7.6 Hz, 3H), 1.53 (d, J (¹H-³¹P) = 14.7 Hz, 9H), 0.99 (d, J (¹H-³¹P) = 14.7 Hz, 9H). **¹³C NMR** (100 MHz, CDCl₃) δ 135.4 (d, J (¹³C-³¹P) = 14.7 Hz), 133.8 (d, J (¹³C-³¹P) = 13.9

UNIVERSITAT ROVIRA I VIRGILI
COMPUTATIONAL MECHANISTIC STUDIES IN GOLD(I) CATALYSIS AND DESIGN OF NEW CHIRAL LIGANDS
Immaculada Escofet Miquel

Chapter III

Hz), 132.4 (d, J (^{13}C-^{31}P) = 2.6 Hz), 131.9 (d, J (^{13}C-^{31}P) = 2.7 Hz), 130.4 (d, J (^{13}C-^{31}P) = 56.8 Hz), 130.0 (d, J (^{13}C-^{31}P) = 12.1 Hz), 129.4 (d, J (^{13}C-^{31}P) = 56.7), 129.0 (d, J (^{13}C-^{31}P) = 12.2 Hz), 102.1 (dd, J (^{13}C-^{31}P) = 16.6, 9.3 Hz), 73.9 (dd, J (^{13}C-^{31}P) = 6.7, 6.6 Hz), 72.5 (d, J (^{13}C-^{31}P) = 5.9 Hz), 72.0 (d, J (^{13}C-^{31}P) = 8.1 Hz), 71.0, 65.4 (dd, J (^{13}C-^{31}P) = 73.1, 2.5 Hz), 38.6 (d, J (^{13}C-^{31}P) = 18.1 Hz), 37.9 (d, J (^{13}C-^{31}P) = 23.5 Hz), 32.0 (d, J (^{13}C-^{31}P) = 5.1 Hz), 31.3 (dd, J (^{13}C-^{31}P) = 20.2, 4.9 Hz), 29.5 (d, J (^{13}C-^{31}P) = 4.7 Hz), 24.1 (d, J (^{13}C-^{31}P) = 3.1 Hz). **^{31}P NMR** (162 MHz, CDCl$_3$) δ 90.00, 23.89. **HRMS** (MALDI) calculated for C$_{32}$H$_{40}$Au$_2$^{35}Cl$_2$^{56}FeP$_2$ (M$^+$): 1006.0663; found: 1006.0647. **Elemental Analysis** calculated for C$_{32}$H$_{40}$Au$_2$Cl$_2$FeP$_2$: C, 38.16; H, 4.00; found: C, 38.06; H, 3.85.

Complex 49-(*S*,*R*$_P$)-B
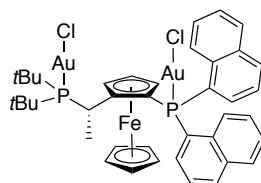
The digold chloride complex was synthesized according to the general procedure from (*S*,*R*$_P$)-Josiphos12 (200 mg, 0.31 mmol) and (Me$_2$S)AuCl (201 mg, 0.68 mmol, 2.2 equiv). The resulting solution was filtered through a Teflon disk, concentrated and layered with pentane. It was allowed to stand in the fridge for 12 h. An orange solid was separated by decantation and washed with pentane (5 mL × 3). The orange solid was purified by flash column chromatography on silica gel (4:1 cyclohexane-ethyl acetate) and the product was obtained in 78% yield (269 mg, 0.25 mmol). X-ray quality crystals were obtained layering a solution of the mixture of complexes (*S*,*R*$_P$)-**B** and in (*S*,*R*$_P$)-**O** CH$_2$Cl$_2$ with hexane. NMR data for a mixture of conformers C1 and C2 in a ratio 70:30 (C1:C2) at 253K.

mp 228-229 °C. **[α]$_D$** = + 83.9° (*c* = 0.09, CHCl$_3$, 25 °C). **^{1}H NMR** (500 MHz, CD$_2$Cl$_2$, 253 K) δ 10.50 (C2, d, J = 8.6 Hz, 0.3H), 9.59 (C1, dd, J = 22.1, 7.2 Hz, 0.7H), 8.40 – 8.02 (C1 + C2, m, 4H), 8.02 – 7.70 (C1 + C2, m, 5H), 7.54 – 7.38 (C1 + C2, m, 2H), 7.35 (C1, ddd, J = 8.4, 6.9, 1.3 Hz, 1.4H), 7.19 (C2, t, J = 7.8 Hz, 0.6H), 5.12 (C2, bs, 0.3H), 5.02 (C1, bs, 0.7H), 4.72 (C2, bs, 0.3H), 4.67 (C1, bs, 0.7H), 4.62 – 4.52 (C1, m, 0.7H), 4.51 – 4.43 (C2, m, 0.3H), 4.40 (C1, bs, 0.7H), 4.03 (C1, s, 3H), 3.98 (C2, bs, 0.3H), 3.91 (C2, s, 2H), 2.23 (C1 + C2, dd, J = 11.0, 7.7 Hz, 3H), 1.62 (C1 + C2, d, J = 14.9 Hz, 9H), 1.00 (C1 +C2, m, 9H). **^{13}C NMR** (125 MHz, CD$_2$Cl$_2$, 253 K) δ 141.0 (C1 + C2), 140.7 (C1 +C2), 136.5 (C1 + C2), 135.4 (C1 +C2), 135.0 (C1 +C2), 134.8 – 134.4 (C1 +C2, m), 134.4 – 134.1 (C1 +C2, m), 133.9 – 133.8 (C2, m), 133.8 – 133.3 (C1, m), 133.2 (C1), 132.9 (C2), 132.3 (C1, d, J (^{13}C-^{31}P) = 12.7 Hz), 131.8 – 131.7 (C2, m), 129.9 (C1 + C2), 129.4 (C1 + C2), 128.1 – 127.8 (C1 + C2, m), 127.5 – 127.2 (C1 + C2, m), 127.0 (C2, d, J (^{13}C-^{31}P) = 12.0 Hz), 126.8 (C1, d, J (^{13}C-^{31}P) = 13.7 Hz), 126.2 (C2), 126.1 (C1), 125.6 – 125.5 (C1 + C2, m), 125.5 – 125.3 (C1 + C2, m), 125.3 – 125.1 (C1 +C2, m), 124.8 – 124.5 (C1 +C2, m), 104.11 – 101.72 (C1, m), 102.3 – 102.0 (C2, m), 76.6 – 76.1 (C2, m), 75.0 – 74.5 (C1, m), 72.6 – 72.1 (C1 + C2, m), 72.0 (C1, d, J = 8.1 Hz), 71.6 (C2, d, J (^{13}C-^{31}P) = 6.4 Hz), 71.3 (C1), 71.0 (C2), 66.9 (C2, d, J (^{13}C-^{31}P) = 80.27 Hz), 66.1 (C1, d, J (^{13}C-^{31}P) = 74.4 Hz), 38.9 –

UNIVERSITAT ROVIRA I VIRGILI
COMPUTATIONAL MECHANISTIC STUDIES IN GOLD(I) CATALYSIS AND DESIGN OF NEW CHIRAL LIGANDS
Immaculada Escofet Miquel

Chapter III

37.8 (2C, C1 +C2, m), 32.0 (C1 +C2), 31.4 – 31.1 (C1, m), 31.0 – 30.9 (C2, m), 30.0 (C2), 29.6 (C1), 25.8 – 25.4 (C1 + C2, m). **^{31}P NMR** (202 MHz, CDCl$_3$, 253 K,) δ 89.42 (C2), 88.82 (C1), 23.26 (C1), −5.39 (C2). **HRMS** (ESI+) calculated for C$_{38}$H$_{52}$Au$_2$Cl$_2$O$_2$FeP$_2$Na (M+Na)$^+$: 1145.1393; found: 1145.1365. **Elemental analysis** Anal. Calc. for C$_{40}$H$_{44}$Au$_2$Cl$_2$FeP$_2$, C, 43.38; H, 4.00; found: C, 43.59; H, 4.19.

Complex 49-(*R,S*$_P$)-C
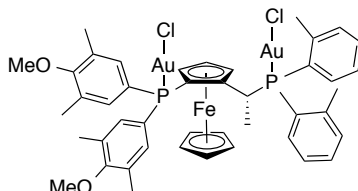
The digold chloride complex was synthetized according to the general procedure from (*R,S*$_P$)-Josiphos13 (90 mg, 0.12 mmol) and (Me$_2$S)AuCl (73.2 mg, 0.25 mmol). The desired complex was obtained as an orange solid in 89% yield (132 mg, 0.11 mmol) after flash column chromatography on silica gel (1:4 cyclohexane-CH$_2$Cl$_2$).

mp > 200 ºC. **[α]$_D$** = −102.4° (*c* = 0.10, CHCl$_3$, 25 ºC). **^{1}H NMR** (400 MHz, CDCl$_3$) δ 7.85-7.79 (m, 1H), 7.51 (dd, *J* (^{1}H-^{31}P) = 14.5, *J* (^{1}H-^{1}H) 7.7 Hz, 1H), 7.47-7.42 (m, 1H), 7.40-7.33 (m, 3H), 7.14-7.09 (m, 1H), 6.99-6.93 (m, 1H), 6.89 (d, *J* (^{1}H-^{31}P) = 13.4 Hz, 2H), 6.81 (t, *J* (^{1}H-^{1}H) = 7.8 Hz, 1H), 6.53 (dt, *J* (^{1}H-^{31}P) = 7.9, *J* (^{1}H-^{1}H) = 2.8 Hz, 1H), 5.31-5.28 (m, 2H), 4.60 (bs, 1H), 4.18 (bs, 1H), 4.03 (bs, 5H), 3.72 (s, 3H), 3.70 (s, 3H), 2.29 (s, 6H), 2.20 (s, 3H), 2.16 (s, 6H), 2.05 (dd, *J* (^{1}H-^{31}P) = 19.5, *J* (^{1}H-^{1}H) = 6.9 Hz, 3H), 1.85 (s, 3H). **^{13}C NMR** (100 MHz, CDCl$_3$) δ 160.2 (d, *J* (^{13}C-^{31}P) = 2.7 Hz), 159.9 (d, *J* (^{13}C-^{31}P) = 2.8 Hz), 141.8 (d, *J* (^{13}C-^{31}P) = 8.5 Hz), 141.6 (d, *J* (^{13}C-^{31}P) = 10.9 Hz), 136.4 (d, *J* (^{13}C-^{31}P) = 14.4 Hz), 135.1 (d, *J* (^{13}C-^{31}P) = 15.8 Hz), 133.4 (d, *J* (^{13}C-^{31}P) = 14.9 Hz), 132.9 (m), 132.2 (d, *J* (^{13}C-^{31}P) = 8.6 Hz), 132.0, 131.8 (m), 131.7, 131.6 (d, *J* (^{13}C-^{31}P) = 2.3 Hz), 131.2 (d, *J* (^{13}C-^{31}P) = 2.6 Hz), 127.1 (d, *J* (^{13}C-^{31}P) = 38.4 Hz), 127.0 (d, *J* (^{13}C-^{31}P) = 9.5 Hz), 126.6 (d, *J* (^{13}C-^{31}P) = 38.1 Hz), 125.7 (d, *J* (^{13}C-^{31}P) = 11.9 Hz), 125.6 (d, *J* (^{13}C-^{31}P) = 32.3 Hz), 125.0 (d, *J* (^{13}C-^{31}P) = 41.7 Hz), 96.1 (dd, *J* (^{13}C-^{31}P) = 17.1, 7.0 Hz), 73.2 (t, *J* (^{13}C-^{31}P) = 8.3 Hz), 72.3 (d, *J* (^{13}C-^{31}P) = 5.1 Hz), 71.2 (d, *J* (^{13}C-^{31}P) = 7.7 Hz), 70.9, 67.6 (dd, *J* (^{13}C-^{31}P) = 69.8, 2.9 Hz), 59.9, 59.6, 29.2 (dd, *J* (^{13}C-^{31}P) = 33.3, 4.6 Hz), 25.5 (d, *J* (^{13}C-^{31}P) = 8.1 Hz), 23.0 (d, *J* (^{13}C-^{31}P) = 8.2 Hz), 22.6 (d, *J* (^{13}C-^{31}P) = 11.0 Hz), 16.6, 16.5. **^{31}P{^{1}H} NMR** (162 MHz, CDCl$_3$) δ 36.60(bs), 20.96(s). **HRMS** (ESI+) calculated for C$_{44}$H$_{48}$Au$_2$Cl$_2$O$_2$FeP$_2$Na (M+Na)$^+$: 1216.1080; found: 1216.1066. **Elemental analysis** calculated for C$_{44}$H$_{48}$Au$_2$Cl$_2$O$_2$FeP$_2$.CH$_2$Cl$_2$: C, 42.34; H, 4.06; found: C, 42.78; H, 4.06.

Complex 49-(*R,S*$_P$)-D
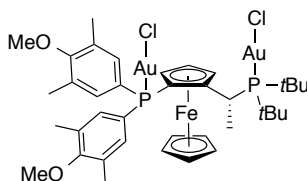
UNIVERSITAT ROVIRA I VIRGILI
COMPUTATIONAL MECHANISTIC STUDIES IN GOLD(I) CATALYSIS AND DESIGN OF NEW CHIRAL LIGANDS
Immaculada Escofet Miquel

Chapter III

The digold chloride complex was synthetized according to the general procedure from (R,S_P)-Josiphos14 (89 mg, 0.14 mmol) and (Me$_2$S)AuCl (80 mg, 0.27 mmol). The desired complex was obtained as an orange solid in 72% yield (109 mg, 0.10 mmol) after flash column chromatography on silica gel (1:4 cyclohexane-CH$_2$Cl$_2$ to 100% CH$_2$Cl$_2$).

mp > 200 ºC. **[α]$_D$** = + 64.2° (c = 0.11, CHCl$_3$, 25 ºC). **^{1}H NMR** (400 MHz, CDCl$_3$) δ 7.45 (d, J (^{1}H-^{31}P) = 13.6 Hz, 2H), 7.29 (d, J (^{1}H-^{31}P) = 13.6 Hz, 2H), 4.88 – 4.82 (m, 1H), 4.66 – 4.59 (m, 1H), 4.18 – 4.07 (m, 7H), 3.77 (s, 3H), 3.67 (s, 3H), 2.33 (s, 6H), 2.31 (s, 6H), 2.19 (dd, J (^{1}H-^{31}P) = 11.1, J (^{1}H-^{1}H) = 7.6 Hz, 3H), 1.55 (d, J (^{1}H-^{31}P) = 15.5 Hz, 9H), 1.00 (d, J (^{1}H-^{31}P) = 14.8 Hz, 9H). **^{13}C NMR** (100 MHz, CDCl$_3$) δ 160.4 (d, J (^{13}C-^{31}P) = 2.6 Hz), 160.2 (d, J (^{13}C-^{31}P) = 2.8 Hz), 135.8 (d, J (^{13}C-^{31}P) = 15.5 Hz), 134.0 (d, J (^{13}C-^{31}P) = 15.0 Hz), 132.7 (d, J (^{13}C-^{31}P) = 13.3 Hz), 132.0 (d, J (^{13}C-^{31}P) = 13.8 Hz), 125.4 (d, J (^{13}C-^{31}P) = 63.2 Hz), 124.5 (d, J (^{13}C-^{31}P) = 69.9 Hz), 102.8 – 101.9 (m), 74.5 (t, J (^{13}C-^{31}P) = 7.5 Hz), 72.6 (d, J (^{13}C-^{31}P) = 6.1 Hz), 71.5 (d, J (^{13}C-^{31}P) = 8.3 Hz), 70.9, 67.0 - 66.3 (m), 60.0 , 59.8, 38.5 (d, J (^{13}C-^{31}P) = 18.4 Hz), 37.6 (d, J (^{13}C-^{31}P) = 23.4 Hz), 32.0 (d, J (^{13}C-^{31}P) = 5.1 Hz), 31.1 (dd, J (^{13}C-^{31}P) = 20.6, 4.5 Hz), 29.6 (d, J (^{13}C-^{31}P) = 4.8 Hz), 25.1 (d, J (^{13}C-^{31}P) = 2.9 Hz), 16.5, 16.4. **^{31}P{^{1}H} NMR** (162 MHz, CDCl$_3$) δ 91.09, 22.12. **HRMS** ESI(+) calculated for C$_{38}$H$_{52}$Au$_2$Cl$_2$Na^{56}FeO$_2$P$_2$ (M+Na)$^+$: 1145.1393; found: 1145.1365. **Elemental analysis** calculated for C$_{38}$H$_{52}$Au$_2$Cl$_2$FeO$_2$P$_2$: C, 40.63; H, 4.67; found: C, 40.26; H, 4.67.

Complex 49-(R,S_P)-E
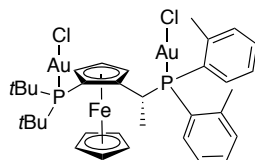
General procedure for the formation of digold chloride complexes afforded the desired complex as a crystalline orange solid in 71% yield (29.5 mg, 0.05 mmol) from (R,S_P)-Josiphos15 (29.5 mg, 0.05 mmol) and (Me$_2$S)AuCl (29.4 mg, 0.10 mmol) after precipitation with diethyl ether. The solid was separated by decantation and washed with 5 mL of dry diethyl ether (x3).

mp > 200 °C. **[α]$_D$** = + 76.4° (c = 0.1, CHCl$_3$, 25 ºC). **^{1}H NMR** (500 MHz, CDCl$_3$) δ 8.22 (bs, 1H), 7.47 - 7.38 (m, 2H), 7.33 - 7.28 (m, 2H), 7.25 - 7.21 (m, 1H), 7.18 - 7.14 (m, 1H), 6.97 - 6.91 (m, 1H), 5.67 - 5.63 (m, 1H), 4.94 - 4.83 (m, 1H), 4.59 - 4.55 (m, 1H), 4.54 (s, 4H), 4.47 (bs, 1H), 2.46 (s, 3H), 2.43 (bs, 3H), 1.86 (dd, J (^{1}H-^{31}P) = 20.0, 6.9 Hz, 3H), 1.78 (d, J = 16.1 Hz, 9H), 1.26 (d, J = 15.6 Hz, 9H). **^{13}C NMR** (125 MHz, CDCl$_3$) δ 142.5 (d, J (^{13}C-^{31}P) = 7.3 Hz), 142.2 (d, J (^{13}C-^{31}P) = 10.8 Hz), 133.1 (m), 132.9 (d, J (^{13}C-^{31}P) = 8.7 Hz), 132.5, 132.4, 131.5 (d, J (^{13}C-^{31}P) = 2.5 Hz), 127.4, 126.9, 126.8 (d, J (^{13}C-^{31}P) = 13.9 Hz), 125.6 (d, J (^{13}C-^{31}P) = 59.4 Hz), 125.3 (d, J (^{13}C-^{31}P) = 9.7 Hz), 96.28 (m), 74.4 (dd, J (^{13}C-^{31}P) = 15.1, 6.9 Hz), 73.22 (d, J (^{13}C-^{31}P) = 3.0 Hz), 72.1, 69.9 (d, J (^{13}C-^{31}P) = 6.4 Hz), 69.3 (dd, J (^{13}C-^{31}P) = 44.8, 8.3 Hz), 39.2 (d, J (^{13}C-^{31}P) = 29.0 Hz), 37.7 (d, J (^{13}C-

UNIVERSITAT ROVIRA I VIRGILI
COMPUTATIONAL MECHANISTIC STUDIES IN GOLD(I) CATALYSIS AND DESIGN OF NEW CHIRAL LIGANDS
Immaculada Escofet Miquel

Chapter III

^{31}P) = 29.4 Hz), 30.7 (d, J (^{13}C-^{31}P) = 5.7 Hz), 30.6 (d, J (^{13}C-^{31}P) = 5.7 Hz), 28.8 (m) 28.19 (d, J (^{13}C-^{31}P) = 7.3 Hz), 22.8, 22.7. **^{31}P{^{1}H} NMR** (203 MHz, CDCl$_3$) δ 59.70, 33.40 (bs). **HRMS (**MALDI+) Calc. for C$_{34}$H$_{44}$Au$_2$Cl$_2$FeP$_2$ [M]$^+$: 1034.0976 Found: 1034.1023 **Elemental analysis** Anal. Calc. for C$_{34}$H$_{44}$Au$_2$Cl$_2$FeP$_2$: C, 39.44; H, 4.53; found: C, 39.22; H, 4.53.

Complex 49-(R,S_P)-F
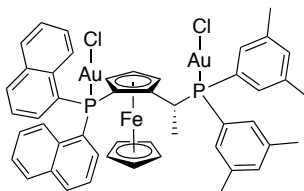
The digold chloride complex was synthetized according to the general procedure from the (R,S_P)-Josiphos16 (285 mg, 0.39 mmol) and (Me$_2$S)AuCl (239 mg, 0.81 mmol). The desired complex was obtained as an orange solid in 92% yield (429 mg, 0.36 mmol) after flash column chromatography on silica gel (9:1 to 3:2 cyclohexane-ethyl acetate).

mp 250-252 °C. **[α]$_D$** = −99.5° (c = 0.15$_2$, 25 ºC). **^{1}H NMR** (500 MHz$_2$, 223 K) δ 10.51 (bd, J = 8.6 Hz, 1H, C1), 9.56 (dd, J (^{1}H-^{31}P) = 22.7, 7.3 Hz, 0.62H, C2), 8.39 (d, J = 8.5 Hz, 0.66H, C2), 8.17 – 7.85 (m, 9H), 7.80 – 7.77 (m, 1H), 7.63 (bd, J = 12.8 Hz, 2H), 7.54 – 7.12 (m, 14.8H), 7.06 – 7.01 (m, 1.6H), 6.88 – 6.84 (m, 0.54H, C2), 6.70 (s, 0.56H, C2), 6.54 – 6.49 (m, 1H, C1), 6.33 (s, 1H, C1), 5.57 – 5.55 (m, 1H, C1, CHP), 5.48 – 5.40 (m, 0.63H, C2, CHP), 5.19 (s, 1H, C1), 5.01 (s, 0.54H, C2), 4.73 (s, 1H, C1), 4.57 (s, 0.59H, C2), 4.45 (s, 0.54H, C2), 3.77 (s, 3.15H, C2), 3.58 (s, 4.45H, C1), 2.41 (s, 9.9H), 1.98 (s, 4.7H), 1.90 – 1.82 (m, 5H), 1.75 (s, 5H). **^{13}C NMR** (100 MHz$_2$) δ 139.2 (d, J (^{13}C-^{31}P) = 12.1 Hz, 2Cq), 138.4 (d, J (^{13}C-^{31}P) = 12.1 Hz, 2C2), 134.4 (d, J (^{13}C-^{31}P) = 7.6 Hz, Cq), 133.8 (d, J (^{13}C-^{31}P) = 2.6 Hz, CH), 133.7 (d, J (^{13}C-^{31}P) = 2.5 Hz, CH), 133.7 (Cq), 133.6 (CH), 132.2 (Cq), 132.1 (CH), 132.08 (CH), 131.9 (d, J (^{13}C-^{31}P) = 13.5 Hz, CH), 131.7 (d, J (^{13}C-^{31}P) = 2.5 Hz, CH), 131.5 (d, J (^{13}C-^{31}P) = 13.3 Hz, CH), 129.7 (d, J (^{13}C-^{31}P) = 1.8 Hz, CH), 129.2 (Cq), 128.9 (d, J (^{13}C-^{31}P) = 1.7 Hz, CH), 128.4 (Cq), 128.3 (Cq), 127.8, 127.7 (Cq), 127.4 (CH), 126.8 (d, J (^{13}C-^{31}P) = 17.8 Hz, CH), 126.4 (CH), 125.6 (d, J (^{13}C-^{31}P) = 11.3 Hz), 125.4 (d, J (^{13}C-^{31}P) = 11.2 Hz, CH), 125.1 (d, J (^{13}C-^{31}P) = 14.8 Hz, CH), 124.9 (d, J (^{13}C-^{31}P) = 14.6 Hz, CH), 96.5 (dd, J (^{13}C-^{31}P) = 16.7, 8.4 Hz, Cq, Cp), 73.8 (t, J (^{13}C-^{31}P) = 8.1 Hz, CH, Cp), 72.8 (d, J (^{13}C-^{31}P) = 5.4 Hz, CH, Cp,), 71.7 (d, J (^{13}C-^{31}P) = 8.0 Hz, CH, Cp), 70.8 (5CH, Cp), 68.2 (d, J (^{13}C-^{31}P) = 2.5 Hz, Cq. Cp), 67.5 (d, J (^{13}C-^{31}P) = 2.4 Hz, Cq, Cp), 31.8 – 30.8 (m, CHP), 23.6 (d, J (^{13}C-^{31}P) = 5.7 Hz, CH3P), 21.1 (2CH3), 20.6 (2CH3). **^{31}P{^{1}H} NMR** (202 MHz, CD$_2$Cl$_2$, 223 K) δ 54.41, 50.38, 22.97, −7.54. **HRMS (**ESI+) Calc. for C$_{48}$H$_{44}$Au$_2$Cl$_2$FeP$_2$Na [M+Na]$^+$: 1225.0870 Found: 1225.0861 **Elemental analysis** Anal. Calc. for C$_{48}$H$_{44}$Au$_2$Cl$_2$FeP$_2$: C, 47.90; H, 3.69; found: C, 47.67; H, 3.63.

UNIVERSITAT ROVIRA I VIRGILI
COMPUTATIONAL MECHANISTIC STUDIES IN GOLD(I) CATALYSIS AND DESIGN OF NEW CHIRAL LIGANDS
Immaculada Escofet Miquel

Chapter III

Complex 49-(*S*,*R*$_P$)-F
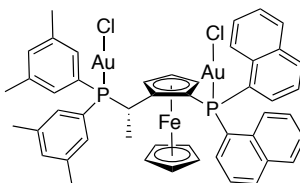
The digold chloride complex was synthetized according to the general procedure from the (*S*,*R*$_P$)-Josiphos16 (285 mg, 0.39 mmol) and (Me$_2$S)AuCl (239 mg, 0.81 mmol). The desired complex was obtained as an orange solid in 92% yield (429 mg, 0.36 mmol) after flash column chromatography on silica gel (9:1 to 3:2 cyclohexane-ethyl acetate). X-ray quality crystals were obtained layering a solution of the mixture of the complex in CH$_2$Cl$_2$ with methanol.

mp 266-268 °C. **[α]$_D$** = +88.38° (*c* = 0.15$_2$, 25 °C). **HRMS** (ESI+) Calc. for C$_{48}$H$_{44}$Au$_2$Cl$_2$FeP$_2$Na [M+Na]$^+$: 1225.0868 Found: 1225.0846 **Elemental analysis** Anal. Calc. for C$_{48}$H$_{44}$Au$_2$Cl$_2$FeP$_2$: C, 47.90; H, 3.69; found: C, 48.22; H, 3.79.

Complex 49-*(S*,*R*$_P$)-O
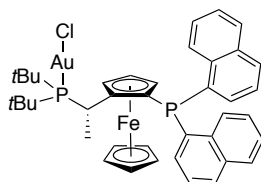
A solution of (SMe$_2$)AuCl (18.3 mg, 0.06 mmol) in 10 mL of dry CH$_2$Cl$_2$ was added dropwise to a solution of (*S*,*R*$_P$)-**L7** (40 mg, 0.06 mmol) in 10 mL of dry CH$_2$Cl$_2$ under argon. It was stirred for 2 h at room temperature. The resulting solution was filtered through a Teflon disk, concentrated and layered with pentane. It was allowed to stand in the fridge for 12 h to give orange crystalline solid separated by decantation and washed with pentane (5mL × 3) (45 mg, 0.05 mmol, 87% yield). X-ray quality crystals were obtained layering a solution of the mixture of complexes **49**-(*S*,*R*$_P$)-**B** and **49**-(*S*,*R*$_P$)-**O** in CH$_2$Cl$_2$ with hexane.

mp 208-208 °C. **^{1}H NMR** (500 MHz, CDCl$_3$) δ 9.63 - 9.57 (m, 1H), 8.09 - 8.05 (m, 1H), 7.97 - 7.94 (m, 1H), 7.90 - 7.85 (m, 2H), 7.81 (ddd, ^3J (^{1}H-^{1}H) = 8.4, ^3J (^{1}H-^{1}H) = 6.8, 1.3 Hz, 1H), ^4J (^{1}H-^{31}P) = 7.79 - 7.74 (m, 3H), f, 7.56 (ddd, ^3J (^{1}H-^{1}H) = 6.9, ^3J (^{1}H-^{1}H) = 5.0, ^4J (^{1}H-^{31}P) = 1.3 Hz, 1H), 7.36 - 7.31 (m, 2H), 7.20 (ddd, ^3J (^{1}H-^{1}H) = 8.4, ^3J (^{1}H-^{1}H) = 6.9, ^4J (^{1}H-^{31}P) = 1.4 Hz, 1H), 4.74 - 4.71 (m, 1H), 4.62 (t, ^3J (^{1}H-^{1}H) = 2.6 Hz, 1H), 4.35 - 4.32 (m, 1H), 4.01 - 3.88 (m, 1H), 3.58 (s, 5H), 2.17 (dd, ^3J (^{1}H-^{31}P) = 11.3, ^3J (^{1}H-^{1}H) = 7.6 Hz, 3H), 1.57 (d, ^3J (^{1}H-^{31}P) = 14.6 Hz, 9H), 0.95 (d, ^3J (^{1}H-^{31}P) = 14.6 Hz, 9H). **^{13}C NMR** (125 MHz, CDCl$_3$) δ 136.5 (d, J (^{13}C-^{31}P) = 27.2 Hz), 135.5 (d, J (^{13}C-^{31}P) = 7.5 Hz), 134.8 (d, J (^{13}C-^{31}P) = 2.7 Hz), 134.5 (dd, J (^{13}C-^{31}P) = 5.5, 0.8 Hz), 134.0 (dd, J (^{13}C-^{31}P) = 22.1, 2.1 Hz), 133.8 - 133.8 (m), 133.4 (d, J (^{13}C-^{31}P) = 4.5 Hz), 129.9, 129.2 (d, J (^{13}C-^{31}P) = 2.2 Hz), 128.9 , 128.6 (d, J (^{13}C-^{31}P) = 2.0 Hz), 127.4 , 126.7 , 126.5 (d, J (^{13}C-^{31}P) = 2.7 Hz),

UNIVERSITAT ROVIRA I VIRGILI
COMPUTATIONAL MECHANISTIC STUDIES IN GOLD(I) CATALYSIS AND DESIGN OF NEW CHIRAL LIGANDS
Immaculada Escofet Miquel

Chapter III

126.5 , 126.2 (d, J (^{13}C-^{31}P) = 2.1 Hz), 125.9 , 125.7 (d, J (^{13}C-^{31}P) = 1.1 Hz) 125.7 , 125.5 , 103.7 (dd, J (^{13}C-^{31}P) = 30.3, 9.5 Hz), 74.1 , 71.8 (dd, J (^{13}C-^{31}P) = 6.1, 3.8 Hz), 71.4 (d, J (^{13}C-^{31}P) = 3.8 Hz), 71.1 , 69.6 , 38.4 (d, J (^{13}C-^{31}P) = 18.4 Hz), 37.5 (d, J (^{13}C-^{31}P) = 23.0 Hz), 32.0 (d, J (^{13}C-^{31}P) = 5.3 Hz), 30.8 (dd, J (^{13}C-^{31}P) = 21.4, 17.5 Hz), 29.6 (d, J (^{13}C-^{31}P)= 3.5 Hz), 24.2. **^{31}P{^{1}H} NMR** (203 MHz, CDCl$_3$) δ 89.50, -50.88 (bs). **HRMS** (MALDI+) Calc. for C$_{40}$H$_{44}$AuClFeP$_2$ [M]$^+$: 874.1622 Found: 874.1619 **Elemental analysis** Anal. Calc. for C$_{40}$H$_{44}$AuClFeP$_2$·CH$_2$Cl$_2$: C, 51.30; H, 4.38; found: C, 51.73; H, 4.91.

General procedure for the preparation of alkenes

To a stirred suspension of methyltriphenylphosphonium bromide in dry diethyl ether under argon was slowly added *n*-BuLi (2.5 M) at 0 ºC. After 1 h, the corresponding ketone was added, and the mixture was stirred at 25 ºC until full conversion. The solution was poured into water and extracted with diethyl ether (×3). The combined organic layers were dried over MgSO$_4$ and the volatiles were removed under reduced pressure at 20 ºC. Purification by flash column chromatography on silica gel (100% pentane) afforded the entitled compounds.

p-Chloro-α-methylstyrene (20c)[69]
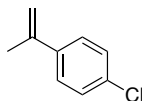
The title alkene was prepared from methyltriphenylphosphonium bromide (9.0 g, 25.2 mmol), *n*BuLi (10.1 mL, 25.2 mmol) and 4-chloroacetophenone (3.2 g, 21 mmol). Colorless oil (1.1 g, 7.0 mmol, 33% yield).

^{1}H NMR (300 MHz, CDCl$_3$) δ 7.45 – 7.37 (m, 2H), 7.35 – 7.27 (m, 2H), 5.41 – 5.34 (m, 1H), 5.15 – 5.09 (m, 1H), 2.19 – 2.14 (m, 3H). **^{13}C NMR** (75 MHz, CDCl$_3$) δ 142.3, 139.8, 133.3, 128.5, 126.9, 113.1, 21.9. The spectroscopic data of the title alkene were identical to those previously reported.

p-Bromo-α-methylstyrene (20d)[70]
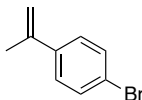
The title alkene was prepared from methyltriphenylphosphonium bromide (6.4 g, 18 mmol), *n*BuLi (7.2 mL, 18 mmol) and 4-bromoacetophenone (3.0 g, 15 mmol). Colorless oil (744 mg, 3.75 mmol, 25% yield).

^{1}H NMR (400 MHz, CDCl$_3$) δ 7.49 – 7.43 (m, 2H), 7.38 – 7.30 (m, 2H), 5.42 – 5.33 (m, 1H), 5.12 (p, J = 1.5 Hz, 1H), 2.14 (bs, 3H). **^{13}C NMR** (101 MHz, CDCl$_3$) δ 142.3, 140.2, 131.4, 127.3, 121.5, 113.2, 21.8. The spectroscopic data of the title alkene were identical to those previously reported.

69   Gupton, J. T.; Layman, W. J. *JOC*, **1987**, *52*, 3683–3686.
70   Fryszkowka, A.; Fisher, K.; Gardiner, J. M.; Stephens, G. M. *JOC*, **2008**, *11*, 4295–4298.

UNIVERSITAT ROVIRA I VIRGILI
COMPUTATIONAL MECHANISTIC STUDIES IN GOLD(I) CATALYSIS AND DESIGN OF NEW CHIRAL LIGANDS
Immaculada Escofet Miquel

Chapter III

*p-i*Propyl-α-methylstyrene (20f)
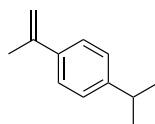
The title alkene was prepared from methyltriphenylphosphonium bromide (8.6 g, 24 mmol), *n*BuLi (9.6 mL, 24 mmol) and 4-isopropylacetophenone (3.2 g, 20 mmol). Colorless oil (1.2 g, 7.4 mmol, 37% yield).

¹H NMR (400 MHz, CDCl₃) δ 7.49 – 7.43 (m, 2H), 7.27 – 7.22 (m, 2H), 5.41 – 5.38 (m, 1H), 5.09 (p, *J* = 1.5 Hz, 1H), 2.96 (hept, *J* = 6.9 Hz, 1H), 2.20 (dd, *J* = 1.5, 0.8 Hz, 3H), 1.31 (d, *J* = 6.9 Hz, 6H). **¹³C NMR** (126 MHz, CDCl₃) δ 148.2, 143.2, 138.9, 126.4, 125.6, 111.8, 33.9, 24.1, 22.0.

p-tert-Butyl-α-methylstyrene (20g)[71]
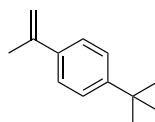
The title alkene was prepared from methyltriphenylphosphonium bromide (11.6 g, 32.5 mmol), *n*BuLi (13 mL, 32.5 mmol) and 4-*tert*-butylacetophenone (4.8 g, 27 mmol). Colorless oil (3.1 g, 17.6 mmol, 65% yield).

¹H NMR (300 MHz, CDCl₃) δ 7.50 – 7.32 (m, 4H), 5.38 (dq, *J* = 1.5, 0.8 Hz, 1H), 5.07 (p, *J* = 1.5 Hz, 1H), 2.17 (dd, *J* = 1.5, 0.8 Hz, 3H), 1.35 (s, 9H). **¹³C NMR** (75 MHz, CDCl₃) δ 150.5, 143.1, 138.4, 125.3, 125.3, 111.8, 34.6, 31.5, 21.9. The spectroscopic data of the title alkene were identical to those previously reported.

2-Phenyl-1-butene (20h)[72]
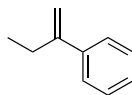
The title alkene was prepared from methyltriphenylphosphonium bromide (15.93 g, 44.6 mmol), *n*BuLi (17.9 mL, 44.7 mmol) and propiophenone (5.0 g, 37.3 mmol). Colorless oil (3.45 g, 26.1 mmol, 70% yield).

¹H NMR (300 MHz, CDCl₃) δ 7.57 – 7.46 (m, 2H), 7.45 – 7.34 (m, 3H), 5.39 (dt, *J* = 1.6, 0.8 Hz, 1H), 5.17 (q, *J* = 1.6 Hz, 1H), 2.62 (qdd, *J* = 7.4, 1.6, 0.8 Hz, 2H), 1.21 (t, *J* = 7.4 Hz, 3H). **¹³C NMR** (75 MHz, CDCl₃) δ 150.2, 141.7, 128.4, 127.4, 126.1, 111.1, 28.2, 13.1. The spectroscopic data of the title alkene were identical to those previously reported.

71   Gerst, M.; Ruechardt, C. *Tetrahedron Lett*., **1993**, *34*, 7733–7736.
72   Emer, E.; Brown, J. M.; Gouverneur, V. *Angew. Chem. Int. Ed.* **2014**, *52*, 4181–4185.

UNIVERSITAT ROVIRA I VIRGILI
COMPUTATIONAL MECHANISTIC STUDIES IN GOLD(I) CATALYSIS AND DESIGN OF NEW CHIRAL LIGANDS
Immaculada Escofet Miquel

Chapter III

2-Cyclohexyl-1-propene (20i)[73]
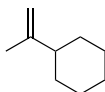
The title alkene was prepared from methyltriphenylphosphonium bromide (16.9 g, 47.4 mmol), *n*BuLi (19 mL, 47.4 mmol) and 1-cyclohexylethan-1-one (5.0 g, 39.6 mmol). Colorless oil (2.8 g, 22.6 mmol, 57% yield).

^{1}H NMR (300 MHz, CDCl$_3$) δ 4.60 – 4.56 (m, 2H), 1.85 – 1.64 (m, 6H), 1.63 (t, J = 1.2 Hz, 3H), 1.30 – 1.00 (m, 5H). **^{13}C NMR** (75 MHz, CDCl$_3$) δ 151.2, 108.0, 45.8, 32.2, 26.9, 26.6, 21.0. The spectroscopic data of the title alkene were identical to those previously reported.

General procedure for the enantioselective gold(I)-catalyzed [2+2] cycloaddition of alkynes with alkenes

Unless otherwise stated, cyclobutenes were prepared following procedure **A**, **B** or **C**.

Procedure A
Alkyne (0.3 mmol) and alkene (0.05 mmol) were added to a solution of **49**-(*S*,*R*$_P$)-**B** (2.5 mol %) in chlorobenzene (0.5 M), followed by the addition of NaBAr$_4^F$ (2.5 mol %) at -20 ºC. Alkene (0.55 mmol) was added slowly to the mixture over 1-12 h. The reaction was quenched adding a drop of NEt$_3$ when no alkyne was observed by GCMS or TLC. Purification by flash column chromatography or preparative TLC (silica gel) afforded the corresponding cyclobutenes.

Procedure B
Alkyne (0.3 mmol) and alkene (1.2 mmol) were added to a solution of **49**-(*S*,*R*$_P$)-**B** (2.5 mol %) in chlorobenzene (0.5 M) followed by the addition of NaBAr$_4^F$ (2.5 mol %) to the resulting solution at -20 ºC. The reaction was quenched adding a drop of NEt$_3$ when no alkyne was observed by GCMS or TLC. Purification by flash column chromatography or preparative TLC (silica gel) afforded the corresponding cyclobutenes.

Procedure C
Alkyne (0.3 mmol) and alkene (1.8 mmol) were added to a solution of **49**-(*R*,*S*$_P$)-**F** (5 mol %) in chlorobenzene (0.5 M) followed by the addition of NaBAr$_4^F$ (5 mol %) to the resulting solution at -20 ºC. The reaction was quenched adding a drop of NEt$_3$ when no alkyne was observed by GCMS or TLC. Purification by flash column chromatography or preparative TLC (silica gel) afforded the corresponding cyclobutenes.

The spectroscopic data for cyclobutenes **21a, c, e-g** and **21h-i** are identical to those previously reported.[20]

---

73   Young, P. C.; Hadfield, M. S.; Arrowsmith, L.; Macleod, K. M.; Mudd, R. J.; Jordan-Hore, J. A.; Lee, A. *Org. Lett.* **2012**, *14*, 898–901.

UNIVERSITAT ROVIRA I VIRGILI
COMPUTATIONAL MECHANISTIC STUDIES IN GOLD(I) CATALYSIS AND DESIGN OF NEW CHIRAL LIGANDS
Immaculada Escofet Miquel

Chapter III

Table 18. Remaining data for reported cyclobutenes **21a, c, e-i**.

Entry[a]	Cyclobutene	Procedure	$[\alpha]_D$ (degcm^{2}g^{-1})	Yield (%)[a]	er[b]
1	**21a**	A	−34.3 (c = 0.23, CHCl$_3$, 27 ºC)	70	90:10
2	**21c**	A	−48.5 (c = 1, CHCl$_3$, 26 ºC)	82	82:18
3	**21e**	A	−65.7 (c = 0.95, CHCl$_3$, 27 ºC)	47	93:7
4	**21f**	B	−55.0 (c = 1, CHCl$_3$, 27 ºC)	45	93:7
5	**21g**	A	−48.5 (c = 1, CHCl$_3$, 26 ºC)	74	90:10
6	**21h**	A	−61.7 (c = 0.75, CHCl$_3$, 27 ºC)	60	91:9
7	**21i**	A	−10.3 (c = 0.55, CHCl$_3$, 26 ºC)	78	84:16

[a] Isolated yield. Average of two runs. [b] Enantiomeric ratio determined by UPC2.

(*R*)-3-Phenyl-1-[(1,1'-diphenyl)-4-yl]-3-methyl-cyclobut-1-ene (21b)
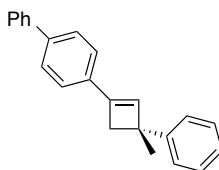
Cyclobutene **21b** was synthetized following procedure A, from(1,1'-biphenyl-4-yl)-acetylene (**19b**) (0.15 mmol, 27 mg) and α-methylstyrene **20a** (0.3 mmol, 35mg, 39 μL). The reaction time was 72 h. The crude product was purified by silica gel flash column chromatography using pentane as eluent to afford **21b** as a white solid (25 mg, 0.086 mmol, 57% yield), 91:9 *er*.

mp 140.7-143.8 °C, **[α]$_D$** = −61.8 ° (*c* = 1, CHCl$_3$, 25 ºC). **^{1}H NMR** (300 MHz, CDCl$_3$) δ 7.65 – 7.57 (m, 4H), 7.51 – 7.40 (m, 6H), 7.40 – 7.31 (m, 3H), 7.25 – 7.18 (m, 1H), 6.78 (s, 1H), 3.03 (d, *J* = 12.5 Hz, 1H), 2.96 (d, *J* = 12.5 Hz, 1H), 1.67 (s, 3H). **^{13}C NMR** (75 MHz, CDCl$_3$) δ 147.7, 143.5, 140.8, 140.5, 134.0, 133.7, 128.8, 128.2, 127.4, 127.1, 127.0, 125.9, 125.7, 125.1, 46.1, 44.4, 27.6. **HRMS** (APCI+) Calc. for C$_{23}$H$_{21}$ [M+H]$^+$: 297.1638 Found: 297.1652.

(*R*)-3-Phenyl-1-*p-tert*butylphenyl-3-methylcyclobut-1-ene (21d)
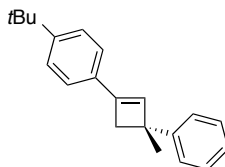
Cyclobutene **21d** was synthetized following procedure A, from 4-*tert*-butylphenylacetylene (**19d**) (0.3 mmol, 47.5 mg, 53 μL) and α-methylstyrene **20a** (0.6 mmol, 70.9 mg, 78 μL).

UNIVERSITAT ROVIRA I VIRGILI
COMPUTATIONAL MECHANISTIC STUDIES IN GOLD(I) CATALYSIS AND DESIGN OF NEW CHIRAL LIGANDS
Immaculada Escofet Miquel

Chapter III

The reaction time was 30 h. The crude product was purified by silica gel flash column chromatography using pentane as eluent to afford **21d** as a colorless oil (66 mg, 0.240 mmol, 80% yield), 87:13 *er*.

$[\alpha]_D$ = −48.5 ° (*c* = 1, CHCl$_3$, 26 ºC). **^{1}H NMR** (300 MHz, CDCl$_3$) δ 7.42 – 7.27 (m, 8H), 7.21 – 7.14 (m, 1H), 6.66 (s, 1H), 2.94 (d, *J* = 12.5 Hz, 1H), 2.88 (d, *J* = 12.5, 1H), 1.61 (s, 3H), 1.31 (s, 9H). **^{13}C NMR** (75 MHz, CDCl$_3$) δ 151.1, 147.9, 143.8, 133.1, 132.2, 128.2, 126.0, 125.8, 125.4, 124.5, 46.0, 44.5, 34.8, 31.4, 27.6. **HRMS** (APCI+) Calc. for C$_{20}$H$_{21}$ [M-CH$_3$]$^+$: 261.1638 Found: 277.1951.

(*R*)-3-*p*-Fluorophenyl-1-phenyl-3-methylcyclobut-1-ene (21j)
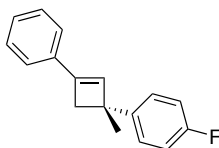
Cyclobutene **21j** was synthetized following procedure A, from phenylacetylene (**19a**) (0.3 mmol, 30.6 mg, 33 μL) and 2-(4-fluorophenyl)-1-propene **20b** (0.6 mmol, 82 mg, 81 μL). The reaction time was 40 h. The crude product was purified by silica gel flash column chromatography using pentane as eluent to afford **21j** as a colorless oil (51 mg, 0.216 mmol, 72% yield), 91:9 *er*.

$[\alpha]_D$ = −59.9 ° (*c* = 0.5, CHCl$_3$, 27 ºC). **^{1}H NMR** (300 MHz, CDCl$_3$) δ 7.50 – 7.34 (m, 6H), 7.34 – 7.28 (m, 1H), 7.12 – 6.96 (m, 2H), 6.73 (s, 1H), 3.00 – 2.92 (m, 2H), 1.66 (s, 3H). **^{13}C NMR** (75 MHz, CDCl$_3$) δ 161.2 (d, *J* (^{13}C-^{19}F) = 243.5 Hz), 144.1, 143.5 (d, *J* (^{13}C-^{19}F) = 3.1 Hz), 134.7, 133.6, 128.5, 128.1, 127.5 (d, *J* (^{13}C-^{19}F) = 7.8 Hz), 124.7, 114.9 (d, *J* (^{13}C-^{19}F) = 21.1 Hz), 45.6, 44.5, 27.7. **^{19}F{^{1}H} NMR** (376 MHz, CDCl$_3$) δ -117.94. **HRMS** (APCI+) Calc. for C$_{17}$H$_{16}$F [M+H]$^+$: 239.1231 Found: 239.1226.

(*R*)-1-Chloro-4-(1-methyl-3-phenylcyclobut-2-en-1-yl)benzene (21k)
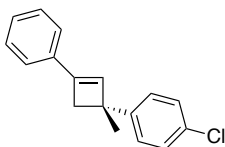
Cyclobutene **21k** was synthetized following procedure B, from phenylacetylene **19i** (0.2 mmol, 20.4 mg) and *p*-chloro-α-methylstyrene **20c** (0.6 mmol, 61 mg). The reaction time was 12 h. The crude product was purified by silica gel flash column chromatography using pentane as eluent to give **21k** as a white solid (49.7 mg, 0.192 mmol, 98% yield), 86:14 *er*.

mp 61.8-63.5 °C, $[\alpha]_D$ = −35.4 ° (*c* = 1.00, CHCl$_3$, 26 ºC). **^{1}H NMR** (500 MHz, CDCl$_3$) δ 7.40 – 7.36 (m, 2H), 7.36 – 7.29 (m, 4H), 7.29 – 7.24 (m, 3H), 6.66 (s, 1H), 2.93 – 2.88 (m, 2H), 1.60 (s, 3H). **^{13}C NMR** (126 MHz, CDCl$_3$) δ 146.3, 144.2, 134.6, 133.4, 131.6, 128.5, 128.3, 128.1, 127.5, 124.8, 45.7, 44.5, 27.4. **HRMS** (ESI+) Calc. for C$_{17}$H$_{16}$Cl [M+H]$^+$:

UNIVERSITAT ROVIRA I VIRGILI
COMPUTATIONAL MECHANISTIC STUDIES IN GOLD(I) CATALYSIS AND DESIGN OF NEW CHIRAL LIGANDS
Immaculada Escofet Miquel

Chapter III

255.0935 Found: 255.0943.

(*R*)-1-Bromo-4-(1-methyl-3-phenylcyclobut-2-en-1-yl)benzene (21l)
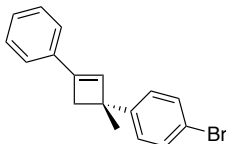
Cyclobutene **21l** was synthetized following procedure B, from phenylacetylene **19i** (0.2 mmol, 20.4 mg) and *p*-bromo-α-methylstyrene **20d** (0.4 mmol, 79 mg). The reaction time was 12 h. The crude product was purified by silica gel flash column chromatography using pentane as eluent to give **21l** as a white solid (31 mg, 0.104 mmol, 52% yield), 87:13 *er*.

mp 68.7-71.5 °C, **[α]**$_D$ = −25.0 ° (*c* = 1.00, CHCl$_3$, 26 ºC). **^{1}H NMR** (400 MHz, Chloroform-*d*) δ 7.47 – 7.43 (m, 2H), 7.42 – 7.39 (m, 2H), 7.36 (ddd, *J* = 7.9, 6.7, 0.9 Hz, 2H), 7.32 – 7.26 (m, 3H), 6.69 (s, 1H), 2.93 (s, 2H), 1.63 (s, 3H). **^{13}C NMR** (101 MHz, Chloroform-*d*) δ 146.8, 144.2, 134.6, 133.3, 131.3, 128.5, 128.1, 127.9, 124.8, 119.6, 45.7, 44.4, 27.4. **HRMS** (ESI+) Calc. for C$_{17}$H$_{16}$Br [M+H]$^+$: 299.0430 Found: 299.0422.

(*R*)-3-Phenyl-1-*p*-tolyl-3-methylcyclobut-1-ene (21m)
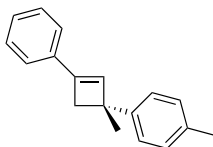
Cyclobutene **21m** was synthetized following procedure B at 25 ºC, from phenylacetylene (**19a**) (0.3 mmol, 31 mg, 33 μL) and α-methyl-*p*-methylstyrene **20e** (1.2 mmol, 159 mg, 0.175 μL). The reaction time was 24 h. The crude product was purified by silica gel flash column chromatography using pentane as eluent to afford **21m** as a white solid (40 mg, 0.171 mmol, 57% yield), 89:11 *er*.

mp 57-59 °C, **[α]**$_D$ = −31.6 ° (*c* = 1, CHCl$_3$, 25 ºC). **^{1}H NMR** (400 MHz, CD$_2$Cl$_2$) δ 7.44 – 7.39 (m, 2H), 7.38 – 7.32 (m, 2H), 7.32 – 7.25 (m, 3H), 7.18 – 7.11 (m, 2H), 6.75 (s, 1H), 2.95 (d, *J* = 12.6, 1H), 2.91 (d, *J* = 12.6 Hz, 1H), 2.33 (s, 1H), 1.61 (s, 1H). **^{13}C NMR** (100 MHz, CD$_2$Cl$_2$) δ 145.3, 144.3, 135.7, 135.4, 134.6, 129.3, 128.9, 128.3, 126.3, 125.1, 46.2, 44.7, 28.1, 21.3. **HRMS** (APCI+) Calc. for C$_{18}$H$_{19}$ [M+H]$^+$: 235.1481 Found: 235.1476.

UNIVERSITAT ROVIRA I VIRGILI
COMPUTATIONAL MECHANISTIC STUDIES IN GOLD(I) CATALYSIS AND DESIGN OF NEW CHIRAL LIGANDS
Immaculada Escofet Miquel

Chapter III

(*R*)-1-Isopropyl-4-(1-methyl-3-phenylcyclobut-2-en-1-yl)benzene (21n)
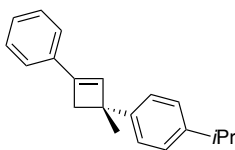
Cyclobutene **21n** was synthetized following procedure B, from phenylacetylene **19i** (0.2 mmol, 20.4 mg) and *p-i*propyl-α-methylstyrene **20f** (0.4 mmol, 64.1 mg). The reaction time was 3 h. The crude product was purified by silica gel flash column chromatography using pentane as eluent (two columns in a row) to give **21n** as a colorless oil (27 mg, 0.104 mmol, 52% yield), 88:12 *er*.

[α]$_D$ = −28.6 ° (*c* = 1.00, CHCl$_3$, 26 ºC). **¹H NMR** (500 MHz, Chloroform-*d*) δ 7.41 – 7.34 (m, 2H), 7.35 – 7.29 (m, 4H), 7.27 – 7.22 (m, 1H), 7.20 – 7.15 (m, 2H), 6.70 (s, 1H), 2.95 (d, *J* = 12.5 Hz, 1H), 2.93 – 2.85 (m, 2H), 1.62 (d, *J* = 0.6 Hz, 3H), 1.24 (d, *J* = 7.0 Hz, 6H). **¹³C NMR** ¹³C NMR (126 MHz, Chloroform-*d*) δ 146.2, 145.0, 143.8, 134.8, 134.1, 128.3, 127.7, 126.2, 125.8, 124.6, 45.7, 44.3, 33.7, 27.5, 24.1. **HRMS** (ESI+) Calc. for C$_{20}$H$_{23}$ [M+H]$^+$: 263.1794 Found: 263.1792.

(*R*)-3-*p-tert*-Butylphenyl-1-phenyl-3-methylcyclobut-1-ene (21o)
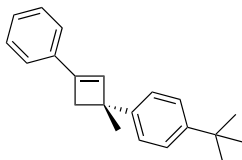
Cyclobutene **21o** was synthetized following procedure B at 25 ºC, from phenylacetylene (**19a**) (0.3 mmol, 33 μL) and 2-methyl-2-(4-*tert*-butyl)ethene **20g** (1.2 mmol, 209 mg). The reaction time was 20 h. The crude product was purified by silica gel flash column chromatography using pentane as eluent to give **21o** as a white solid (74 mg, 0.267 mmol, 89% yield), 88:12 *er*.

mp 79-84 °C, [α]$_D$ = −24.0 ° (*c* = 0.45, CHCl$_3$, 25 ºC). **¹H NMR** (400 MHz, CDCl$_3$) δ 7.43 – 7.39 (m, 2H), 7.38 – 7.33 (m, 6H), 7.30 – 7.26 (m, 1H), 6.74 (s, 1H), 2.99 (d, *J* = 12.4 Hz, 1H), 2.91 (d, *J* = 12.4 Hz, 1H), 1.65 (s, 3H), 1.34 (s, 9H). **¹³C NMR** (75 MHz, CDCl$_3$) δ 148.6, 144.7, 143.9, 134.9, 134.2, 128.4, 127.9, 125.7, 125.1, 124.7, 45.7, 44.4, 34.5, 31.6, 27.5. **HRMS** (APCI+) Calc. for C$_{21}$H$_{25}$ [M+H]$^+$: 277.1951 Found: 277.1948.

UNIVERSITAT ROVIRA I VIRGILI
COMPUTATIONAL MECHANISTIC STUDIES IN GOLD(I) CATALYSIS AND DESIGN OF NEW CHIRAL LIGANDS
Immaculada Escofet Miquel

Chapter III

(*R*)-3-*p*-Fluorophenyl-1-*p*-*tert*butylphenyl-3-methylcyclobut-1-ene (21p)
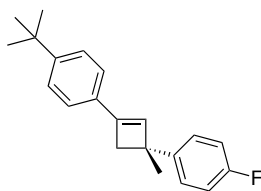
Cyclobutene **21p** was synthetized following procedure B, from 4-*tert*-butylphenylacetylene **19d** (0.3 mmol, 47.5 mg, 53 μl) and methyl-2-(4-fluoro)-ethene **20b** (1.2 mmol, 163 mg). The reaction time was 20 h. The crude product was purified by silica gel flash column chromatography using pentane as eluent to obtain **21p** as a yellowish oil (74.7 mg, 0.254 mmol, 85% yield), 87:13 *er*.

[α]$_D$ = −49.4 ° (*c* = 1.00, CHCl$_3$, 25 ºC). **¹H NMR** (300 MHz, CDCl$_3$) δ 7.45 – 7.33 (m, 6H), 7.06 – 6.97 (m, 2H), 6.66 (s, 1H), 2.95 – 2.89 (m, 2H), 1.64 (s, 3H), 1.36 (s, 9H). **¹³C NMR** (101 MHz, CDCl$_3$) δ 161.2 (d, *J* (¹³C-¹⁹F) = 243.5 Hz), 151.3, 143.9, 143.6 (d, *J* (¹³C-¹⁹F) = 3.1 Hz), 132.9, 132.0, 127.4 (d, *J* (¹³C-¹⁹F) = 7.7 Hz), 125.4, 124.5, 114.9 (d, *J* (¹³C-¹⁹F) = 21.1 Hz), 45.5, 44.7, 34.8, 31.4, 27.6. **¹⁹F NMR** (376 MHz, CDCl$_3$) δ −118.04 . **HRMS** (APCI+) Calc. for C$_{21}$H$_{24}$F [M+H]$^+$: 295.1857 Found: 295.1852.

(*R*)-3-*p*-Fluorophenyl-1-*p*-chlorophenyl-3-methylcyclobut-1-ene (21q)
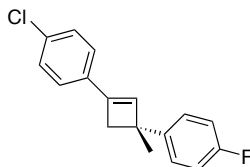
Cyclobutene **21q** was synthetized following procedure B, from 4-chlorophenylacetylene **19e** (0.3 mmol, 41 mg) and 2-methyl-2-(4-fluorophenyl)-ethene **20b** (1.2 mmol, 163 mg, 162 μl). The reaction time was 72 h. The crude product was purified by silica gel flash column chromatography using cyclohexane as eluent to obtain **21q** as a white solid (30 mg, 0.111 mmol, 37% yield), 91:9 *er*.

m.p. 59.9-63.0 °C, [α]$_D$ = −68.0 ° (*c* = 1, CHCl$_3$, 26 ºC). **¹H NMR** (400 MHz, CDCl$_3$) δ 7.36 – 7.31 (m, 2H), 7.31 (s, 4H), 7.04 – 6.96 (m, 2H), 6.69 (s, 1H), 2.93 – 2.86 (m, 2H), 1.61 (s, 3H). **¹³C NMR** (101 MHz, CDCl$_3$) δ 161.3 (d, *J* (¹³C-¹⁹F) = 243.8 Hz), 143.2 (d, *J* (¹³C-¹⁹F) = 3.2 Hz), 143.0, 134.3, 133.8, 133.2, 128.7, 127.4 (d, *J* (¹³C-¹⁹F) = 7.9 Hz), 126.1, 115.0 (d, *J* (¹³C-¹⁹F) = 21.0 Hz), 45.7, 44.4, 27.7. **¹⁹F{¹H} NMR** (376 MHz, CDCl$_3$) δ −117.79. **HRMS** (APCI+) Calc. for C$_{17}$H$_{15}$ClF [M+H]$^+$: 273.0841 Found: 273.0836.

```
UNIVERSITAT ROVIRA I VIRGILI
COMPUTATIONAL MECHANISTIC STUDIES IN GOLD(I) CATALYSIS AND DESIGN OF NEW CHIRAL LIGANDS
Immaculada Escofet Miquel
```
Chapter III

(*R*)-3-*p*-Fluorophenyl-1-*p*-bromophenyl-3-methylcyclobut-1-ene (21r)
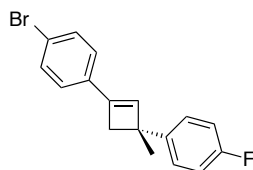
Cyclobutene **21r** was synthetized following procedure B at 25 ºC, from 4-bromophenylacetylene **19f** (0.3 mmol, 54.3 mg) and 2-methyl-2-(4-fluoro)-ethene **20b** (1.2 mmol, 163 mg). The reaction time was 12 h. The crude product was purified by silica gel flash column chromatography (two in a row) using pentane as eluent to obtain **21r** as a white solid (80 mg, 0.252 mmol, 84% yield), 88:12 *er*.

m.p. 77.1-80.2 °C, **[α]$_D$** = −48.7 ° (*c* = 1, CHCl$_3$, 26 ºC). **^{1}H NMR** (400 MHz, CDCl$_3$) δ 7.49 – 7.42 (m, 2H), 7.35 – 7.28 (m, 2H), 7.26 – 7.21 (m, 2H), 7.03 – 6.95 (m, 2H), 6.70 (s, 1H), 2.86 - 2,93 (m, 2H), 1.60 (s, 3H). **^{1}H{^{19}F} NMR** (400 MHz, CDCl$_3$) δ 7.48 – 7.43 (m, 2H), 7.34 – 7.29 (m, 2H), 7.25 – 7.21 (m, 2H), 7.02 – 6.97 (m, 2H), 6.70 (s, 1H), 2.86 – 2.93 (m, 2H), 1.60 (s, 3H). **^{13}C NMR** (100 MHz, CDCl$_3$) δ 161.3 (d, *J* (^{13}C-^{19}F) = 243.8 Hz), 143.2 (d, *J* (^{13}C-^{19}F) = 3.1 Hz), 143.0, 134.5, 133.6, 131.6, 127.4 (d, *J* (^{13}C-^{19}F) = 7.9 Hz), 126.4, 122.0, 115.0 (d, *J* (^{13}C-^{19}F) = 21.0 Hz), 45.7, 44.4, 27.7. **^{19}F NMR** (376 MHz, CDCl$_3$) δ −117.81. **HRMS** (APCI+) Calc. for C$_{17}$H$_{15}$BrF [M+H]$^+$: 317.0336 Found: 317.0325.

(*R*)-3-*p*-Fluoro-phenyl-1-(3-methoxyphenyl) -3-methylcyclobut-1-ene (21s)
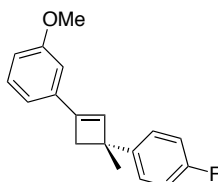
Cyclobutene **21s** was synthetized following procedure B, from 3-metoxyphenylacetylene **19h** (0.3 mmol, 39.6 mg) and 2-methyl-2-(4-fluoro)-ethene **20b** (1.2 mmol, 163 mg, 162 µl). The reaction time was 72 h. The crude product was purified by silica gel flash column chromatography using pentane: CH$_2$Cl$_2$ (9:1) as eluent to obtain **21s** as a yellowish oil (32 mg, 0.120 mmol, 40% yield), 89:11 *er*.

[α]$_D$ = −32.4 ° (*c* = 0.59, CHCl$_3$, 26 ºC). **^{1}H NMR** (400 MHz, CDCl$_3$) δ 7.38 – 7.32 (m, 2H), 7.31 – 7.24 (m, 1H), 7.05 – 6.96 (m, 3H), 6.94 – 6.92 (m, 1H), 6.84 (ddd, *J* = 8.2, 2.6, 1.0 Hz, 1H), 6.70 (s, 1H), 3.84 (s, 3H), 2.96 – 2.87 (m, 2H), 1.63 (s, 3H). **^{13}C NMR** (100 MHz, CDCl$_3$) δ 161.2 (d, *J* (^{13}C-^{19}F) = 243.6 Hz), 159.89, 144.0, 143.4 (d, *J* (^{13}C-^{19}F) = 3.0 Hz), 136.1, 134.1, 129.6, 127.5 (d, *J* (^{13}C-^{19}F) = 7.8 Hz), 117.4, 114.9 (d, *J* (^{13}C-^{19}F) = 21.1 Hz), 113.9, 110.0, 55.4, 45.5, 44.6, 27.6. **^{19}F NMR** (376 MHz, CDCl$_3$) δ −117.95. **HRMS** (ESI+) Calc. for C$_{18}$H$_{18}$FO [M+H]$^+$: 269.1336 Found: 269.1343.

UNIVERSITAT ROVIRA I VIRGILI
COMPUTATIONAL MECHANISTIC STUDIES IN GOLD(I) CATALYSIS AND DESIGN OF NEW CHIRAL LIGANDS
Immaculada Escofet Miquel

Chapter III

(*R*)-3-Phenyl-1-(thiophen-3-yl) -3-methylcyclobut-1-ene (21t)
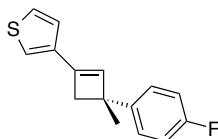
Cyclobutene **21t** was synthetized following procedure B, from 3-ethynylthiophene **19i** (0.3 mmol, 32 mg) and 2-methyl-2-(4-fluoro)-ethene **20b** (1.2 mmol, 163 mg). The reaction time was 20 h. The crude product was purified by silica gel flash column chromatography using pentane as eluent to obtain **21t** as a white solid (62 mg, 0.252 mmol, 85% yield), 86:14 *er*.

m.p. 71.2-74.1 ºC, **[α]$_D$** = −27.3 ° (*c* = 1.00, CHCl$_3$, 26 ºC). **^{1}H NMR** (400 MHz, CDCl$_3$) δ 7.39 – 7.33 (m, 2H), 7.31 (dd, J = 5.0, 2.9 Hz, 1H), 7.23 (dd, J = 5.0, 1.2 Hz, 1H), 7.18 (dd, J = 2.9, 1.2 Hz, 1H), 7.06 – 6.98 (m, 2H), 6.47 (s, 1H), 2.92 (s, 2H), 1.64 (s, 3H). **^{13}C NMR** (100 MHz, CDCl$_3$) δ 161.2 (d, *J* (^{13}C-^{19}F) = 243.5 Hz), 143.5 (d, *J* (^{13}C-^{19}F) = 3.3 Hz), 139.5, 137.7, 132.5, 127.4 (d, *J* (^{13}C-^{19}F) = 7.8 Hz), 126.1, 125.1, 121.3, 114.9 (d, *J* (^{13}C-^{19}F) = 21.0 Hz), 46.6, 45.3, 27.7. **^{19}F NMR** (376 MHz, CDCl$_3$) δ −117.90. **HRMS** (ESI+) Calc. for C$_{15}$H$_{14}$S [M+H]$^+$: 245.0795 Found: 245.0805.

(*R*)-3-*p-tert*-Butylphenyl-1-*p-tert*-butylphenyl-3-methylcyclobut-1-ene (21u)
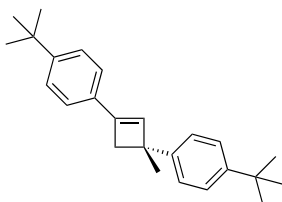
Cyclobutene **21u** was synthetized following procedure B, from 4-*tert*-butylphenylacetylene **19d** (0.3 mmol, 47 mg) and *p*-tert-butyl-α-methylstyrene **20g** (1.2 mmol, 209 mg). The reaction time was 40 h. The crude product was purified by silica gel flash column chromatography using pentane as eluent to give **21u** as a white solid (63 mg, 0.189 mmol, 63% yield), 89:11 *er*. X-ray quality crystals were obtained by slow evaporation of a CH$_2$Cl$_2$ solution of **21u**.

mp 51-54 °C, **[α]$_D$** = −23.6 ° (*c* = 1, CHCl$_3$, 25 ºC). **^{1}H NMR** (300 MHz, CDCl$_3$) δ 7.44 – 7.33 (m, 8H), 6.69 (s, 1H), 2.99 (d, *J* = 12.5 Hz, 1H), 2.90 (d, *J* = 12.5 Hz, 1H), 1.66 (s, 3H), 1.40 – 1.32 (m, 18H). **^{13}C NMR** (75 MHz, CDCl$_3$) δ 151.0, 148.5, 144.8, 143.8, 133.5, 132.3, 125.7, 125.4, 125.1, 124.5, 45.6, 44.6, 34.8, 34.5, 31.6, 31.5, 27.4. **HRMS** (APCI+) Calc. for C$_{25}$H$_{33}$ [M+H]$^+$: 333.2577 Found: 333.2563.

UNIVERSITAT ROVIRA I VIRGILI
COMPUTATIONAL MECHANISTIC STUDIES IN GOLD(I) CATALYSIS AND DESIGN OF NEW CHIRAL LIGANDS
Immaculada Escofet Miquel

Chapter III

(*R*)-3-*p-tert*-Butylphenyl-1-(thiophen-3-yl)-3-methylcyclobut-1-ene (21v)
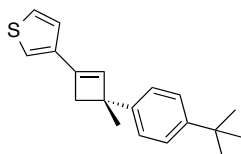
Cyclobutene **21v** was synthetized following procedure B, from 3-ethynylthiophene **19i** (0.3 mmol, 32.4 mg) and *p-tert*-butyl-α-methylstyrene **20g** (1.2 mmol, 209 mg). The reaction time was 24 h. The crude product was purified by silica gel flash column chromatography using pentane as eluent to give **21v** as a white solid (47.2 mg, 0.167 mmol, 56% yield), 96:4 *er*. X-ray quality crystals were obtained by slow evaporation of a CH_2Cl_2 solution of **21v**.

mp 107-110 °C, $[α]_D$ = + 11.3 ° (*c* = 1.00, CHCl₃, 25 ºC). **¹H NMR** (300 MHz, CDCl₃) $δ$ 7.40 – 7.32 (m, 4H), 7.29 (dd, *J* = 5.1, 2.2 Hz, 1H), 7.22 (dd, *J* = 5.1, 1.2 Hz, 1H), 7.16 (dd, *J* = 2.9, 1.2 Hz, 1H), 6.50 (s, 1H), 2.97 (d, *J* = 12.5 Hz, 1H), 2.89 (d, *J* = 12.5 Hz, 1H), 1.65 (s, 3H), 1.34 (s, 9H). **¹³C NMR** (75 MHz, CDCl₃) $δ$ 148.6, 144.7, 139.3, 138.0, 133.1, 126.0, 125.6, 125.1, 125.1, 121.0, 46.8, 45.2, 34.5, 31.6, 27.6. **HRMS** (APCI+) Calc. for $C_{19}H_{23}S$ [M+H]⁺: 283.1515 Found: 283.1515.

(*R*)-3-Phenyl-1-phenyl-3-ethylcyclobut-1-ene (21w)
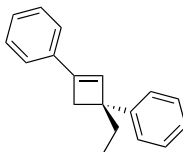
Cyclobutene **21w** was synthetized following procedure A, from phenylacetylene **19a** (0.3 mmol, 30.6 mg, 33 µL) and 2-phenyl-1-butene **20h** (0.6 mmol, 79 mg). The reaction time was 96 h. The crude product was purified by silica gel column chromatography using pentane as eluent to give **21w** as a colorless oil (58 mg, 0.25 mmol, 83% yield), 83:17 *er*.

$[α]_D$ = −78.6 ° (*c* = 1, CHCl₃, 26 ºC). **¹H NMR** (300 MHz, CDCl₃) $δ$ 7.49 – 7.43 (m, 2H), 7.43 – 7.35 (m, 6H), 7.34 – 7.22 (m, 2H), 6.91 (s, 1H), 3.00 (m, 2H), 2.08 (dq, *J* = 13.3, 7.4 Hz, 1H), 1.90 (dq, *J* = 13.3, 7.4 Hz, 1H), 0.91 (t, *J* = 7.4 Hz, 3H). **¹³C NMR** (75 MHz, CDCl₃) $δ$ 146.3, 144.5, 134.8, 131.7, 128.4, 128.0, 127.9, 126.9, 125.7, 124.7, 50.7, 42.4, 34.4, 10.4. **HRMS** (APCI+) Calc. for $C_{18}H_{19}$ [M+H]⁺: 235.1481 Found: 235.1474.

(*R*)-3-Phenyl-1-*p*-chlorophenyl-3-ethylcyclobut-1-ene (21x)

UNIVERSITAT ROVIRA I VIRGILI
COMPUTATIONAL MECHANISTIC STUDIES IN GOLD(I) CATALYSIS AND DESIGN OF NEW CHIRAL LIGANDS
Immaculada Escofet Miquel

Chapter III
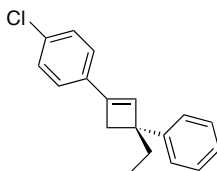
Cyclobutene **21x** was synthetized following procedure B, from 4-chlorophenylacetylene **19e** (0.3 mmol, 41 mg) and 2-phenyl-1-butene **20h** (1.2 mmol, 159 mg). The reaction time was 72 h. The crude product was purified by silica gel flash column chromatography using pentane as eluent to give **21x** as a yellowish oil (74 mg, 0.275 mmol, 92% yield), 88:12 *er*.

[α]$_D$ = −56.4 ° (*c* = 0.86, CHCl$_3$, 27 ºC). **^{1}H NMR** (400 MHz, CDCl$_3$) δ 7.35 − 7.29 (m, 8H), 7.25 − 7.18 (m, 1H), 6.85 (s, 1H), 2.93 (s, 2H), 2.02 (dq, *J* = 13.4, 7.4 Hz, 1H), 1.85 (dq, *J* = 13.4, 7.4 Hz, 1H), 0.85 (t, *J* = 7.4 Hz, 3H). **^{13}C NMR** (100 MHz, CDCl$_3$) δ 146.0, 143.5, 133.6, 133.3, 132.5, 128.6, 128.1, 126.9, 126.0, 125.8, 50.9, 42.3, 34.4, 10.3. **HRMS** (APCI+) Calc. for C$_{18}$H$_{18}$Cl [M+H]$^+$: 269.1092 Found: 269.1084.

(*R*)-3-Phenyl-1-*p*-bromophenyl-3-ethylcyclobut-1-ene (21y)
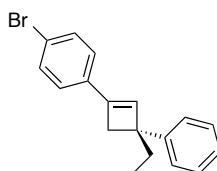
Cyclobutene **21y** was synthetized following procedure B at 25 ºC, from 4-bromophenylacetylene **19f** (0.3 mmol, 54 mg) and 2-phenyl-1-butene **20h** (1.2 mmol, 159 mg). The reaction time was 24 h. The crude product was purified by silica gel flash column chromatography using pentane as eluent to give **21y** as a colorless oil (76 mg, 0.243 mmol, 81% yield), 85:15 *er*.

[α]$_D$ = −60.5 ° (*c* = 1.00, CHCl$_3$, 25 ºC). **^{1}H NMR** (300 MHz, CDCl$_3$) δ 7.49 − 7.36 (m, 2H), 7.33 − 7.25 (m, 4H), 7.24 − 7.13 (m, 3H), 6.83 (s, 1H), 2.88 (s, 2H), 1.97 (dq, *J* = 13.4, 7.4 Hz, 1H), 1.80 (dq, *J* = 13.4, 7.4 Hz, 1H), 0.80 (t, *J* = 7.4 Hz, 3H). **^{13}C NMR** (100 MHz, CDCl$_3$) δ 146.0, 143.5, 133.7, 132.7, 131.6, 128.1, 126.9, 126.3, 125.8, 121.8, 50.9, 42.2, 34.3, 10.3. **HRMS** (APCI+) Calc. for C$_{18}$H$_{18}$Br [M+H]$^+$: 313.0586 Found: 313.0598.

(*R*)-3-Phenyl-1-(3-methoxyphenyl)-3-ethylcyclobut-1-ene (21z)
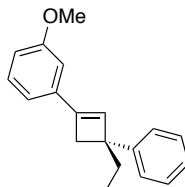
Cyclobutene **21z** was synthetized following procedure B, from 3-metoxyphenylacetylene (**19h**) (0.3 mmol, 39.6 mg) and 2-phenyl-1-butene **20h** (1.2 mmol, 159 mg). The reaction time was 72 h. The crude product was purified by silica gel flash column chromatography using 9:1 pentane-CH$_2$Cl$_2$ as eluent to give **21z** as a yellowish oil (70.1 mg, 0.265 mmol, 88% yield), 89:11 *er*.

UNIVERSITAT ROVIRA I VIRGILI
COMPUTATIONAL MECHANISTIC STUDIES IN GOLD(I) CATALYSIS AND DESIGN OF NEW CHIRAL LIGANDS
Immaculada Escofet Miquel

Chapter III

[α]$_D$ = −86.9 ° (*c* = 1.00, CHCl$_3$, 27 ºC). **^{1}H NMR** (400 MHz, CDCl$_3$) δ 7.41 – 7.35 (m, 4H), 7.34 – 7.29 (m, 1H), 7.29 – 7.23 (m, 1H), 7.08 – 7.05 (m, 1H), 7.01 – 6.98 (m, 1H), 6.91 (s, 1H), 6.90 – 6.86 (m, 1H), 3.88 (s, 3H), 3.04 – 2.93 (m, 2H), 2.08 (dq, *J* = 13.2, 7.4 Hz, 1H), 1.91 (dq, *J* = 13.2, 7.4 Hz, 1H), 0.91 (t, *J* = 7.4 Hz, 3H). **^{13}C NMR** (100 MHz, CDCl$_3$) δ 159.7, 146.2, 144.4, 136.2, 132.1, 129.4, 127.9, 126.8, 125.6, 117.3, 113.7, 109.9, 55.3, 50.6, 42.3, 34.3, 10.3. **HRMS** (ESI+) Calc. for C$_{19}$H$_{21}$O [M+H]$^+$: 265.1587 Found: 265.1596.

(*R*)-3-Phenyl-1-(thiophen-3-yl)-3-ethylcyclobut-1-ene (21aa)
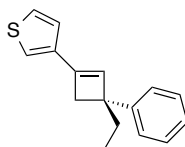
Cyclobutene **21aa** was synthetized following procedure B, from 3-ethynylthiophene **19i** (0.3 mmol, 32.4 mg) and 2-phenyl-1-butene **20h** (1.2 mmol, 159 mg). The reaction time was 72 h. The crude product was purified by silica gel flash column chromatography using pentane as eluent to give **21aa** as a yellowish oil (63 mg, 0.261 mmol, 87% yield), 83:17 *er*.

[α]$_D$ = −29.2 ° (*c* = 1.00, CHCl$_3$, 26 ºC). **^{1}H NMR** (500 MHz, CDCl$_3$) δ 7.35 – 7.32 (m, 4H), 7.29 (dd, *J* = 5.0, 2.9 Hz, 1H), 7.24 – 7.19 (m, 2H), 7.17 (dd, *J* = 2.9, 1.2 Hz, 1H), 6.62 (s, 1H), 2.93 (s, 2H), 2.03 (dq, *J* = 13.4, 7.4 Hz, 1H), 1.87 (dq, *J* = 13.4, 7.4 Hz, 1H), 0.86 (t, *J* = 7.4 Hz, 5H). **^{13}C NMR** (100 MHz, CDCl$_3$) δ 146.3, 140.0, 137.9, 130.6, 128.0, 126.9, 126.0, 125.7, 125.1, 121.1, 51.8, 43.2, 34.4, 10.4. **HRMS** (ESI+) Calc. for C$_{16}$H$_{17}$S [M+H]$^+$: 241.1045 Found: 241.1043.

(*R*)-3-Cyclohexyl-1-phenyl-3-methylcyclobut-1-ene (21ab)
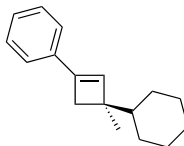
Cyclobutene **21ab** was synthetized following procedure B at 25 ºC, from phenylacetylene (**19a**) (0.3 mmol, 30.6 mg, 33 μL) and 2-cyclohexyl-1-propene **20i** (1.2 mmol, 149 mg). The reaction time was 24 h. The crude product was purified by silica gel flash column chromatography (two in a row, first using pentane and then using cyclohexane as eluents), to give **21ab** as a colorless oil (46 mg, 0.201 mmol, 67% yield), 64:36 *er*.

[α]$_D$ = + 8.3 ° (*c* = 0.3, CHCl$_3$, 25 ºC). **^{1}H NMR** (300 MHz, CDCl$_3$) δ 7.39 – 7.28 (m, 4H), 7.26 – 7.19 (m, 1H), 6.51 (s, 1H), 2.58 (d, *J* = 12.5 Hz, 1H), 2.33 (d, *J* = 12.5 Hz, 1H), 1.86 – 1.59 (m, 5H), 1.49 – 0.96 (m, 6H), 1.16 (s, 3H). **^{13}C NMR** (75 MHz, CDCl$_3$) δ 143.1,

UNIVERSITAT ROVIRA I VIRGILI
COMPUTATIONAL MECHANISTIC STUDIES IN GOLD(I) CATALYSIS AND DESIGN OF NEW CHIRAL LIGANDS
Immaculada Escofet Miquel

Chapter III

136.1, 135.4, 128.4, 127.5, 124.4, 46.5, 46.0, 40.0, 28.7, 28.5, 27.0, 27.0, 26.8, 20.4. **HRMS** (APCI+) Calc. for $C_{17}H_{23}$ [M]$^+$: 227.1794 Found: 227.1787.

(*R*)-3-Phenyl-1-phenyl-cyclobut-1-ene (21ac)
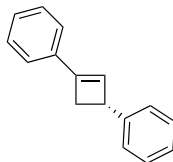
Cyclobutene **21ac** was synthetized following procedure A at 25ºC, from phenylacetylene **19a** (0.3 mmol, 31 mg, 33 μL) and styrene **20i** (1.2 mmol, 125 mg, 138 μL). The reaction time was 72 h. The crude product was purified by silica gel column chromatography using pentane as eluent to afford **21ac** as a colorless oil (33 mg, 0.160 mmol, 53% yield), 66:34 *er*.

[α]$_D$ = + 4.4 ° (*c* = 0.25, CHCl$_3$, 27 ºC). **^{1}H NMR** (500 MHz, CDCl$_3$) δ 7.45 – 7.41 (m, 2H), 7.38 – 7.34 (m, 2H), 7.33 – 7.26 (m, 5H), 7.24 – 7.19 (m, 1H), 6.55 (d, *J* = 1.3 Hz, 1H), 4.02 (dt, *J* = 4.9, 1.5 Hz, 1H), 3.32 (dd, *J* = 12.8, 4.8 Hz, 1H), 2.67 (dd, *J* = 12.8, 1.9 Hz, 1H). **^{13}C NMR** (125 MHz, CDCl$_3$) δ 146.6, 143.9, 134.6, 129.8, 128.5, 128.5, 128.0, 126.9, 126.4, 124.8, 43.1, 38.6. **HRMS** (APCI+) Calc. for $C_{16}H_{13}$ [M]$^+$: 205.1012 Found: 205.1009.

1,4-Bis-((*R*)-3-(4-fluorophenyl)-3-methylcyclobut-1-en-1-yl)benzene (21ad)
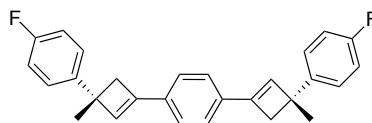
Biscyclobutene **21ad** was synthetized following procedure A with 5 mol% of **49-(*S*,*R*$_P$)-B** and NaBAr$_4$^{F}, from 1,4-diethynylbenzene **19j** (0.3 mmol, 37.8 mg) and 2-methyl-2-(4-fluoro)-ethene **20b** (1.8 mmol, 245 mg) at 25 ºC. The crude product was purified by silica gel flash column chromatography using a mixture of 10:1 pentane-CH$_2$Cl$_2$ as eluent to give **21ad** as a white solid (48.8 mg, 0.122 mmol, 41% yield, 28% meso), 97:3 *er*. **21ad** could also be prepared at −20 ºC (38.2 mg, 0.096 mmol, 32% yield, 21% meso), 98:2 *er*. X-ray quality crystals were obtained by slow diffusion of methanol over a CH$_2$Cl$_2$ solution of **21ad**.

NMR spectroscopy signals are overlapped for the meso form and the enantiomers.

mp 152-158 °C, [α]$_D$ = −91.7 ° (*c* = 0,48, CHCl$_3$, 24 ºC). **^{1}H NMR** (300 MHz, CDCl$_3$) δ 7.46 – 7.28 (m, 8H), 7.11 – 6.89 (m, 4H), 6.70 (s, 2H), 2.92 (s, 4H), 1.62 (s, 6H). **^{13}C NMR** (75 MHz, CDCl$_3$) δ 161.2 (d, *J* (^{13}C-^{19}F) = 243.7 Hz), 143.7, 143.5 (d, *J* (^{13}C-^{19}F) = 3.2 Hz), 134.2, 133.9, 127.5 (d, *J* (^{13}C-^{19}F) = 7.7 Hz), 124.8, 114.9 (d, *J* (^{13}C-^{19}F) = 20.9 Hz), 45.7, 44.5, 27.8. **^{19}F NMR** (376 MHz, CDCl$_3$) δ −117.91. **HRMS** (APCI+) Calc. for $C_{28}H_{25}F_2$ [M+H]$^+$: 399.1919 Found: 399.1914.

UNIVERSITAT ROVIRA I VIRGILI
COMPUTATIONAL MECHANISTIC STUDIES IN GOLD(I) CATALYSIS AND DESIGN OF NEW CHIRAL LIGANDS
Immaculada Escofet Miquel

Chapter III

1,4-Bis-((*R*)-3-(4-(*tert*-butyl)phenyl)-1-methylcyclobut-2-en-1-yl)benzene (21ae)
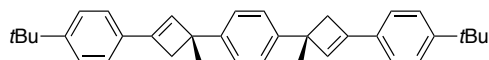
Biscyclobutene **21ae** was synthetized following procedure B with 5 mol % of **49**-(*S*,*R*$_P$)-**B** and NaBAr$^F_4$, from 4-*tert*-butylphenylacetylene **19d** (0.9 mmol, 142 mg) and 1,4-diisocraticpropenylbenzene **20k** (0.3 mmol, 47.5 mg) at 25 ºC. The crude product was purified by silica gel flash column chromatography using a mixture of 19:1 pentane-CH$_2$Cl$_2$ as eluent to give **21ae** as a white solid (86 mg, 0.181 mmol, 60% yield, 32% meso), 95:5 *er*. **21ae** could also be prepared at −20 ºC (46 mg, 0.097 mmol, 32% yield, 22% meso), 98:2 *er*. X-ray quality crystals were obtained by slow diffusion of pentane over a CH$_2$Cl$_2$ solution of **21ae**. Enantiomers (e) and Meso (m).

mp 183-187 °C, **[α]$_D$** = −24.1 ° (*c* = 0.37, CHCl$_3$, 24 ºC). **^{1}H NMR** (400 MHz, CDCl$_3$) δ 7.39 – 7.37 (m, 1H) (e + m), 7.36 (s, 3H) (e + m), 7.37 – 7.35 (m, 7H) (e + m), 7.33 – 7.32 (m, 1H) (e + m), 6.66 (bs, 2H) (e + m), 3.06 – 2.90 (m, 2H) (e + m), 2.87 (d, *J* = 12.4 Hz, 2H) (e + m), 1.62 (s, 6H) (e + m), 1.32 (s, 18H) (e + m). **^{13}C NMR** (100 MHz, CDCl$_3$) δ 151.0 (e + m), 145.2 (e + m), 143.8 (e + m), 133.4 (m), 133.4 (e), 132.3 (e + m), 125.7 (e + m), 125.4 (e + m), 124.5 (e + m), 45.7 (e + m), 44.6 (e + m), 34.8 (e + m), 31.4 (e + m), 27.5 (e + m). **HRMS** (APCI+) Calc. for C$_{36}$H$_{43}$ [M+H]$^+$: 475.3359 Found: 475.3360.

1,3-Bis-((*R*)-1-Methyl-3-(*m*-tolyl)cyclobut-2-en-1-yl)benzene (21af)
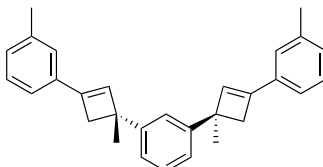
Biscyclobutene **21af** was synthetized following procedure A with 5 mol % of **49**-(*S*,*R*$_P$)-**B** and NaBAr$_4$^{F}, from 3-ethynyltoluene **19g** (0.9 mmol, 105 mg) and 1,3-diisoprenylbenzene **20l** (0.3 mmol, 47.5 mg). The reaction time was 14 h. The crude product was purified by silica gel flash column chromatography using from 97:3 to 95:5 pentane-CH$_2$Cl$_2$ as eluent to give **21af** as a yellowish oil (52.4 mg, 0.134 mmol, 45% yield, 23% meso), 98:2 *er*. Enantiomers (e) and Meso (m).

[α]$_D$ = −35.8 ° (*c* = 0.43, CHCl$_3$, 25 ºC). **^{1}H NMR** (400 MHz, CDCl$_3$) δ 7.46 -7.42 (m, 1H) (e + m), 7.35 – 7.25 (m, 9H) (e + m), 7.15 – 7.10 (m, 2H) (e + m), 6.78 (s, 1.5H) (e), 6.77 (s, 0.5H) (m), 3.09 – 3.00 (m, 2H) (e + m), 2.98 – 2.92 (m, 2H) (e + m), 2.40 (s, 6H) (e + m), 1.68 (s, 6H) (e + m). **^{13}C NMR** (100 MHz, CDCl$_3$) δ 147.7 (e), 147.7 (m), 144.0 (e + m), 138.0 (e + m), 134.9 (e + m), 133.8 (m), 133.8 (e), 128.7 (e + m), 128.4 (e + m), 128.0 (e + m), 125.4 (e + m), 123.4 (e), 123.39 (m), 121.9 (e + m), 46.3 (e + m), 44.5 (e), 44.4

UNIVERSITAT ROVIRA I VIRGILI
COMPUTATIONAL MECHANISTIC STUDIES IN GOLD(I) CATALYSIS AND DESIGN OF NEW CHIRAL LIGANDS
Immaculada Escofet Miquel

Chapter III

(m), 28.1 (m), 28.1 (e) , 21.52 (e + m). **HRMS** (APCI+) Calc. for $C_{30}H_{31}$ [M+H]$^+$: 391.2420 Found: 391.2415.

1,3-Bis-((*R*)-3-(4-(*tert*-Butyl)phenyl)-1-methylcyclobut-2-en-1-yl)benzene (21ag)
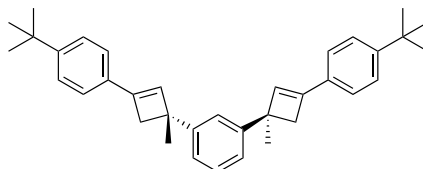
Biscyclobutene **21ag** was synthetized following procedure A with 5 mol % of **49**-(*S,R*$_P$)-**B** and NaBAr$_4$^{F}, from 4-*tert*-butylphenylacetylene **19d** (0.9 mmol, 142 mg) and 1,3-diisoprenylbenzene **20l** (0.3 mmol, 47.5 mg). The reaction time was 12 h. The reaction crude product was purified by silica gel flash column chromatography using a 19:1 pentane-CH$_2$Cl$_2$ as eluent to give **21ag** as a white solid (94.8 mg, 0.200 mmol, 67% yield, 27% meso), 96:4 *er*. Enantiomers (e) and meso (m).

mp 72-77 °C, [**α**]$_D$ = −42.3 ° (*c* = 0.48, CHCl$_3$, 25 ºC). **¹H NMR** (400 MHz, CDCl$_3$) δ 7.45 − 7.42 (m, 2H) (e + m), 7.43 − 7.39 (m, 6H) (e + m), 7.39 − 7.37 (m, 1H) (e + m), 7.33 − 7.24 (m, 3H) (e + m), 6.75 − 6.72 (m, 2H) (e + m), 3.07 − 2.99 (m, 2H) (e + m), 2.97 − 2.91 (m, 2H) (e + m), 1.67 (s, 6H) (e + m), 1.38 (s, 18H) (e + m). **¹³C NMR** (100 MHz, CDCl$_3$) δ 151.0 (e + m), 147.8 (e), 147.7 (m), 143.8 (e + m), 133.2 (m), 133.2 (e), 132.3 (e + m), 127.9 (e + m), 125.4 (e + m), 124.6 (e + m), 123.4 (e + m), 123.4 (e + m), 46.3 (e + m), 44.6 (e), 44.5 (m), 34.8 (e + m), 31.5 (e + m), 28.0 (m), 28.0 (e). **HRMS** (APCI+) Calc. for $C_{36}H_{43}$ [M+H]$^+$: 475.3359 Found: 475.3367.

1,3-Bis-((*R*)-1-Methyl-3-(thiophen-3-yl)cyclobut-2-en-1-yl)benzene (21ah)
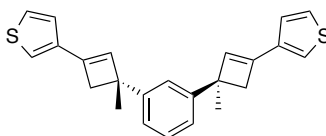
Cyclobutene **21ah** was synthetized following procedure A with 5 mol % of **49**-(*S,R*$_P$)-**B** and NaBAr$_4$^{F}, from 3-ethynylthiophene **19i** (0.9 mmol, 97 mg) and 1,3-diisoprenylbenzene **20l** (0.3 mmol, 47.5 mg). The reaction time was 72 h. The crude product was purified by silica gel flash column chromatography using a mixture of 19:1 pentane-CH$_2$Cl$_2$ as eluent to give **21ah** as a white solid (78.9 mg, 0.211 mmol, 70% yield, 26% meso), 96:4 *er*. Enantiomers (e) and Meso (m).

mp 69-74 °C, [**α**]$_D$ = −3.1 ° (*c* = 0.12, CHCl$_3$, 25 ºC). **¹H NMR** (400 MHz, CDCl$_3$) δ 7.38 − 7.36 (m, 1H) (e + m), 7.31 − 7.26 (m, 3H) (e + m), 7.25 − 7.20 (m, 4H) (e + m), 7.16 (dd, *J* = 2.9, 1.2 Hz, 2H) (e + m), 6.53 (s, 1.5H) (e), 6.52 (s, 0.5H) (m), 3.03 − 2.95 (m, 2H) (e + m), 2.93 − 2.87 (m, 2H) (e + m), 1.64 (s, 6H) (e + m). **¹³C NMR** (100 MHz, CDCl$_3$) δ 147.7 (e), 147.7 (m), 139.3 (e + m), 138.0 (e + m), 132.84 (m), 132.79 (e), 128.0 (e + m), 126.0

UNIVERSITAT ROVIRA I VIRGILI
COMPUTATIONAL MECHANISTIC STUDIES IN GOLD(I) CATALYSIS AND DESIGN OF NEW CHIRAL LIGANDS
Immaculada Escofet Miquel

Chapter III

(e + m), 125.2 (e + m), 123.4 (e + m), 123.3 (e + m), 121.1 (e + m), 47.4 (e + m), 45.2 (e), 45.1 (m), 28.2 (m), 28.1 (e). **HRMS** (APCI+) Calc. for $C_{24}H_{23}S_2$ [M+H]$^+$: 375.1236 Found: 375.1237.

(*S*)-(2-(4,4-Dimethyl-2-phenylcyclobut-2-en-1-yl)ethyl)benzene (21ai)
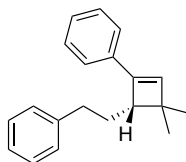
Cyclobutene **21ai** was synthetized following procedure C, from phenylacetylene (0.3 mmol, 30.6 mg) and (4-methylpent-3-en-1-yl)benzene (0.6 mmol, 96 mg). The reaction time was 36 h. The crude product was purified by silica gel flash column chromatography using pentane as eluent to give **21ai** as a colorless oil 7:1 mixture of regioisomers (40.2 mg, 0.153 mmol, 51% yield), 90:10 *er*. Major regioisomer (Mr), minor regioisomer (mr).

[α]$_D$ = −2.3 ° (*c* = 0.6, CHCl$_3$, 23 ºC). **^{1}H NMR** (500 MHz, CDCl$_3$) δ 7.39 – 7.35 (m, 0.3H, mr), 7.33 – 7.27 (m, 5.60H, Mr + mr), 7.25 – 7.17 (m, 4.6H Mr + mr), 6.33 (d, *J* = 1.3 Hz, 0.15H, mr), 6.31 (s, 1H, Mr), 2.84 – 2.75 (m, 2.15H Mr + mr), 2.75 – 2.71 (m, 0.15H, mr), 2.67 (ddd, *J* = 14.2, 10.2, 6.7 Hz, 1H, Mr), 2.44 (dd, *J* = 9.6, 4.8 Hz, 0.15H, mr), 2.16 – 2.07 (m, 1H, Mr), 1.91 (ddt, *J* = 13.2, 9.0, 6.3 Hz, 0.15H, mr), 1.80 (dtd, *J* = 14.2, 10.4, 4.9 Hz, 1H, Mr), 1.69 (dtd, *J* = 13.2, 9.6, 6.3 Hz, 0.15H, mr), 1.41 (s, 0.45H, mr), 1.32 (s, 0.45H, mr), 1.29 (s, 3H, Mr), 1.25 (s, 3H, Mr). **^{13}C NMR** (126 MHz, CDCl$_3$) δ 145.8 (Mr), 142.9 (mr), 142.8 (Mr), 136.5 (Mr), 134.9 (Mr), 128.6 (mr), 128.5 (mr), 128.5 (Mr), 128.5 (Mr), 128.4 (Mr), 128.1 (mr), 127.5 (mr), 127.4 (Mr), 125.9 (Mr), 125.8 (mr), 125.4 (mr), 125.2 (Mr), 51.6 (mr), 51.5 (Mr), 43.1 (Mr), 35.3 (Mr), 34.9 (mr), 32.2 (mr), 31.4 (Mr), 28.0 (Mr), 26.8 (mr), 22.1 (Mr), 21.6 (mr). Some signals from the minor regioisomer are missing. **HRMS** (APCI+) Calc. for $C_{20}H_{23}$ [M+H]$^+$: 263.1794 Found: 263.1796.

(*S*)-1-(*tert*-Butyl)-4-(3,3,4-trimethylcyclobut-1-en-1-yl)benzene (21ak)
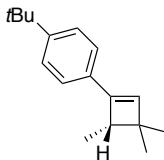
Cyclobutene **21ak** was synthetized following procedure C, from 4-*tert*-butylphenylacetylene (0.3 mmol, 47.5 mg) and 2-methylbut-2-ene (1.8 mmol, 126 mg). The reaction time was 36 h. The crude product was purified by silica gel flash column chromatography using pentane as eluent to give **21ak** as a colorless oil 17:1 mixture of regioisomers (58.4 mg, 0.255 mmol, 85% yield), 89:11 *er*. Major regioisomer (Mr), minor regioisomer (mr).

UNIVERSITAT ROVIRA I VIRGILI
COMPUTATIONAL MECHANISTIC STUDIES IN GOLD(I) CATALYSIS AND DESIGN OF NEW CHIRAL LIGANDS
Immaculada Escofet Miquel

Chapter III

$[\alpha]_D$ = +10.8 ° (c = 0.9, CHCl$_3$, 23 ºC). **^{1}H NMR** (500 MHz, CDCl$_3$) δ 7.36 – 7.32 (m, 2H, Mr), 7.31 – 7.27 (m, 2H, Mr), 6.28 (s, 1H, Mr), 6.23 (d, J = 1.3 Hz, 0.06H, mr), 2.79 (q, J = 7.1 Hz, 1H, Mr), 1.31 (s, 9H, Mr), 1.21 – 1.17 (m, 6H, Mr), 1.09 (s, 3H, Mr). **^{13}C NMR** (126 MHz, CDCl$_3$) δ 150.5 (Mr), 146.9 (Mr), 135.2 (Mr), 132.2 (Mr), 125.4 (mr), 125.4 (Mr), 125.1 (mr), 124.9 (Mr), 46.1 (Mr), 45.6 (mr), 42.4 (Mr), 42.3 (mr) 34.8 (Mr), 31.8 (mr), 31.6 (mr), 31.5 (Mr), 27.5 (Mr), 26.5 (mr), 21.9 (Mr), 21.7 (mr), 14.6 (mr), 14.3 (Mr). Some signals from the minor regioisomer are missing. **HRMS** (APCI+) Calc. for C$_{17}$H$_{25}$ [M+H]$^+$: 229.1951 Found: 229.1949.

(*S*)-1-(*tert*-Butyl)-4-(4-ethyl-3,3-dimethylcyclobut-1-en-1-yl)benzene (21aj)
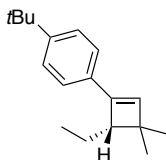
Cyclobutene **21aj** was synthetized following procedure C, from 4-*tert*-butylphenylacetylene (0.3 mmol, 47.5 mg) and 2-methylpent-2-ene (1.8 mmol, 151 mg) at 0 ºC. The reaction time was 36 h. The crude product was purified by silica gel flash column chromatography using pentane as eluent to give **21aj** as a colorless oil 12:1 mixture of regioisomers (56.0 mg, 0.234 mmol, 78% yield), 89:11 *er*. Major regioisomer (Mr), minor regioisomer (mr).

$[\alpha]_D$ = −16.4° (c = 0.7, CHCl$_3$, 24 ºC). **^{1}H NMR** (400 MHz, CDCl$_3$) δ 7.41 – 7.37 (m, 2H, Mr), 7.36 – 7.31 (m, 2H, Mr), 6.38 (d, J = 1.3 Hz, 0.9H, mr), 6.30 (s, 1H, Mr), 2.69 (dd, J = 10.6, 4.1 Hz, 1H, Mr), 1.92 – 1.81 (m, 1H, Mr), 1.57 – 1.47 (m, 1H, Mr), 1.36 (s, 9H, Mr), 1.29 (s, 3H, Mr), 1.22 (s, 3H, Mr), 1.05 (t, J = 7.4 Hz, 3H, Mr). **^{13}C NMR** (101 MHz, CDCl$_3$) δ 152.9 (Mr), 150.4 (Mr), 145.9 (Mr), 135.6 (Mr), 132.4 (Mr), 129.9 (mr), 128.8 (mr), 127.4 (mr), 125.4 (mr), 125.3 (Mr), 125.1 (mr), 125.0 (Mr), 53.9 (mr), 53.9 (Mr), 45.8 (mr), 43.0 (Mr), 34.8 (mr), 31.5 (Mr), 28.2 (Mr), 26.9 (mr), 23.1 (mr), 22.5 (Mr), 21.9 (Mr), 21.5 (mr), 13.6 (Mr), 12.8 (mr). Some signals from the minor regioisomer are missing. **HRMS** (+) Calc. for C$_{18}$H$_{27}$ [M+H]$^+$: 243.2107 Found: 243.2103.

(*S*)-1-Bromo-4-(3,3-dimethyl-4-phenethylcyclobut-1-en-1-yl)benzene (21an)
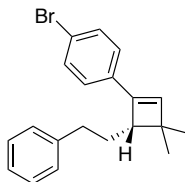
Cyclobutene **21an** was synthetized following procedure C, from 4-bromophenylacetylene (0.1 mmol, 18.1 mg) and (4-methylpent-3-en-1-yl)benzene (0.2 mmol, 32.1 mg). The reaction time was 20 h. The crude product was purified by silica gel flash column

UNIVERSITAT ROVIRA I VIRGILI
COMPUTATIONAL MECHANISTIC STUDIES IN GOLD(I) CATALYSIS AND DESIGN OF NEW CHIRAL LIGANDS
Immaculada Escofet Miquel

Chapter III

chromatography using pentane as eluent to give **21an** as a colorless oil >99:1 mixture of regioisomers (17.2 mg, 0.05 mmol, 50% yield), 85:15 *er*.

$[\alpha]_D$ = −17.0 ° (c = 0.1, CHCl₃, 24 ºC). **¹H NMR** (500 MHz, CDCl₃) δ 7.43 – 7.39 (m, 1H), 7.31 – 7.26 (m, 1H), 7.22 – 7.18 (m, 1H), 7.17 – 7.13 (m, 1H), 6.31 (s, 0H), 2.76 (td, J = 10.7, 4.3 Hz, 1H), 2.67 – 2.58 (m, 0H), 2.08 – 1.98 (m, 0H), 1.78 (dtd, J = 14.1, 10.4, 4.9 Hz, 0H), 1.27 (s, 1H), 1.23 (s, 1H). **¹³C NMR** (126 MHz, CDCl₃) δ 144.8, 142.6, 137.4, 133.8, 131.6, 128.5, 128.5, 126.8, 125.9, 121.2, 51.4, 43.3, 35.2, 31.3, 27.9, 21.9. **HRMS** (APCI+) Calc. for $C_{20}H_{22}Br$ [M+H]⁺: 341.0899 Found: 339.0735.

(*S*)-1-Chloro-4-(3,3,4-trimethylcyclobut-1-en-1-yl)benzene (21al)
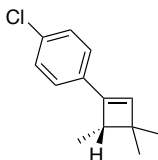
Cyclobutene **21al** was synthetized following procedure C, from 4-chlorophenylacetylene (0.3 mmol, 41 mg) and 2-methylbut-2-ene (1.8 mmol, 126 mg). The reaction time was 24 h. The crude product was purified by silica gel flash column chromatography using pentane as eluent to give **21al** as a colorless oil 6:1 mixture of regioisomers (23.6 mg, 0.114 mmol, 38% yield), 83:17 *er*. Major regioisomer (Mr), minor regioisomer (mr).

$[\alpha]_D$ = +15.0 ° (c = 0.06, CHCl₃, 24 ºC). **¹H NMR** (500 MHz, CDCl₃) δ 7.27 – 7.26 (m, 2H, Mr), 7.26 (s, 2H, Mr), 6.32 (s, 1H, Mr), 6.27 (d, J = 1.3 Hz, 0.16H, mr), 2.77 (q, J = 7.2 Hz, 1H, Mr), 1.21 (s, 3H, Mr), 1.17 (d, J = 7.2 Hz, 3H, Mr), 1.10 (s, 3H, Mr). **¹³C NMR** (126 MHz, CDCl₃) δ 145.9 (Mr), 140.0 (mr), 136.5 (Mr), 133.1 (Mr), 132.8 (mr), 131.4 (Mr), 128.6 (mr), 128.5 (Mr), 128.2 (mr), 127.1 (mr), 126.5 (mr), 126.3 (Mr), 46.0 (Mr), 42.5 (Mr), 27.2 (Mr), 26.2 (mr), 22.8 (mr), 21.6 (Mr), 19.8 (mr), 18.6 (mr), 14.2 (mr), 13.9 (Mr). Some signals from the minor regioisomer are missing. **HRMS** (APCI+) Calc. for $C_{13}H_{14}Cl$ [M+H]⁺: 205.0779 Found: 205.0779.

(*S*)-1-bromo-4-(3,3,4-trimethylcyclobut-1-en-1-yl)benzene (21am)
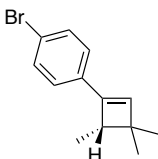
Cyclobutene **21am** was synthetized following procedure C, from 4-bromophenylacetylene (0.3 mmol, 54.3 mg) and 2-methylbut-2-ene (1.8 mmol, 126 mg). The reaction time was 24 h. The crude product was purified by silica gel flash column chromatography using pentane as eluent to give **21am** as a colorless oil 8:1 mixture of regioisomers (58.9 mg, 0.234 mmol, 78% yield), 83:17 *er*. Major regioisomer (Mr), minor regioisomer (mr).

UNIVERSITAT ROVIRA I VIRGILI
COMPUTATIONAL MECHANISTIC STUDIES IN GOLD(I) CATALYSIS AND DESIGN OF NEW CHIRAL LIGANDS
Immaculada Escofet Miquel

Chapter III

[α]$_D$ = +7.9 ° (c = 0.5, CHCl$_3$, 24 ºC). **^{1}H NMR** (500 MHz, CDCl$_3$) δ 7.45 – 7.40 (m, 2.24H, Mr + mr), 7.21 – 7.17 (m, 2.24H, Mr + mr), 6.34 (s, 1H, Mr), 6.29 (d, J = 1.3 Hz, 0.12H, mr), 2.78 (q, J = 7.2 Hz, 1H, Mr), 2.46 (qd, J = 7.1, 1.3 Hz, 0.12H, mr), 1.34 (s, 0.36H, mr), 1.22 (s, 0.36H, mr), 1.21 (s, 3H, Mr), 1.17 (d, J = 7.1 Hz, 3H, Mr), 1.10 (s, 3H, Mr), 1.07 (d, J = 7.2 Hz, 0.36H, mr). **^{13}C NMR** (126 MHz, CDCl$_3$) δ 146.0 (Mr), 136.9 (Mr), 133.7 (Mr), 131.7 (mr), 131.6 (Mr), 126.9 (mr), 126.8 (Mr), 121.1 (Mr), 46.1 (Mr), 42.6 (Mr), 27.3 (Mr), 21.7 (Mr), 21.5 (mr), 14.3 (mr), 14.1 (Mr). Some signals from the minor regioisomer are missing. **HRMS** (APCI+) Calc. for C$_{13}$H$_{14}$Br [M-H]$^+$: 249.0273 Found: 249.0270.

(*S*)-1-Chloro-4-(4-ethyl-3,3-dimethylcyclobut-1-en-1-yl)benzene (21ao)
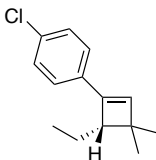
Cyclobutene **21ao** was synthetized following procedure C, from 4-chlorophenylacetylene (0.3 mmol, 41 mg) and 2-methylpent-2-ene (1.8 mmol, 151 mg) at 0 ºC. The reaction time was 36 h. The formation of 1,3-diene was observed in the crude product in a ratio of 10:2:1. The crude product was purified by silica gel flash column chromatography using pentane as eluent to give **21ao** as a colorless oil 4:1 mixture of regioisomers (58.0 mg, 0.264 mmol, 88% yield), 86:14 *er*. Major regioisomer (Mr), minor regioisomer (mr).

[α]$_D$ = −28.5 ° (c = 0.03, CHCl$_3$, 24 ºC). **^{1}H NMR** (500 MHz, CDCl$_3$) δ 7.28 – 7.23 (m, 5H, Mr + mr), 6.36 (d, J = 1.3 Hz, 0.25H, mr), 6.28 (s, 1H, Mr), 2.62 (dd, J = 10.6, 4.1 Hz, 1H, Mr), 2.32 – 2.24 (m, 0.25H, mr), 1.83 – 1.70 (m, 1.25H, Mr + mr), 1.51 – 1.40 (m, 1.25H, Mr + mr), 1.37 (s, 0.75H, mr), 1.26 (s, 0.25H), 1.25 (s, 3H, Mr), 1.16 (s, 3H, Mr), 1.02 – 0.94 (m, 3.75H, Mr + mr). **^{13}C NMR** (101 MHz, CDCl$_3$) δ 151.8 (mr), 145.0 (Mr), 137.1 (Mr), 133.6 (Mr), 132.9 (Mr), 129.1 (mr), 128.7 (mr), 128.6 (Mr), 126.6 (mr), 126.6 (Mr), 54.0 (mr), 53.8 (Mr), 43.2 (Mr), 28.0 (Mr), 26.7 (mr), 22.9 (mr), 22.3 (Mr), 21.8 (Mr), 21.3 (mr), 14.2 (mr), 13.4 (Mr), 12.8 (mr). Some signals from the minor regioisomer are missing. **HRMS** (APCI+) Calc. for C$_{14}$H$_{16}$Cl [M+H]$^+$: 219.0935 Found: 219.0928.

(*S*)-1-Bromo-4-(4-ethyl-3,3-dimethylcyclobut-1-en-1-yl)benzene (21ap)
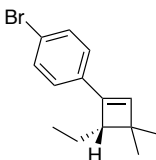
Cyclobutene **21ap** was synthetized following procedure C, from 4-bromophenylacetylene (0.3 mmol, 54.3 mg) and 2-methylpent-2-ene (1.8 mmol, 151 mg) at 25 ºC. The reaction time was 36 h. The formation of 1,3-diene was observed in the crude product in a ratio of 10:2:1 (Mr:mr:1,3-diene). The crude product was purified by silica gel flash column

UNIVERSITAT ROVIRA I VIRGILI
COMPUTATIONAL MECHANISTIC STUDIES IN GOLD(I) CATALYSIS AND DESIGN OF NEW CHIRAL LIGANDS
Immaculada Escofet Miquel

Chapter III

chromatography using pentane as eluent to give **21ap** as a colorless oil 5:1 mixture of regioisomers (61.7 mg, 0.234 mmol, 78% yield), 83:17 *er*. Major regioisomer (Mr), minor regioisomer (mr).

$[\alpha]_D$ = −5.0 ° (c = 0.7, CHCl$_3$, 24 ºC). **^{1}H NMR** (400 MHz, CDCl$_3$) δ 7.45 – 7.39 (m, 2H, Mr), 7.24 – 7.20 (m, 0.4H, mr), 7.20 – 7.15 (m, 2H, Mr), 6.38 (d, *J* = 1.4 Hz, 0.2H, mr), 6.30 (s, 1H, Mr), 2.63 (dd, *J* = 10.5, 4.2 Hz, 1H, Mr), 2.31 – 2.23 (m, 0.2H, mr), 1.82 – 1.69 (m, 1.2H, Mr + mr), 1.52 – 1.40 (m, 1.2H, Mr + mr), 1.37 (s, 0.6H, mr), 1.26 (s, 0.2H, mr), 1.25 (s, 3H, Mr), 1.16 (s, 3H, Mr), 1.03 – 0.95 (m, 3.60H, Mr + mr). **^{13}C NMR** (75 MHz, CDCl$_3$) δ 145.1 (Mr), 137.4 (Mr), 134.0 (Mr), 131.7 (mr), 131.5 (Mr), 126.9 (mr), 126.9 (Mr), 121.1 (Mr), 53.8 (Mr), 43.2 (Mr), 28.0 (Mr), 22.3 (Mr), 21.7 (Mr), 13.4 (Mr). Some signals from the minor regioisomer are missing. **HRMS** (APCI+) Calc. for C$_{14}$H$_{18}$Br [M+H]$^+$: 265.0586 Found: 265.0581.

General procedure for the enantioselective gold(I)-catalyzed [4+2] annulation

Alkyne (0.3 mmol) and alkene (1.5 mmol) were added to a solution of **49**-(*S*,*R*$_P$)-**D** (2.5 mol %) in dichloromethane (0.1 M), followed by the addition of NaBAr$_4^F$ (2.5 mol %) at 25 ºC. The mixture was stirred for 24h at 25 ºC. The reaction was quenched adding a drop of NEt$_3$ and concentrated in vacuo. Purification by flash column chromatography or preparative TLC (silica gel) afforded the corresponding lactones.

(*R*)-5,6,6-trimethyl-5,6-dihydro-2*H*-pyran-2-one (50)
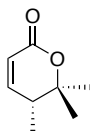
Lactorne **50** was synthetized from 2-methyl-2-butene **20m** (105.2 mg, 1.5 mmol) and *tert*-butyl propiolate **19j** (37.8 mg, 0.30 mmol) at 25 ºC. The reaction time was 24 h. The crude product was purified by silica gel flash column chromatography using cyclohexane/ethyl acetate 5:1 to give **50** as a colorless oil (56.9 mg, 0.216 mmol, 72% yield), 84:16 *er*. The analytical data corresponds to the one reported.[56]

^{1}H NMR (400 MHz, CDCl$_3$): 6.62 (dd, *J* = 9.7, 3.8 Hz, 1H), 5.97 (dd, *J* = 9.8, 2.1 Hz, 1H), 2.57-2.49 (m, 1H), 1.45 (s, 3H), 1.33 (s, 3H), 1.11 (d, *J* = 7.4 Hz, 3H). **^{13}C NMR** (101 MHz, CDCl$_3$): 164.04 , 149.98 , 120.09 , 83.40 , 38.15 , 29.85 , 22.73 , 15.13 .

UNIVERSITAT ROVIRA I VIRGILI
COMPUTATIONAL MECHANISTIC STUDIES IN GOLD(I) CATALYSIS AND DESIGN OF NEW CHIRAL LIGANDS
Immaculada Escofet Miquel

Chapter III

Crystallographic Data

Complex 48(AuCl)a
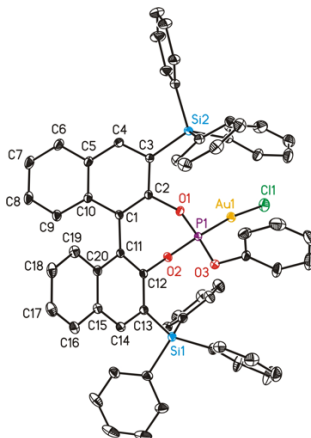
Table 19. Crystal data and structure refinement for **48(AuCl)a**.

Identification code	CBO416_0m
Empirical formula	C62 H45 Au Cl O3 P Si2
Formula weight	1157.55
Temperature	100(2) K
Wavelength	0.71073 Å
Crystal system	Orthorhombic
Space group	P2(1)2(1)2(1)
Unit cell dimensions	a = 9.7873(3) Å a= 90.00 °.
	b = 12.8393(4) Å b = 90.00 °.
	c = 39.6173(13) Å g = 90.00 °.
Volume	4978.4(3) Å^3
Z	4
Density (calculated)	1.544 Mg/m^3
Absorption coefficient	3.137 mm^{-1}
F(000)	2320
Crystal size	0.3 x 0.15 x 0.1 mm^3
Theta range for data collection	2.62 to 39.97 °.
Index ranges	-16 <=h<=10 ,-22 <=k<=16 ,-70 <=l<=62
Reflections collected	70648
Independent reflections	27809 [R(int) = 0.0330]
Completeness to theta =39.97 °	0.952 %
Absorption correction	Empirical
Max. and min. transmission	0.7444 and 0.4529
Refinement method	Full-matrix least-squares on F^2
Data / restraints / parameters	27809 / 0 / 631
Goodness-of-fit on F^2	1.118
Final R indices [I>2sigma(I)]	R1 = 0.0360 , wR2 = 0.0841
R indices (all data)	R1 = 0.0389 , wR2 = 0.0850
Largest diff. peak and hole	3.589 and -3.318 e.Å^{-3}

UNIVERSITAT ROVIRA I VIRGILI
COMPUTATIONAL MECHANISTIC STUDIES IN GOLD(I) CATALYSIS AND DESIGN OF NEW CHIRAL LIGANDS
Immaculada Escofet Miquel

Chapter III
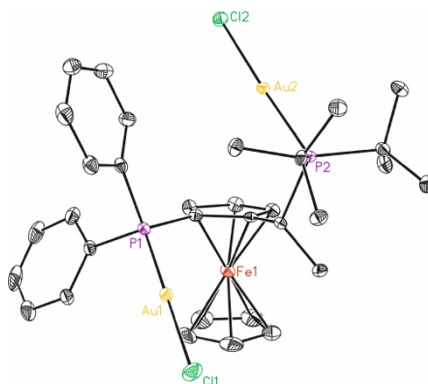
Complex (*S*,*R*$_P$)-A

Table 20. Crystal data and structure refinement for complex **49-(*S*,*R*$_P$)-A**. Absolute configuration was determined.

Deposition number at CCDC	**CCDC 1563807**
Identification code	mo_CG341c_0m
Empirical formula	C64 H80 Au4 Cl4 Fe2 P4
Formula weight	2014.52
Temperature	100(2) K
Wavelength	0.71073 Å
Crystal system	Orthorhombic
Space group	P2(1)2(1)2(1)
Unit cell dimensions	a = 8.6631(2)Å a = 90°.
	b = 11.5159(3)Å b = 90°.
	c = 33.5456(9)Å g = 90°.
Volume	3346.62(15) Å^3
Z	2
Density (calculated)	1.999 Mg/m^3
Absorption coefficient	9.449 mm^{-1}
F(000)	1920
Crystal size	0.20 x 0.20 x 0.10 mm^3
Theta range for data collection	1.214 to 35.010°.
Index ranges	-12<=h<=7,-15<=k<=18,-36<=l<=53
Reflections collected	28510
Independent reflections	13019[R(int) = 0.0225]
Completeness to theta =35.010°	92.4%
Absorption correction	Multi-scan
Max. and min. transmission	0.452 and 0.359
Refinement method	Full-matrix least-squares on F^2
Data / restraints / parameters	13019/ 0/ 359
Goodness-of-fit on F^2	1.084
Final R indices [I>2sigma(I)]	R1 = 0.0237, wR2 = 0.0476
R indices (all data)	R1 = 0.0260, wR2 = 0.0536
Flack parameter	x =-0.010(3)
Largest diff. peak and hole	1.916 and -1.234 e.Å^{-3}

UNIVERSITAT ROVIRA I VIRGILI
COMPUTATIONAL MECHANISTIC STUDIES IN GOLD(I) CATALYSIS AND DESIGN OF NEW CHIRAL LIGANDS
Immaculada Escofet Miquel

Chapter III

Complex 49-(*S*,*R*$_P$)-B and 49-(*S*,*R*$_P$)-O
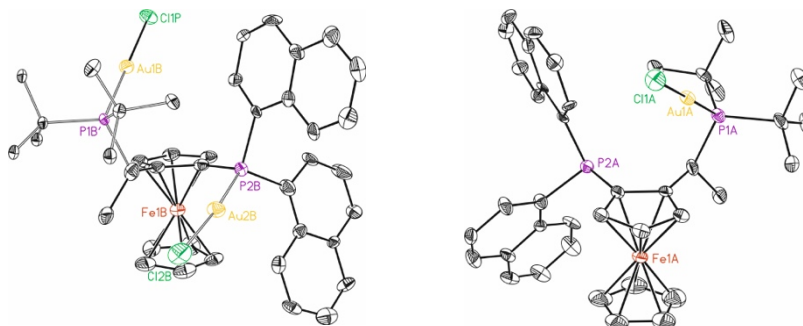
Table 21. Crystal data and structure refinement for IE-JosiPhosMAuCl2. Absolute configuration was determined. The crystal was formed for a mixture of **49-(*S*,*R*$_P$)-O** and **49-(*S*,*R*$_P$)-B**, 9:1.

Depostion number at CCDC	**CCDC 1563811**
Identification code	IE-JosiPhosMAuCl2
Empirical formula	C40.40 H44.80 Au1.10 Cl1.90 Fe P2
Formula weight	932.17
Temperature	100(2) K
Wavelength	0.71073 ≈
Crystal system	Orthorhombic
Space group	P2(1)2(1)2(1)
Unit cell dimensions	a = 14.788(3)≈ a = 90º.
	b = 18.134(4)≈ b = 90º.
	c = 28.447(6)≈ g = 90º.
Volume	7629(3) ≈^{3}
Z	8
Density (calculated)	1.623 Mg/m^3
Absorption coefficient	4.849 mm^{-1}
F(000)	3699
Crystal size	0.20 x 0.20 x 0.20 mm^3
Theta range for data collection	2.246 to 26.373∞.
Index ranges	-18<=h<=18,-22<=k<=22,-35<=l<=34
Reflections collected	43920
Independent reflections	15132[R(int) = 0.0737]
Completeness to theta =26.373∞	99.0%
Absorption correction	Multi-scan
Max. and min. transmission	0.444 and 0.342
Refinement method	Full-matrix least-squares on F^2
Data / restraints / parameters	15132/ 405/ 985
Goodness-of-fit on F^2	1.151
Final R indices [I>2sigma(I)]	R1 = 0.0511, wR2 = 0.0781
R indices (all data)	R1 = 0.0959, wR2 = 0.1000
Flack parameter	x =-0.017(9)
Largest diff. peak and hole	1.535 and -1.150 e.≈$^{-3}$

UNIVERSITAT ROVIRA I VIRGILI
COMPUTATIONAL MECHANISTIC STUDIES IN GOLD(I) CATALYSIS AND DESIGN OF NEW CHIRAL LIGANDS
Immaculada Escofet Miquel

Chapter III
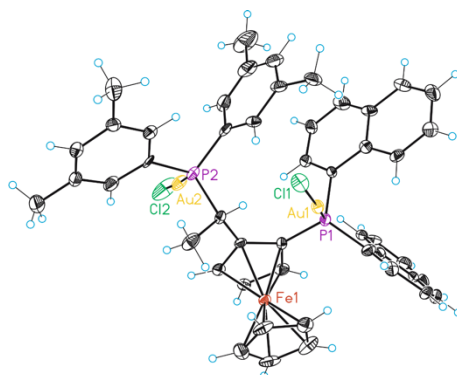
Complex 49-(S,R_P)-F

Table 22. Crystal data and structure refinement for complex **49-(S,R_P)-F**. Absolute configuration was determined.

Depostion number at CCDC	**CCDC 1563812**
Identification code	mo_BR688_0m
Empirical formula	C48.50 H45 Au2 Cl3 Fe P2
Formula weight	1245.92
Temperature	100(2) K
Wavelength	0.71073 Å
Crystal system	Monoclinic
Space group	P2(1)
Unit cell dimensions	a = 10.7462(8)Å a = 90°.
	b = 10.3072(9)Å b = 90.695(4)°.
	c = 20.126(3)Å g = 90°.
Volume	2229.1(4) Å^3
Z	2
Density (calculated)	1.856 Mg/m^3
Absorption coefficient	7.172 mm^{-1}
F(000)	1202
Crystal size	0.25 x 0.15 x 0.12 mm^3
Theta range for data collection	1.012 to 30.049°.
Index ranges	-15<=h<=12,-13<=k<=14,-27<=l<=27
Reflections collected	22601
Independent reflections	10444[R(int) = 0.0437]
Completeness to theta =30.049°	89.4%
Absorption correction	Empirical
Max. and min. transmission	0.480 and 0.282
Refinement method	Full-matrix least-squares on F^2
Data / restraints / parameters	10444/ 60/ 547
Goodness-of-fit on F^2	1.018
Final R indices [I>2sigma(I)]	R1 = 0.0408, wR2 = 0.0883
R indices (all data)	R1 = 0.0496, wR2 = 0.0940
Flack parameter	x =-0.026(6)
Largest diff. peak and hole	2.077 and -1.053 e.Å^{-3}

UNIVERSITAT ROVIRA I VIRGILI
COMPUTATIONAL MECHANISTIC STUDIES IN GOLD(I) CATALYSIS AND DESIGN OF NEW CHIRAL LIGANDS
Immaculada Escofet Miquel

Chapter III

(*R*)-3-*p*-Bromophenyl-1-phenyl-3-methylcyclobut-1-ene (21f)
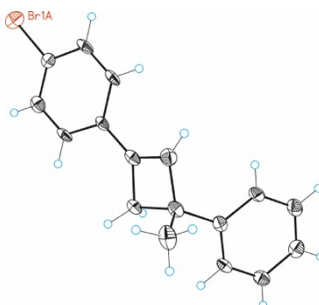
Table 23. Crystal data and structure refinement for **21f**. Absolute configuration was determined.

Depostion number at CCDC	**CCDC 1563806**
Identification code	CG-3-104
Empirical formula	C17 H15 Br
Formula weight	299.20
Temperature	100(2) K
Wavelength	0.71073 Å
Crystal system	Monoclinic
Space group	P2(1)
Unit cell dimensions	a = 6.0054(7)Å a = 90°.
	b = 31.426(4)Å b = 90.918(7)°.
	c = 7.3514(10)Å g = 90°.
Volume	1387.2(3) Å^3
Z	4
Density (calculated)	1.433 Mg/m^3
Absorption coefficient	2.943 mm^{-1}
F(000)	608
Crystal size	0.20 x 0.20 x 0.20 mm^3
Theta range for data collection	2.592 to 28.280°.
Index ranges	-8<=h<=8,-41<=k<=41,-9<=l<=9
Reflections collected	20099
Independent reflections	6327[R(int) = 0.0810]
Completeness to theta =28.280°	98.9%
Absorption correction	Multi-scan
Max. and min. transmission	0.591 and 0.455
Refinement method	Full-matrix least-squares on F^2
Data / restraints / parameters	6327/ 1/ 327
Goodness-of-fit on F^2	1.174
Final R indices [I>2sigma(I)]	R1 = 0.0791, wR2 = 0.1903
R indices (all data)	R1 = 0.0864, wR2 = 0.1934
Flack parameter	x =0.020(12)
Largest diff. peak and hole	2.703 and -1.993 e.Å^{-3}

UNIVERSITAT ROVIRA I VIRGILI
COMPUTATIONAL MECHANISTIC STUDIES IN GOLD(I) CATALYSIS AND DESIGN OF NEW CHIRAL LIGANDS
Immaculada Escofet Miquel

Chapter III

3-*p-tert*-Butylphenyl-1-*p-tert*butylphenyl-3-methylcyclobut-1-ene (21u)
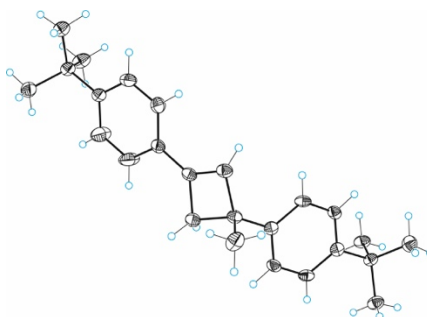
Table 24. Crystal data and structure refinement for **21u**.

Depostion number at CCDC	**CCDC 1563808**
Identification code	CG3_49
Empirical formula	C25 H32
Formula weight	332.50
Temperature	100(2) K
Wavelength	0.71073 Å
Crystal system	Monoclinic
Space group	P2(1)
Unit cell dimensions	a = 10.1094(6)Å α= 90°.
	b = 6.1675(4)Å β = 91.584(6)°.
	c = 16.2477(12)Å γ = 90°.
Volume	1012.66(12) Å^3
Z	2
Density (calculated)	1.090 Mg/m^3
Absorption coefficient	0.061 mm^{-1}
F(000)	364
Crystal size	0.15 x 0.10 x 0.04 mm^3
Theta range for data collection	2.344 to 30.190°.
Index ranges	-12<=h<=14,-8<=k<=8,-21<=l<=21
Reflections collected	13423
Independent reflections	5030[R(int) = 0.0717]
Completeness to theta =30.190°	89.3%
Absorption correction	Multi-scan
Max. and min. transmission	0.998 and 0.768
Refinement method	Full-matrix least-squares on F^2
Data / restraints / parameters	5030/ 1/ 233
Goodness-of-fit on F^2	1.044
Final R indices [I>2sigma(I)]	R1 = 0.0703, wR2 = 0.1616
R indices (all data)	R1 = 0.1045, wR2 = 0.1777
Largest diff. peak and hole	0.422 and -0.286 e.Å^{-3}

UNIVERSITAT ROVIRA I VIRGILI
COMPUTATIONAL MECHANISTIC STUDIES IN GOLD(I) CATALYSIS AND DESIGN OF NEW CHIRAL LIGANDS
Immaculada Escofet Miquel

Chapter III

(*R*)-3-Phenyl-1-(thiophen-3-yl) -3-methylcyclobut-1-ene (21v)
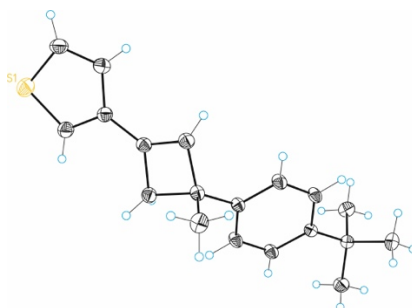
Table 25. Crystal data and structure refinement for **21v**. Absolute configuration was determined.

Depostion number at CCDC	**CCDC 1563810**
Identification code	CG-3-498-2a
Empirical formula	C19 H22 S
Formula weight	282.42
Temperature	100(2) K
Wavelength	0.71073 Å
Crystal system	Monoclinic
Space group	P2(1)
Unit cell dimensions	a = 8.3202(3)Å a = 90°.
	b = 6.0778(2)Å b = 98.970(3)°.
	c = 16.2853(5)Å g = 90°.
Volume	813.45(5) Å^3
Z	2
Density (calculated)	1.153 Mg/m^3
Absorption coefficient	0.188 mm^{-1}
F(000)	304
Crystal size	0.15 x 0.1 x 0.04 mm^3
Theta range for data collection	2.478 to 37.314°.
Index ranges	-14<=h<=14,-10<=k<=10,-27<=l<=27
Reflections collected	34968
Independent reflections	8189[R(int) = 0.0455]
Completeness to theta =37.314°	98.4%
Absorption correction	Multi-scan
Max. and min. transmission	0.993 and 0.764
Refinement method	Full-matrix least-squares on F^2
Data / restraints / parameters	8189/ 1/ 185
Goodness-of-fit on F^2	1.037
Final R indices [I>2sigma(I)]	R1 = 0.0473, wR2 = 0.1222
R indices (all data)	R1 = 0.0581, wR2 = 0.1284
Flack parameter	x =0.01(2)
Largest diff. peak and hole	0.526 and -0.516 e.Å^{-3}

UNIVERSITAT ROVIRA I VIRGILI
COMPUTATIONAL MECHANISTIC STUDIES IN GOLD(I) CATALYSIS AND DESIGN OF NEW CHIRAL LIGANDS
Immaculada Escofet Miquel

Chapter III

1,4-Bis-[3-(4-fluorophenyl)-3-methylcyclobut-1-en-1-yl]benzene (21ad)
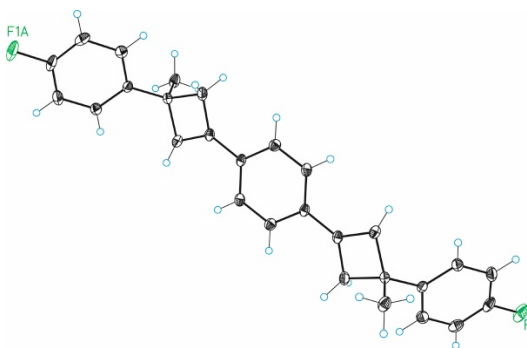
Table 26. Crystal data and structure refinement for **21ad**.

Depostion number at CCDC	**CCDC 1563805**
Identification code	mo_CG30531_0m
Empirical formula	C28 H24 F2
Formula weight	398.47
Temperature	100(2) K
Wavelength	0.71073 Å
Crystal system	Monoclinic
Space group	C2/c
Unit cell dimensions	a = 23.1418(14)Å a= 90°.
	b = 5.7036(3)Å b = 101.5997(19)°.
	c = 15.8393(10)Å g = 90°.
Volume	2048.0(2) Å^3
Z	4
Density (calculated)	1.292 Mg/m^3
Absorption coefficient	0.086 mm^{-1}
F(000)	840
Crystal size	0.15 x 0.05 x 0.01 mm^3
Theta range for data collection	1.797 to 29.653°.
Index ranges	-32<=h<=29,-7<=k<=7,-19<=l<=22
Reflections collected	16858
Independent reflections	2882[R(int) = 0.0482]
Completeness to theta =29.653°	99.7%
Absorption correction	Multi-scan
Max. and min. transmission	0.999 and 0.915
Refinement method	Full-matrix least-squares on F^2
Data / restraints / parameters	2882/ 0/ 137
Goodness-of-fit on F^2	1.159
Final R indices [I>2sigma(I)]	R1 = 0.0710, wR2 = 0.1474
R indices (all data)	R1 = 0.0920, wR2 = 0.1551
Largest diff. peak and hole	0.421 and -0.351 e.Å^{-3}

UNIVERSITAT ROVIRA I VIRGILI
COMPUTATIONAL MECHANISTIC STUDIES IN GOLD(I) CATALYSIS AND DESIGN OF NEW CHIRAL LIGANDS
Immaculada Escofet Miquel

Chapter III

1,4-Bis-[3-(4-(*tert*-butyl)phenyl)-1-methylcyclobut-2-en-1-yl]benzene (21ae)
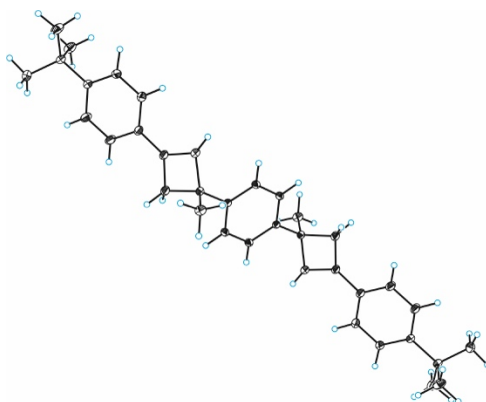
Table 27. Crystal data and structure refinement for **21ae**.

Depostion number at CCDC	**CCDC 1563809**
Identification code	CG-3-0574_P21
Empirical formula	C36 H42
Formula weight	474.69
Temperature	100(2) K
Wavelength	0.71073 Å
Crystal system	Monoclinic
Space group	P2(1)
Unit cell dimensions	a = 15.4670(5)Å a = 90°.
	b = 6.10912(17)Å b = 115.627(4)°.
	c = 16.5386(5)Å g = 90°.
Volume	1409.00(8) Å^3
Z	2
Density (calculated)	1.119 Mg/m^3
Absorption coefficient	0.062 mm^{-1}
F(000)	516
Crystal size	0.2 x 0.15 x 0.1 mm^3
Theta range for data collection	2.392 to 64.554°.
Index ranges	-25<=h<=38,-11<=k<=12,-41<=l<=37
Reflections collected	59815
Independent reflections	28367[R(int) = 0.0334]
Completeness to theta =64.554°	70.9%
Absorption correction	Multi-scan
Max. and min. transmission	0.994 and 0.765
Refinement method	Full-matrix least-squares on F^2
Data / restraints / parameters	28367/ 2/ 485
Goodness-of-fit on F^2	0.725
Final R indices [I>2sigma(I)]	R1 = 0.0422, wR2 = 0.1199
R indices (all data)	R1 = 0.0581, wR2 = 0.1351
Flack parameter	x =-4.3(10)
Largest diff. peak and hole	0.591 and -0.306 e.Å^{-3}

UNIVERSITAT ROVIRA I VIRGILI
COMPUTATIONAL MECHANISTIC STUDIES IN GOLD(I) CATALYSIS AND DESIGN OF NEW CHIRAL LIGANDS
Immaculada Escofet Miquel

Chapter III

Computational Methods

Calculations were performed by means of the Gaussian 09 suite of programs.[74] DFT was applied using BP86-D3 that has proved its efficiency in other DFT studies of gold-catalyzed transformations.[75] The SDD basis set and ECP was used to describe Au.[76] The 6-31G(d) basis set[77] was employed for all remaining atoms (C, H, P, F, O and N). Full geometry optimizations were carried out in dichloromethane, through an implicit polarizable continuum model (PCM).[78] The stationary points were characterized by vibrational analysis. Transition states were identified by the presence of one imaginary frequency while minima by a full set of real frequencies. The connectivity of the transition states was confirmed by the relaxation of each transition state towards both the reactant and the product or, in some cases, by IRC[79] calculations. NCIPlot was used to obtain the grid data for NCI (non-covalent interactions) analysis[80] and the corresponding results were visualized with the VMD software.[81] Reported energies are potential energies (E) and free energies (G) in solution, computed at 298 K and 1 atm.

A dataset collection of computational results of this chapter is available in the ioChem-BD[82] repository and can be accessed through: https://doi.org/10.19061/iochem-bd-1-166.

74   Gaussian 09, Revision B.1, Frisch, M. J.; Trucks, G. W.; Schlegel, H. B.; Scuseria, G. E.; Robb, M. A.; Cheeseman, J. R.; Scalmani, G.; Barone, V.; Mennucci, B.; Petersson, G. A.; Nakatsuji, H.; Caricato, M.; Li, X.; Hratchian, H. P.; Izmaylov, A. F.; Bloino, J.; Zheng, G.; Sonnenberg, J. L.; Hada, M.; Ehara, M.; Toyota, K.; Fukuda, R.; Hasegawa, J.; Ishida, M.; Nakajima, T.; Honda, Y.; Kitao, O.; Nakai, H.; Vreven, T.; Montgomery, J. A.; Peralta, Jr. J. E.; Ogliaro, F.; Bearpark, M.; Heyd, J. J.; Brothers, E.; Kudin, K. N.; Staroverov, V. N.; Kobayashi, R.; Normand, J.; Raghavachari, K.; Rendell, A.; Burant, J. C.; Iyengar, S. S.; Tomasi, J.; Cossi, M.; Rega, N.; Millam, J. M.; Klene, M.; Knox, J. E.; Cross, J. B.; Bakken, V.; Adamo, C.; Jaramillo, J.; Gomperts, R.; Stratmann, R. E.; Yazyev, O.; Austin, A. J.; Cammi, R.; Pomelli, C.; Ochterski, J. W.; Martin, R. L.; Morokuma, K.; Zakrzewski, V. G.; Voth, G. A.; Salvador, P.; Dannenberg, J. J.; Dapprich, S.; Daniels, A. D.; Farkas, Ö.; Foresman, J. B.; Ortiz, J. V.; Cioslowski, J.; Fox, D. J. Gaussian, Inc., Wallingford CT **2009**.

75   (a) Kang, R., Chen, H., Shaik, S., Yao, J. *J. Chem. Theory Comput.* **2011**, 7, 4002−4011. (b) Ciancaleoni, G.; Rampino, S.; Zuccaccia, D.; Tarantelli, F.; Belanzoni, P.; Belpassi, L. *J. Chem. Theory Comput.* **2014**, *10*, 1021−1034.

76   Andrae, D.; Haussermann, U.; Dolg, M.; Stoll, H.; Preuss, H. *Theor. Chim. Acta.* **1990**, *77*, 123–141.

77   Hehre, W. J.; Ditchfield, R.; Pople, J. A. *J. Chem. Phys.* **1972**, *56*, 2257–2261.

78   Cancès, M. T.; Mennucci, B. B.; Tomasi, J. *J. Chem. Phys.* **1997**, *107*, 3032−3041.

79   Gonzalez, C., Schlegel, H. B., *J. Phys. Chem.* **1990**, *94,* 5523−5527.

80   (a) Johnson, E. R.; Keinan, S.; Mori-Sanchez, P.; Contreras-Garcia, J.; Cohen, A. J.; Yang, W. *J. Am. Chem. Soc.* **2010**, *132*, 6498–6506. (b) Contreras-Garcia, J.; Johnson, E. R.; Keinan, S.; Chaudret, R.; Piquemal, J. P.; Beratan, D. N.; Yang, W. *J. Chem. Theory Comput.* **2011**, *7*, 625–632.

81   Humphrey, W.; Dalke, A.; Schulten, K. *J. Mol. Graphics.* **1996**, *14*, 33–38.

82   Álvarez-Moreno, M.; de Graaf, C.; Lopez, N.; Maseras, F.; Poblet, J. M.; Bo, C. *J. Chem. Inf. Model.* **2015**, *55*, 95−103.

UNIVERSITAT ROVIRA I VIRGILI
COMPUTATIONAL MECHANISTIC STUDIES IN GOLD(I) CATALYSIS AND DESIGN OF NEW CHIRAL LIGANDS
Immaculada Escofet Miquel

Chapter III

NCI Plots

A-TS_{Int1a-2a}

A-TS_{Int1c-2c}

B-TS_{Int1d-2d}

B-TS_{Int1b-2b}

UNIVERSITAT ROVIRA I VIRGILI
COMPUTATIONAL MECHANISTIC STUDIES IN GOLD(I) CATALYSIS AND DESIGN OF NEW CHIRAL LIGANDS
Immaculada Escofet Miquel

Chapter III
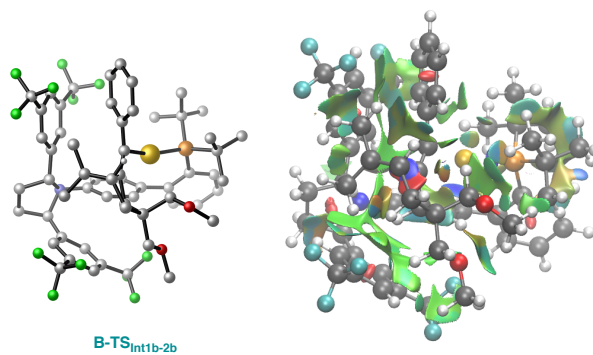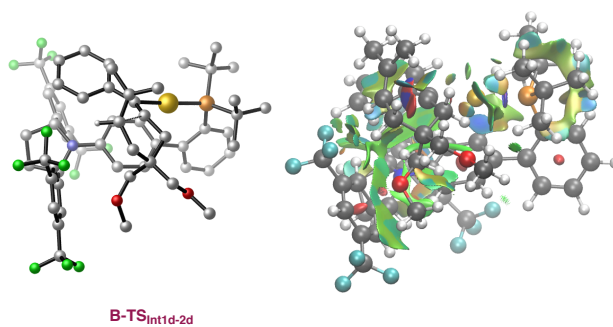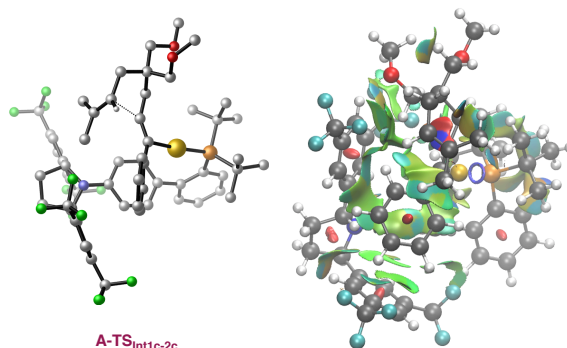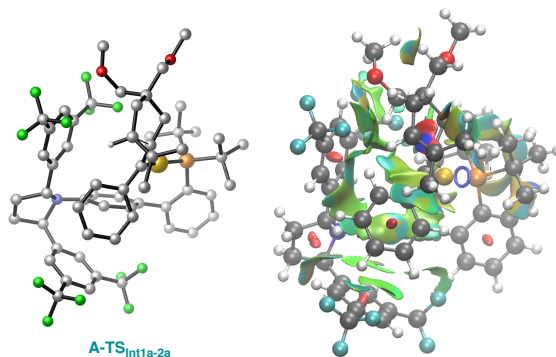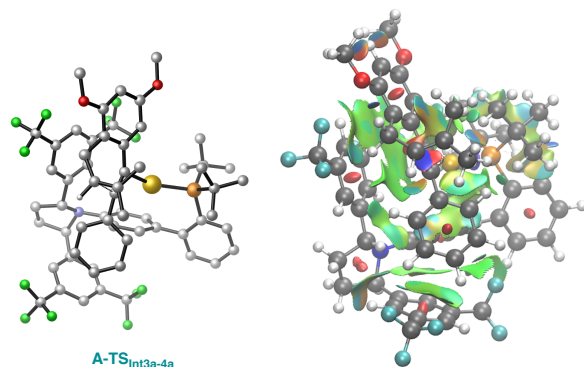
A-TS_{Int3a-4a}
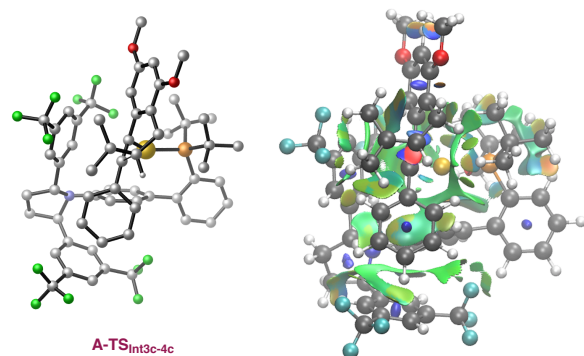
A-TS_{Int3c-4c}

B-TS_{Int3d-4d}

B-TS_{Int3b-4b}

UNIVERSITAT ROVIRA I VIRGILI
COMPUTATIONAL MECHANISTIC STUDIES IN GOLD(I) CATALYSIS AND DESIGN OF NEW CHIRAL LIGANDS
Immaculada Escofet Miquel

Chapter III
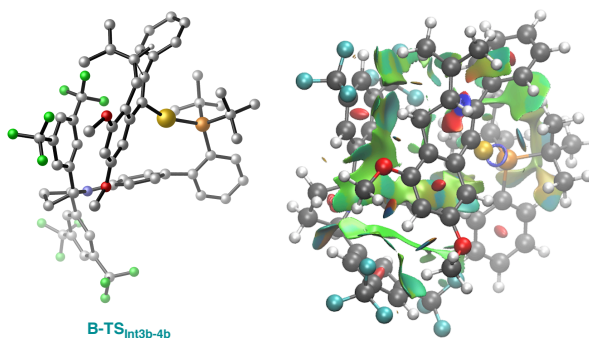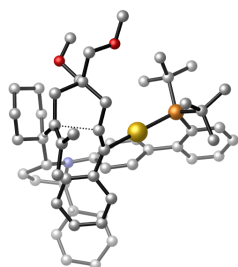
A-TS_{Int5a-6a}
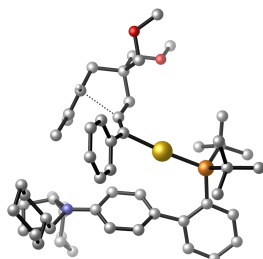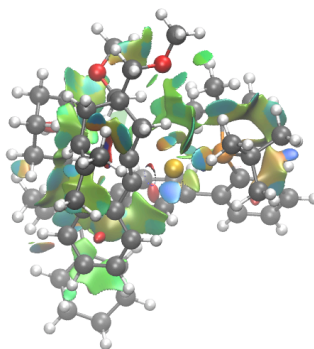
A-TS_{Int5c-6c}

B-TS_{Int5d-6d}

B-TS_{Int5b-6b}

UNIVERSITAT ROVIRA I VIRGILI
COMPUTATIONAL MECHANISTIC STUDIES IN GOLD(I) CATALYSIS AND DESIGN OF NEW CHIRAL LIGANDS
Immaculada Escofet Miquel

Chapter III

A-TS$_{Int7a-8a}$

A-TS$_{Int7c-8c}$

B-TS$_{Int7d-8d}$

B-TS$_{Int7b-8b}$

UNIVERSITAT ROVIRA I VIRGILI
COMPUTATIONAL MECHANISTIC STUDIES IN GOLD(I) CATALYSIS AND DESIGN OF NEW CHIRAL LIGANDS
Immaculada Escofet Miquel

Chapter III
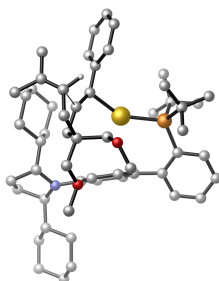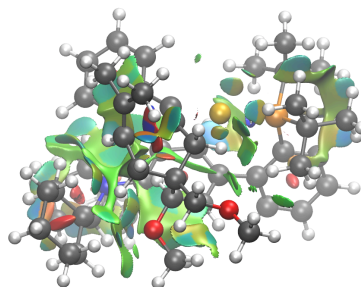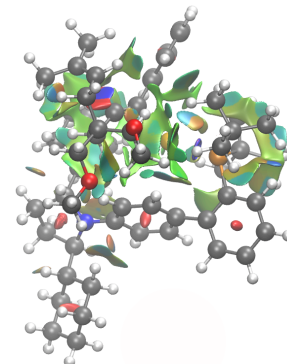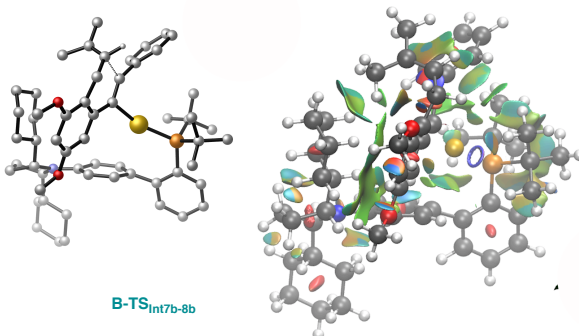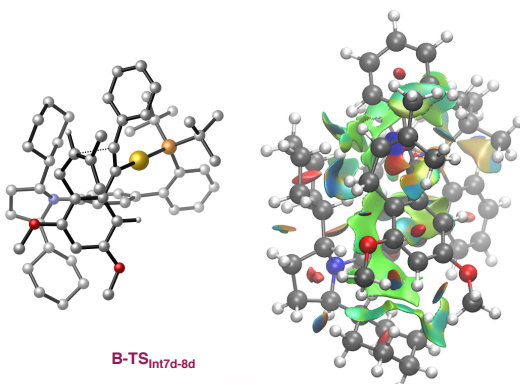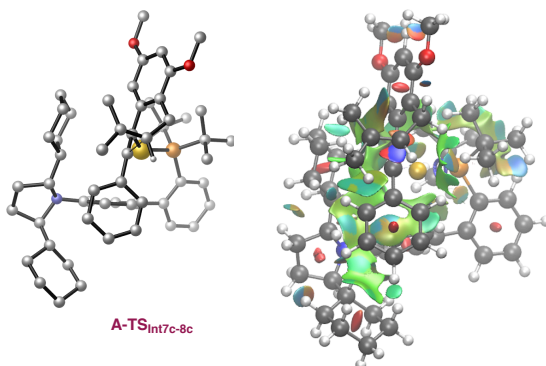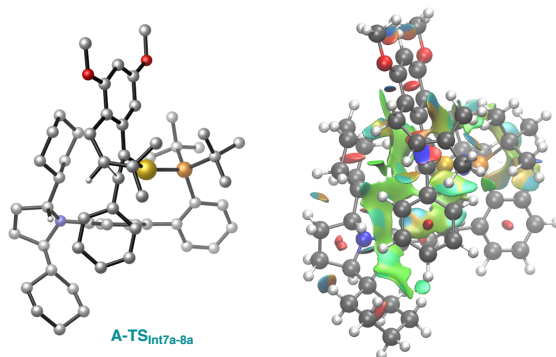
Computed Structures and Energies (BP86-D3)

A-Int1a
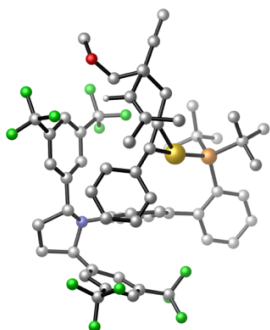
E = - 4167.37188981 Hartrees
G = - 4166.394407 Hartrees

A-Int1c
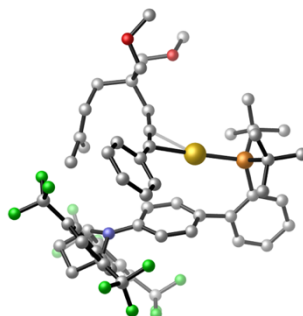
E = - 4167.36318320 Hartrees
G = - 4166.390366 Hartrees

A-Int2a
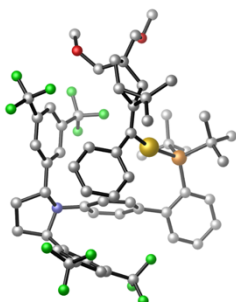
E = - 4167.38032723 Hartrees
G = - 4166.401105 Hartrees

A-Int2c
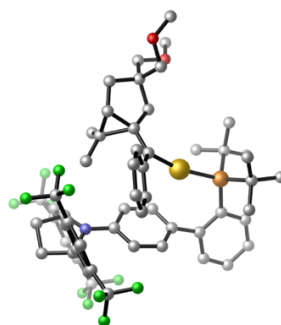
E = - 4167.37405374 Hartrees
G = - 4166.400970 Hartrees

A-Int3a
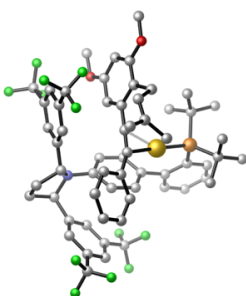
E = - 4241.19803338 Hartrees
G = -4240.254451 Hartrees

A-Int3c
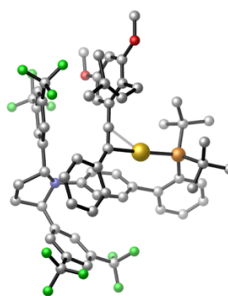
E = - 4241.19411247 Hartrees
G = - 4240.253519 Hartrees

UNIVERSITAT ROVIRA I VIRGILI
COMPUTATIONAL MECHANISTIC STUDIES IN GOLD(I) CATALYSIS AND DESIGN OF NEW CHIRAL LIGANDS
Immaculada Escofet Miquel

Chapter III
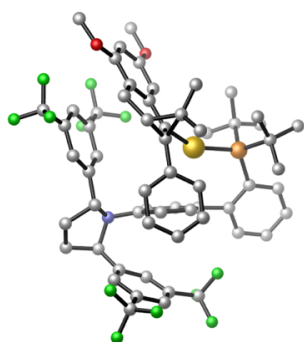
A-Int4a

E = - 4241.22251705 Hartrees
G = - 4240.271284 Hartrees

A-Int4c
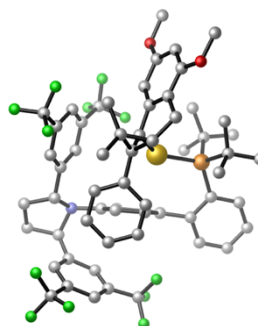
E = - 4241.20737493 Hartrees
G = - 4240.258695 Hartrees

A-TSInt₁ₐ₋₂ₐ
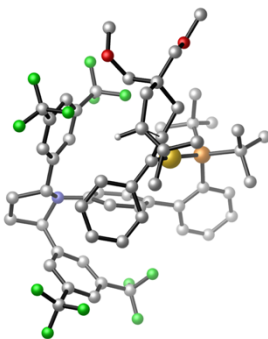
E = - 4167.36450210 Hartrees
G = - 4166.387486 Hartrees

A-TSInt₁c₋₂c
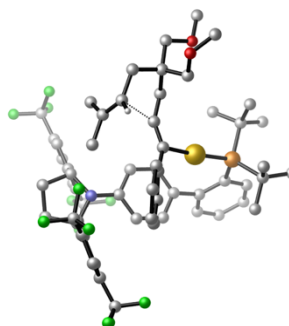
E = - 4167.35316045 Hartrees
G = - 4166.380823 Hartrees

A-TSInt₃ₐ₋₄ₐ
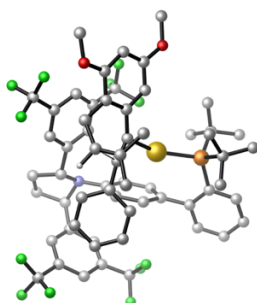
E = - 4241.19083258 Hartrees
G = - 4240.247829 Hartrees

A-TSInt₃c₋₄c
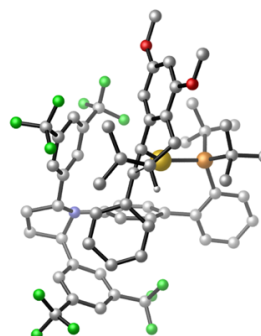
E = - 4241.18599520 Hartrees
G = - 4240.241784 Hartrees

UNIVERSITAT ROVIRA I VIRGILI
COMPUTATIONAL MECHANISTIC STUDIES IN GOLD(I) CATALYSIS AND DESIGN OF NEW CHIRAL LIGANDS
Immaculada Escofet Miquel

Chapter III
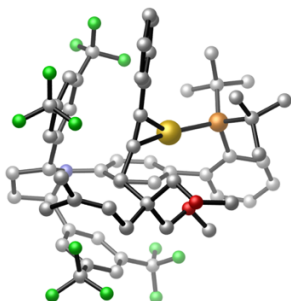
B-Int1b

E = - 4167.38134937 Hartrees
G = - 4166.399435 Hartrees

B-Int1d
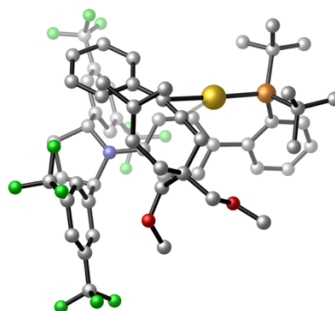
E = - 4167.37466010 Hartrees
G = - 4166.398710 Hartrees

B-Int2b
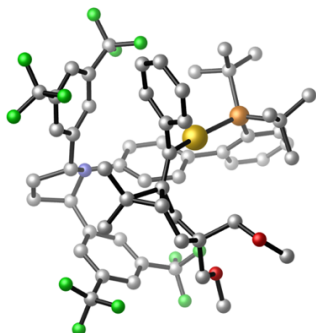
E = - 4167.37236583 Hartrees
G = - 4166.391239 Hartrees

B-Int2d
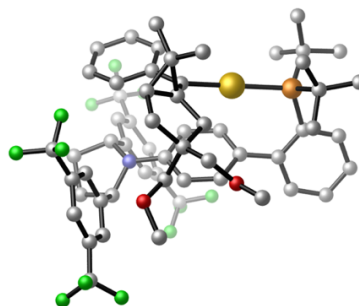
E = - 4167.38367926 Hartrees
G = - 4166.407002 Hartrees

B-Int3b
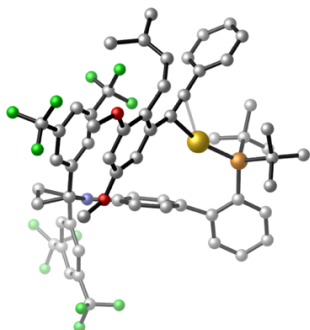
E = - 4241.19177511 Hartrees
G = - 4240.251004 Hartrees

B-Int3d
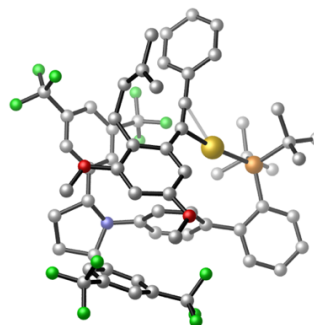
E = - 4241.19076567 Hartrees
G = - 4240.247438 Hartrees

UNIVERSITAT ROVIRA I VIRGILI
COMPUTATIONAL MECHANISTIC STUDIES IN GOLD(I) CATALYSIS AND DESIGN OF NEW CHIRAL LIGANDS
Immaculada Escofet Miquel

Chapter III
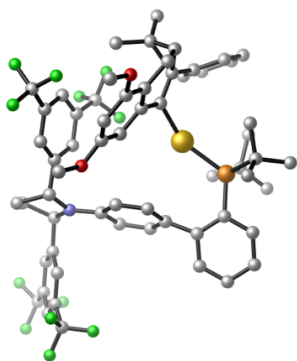
B-Int4b

E = - 4241.21208077 Hartrees
G = - 4240.266842 Hartrees

B-Int4d
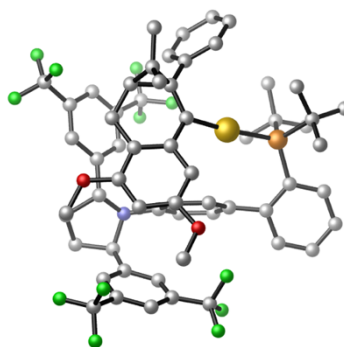
E = - 4241.21640352 Hartrees
G = -4240.268278 Hartrees

B-TSInt1b-2b
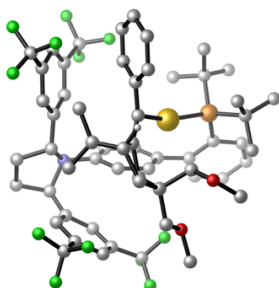
E = - 4167.35742293 Hartrees
G = - 4166.380281 Hartrees

B-TSInt1d-2d
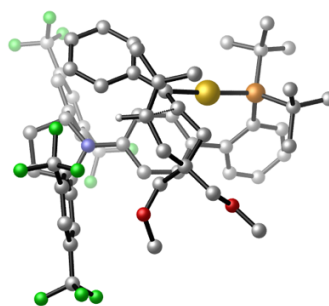
E = - 4167.36280837 Hartrees
G = - 4166.391606 Hartrees

B-TSInt3b-4b
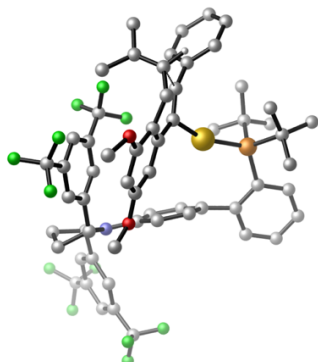
E = - 4241.18953982 Hartrees
G = - 4240.246245 Hartrees

B-TSInt3d-4d
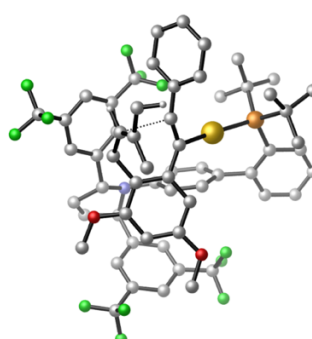
E = - 4241.18893406 Hartrees
G = - 4240.243709 Hartrees

UNIVERSITAT ROVIRA I VIRGILI
COMPUTATIONAL MECHANISTIC STUDIES IN GOLD(I) CATALYSIS AND DESIGN OF NEW CHIRAL LIGANDS
Immaculada Escofet Miquel

Chapter III

Enyne 8b
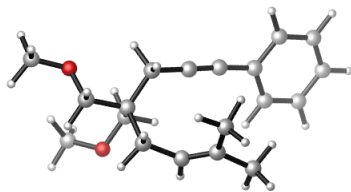
E = - 890.034548813 Hartrees
G = -889.691653 Hartrees

Enyne 38k
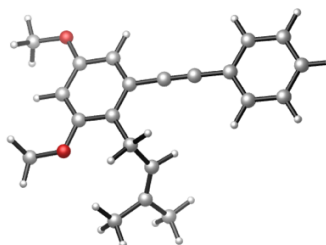
E = - 963.859114793 Hartrees
G = - 963.551049 Hartrees

LAu
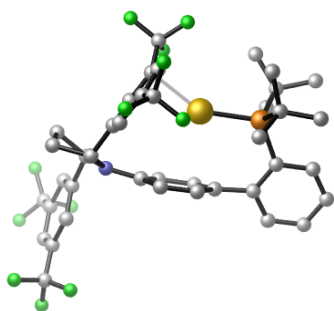
E = - 3277.27892571 Hartrees
G = - 3276.677658 Hartrees

38k-Int1
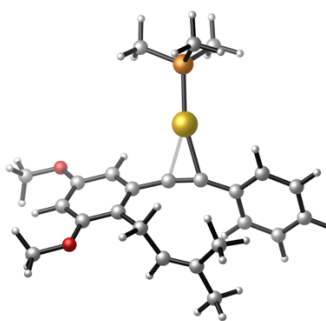
E = - 1560.79016818 Hartrees
G = - 1560.380559 Hartrees

38k-TS$_{1-2b}$
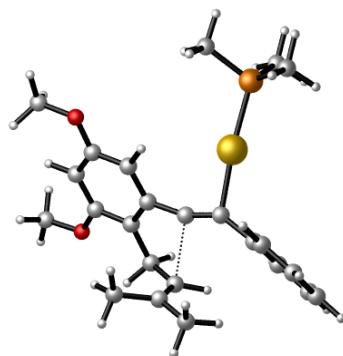
E = - 1560.78286990 Hartrees
G = - 1560.373263 Hartrees

38k-Int3b
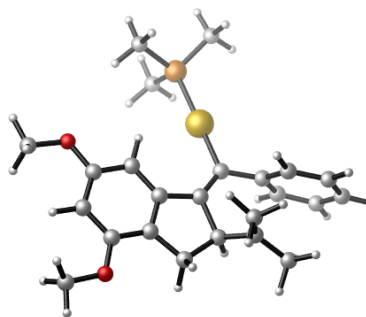
E = - 1560.79937715 Hartrees
G = - 1560.384897 Hartrees

UNIVERSITAT ROVIRA I VIRGILI
COMPUTATIONAL MECHANISTIC STUDIES IN GOLD(I) CATALYSIS AND DESIGN OF NEW CHIRAL LIGANDS
Immaculada Escofet Miquel

Chapter III
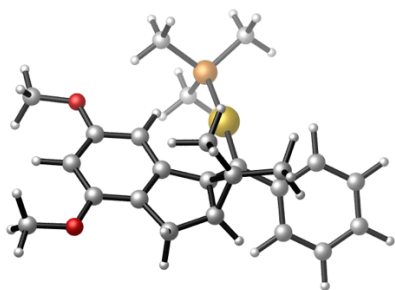
38k-Int2b

E = -1560.80195382 Hartrees
G = -1560.388248 Hartrees

38k-TS₃ᵦ₋₂ᵦ
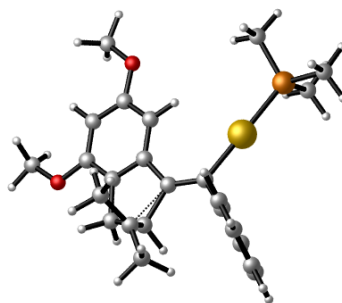
E = -1560.79723704 Hartrees
G = -1560.383233 Hartrees

38k-TS₁₋₃ᵦ
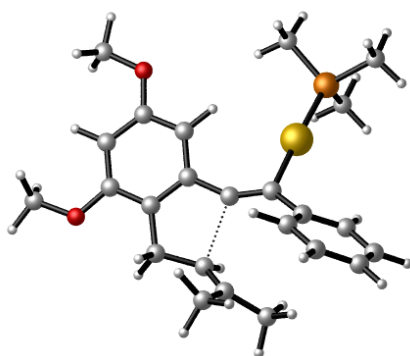
E = -1560.78034047 Hartrees
G = -1560.369283 Hartrees

38k-TS₁₋₂ₐ
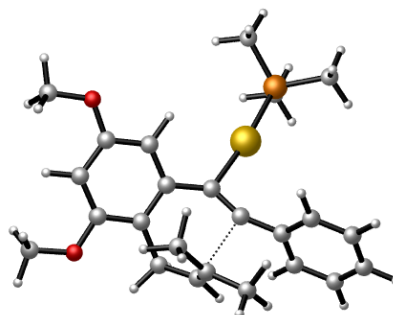
E = -1560.78435382 Hartrees
G = -1560.374309 Hartrees

38k-Int3a
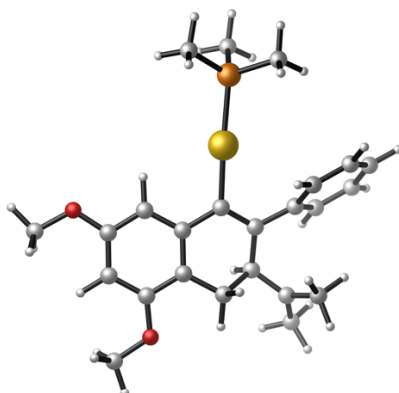
E = -1560.79641003 Hartrees
G = -1560.384329 Hartrees

38k-Int2a
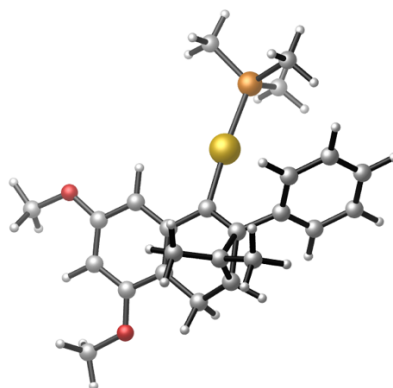
E = -1560.81621241 Hartrees
G = -1560.400681 Hartrees

263

UNIVERSITAT ROVIRA I VIRGILI
COMPUTATIONAL MECHANISTIC STUDIES IN GOLD(I) CATALYSIS AND DESIGN OF NEW CHIRAL LIGANDS
Immaculada Escofet Miquel

Chapter III

38k-TS$_{1\text{-}3a}$
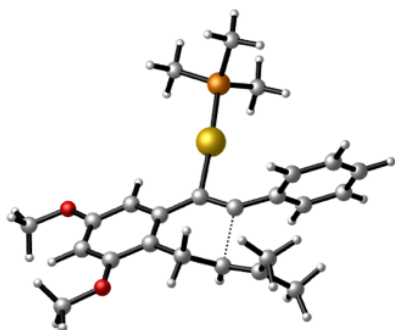
E = -1560.78135974 Hartrees
G = -1560.370725 Hartrees

38k-TS$_{3a\text{-}2a}$
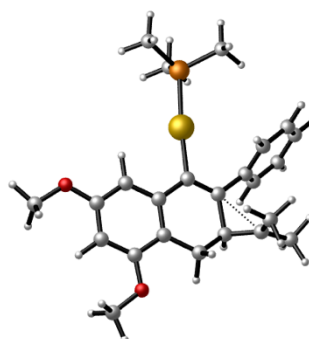
E = -1560.78909454 Hartrees
G = -1560.375779 Hartrees

A-Int5a
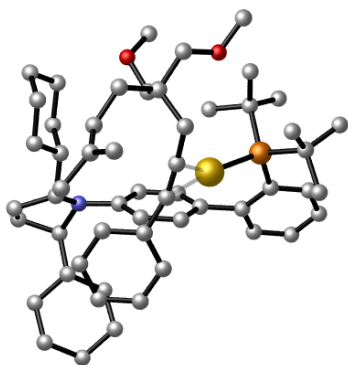
E = -2826.44106958 Hartrees
G = -2825.326885 Hartrees

A-Int5c
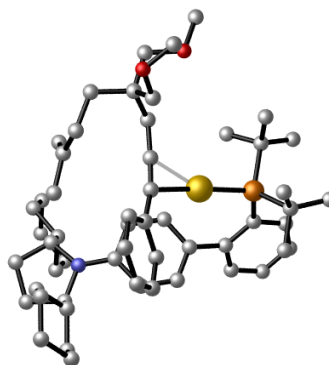
E = -2826.44487863 Hartrees
G = -2825.333112 Hartrees

A-Int6a
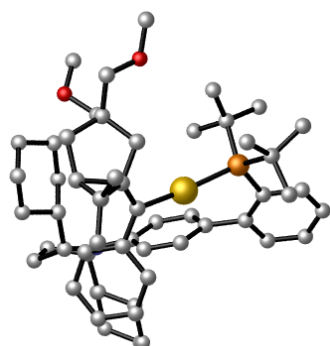
E = -2826.44744341 Hartrees
G = -2825.333102 Hartrees

A-Int6c
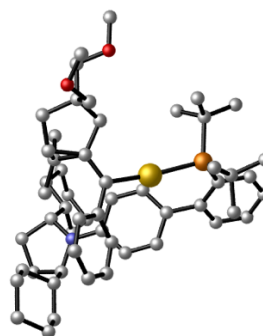
E = -2826.45832761 Hartrees
G = -2825.342285 Hartrees

264

UNIVERSITAT ROVIRA I VIRGILI
COMPUTATIONAL MECHANISTIC STUDIES IN GOLD(I) CATALYSIS AND DESIGN OF NEW CHIRAL LIGANDS
Immaculada Escofet Miquel

Chapter III
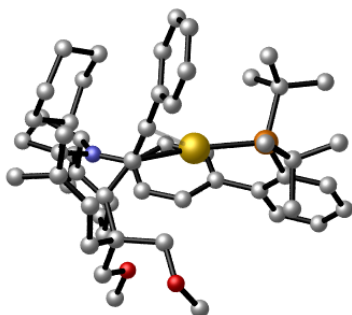
B-Int5b

E = -2826.44904003 Hartrees
G = -2825.339128 Hartrees

B-Int5d
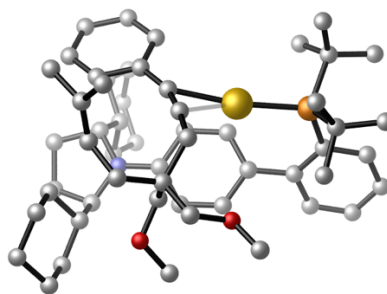
E = -2826.45719538 Hartrees
G = -2825.341861 Hartrees

B-Int6b
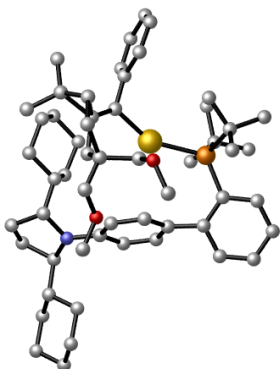
E = -2826.44782475 Hartrees
G = -2825.331116 Hartrees

B-Int6d
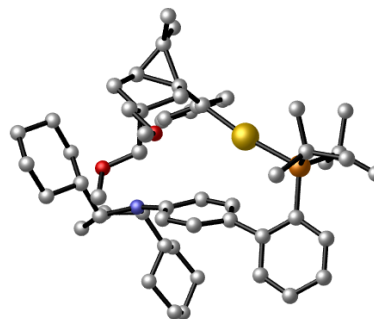
E = -2826.46322434 Hartrees
G = -2825.342982 Hartrees

A-TSInt₅ₐ₋₆ₐ
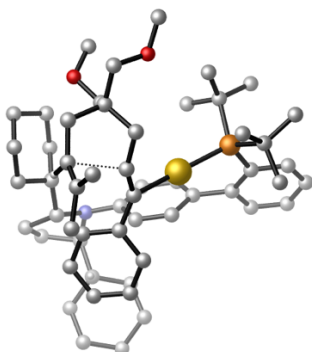
E = -2826.42764589 Hartrees
G = -2825.316494 Hartrees

A-TSInt₅c₋₆c
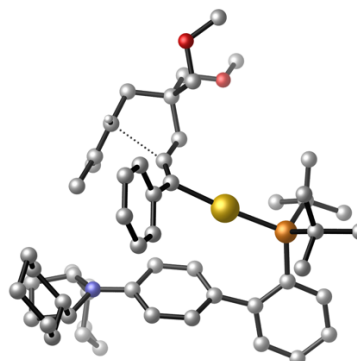
E = -2826.43681900 Hartrees
G = -2825.325915 Hartrees

UNIVERSITAT ROVIRA I VIRGILI
COMPUTATIONAL MECHANISTIC STUDIES IN GOLD(I) CATALYSIS AND DESIGN OF NEW CHIRAL LIGANDS
Immaculada Escofet Miquel

Chapter III

B-TSInt$_{5b-6b}$
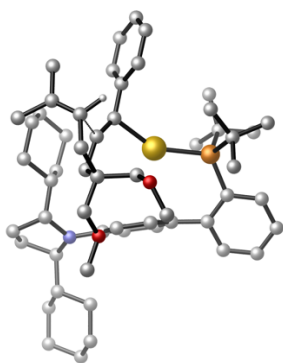
E = -2826.43590736 Hartrees
G = -2825.323211 Hartrees

B-TSInt$_{5d-6d}$
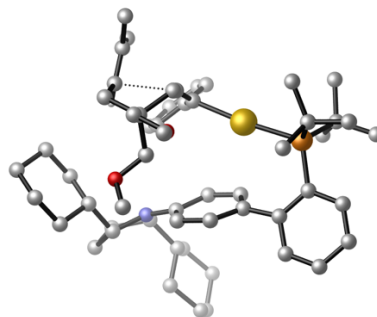
E = -2826.44614476 Hartrees
G = -2825.331451 Hartrees

A-Int7a
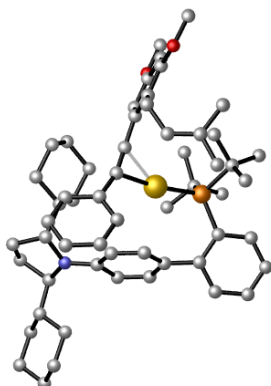
E = -2900.27214391 Hartrees
G = -2899.191336 Hartrees

A-Int7c
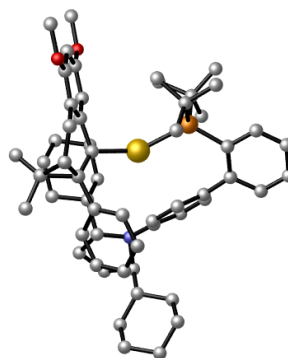
E = -2900.27619725 Hartrees
G = -2899.189855 Hartrees

A-Int8c
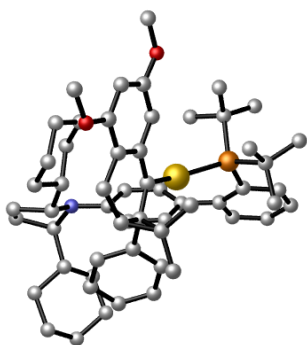
A-Int8a

E = -2900.28573941 Hartrees
G = -2899.199689 Hartrees
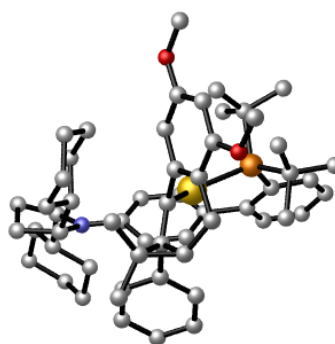
E = -2900.28252416 Hartrees
G = -2899.197569 Hartrees

UNIVERSITAT ROVIRA I VIRGILI
COMPUTATIONAL MECHANISTIC STUDIES IN GOLD(I) CATALYSIS AND DESIGN OF NEW CHIRAL LIGANDS
Immaculada Escofet Miquel

Chapter III
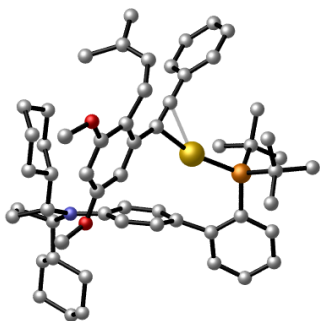
B-Int7b

E = -2900.25971133 Hartrees
G = -2899.183591 Hartrees

B-Int7d
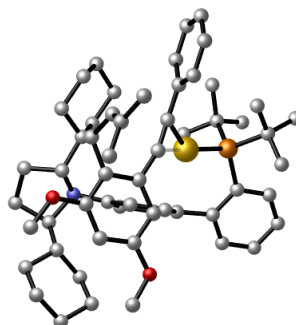
E = -2900.26086151 Hartrees
G = -2899.181521 Hartrees

B-Int8b
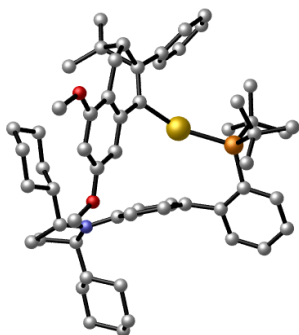
E = -2900.28648443 Hartrees
G = -2899.201688 Hartrees

B-Int8d
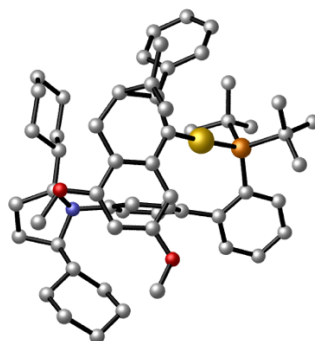
E = -2900.28359318 Hartrees
G = -2899.197048 Hartrees

A-TSInt7a-8a
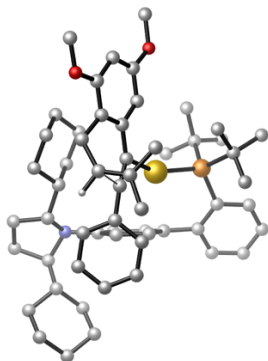
E = -2900.25484053 Hartrees
G = -2899.174841 Hartrees

A-TSInt7c-8c
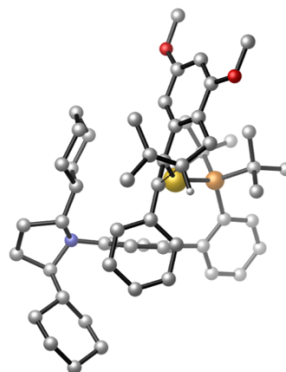
E = -2900.25391074 Hartrees
G = -2899.173854 Hartrees

UNIVERSITAT ROVIRA I VIRGILI
COMPUTATIONAL MECHANISTIC STUDIES IN GOLD(I) CATALYSIS AND DESIGN OF NEW CHIRAL LIGANDS
Immaculada Escofet Miquel

Chapter III

B-TSInt_{7b-8b}
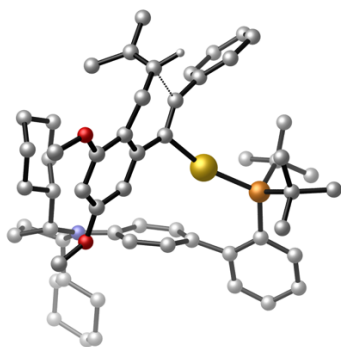
B-TSInt_{7d-8d}

E = -2900.25998006 Hartrees
G = -2899.180304 Hartrees
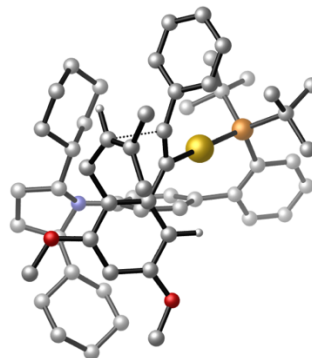
E = -2900.25430614 Hartrees
G = -2899.172705 Hartrees

UNIVERSITAT ROVIRA I VIRGILI
COMPUTATIONAL MECHANISTIC STUDIES IN GOLD(I) CATALYSIS AND DESIGN OF NEW CHIRAL LIGANDS
Immaculada Escofet Miquel

UNIVERSITAT ROVIRA I VIRGILI
COMPUTATIONAL MECHANISTIC STUDIES IN GOLD(I) CATALYSIS AND DESIGN OF NEW CHIRAL LIGANDS
Immaculada Escofet Miquel

UNIVERSITAT ROVIRA I VIRGILI
COMPUTATIONAL MECHANISTIC STUDIES IN GOLD(I) CATALYSIS AND DESIGN OF NEW CHIRAL LIGANDS
Immaculada Escofet Miquel

General Conclusions

General Conclusions

The present thesis addresses the computational study of intriguing mechanisms of gold(I)-catalyzed transformations together with the development of new chiral gold(I) catalysts based on new designs. The main conclusions of this work are the following:

Our computational studies on the nature of intermediates in cycloisomerizations of 1,6-enynes provides an evidence on the existance of different possible intermediates depending on the substitution of the substrate. Benchmark of DFT functionals with DLPNO-CCSD(T), allowed us to select the most appropriated functional for these systems. The QTAIM theory confirms that the molecular representation of the different types of intermediates was accurate. Moreover, the metal carbenic or cationic character of these intermediates was confirmed by NBO analysis since NPA charges were clearly delocalized.
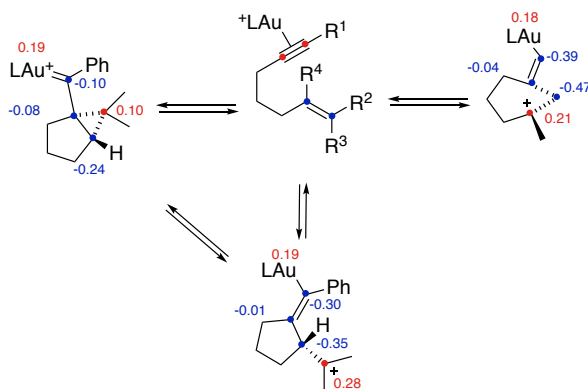
Our group developed a new gold(I)-catalyzed cyclization cascade of substituted dienynes that can lead to selective formation of unexpected *trans*-fused cyclopropanes within a *trans*-bicyclo[5.1.0]octane framework, depending on the substrate geometry. DFT calculations showed that this specific transformation is directed by the rigidity of the system. Likewise, computed pathways provide a rational for the role played by the fused tetrahydrofuran ring in the final cyclopropanation step.

The formation of *meso*-biscyclopropanes by reaction of *trans*-stilbene with acetylenein the presence og gold(I) catalysts has been rationalized by means of DFT calculations. The selectivity on the one step total synthesis of waitzacuminone has also been rationalzed computationally.

UNIVERSITAT ROVIRA I VIRGILI
COMPUTATIONAL MECHANISTIC STUDIES IN GOLD(I) CATALYSIS AND DESIGN OF NEW CHIRAL LIGANDS
Immaculada Escofet Miquel

General Conclusions

waitziacuminone
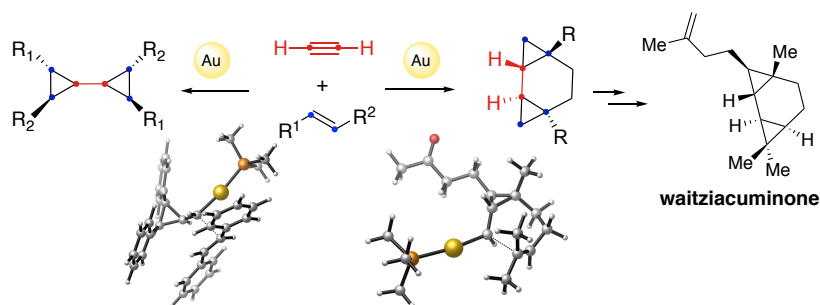
We have prepared a of series of chiral phosphite gold(I) complexes in a modular manner. Enantioenriched products of formal [4+2] cycloaddition were obtained from the corresponding 1,6-arylenynes in up to 88% *ee*.
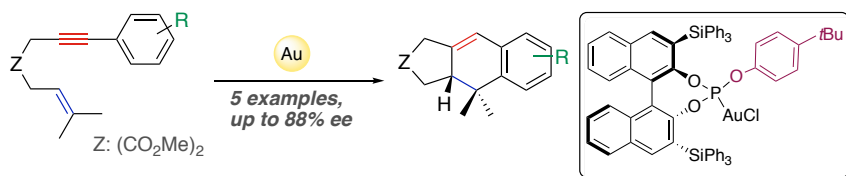
The first general strategy for the asymmetric synthesis of cyclobutenes by intermolecular gold(I)-catalyzed [2+2] cycloaddition has been developed. This was enabled by the use of a chiral non-C_2 symmetrical Josiphos digold(I) complexes. Mechanistic investigations suggest that both ligand exchange and electrophilic addition can be turnover-limiting steps of the catalytic cycle.
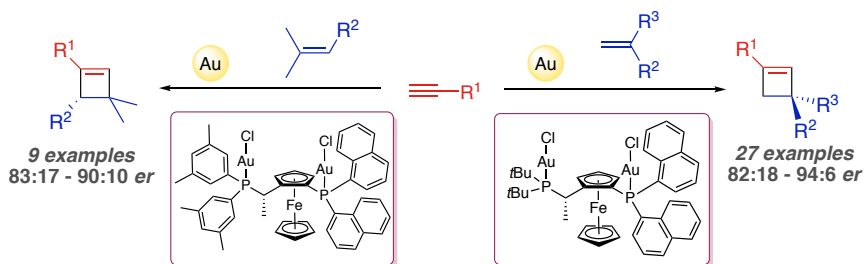
A model for the enantioinduction of new chiral ligand containing remote C_2-symmetric 2,5-disusbtituted pyrrolidines has been developed. As revealed by NCI plots, attractive non-covalent interactions between stereodirecting component of the substrates and the aromatic substituents of the chiral pyrrolidine are key to achieve high enantioinduction in the chiral pocket. The computational study of a 2nd of generation of catalysts openes the door for the preparation of more efficient gold(I) chiral catalysts.

UNIVERSITAT ROVIRA I VIRGILI
COMPUTATIONAL MECHANISTIC STUDIES IN GOLD(I) CATALYSIS AND DESIGN OF NEW CHIRAL LIGANDS
Immaculada Escofet Miquel

General Conclusions

favoured orientation A (ΔG = 0)
ΔG‡ = 4.2 - reaction through *Re* face

favoured orientation B (ΔG = 0)
ΔG‡ = 4.5 - reaction through *Si* face

UNIVERSITAT ROVIRA I VIRGILI
COMPUTATIONAL MECHANISTIC STUDIES IN GOLD(I) CATALYSIS AND DESIGN OF NEW CHIRAL LIGANDS
Immaculada Escofet Miquel

UNIVERSITAT ROVIRA I VIRGILI
COMPUTATIONAL MECHANISTIC STUDIES IN GOLD(I) CATALYSIS AND DESIGN OF NEW CHIRAL LIGANDS
Immaculada Escofet Miquel

UNIVERSITAT
ROVIRA i VIRGILI